MULTI-PROXY RESPONSES OF ICELANDIC LAKES TO HOLOCENE TEPHRA PERTURBATIONS

by

CELENE LOUISE CHRISTENSEN

H.B.S., Oregon State University, 2011

A thesis submitted to the

Faculty of the Graduate School of the

University of Colorado in partial fulfillment

of the requirement for the degree of

Master of Science

Department of Geological Sciences

2013

This thesis entitled:

Multi-proxy Responses of Icelandic Lakes to Holocene Tephra Perturbations

written by Celene Louise Christensen

has been approved for the Department of Geological Sciences

____

Gifford H. Miller

____

Áslaug Geirsdóttir

Date _____________

The final copy of this thesis has been examined by the signatories, and we
Find that both the content and the form meet acceptable presentation standards
Of scholarly work in the above mentioned discipline.

Christensen, Celene Louise (M.S., Geological Sciences)

Multi-proxy Responses of Icelandic Lakes to Holocene Tephra Perturbations

Thesis directed by Professor Gifford H. Miller

This thesis presents two independent studies in which sediment records from Icelandic lakes are utilized to interpret past environmental change related to climate evolution and tephra deposition on the landscape. Chapter 4, a multi-proxy high-resolution Holocene record from Vestra Gíslholtsvatn (VGHV), describes ecosystem development and variability over the last ~11 ka in southern Iceland. Proxies indicate ecosystem development in the lake took >2000 years following landscape deglaciation. Principle component analysis (PCA) of the VGHV multi-proxy data set indicate irreversible changes in the environmental state at ~5.5 ka and ~4.2 ka coinciding with onset and intensification of Neoglaciation in Iceland. Changes in proxy values and relationships following Icelandic settlement (871± 2 AD) indicate a strong anthropogenic signal in the last 1.2 ka of the proxy record. Additionally, abundant tephra fall in VGHV contributed to transient variability in lake proxies throughout the Holocene.

In Chapter 6, PCAs were conducted using ultrahigh-resolution multi-proxy records from four diverse Icelandic lakes: Vestra Gíslholtsvatn, Hvítárvatn, Haukadalsvatn, Torfadalsvatn; before and after four significant Holocene tephra fall events: T-tephra (~5650 BP), H4 (~4200 BP), KN (~3500 BP), and H3 (~3000 BP). Landscape and ecosystem processes were inferred from component relationships with pre- and post- tephra deposition states compared between events and lakes. Results indicate all substantial tephra deposition events, regardless of composition produce decadal to centennial scale disturbances to the lakes and catchments. Between the two tephra geochemical endmembers represented rhyolitic tephra was most disruptive to the landscape. Basaltic tephra sometimes appeared to improve lake and catchment productivity. Our observations indicate rhyolitic tephra deposition on relatively step slopes with thin soils during episodes of decreasing summer temperatures have the highest probability of producing sustained transitions into less ecologically productive states. Smaller lakes with greater background primary productivity and relatively thick, well-vegetated soils mantling low-relief catchments were able to return to pre-eruption ecosystem states within 100 years of significant tephra fall events. Therefore, it is important to consider how different tephra composition, thickness, lake properties, and climate state may influence a lacustrine ecosystem following a tephra fall event when analyzing abrupt transitions in Icelandic Holocene proxy records.

DEDICATION

To Cody A. Blair

And, as the stones that (Hekla) sees
Flung up to heaven through fiery rain
Descend like thunderbolts again
Upon the distant Faröese…

Ferdinand Freiligrath (1810-1876)

ACKNOWLEDGEMENTS

I want to first and foremost thank my advisors, Giff Miller and Áslaug Geirsdóttir for providing a unique and incomparable research experience. They also deserve thanks for their patience, assistance, and suggestions over the past two years. I also want to thank my other committee member, Tom Marchitto, for his time and inspiration as an educator.

There are many others who deserve thanks for their contributions to this thesis. I want to express my gratitude for the other students in my research group; Chris Florian, Darren Larsen, and Kate Zalzal for their help, encouragement, and recommendations, both in the field and the lab. I offer thanks to the wonderful people at the Limnological Research Center at the University of Minnesota for making sampling a simple and efficient process. Additional thanks are given to the staff at the Stable Isotope Facility at the University of California, Davis for painless and relatively fast sample processing and analysis. Appreciation is given to Yarrow Axford for constructing the Holocene chironomid record for Vestra Gíslholtsvatn and helping me interpret it. I thank Thorvaldur Thordarson, Gudrun Eva Jóhannsdóttir, and Anna Jagan for their extensive work on the tephra horizons in the lake records used in this thesis.

Furthermore, I thank my friends and family, especially Emily and my parents, Lyle and Cynthia, for their unending encouragement and eternal belief in my ability to pull this off. Finally, I want to thank Cody for always holding the shining light at the end of the tunnel, putting things in perspective, and reminding me I live in “real life”.

Table of Contents

LIST OF TABLES

LIST OF FIGURES

CHAPTER 1: INTRODUCTION

Icelandic lake sediment cores have been used to produce records of Holocene environmental change in lacustrine ecosystems and their surrounding landscapes (e.g. Björck et al., 1992; Hallsdóttir, 1995; Rundgren et al., 1995; 1998; Hallsdóttir and Caseldine; 2005; Caseldine et al., 2003; 2006; Wooller et al., 2008; Langdon et al., 2010; Larsen et al., 2011; 2012; Geirsdóttir et al., 2009a; 2013). In Iceland mobile soil, soft bedrock, sufficient erosional processes (i.e. wind, water, and glaciers) (Arnalds, 2008b; Óskarsson et al., 2010; Arnalds et al., 2012), and adequate lacustrine productivity contribute to high sediment accumulation rates in lake basins. This allows for sub-decadal to decadal sample resolution throughout the Holocene for a variety of biological and physical proxies. These proxies are representative of ecosystem stability and structure in lakes and their catchments, processes associated with the climate state (e.g. Bigelow et al., 2003; Kaplan et al., 2003). As Iceland is at a thermally sensitive location in the northern North Atlantic (e.g. Knudsen and Eiríksson, 2002) regional changes in Holocene climate are well represented in environmental proxy records. Spatial variability across the island is related to the proximity of warm and cold ocean surface currents and orography (e.g. Bromwich et al., 2005; Logemann and Harms, 2006; Rousse et al., 2006).

Iceland also has means of producing exceptionally well-dated Holocene sediment records despite handicaps with radiocarbon in some lakes due to remobilization of old carbon within their catchments (Black et al., 2008; Geirsdóttir et al., 2009a; Larsen et al., 2011). Age models are applied to lake sediment cores using tephrochronology from abundant Holocene volcanism (Jóhannsdóttir, 2007; Larsen and Eiríksson, 2008; Thordarson and Höskuldsson 2008; Jagan, 2010), synchronization of paleomagnetic secular variation (PSV) between sediment cores (Ólafsdóttir, 2010), and radiocarbon when appropriate. This allows for the observation of subtle changes in sediment accumulation rates that would otherwise be missed when using linear interpolation between limited tie points (Hardardóttir, 1999; Geirsdóttir et al., 2013; Ólafsdóttir et al., 2013).

Expanding the spatial extent of highly resolved Holocene records of climate and environmental change improves understanding of regional climate variability and occurrence of synchronized climate events. Several large scale climate events are well documented within Icelandic terrestrial and marine records including the transition from deglaciation (Björck et al., 1992; Rundgren, 1995; Black et al., 2004; Caseldine et al., 2006; Hannesdóttir et al; 2009; Langdon et al., 2010), the 8.2 ka cold event (Alley and Ágústsdóttir, 2005; Larsen et al., 2012; Quillmann et al., 2012; Geirsdóttir et al., 2009b; 2013), Holocene Thermal Maximum (HTM) (Andrews et al., 2003; Kaufman et al., 2004; Caseldine et al., 2006), and Neoglaciation beginning ~5.5 ka (Larsen et al., 2012; Geirsdóttir et al., 2013). The Neoglacial includes intensification at 4.2 ka, a decline into the Dark Ages Cold Period (DACP) at 550 AD, the Medieval Warm Period (MWP) from 950 to 1250 AD, and onset of the Little Ice Age (LIA) at 1250 AD (Larsen et al., 2011; 2012; Geirsdóttir et al., 2009b; 2013). However, how these periods of transient stability and systematic shifts are represented in sediment proxy records depends upon individual properties of each lake and its catchment. This makes it important to have an array of lakes with high-resolution, multi-proxy records to appropriately describe regional Holocene environmental variability across Iceland.

Explosive volcanism is a common occurrence in the Iceland throughout the Holocene (Larsen and Eiríksson, 2008; Thordarson and Höskuldsson, 2008) producing widespread tephra horizons that can be geochemically characterized; correlated between accumulation sites (i.e. lakes, ice cores, soil profiles, and peat bogs), and dated with historical records after ~1.1 ka and radiocarbon ages of adjacent organic material for prehistoric eruptions (e.g. Larsen and Thorarinsson, 1977; Thorarinsson, 1979; Mangerud, 1986; Róbertsdóttir, 1992; Dugmore, 1995; Jóhannsdóttir, 2007; Óladóttir et al., 2008; Jagan, 2010; Myers, 2011). Most lake studies in Iceland only use tephra layers as chronostratigraphic constraints. Some have noted transient periods of change in physical and/or biological proxies following prominent tephra deposition events such as Hekla 3 (H3) and Hekla 4 (H4) (e.g. Hardardóttir, 2001; Larsen et al., 2011, 2012; Geirsdóttir et al., 2013) at ~3.0 ka and ~4.2 ka respectively (Dugmore et al., 1995) and Saksunarvatn (e.g. Björck et al., 1992; Axford et al., 2007; Wooller et al., 2008; Langdon et al., 2010) at 10.3 ka (Jóhannsdóttir, 2007; Davies et al., 2012).

Despite their prominence in the sediment record and the general observation that large tephra deposition events create significant and long lasting environmental disturbances (Thordarson, 1979; Gudmundsson et al., 2008; Ayris and Delmelle, 2012) no one has produced an ultrahigh-resolution, multi-proxy study focusing on substantial ash fall events. Nor has anyone methodically compared landscape and ecosystem responses between lakes to tephra deposition. Better knowledge of how different lakes and their catchments respond to significant tephra fall events is important for the understanding of connectivity between volcanic disturbance, climate, and ecosystem succession and could be valuable when considering the inevitability of future explosive volcanic eruptions in Iceland.

CHAPTER 2: AIMS AND OBJECTIVES

The purpose of this thesis, which is divided into seven chapters, is to provide high-resolution records of environmental change as recorded in Holocene lake sediments in southern and western Iceland. Chapters 1 and 3 provide an introduction and background on the use of high latitude lake sediment records, Holocene climate in the northern North Atlantic, and post-glacial volcanism in Iceland. This chapter (Chapter 2) offers rationale behind three studies (Chapters 4, 5, and 6) in this thesis, two of which (Chapters 4 and 5) are to be submitted as independent papers to peer-reviewed journals. The final chapter (Chapter 7) summarizes conclusions and suggests additional research that would broaden our understanding of Holocene climate and lacustrine ecosystem dynamics in Iceland.

Chapter 4 presents an ~11,000 year record of environmental change and variability in ecosystem structure and function at Vestra Gíslholtsvatn, a small lake in southern Iceland. This record utilizes multiple physical (MS, density, tephra abundance and layer thickness) and biological (%TOC, %N, C:N, $\delta^{13}C$, $\delta^{15}N$, %BSi, midge temperature reconstructions) proxies collected from lake sediment to characterize ecosystem evolution of the basin and catchment, periods of tephra disturbance, climate driven transitions, and anthropogenic influence.

Chapter 5 presents a study using four Icelandic lakes: Vestra Gíslholtsvatn, Hvítárvatn, Haukadalsvatn, and Torfadalsvatn comparing sub-decadal to decadal resolution multi-proxy records 200 years before and after tephra fall events. Principal component analysis (PCA) was preformed for each lake and eruption using physical (MS and bulk sediment density) and organic matter (OM) proxies (%TOC, C:N, and $\delta^{13}C$) to determine the strength of individual components and observe shifts in the state and function of lake and catchment ecosystems. We compare lake responses following two substantial rhyolitic tephra (H3 and H4) and two widespread basaltic tephra (KN and T-tephra) contributing an additional element to the study. Thickness, timing, and composition of additional tephra horizons observed within each time window were recorded and also used to interpret changes in the component scores through time.

Chapter 6 is a smaller study using high-resolution multi-proxy lake sediment records from Hvítárvatn, a high elevation, proglacial lake in the central highlands of Iceland. For this study we emphasize time windows falling 500 years before and after the significant rhyolitic tephra deposition events, Hekla 3 (H3) and Hekla 4 (H4). In doing so, we identify in the proxy record periods of tephra disturbance in the lake catchment related to tephra fall. As Hvítárvatn is the most sensitive lake in our Chapter 5 study we are able to determine an appropriate time interval in which to conduct high-resolution sampling surrounding thick tephra horizons that sufficiently captures landscape and ecosystem perturbations attributable to tephra fall events.

The results of these studies enable us to better understand lake ecosystem development and sustainability in Iceland through the Holocene as related to climate, tephra fall, and anthropogenic influence. They also provide a preliminary interpretation as to how and why lacustrine and terrestrial ecosystems change following tephra deposition events. As Iceland is a volcanically active region, any information on landscape and ecosystem resilience to tephra fall is valuable to its inhabitants.

CHAPTER 3: BACKGROUND

3.1 High Latitude Lake Studies in the North Atlantic Region

Lake basins are locations of deposition, continuously collecting sediment and in doing so preserving records of lacustrine ecosystems and terrestrial landscape stability, processes reflective of the climate at specific locations and time periods (e.g. Bigelow et al., 2003; Kaplan et al., 2003). At high latitudes in the North Atlantic, lake sediment studies have been successful at reconstructing signals of environmental change related to climate and other external forcings, such as explosive volcanism and anthropogenic influences. However, many studies are poorly resolved, inadequately constrained, and span only a portion of the Holocene while others utilize high-resolution sampling, multiple lakes, and constrain age models with more than one method.

Despite some inequality in methodology most studies possess a multi-proxy approach making it possible to test the interpretation of each variable with a spectrum of physical and organic matter (OM) proxies. Some studies emphasize a single proxy such as chironomid inferred temperature reconstructions (Caseldine et al., 2003; 2006; Wooller et al., 2008; Axford et al., 2007; 2009; Langdon et al., 2010) or pollen assemblages (Hallsdóttir, 1995; Rundgren, 1995; 1998; Rundgren and Ingólfsson, 1999; Hallsdóttir and Caseldine, 2005; Payne et al., 2013) comparing the chosen variable to additional physical and OM proxies. Others use an array of proxies including but not limited to: the presence of ice rafted debris (IRD), magnetic susceptibility (MS), bulk sediment density, sediment mineralogy, total carbon (%C), total nitrogen (%N), C:N, $\delta^{13}C$, $\delta^{15}N$, diatom assemblages, and percent biogenic silica (%BSi) (e.g. Björck et al., 1992; Hardardóttir; 1999; Kaufman et al., 2004; Black, 2008; Lennox et al., 2010; Janbu et al., 2011; Larsen et al., 2011; 2012; Geirsdóttir et al., 2009 a; b; 2013). These proxies are used to infer relative summer temperature, terrestrial vegetation assemblages, glacial advance into a basin, terrestrial erosion, and lacustrine ecosystem structure and function, all indirect measures of climate that are most robust when signals are coherent between proxies and study sites.

In Iceland, correlation between lake sediment cores can be a relatively simple first order process if conspicuous tephra layers are present producing rough synchronization (e.g. Thordarson and Höskuldsson, 2008; Larsen et al., 2011; 2012). Unfortunately radiocarbon dating is often inappropriate for dating high latitude lake sediments due to the remobilization of old carbon in lake catchments making it difficult to establish age model tie points (Black, 2008; Geirsdóttir et al., 2009a). However, in some relatively productive lakes and catchments, radiocarbon works well (e.g. Lennox et al., 2010). A lack of age constraints forces linear interpolations and smoothing between known tie-points reducing age model accuracy and producing unrealistic sediment accumulation rates (Hardardóttir, 2001). A more precise method of core comparison uses paleomagnetic secular variation (PSV) records (Ólafsdóttir, 2010) improving correlation of multi-proxy responses between lake sediment cores and observation of coherent transitions in proxy records at different locations (e.g. Geirsdóttir et al., 2013; Ólafsdóttir et al., 2013).

3.2 Non-linear Holocene Climate Change in Iceland

Holocene climate in Iceland has been inferred from a variety of proxy records including lake sediment cores (e.g. Björck et al., 1992; Rundgren et al., 1995, 1998; Hardardóttir et al., 1999; Rundgren and Ingólfsson, 1999; Hallsdóttir and Caseldine, 2005; Wooller et al., 2008; Axford et al., 2007; 2009; Langdon et al., 2010; Larsen et al., 2011; 2012; Geirsdóttir et al., 2009; 2013), peat bogs (e.g. Gudmundsson, 1997 and references therein), marine sediment cores (Knudsen and Eiríksson, 2002; Andrews et al., 2003; Giraudeau et al., 2004; Sicre et al., 2008; Quillmann et al., 2012), and glacial moraines (Gudmundsson, 1997; Mackintosh et al., 2002; Kirkbride and Dugmore, 2006; Geirsdóttir et al., 2008) indicating coherent centennial and millennial scale climate events controlled by decreasing solar insolation, variability in atmospheric and oceanic circulation, and external forcings such as explosive volcanism (e.g. Bond et al., 2001; Mayewski et al., 2004; Miller et al., 2012). From this information the Icelandic Holocene is broken into three broad climate periods: deglaciation (pre ~8 ka), the Holocene Thermal Maximum (HTM) (~8 ka to ~5.5 ka) and Neoglaciation (~5.5 ka to present) (e.g. Geirsdóttir et al., 2013). Within these broad time periods fall short-lived climate events that often produced substantial changes in proxy records.

Deglaciation is notable in Iceland with an early Holocene warming that led to the rapid removal of ice and development of soils and fauna across Iceland (Björck et al., 1992; Rundgren et al., 1995; Caseldine et al., 2006; Langdon et al., 2010; Geirsdóttir et al., 2009b; 2013). This initial terrestrial success was offset by the deposition of the Saksunarvatn tephra producing decades of landscape instability across the country (Hallsdóttir and Caseldine, 2005). A multi-century cold event at ~8.2 ka due to freshening of the North Atlantic (Alley and Ágústsdóttir, 2005; Quillmann et al., 2012) further impacted terrestrial and lacustrine environments (e.g. Caseldine et al., 2006; Larsen et al., 2012; Geirsdóttir et al., 2013). However, ecosystems quickly recovered with the terrestrial signals indicating maximum Holocene warmth at ~8.0 ka supporting onset of the HTM.

Both terrestrial and marine records indicate a HTM in Iceland from ~8.0 ka to between 6.0 ka and ~5.5 ka (e.g. Andrews et al., 2003; Kaufman et al., 2004; Caseldine et al., 2006; Larsen et al., 2012; Geirsdóttir et al., 2013). In this time period pollen records show an expansion of birch forests (Hallsdóttir et al., 1995), physical proxies imply limited watershed erosion, and OM proxies suggest productive lacustrine ecosystems all indicators of a warm and stable climate. Sediment records from higher latitude coastal lakes observe a delay in onset of the HTM. This is explained with suppression of the terrestrial system by the maritime climate overwhelming temperatures on land (Caseldine et al., 2003; Axford et al., 2007). The strong temperature gradient across Iceland produced by variability in ocean surface currents also contributed to variations in vegetational colonization between northern and southern Iceland in the HTM (Caseldine and Hallsdóttir, 2005).

Between 6.0 ka and 5.5 ka Neoglacial cooling began across Iceland (Geirsdóttir et al., 2013). Neoglaciation is distinguished by the presence of persistent cool summers, increased variability in the lake proxy records, greater sediment accumulation rates, and the readvance of glaciers across Iceland (Gudmundsson, 1997; Kirkbride and Dugmore, 2006; Geirsdóttir et al., 2009a and b; Larsen et al., 2011; 2012). Noteworthy periods of cooling include ~4.2 ka; ~3.0 ka, 2.0 ka, ~1.5 ka, 0.7 ka, and 0.2 ka

(Geirsdóttir et al., 2013). The intervals of cooling at 4.2 ka and 3.0 ka coincide with the substantial rhyolitic eruptions H4 and H3 respectively (Larsen and Thorarinsson, 1977; Dugmore et al., 1995) complicating the climate signals observed in the proxy record. A significant shift in proxies at ~1.5 ka signifies the DACP which is followed by a less cold MWP from ~1.0 ka to 0.7 ka (Geirsdóttir et al., 2013). The LIA began following an initial summer cooling at 0.7 ka reaching its maximum intensity at ~0.2 ka (e.g. Larsen et al., 2011). The complicated structure of proxy records during the last ~2 ka is further convoluted by anthropogenic erosion related to the settlement of Iceland (874 AD) obscuring climate driven signals (e.g. Hardardóttir, 1999; Ólafsdóttir et al., 2002; Óskarsson et al., 2004).

3.3 Explosive Holocene Volcanism in Iceland

Volcanism in Iceland is driven by the collaborative influence of a mantle plume hotspot (e.g. Wolfe et al., 1997) and the divergence of the North American and Eurasian tectonic plates along the Mid-Atlantic Ridge (Sæmundsson, 1979; Einarsson, 1991). From this interaction a diverse collection of volcanoes and eruption styles are present throughout the Holocene dominated by explosive eruptions of basaltic magma (Thordarson and Höskuldsson, 2008) (See Fig. 3.1). Tephra, glassy airborne ejecta, is a product of explosive volcanism varying in geochemical composition between mafic (basaltic) and felsic (rhyolitic) endmembers (e.g. Thordarson and Larsen, 2007). These vitric fragments can travel great distances and repeatedly remobilize before permanent deposition (e.g. Thorarinsson, 1979; Ayris and Delmelle, 2012 and references therein). Thus, tephra horizons in the sediment record can be widespread but variable and incomplete (e.g. Jóhannsdóttir, 2007; Larsen and Eiríksson, 2008; Jagan, 2010).

Figure 3.1 Distribution of active volcanic zones and belts in Iceland. The approximate location lakes used in this thesis are marks with black circles and labeled. Abbreviations are as follows: RR- Reykjanes Ridge; RVB- Reykjanes Volcanic Belt; SISZ- South Iceland Seismic Zone; WVZ- West Volcanic Zone; MIB- Mid-Iceland Belt; EVZ- East Volcanic Zone; NVZ- North Volcanic Zone; TFZ- Tjörnes Fracture Zone; KR- Kolbeinsey Ridge; ÖVB- Öræfi Volcanic Belt; and SVB- Snæfellsnes Volcanic Belt. Numbers refer to volcanic systems listed in Thordarson and Höskuldsson, (2008). Systems relevant to this study include numbers: 14- Katla; 16- Hekla; 17- Torfajökull; 18- Bárdarbunga-Veiđivötn; 19- Grímsvötn; 20- Kverkfjöll; 21- Askja. The large open circle indicates the approximate center of the Icelandic mantle plume as depicted by Wolfe et al., (1997). Figure adapted from Jóhannesson and Sæmundsson (1998) and Thordarson and Höskuldsson, (2008).

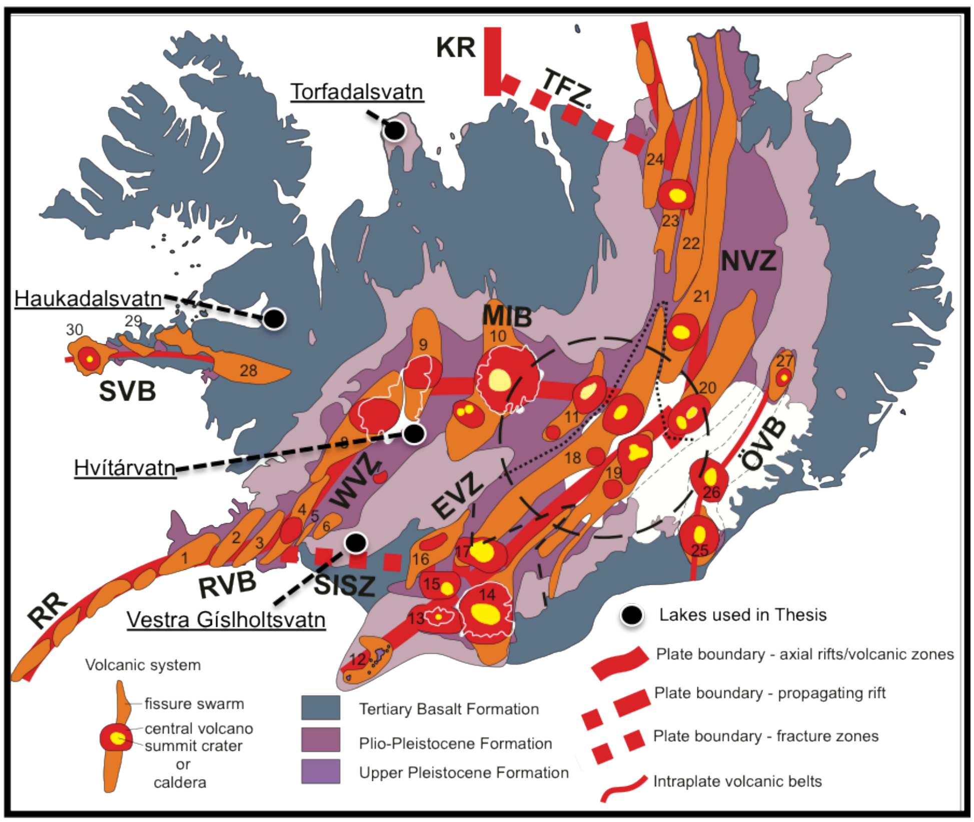

Explosive eruptive events are more common in Iceland than in other comparable volcanic regions due to the high frequency of eruptions and unique environmental conditions. Most of the active Icelandic volcanoes are covered or capped by glaciers and in close proximity of the North Atlantic Ocean promoting interactions between magma and ice or seawater (e.g. Gudmundsson, 2005; Thordarson and Höskuldsson, 2008). Determining the number and magnitude of explosive Holocene eruptions is difficult as <35% of tephra producing eruptions are preserved in sediment archives, tephra geochemistry from specific eruptions can be variable covering a range of compositions, <10% of known tephra layers have been mapped across Iceland, and post glacial tephra stratigraphy for the island is not complete or fully synchronized between research groups (Larsen and Eiríksson, 2008; Thordarson and Höskuldsson, 2008). Thus, there is no complete record of Holocene explosive volcanism in Iceland. Written accounts indicate Iceland was settled by the Norse in 871±2 AD shortly after deposition of the Settlement Tephra Layer (Vö), observed in the Greenland ice core at 871±2 AD (Grönvold et al., 1995). After settlement, the eruption history of Iceland is well documented with 205 confirmed historical eruptions of which 124 are categorized as explosive eruptions. The majority of these eruptions propagated from the East Volcanic Zone (EVZ) where the prolific Grímsvötn, Hekla, Katla, and Bárdarbunga-Veiđivötn volcanic systems reside (Thordarson and Larsen, 2007). In the Holocene record it is estimated that one out of four eruptions were explosive with ~86% of classified as “wet” (hydromagmatic) while ~14% are categorized as “dry” (magmatic) (Thordarson and Höskuldsson, 2008).

In the Holocene >90% of explosive eruptions have been of mafic (basaltic) composition making rhyolitic eruptions noteworthy in the sediment record. Estimates suggest explosive rhyolitic eruptions occur with a frequency of 1 every 200 to 300 years (Thordarson and Höskuldsson, 2008). However, the largest rhyolitic eruptions have an event frequency of 1 every 10^3 to 10^5 years (Thordarson and Larsen, 2007) making them unique in the Holocene sediment record. For this reason, substantial rhyolitic tephra horizons are most typically used as chronostratigraphic marker beds (e.g. Larsen and Thorarinsson, 1977; Haflidason et al., 2000; Kristjánsdóttir et al., 2007) but, significant work has been done in recent years resolving the age, composition, and distribution of basaltic tephra layers using geochemical compositions collected from electron microprobe analysis (e.g. Jóhannsdóttir, 2007; Óladóttir et al., 2008; Jagan, 2010).

CHAPTER 4: A HIGH RESOLUTION MULTI-PROXY LAKE RECORD OF HOLOCENE ENVIRONMENTAL CHANGE IN SOUTHERN ICELAND FROM VESTRA GÍSLHOLTSVATN

Celene L. Christensen[1], Áslaug Geirsdóttir[2], Gifford H. Miller[1,2], Thorvaldur Thordarson[3], and Yarrow Axford[4]

1. INSTAAR and Department of Geological Sciences, University of Colorado at Boulder, Boulder, CO, USA

2. Institute of Earth Sciences, University of Iceland, Reykjavik, Iceland

3. School of GeoSciences, University of Edinburgh, Edinburgh, United Kingdom

4. Department of Earth and Planetary Sciences, Northwestern University, Evanston, IL, USA

4.1 Introduction

Throughout the Holocene, climate in the Northern Hemisphere has responded to a relatively simple decreasing trend of solar insolation with non-linearities and spatial heterogeneity (e.g. Bond et al., 2001; Kaufman et al., 2004; Alley and Ágústsdóttir, 2005; Wanner et al., 2008; Larsen et al., 2012; Geirsdóttir et al., 2013). The most feasible rational for these irregularities are local and regional scale factors which complicate the climate response to radiative forcing producing a signal dependent on interconnected variables (Wanner et al., 2011). Previous studies have shown Icelandic lake sediment records reflect centennial and millennial scale environmental variability related to complex changes in northern North Atlantic ocean and atmosphere circulation, local and global volcanism, and solar variability (e.g. Axford et al., 2007; Larsen et al., 2011; 2012; Miller et al., 2012; Geirsdóttir et al., 2009a; 2013). Short-term deviations from the background state are typically attributed to local phenomenon while persistent changes are associated with regional and global signals.

Iceland (~103,000 km^2) is located in the north central Atlantic Ocean at the intersection of the relatively warm salty North Atlantic Current (NAC) and currents originating in the cold fresh Arctic Ocean (Fig. 4.1). This produces strong oceanic and atmospheric thermal gradients creating an ideal location for terrestrially based paleoenvironmental studies. Branching off the NAC is the Irminger Current (IC), which

Figure 4.1 Location map of Iceland in the North Atlantic with simplified ocean current circulation. Note the intersection of the warm and cold currents. The Irminger Current (IC) branches off the North Atlantic Current (NAC) flowing west bringing warmth to the southern coast of Iceland before bifurcating with one branch (the Northern Iceland Irminger Current) flowing north along the Western Icelandic shelf and the other branch flowing south next to the East Greenland current (EGC). Figure unaltered from Larsen et al., (2012).

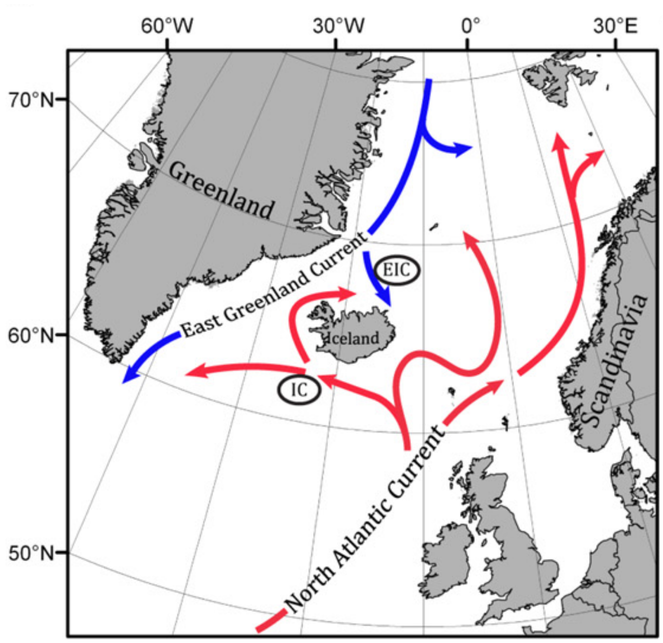

brings warm water along the southern and western coastlines of Iceland subsequently moderating the regional climate (See Fig. 4.1). The IC bifurcates south of the Denmark Strait where one branch turns west flowing southward mixing with the East Greenland Current (EGC) along the East Greenland shelf (Malmberg & Kristmannsson, 1992). The other branch, the North Icelandic Irminger Current (NIIC), continues north-eastward on the North Icelandic shelf (Logemann and Harms, 2006). Fluctuations in the NIIC have been linked to climate variability around and across Iceland (e.g. Andrews et al., 2003; Rousse et al., 2006; Sicre et al., 2008; Geirsdóttir et al., 2009b; Ólafsdóttir et al, 2010).

Several studies use well-dated high-resolution lake sediment proxy records to reconstruct Holocene environmental change in Iceland. However, no complete contemporary Holocene record exists for southern Iceland (e.g. Hallsdóttir, 1995; Hallsdóttir and Caseldine, 2005; Axford et al., 2007; Hannesdóttir et al., 2009; Larsen et al., 2011; 2012; Geirsdóttir et al., 2009a; 2013). As south Iceland is close to the less variable portion of the IC it is important to understand how Holocene climate variability is expressed in the terrestrial archive for this region. The objective of this paper is to present a 10.3 ka high-resolution paleoenvironmental record from the small, low-elevation, non-glacial lake, Vestra Gíslholtsvatn, located in southern Iceland (Fig. 4.2). Notable in the record is an extended period of lake development and stabilization following deglaciation; repeated short-lived disturbances related to tephra fall events from nearby explosive volcanism; and an overprint of settlement on the climate record over the last millennium. A sediment core was first collected from Vestra Gíslholtsvatn in 1994 and used to produce a record of tephrochronology, pollen assemblages, and

Figure 4.2 a. Map of Iceland with location of Vestra Gíslholtsvatn marked by a star (Google Earth). b. Satellite image of Vestra and Eystra Gíslholtsvatn and surroundings (Google Earth) overlain with topographic map (Raforkumálastjóri (Electrical Authorities), 1967). c. The bathymetry of the lake (Rist, 1975).

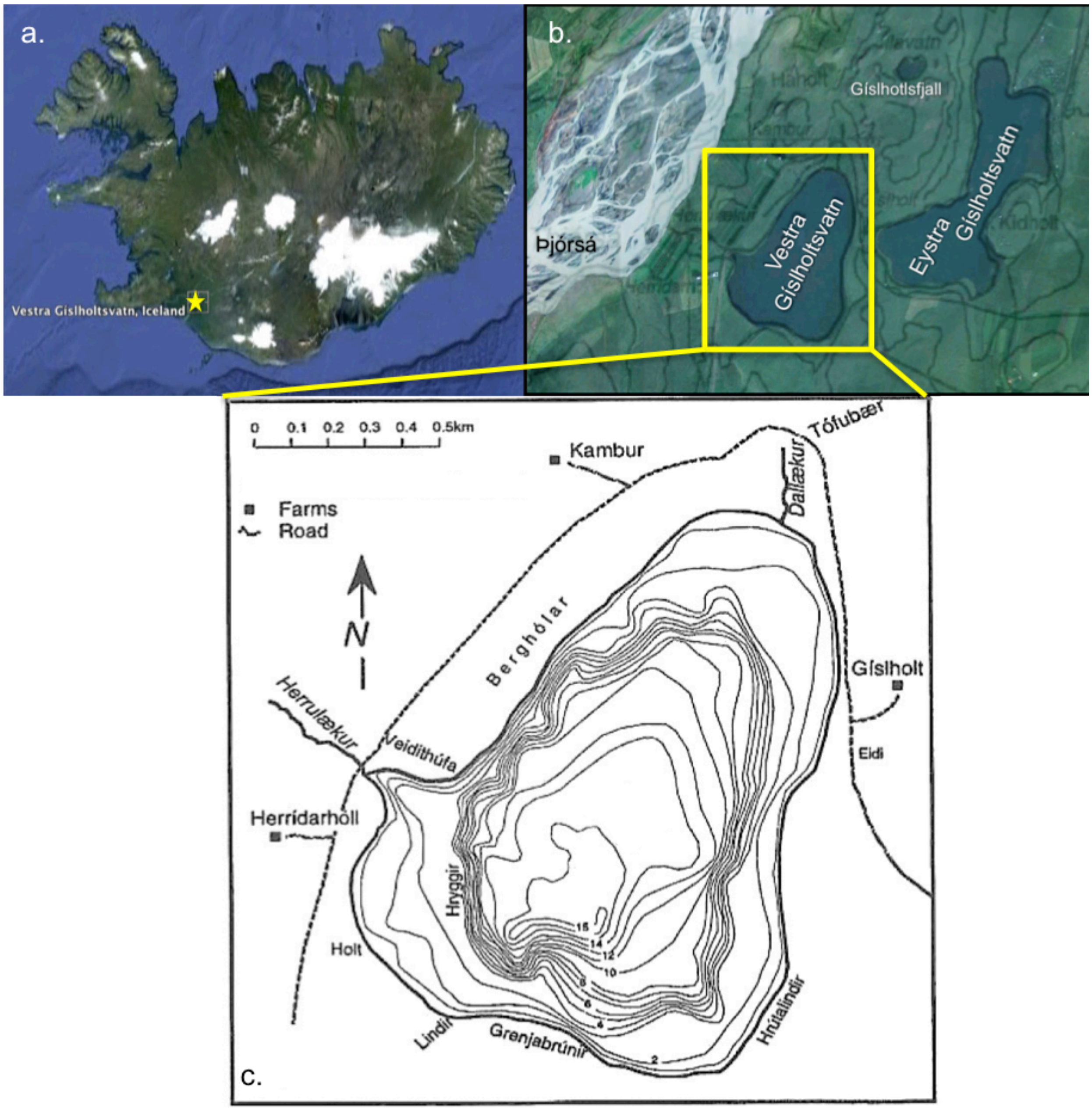

sediment physical characteristics for the last ~5.6 ka BP (Hardardóttir, 1999; Hallsdóttir and Caseldine, 2003; Jagan, 2010). Our record covers nearly twice the time interval, has higher resolution sampling of both organic matter (OM) and physical proxies, and uses an improved age model. Therefore our Vestra Gíslholtsvatn record strengthens knowledge and understanding of Holocene climate and environmental variability in southern Iceland.

4.2 Physical Setting

Vestra Gíslholtsvatn is a non-glacial lake in the lowlands of south Iceland (63°56', -20°31') approximately 0.25 km west of the neighboring lake, Eystra Gíslholtsvatn (Fig. 4.2a, b). Both lakes reside in glacially scoured bedrock basins >15 m above the Þjórsá, a large river northwest of the lakes, flowing from the glacier, Hofsjökull, to the Atlantic Ocean. This topographic relationship allows us to assume there has been no direct interaction between the lakes and the river since deglaciation. Maps from the Icelandic Geodetic Institute indicate the lake levels are 61 m asl; but, as of 1975 the lake level of Vestra Gíslholtsvatn is approximately 9 m lower than that of Eystra Gíslholtsvatn (Rist, 1975). Dallækur; a stream fed by bogs located at the northern part of the lake and atop Gíslholtsfjall, a small fell (168 m asl) situated between the two lakes, provides the primary inflow into Vestra Gíslholtsvatn. There are no major drainages into or out of the lake and additional inflow from small brooks enters along the southern and southeastern ends of the basin (Fig. 4.2c) (Hardardóttir, 1999).

Since settlement of Iceland (871±2 AD) the land surrounding the lake has been predominately used for farming and the grazing of sheep due to the presence of fertile soils and a relatively mild climate. Large planted hayfields, shrub-heath, and fen/mires make up the modern vegetation in the area. Shrub-heath is found near bedrock outcrops on elevated areas while fen/mires prefer places where water can accumulate such as atop Gíslholtsfjall and at lower elevations in valley bottoms (Hardardóttir, 1999). The pollen record from the lake extending ~5.6 ka indicates abundant trees with most disappearing in less than a generation after settlement to be replaced with herbs and shrubs (Hallsdóttir and Caseldine, 2005). Erosional features are evident on the hillsides indicating the watershed has endured erosion for an unknown period of time (Hardardóttir, 1999).

4.3 Materials and Methods

4.3.1 Sediment core collection

In the winter of 2008 an 8.14 m sediment core was collected from the deep central basin of Vestra Gíslholtsvatn using a Bolivia piston coring system (Wright, 1967) (See Fig. 4.2c.). Seven 1.5 m drives were completed of which the upper six were recovered (Fig. 4.3). Cores were packed in the field and shipped to the Limnological Research Center (UM-LRC) at the University of Minnesota for initial core processing, description, and sub-sampling.

Surface cores were taken in August 2008 using a Universal coring system capturing the undisturbed upper sediments and the sediment-water interface following methodology outlined in Glew (1991). Comparison of magnetic susceptibility (MS) and bulk sediment density in the surface cores to the top of the Bolivia core allows us to assume near complete recovery of the spliced core.

Figure 4.3 Vestra Gíslholtsvatn Core VGHV08-1A-1B arranged in sections from top (upper left) to bottom (lower right). The core captures the entire Holocene record constrained by the Saksunarvatn tephra at 10.3 ka. Geochemically identified tephra horizons used in the age model are labeled with arrows pointing to base of the respective layer in the core.

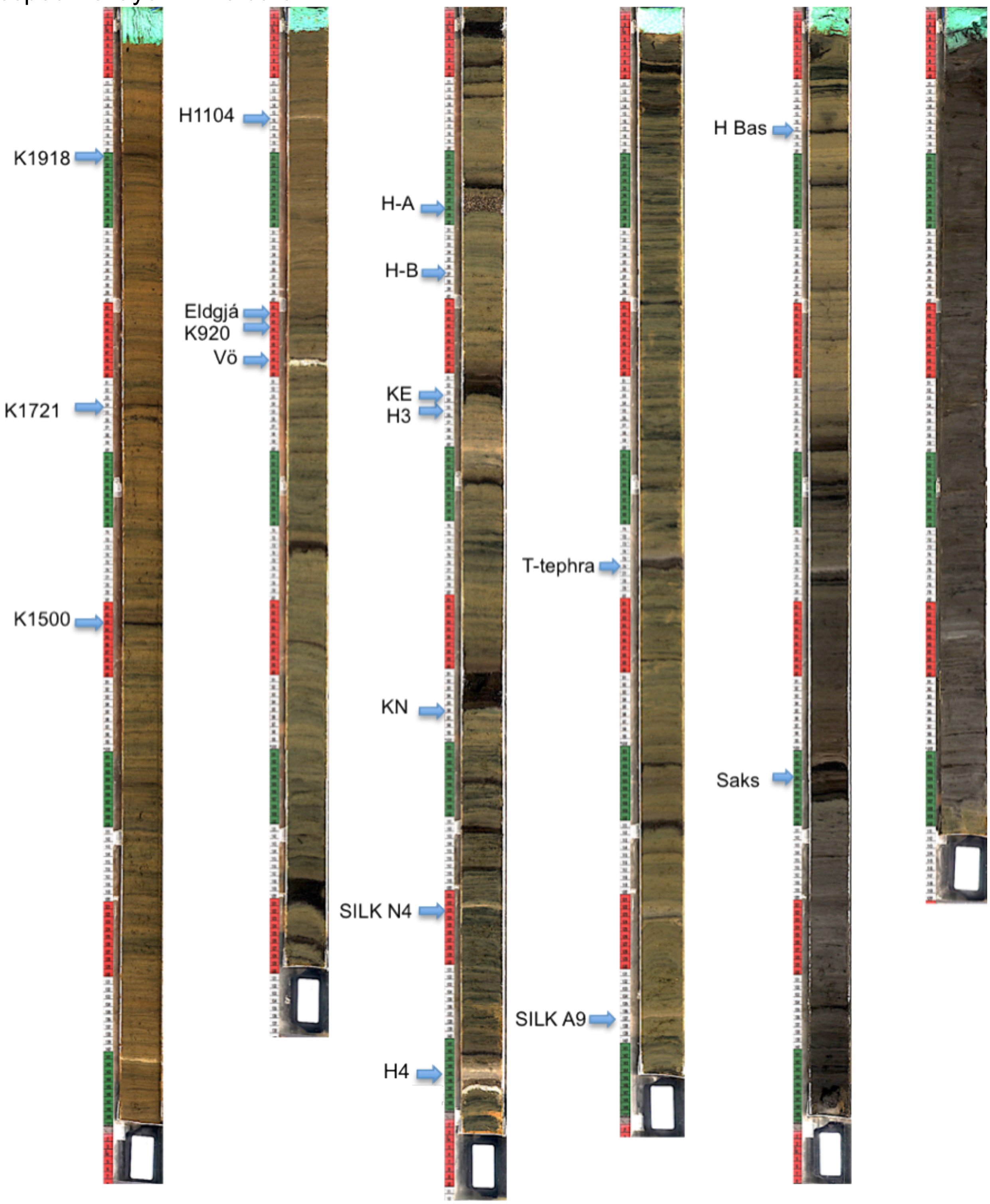

4.3.2 Physical Proxies

The Vestra Gíslholtsvatn cores were analyzed for multiple physical and OM proxies directly related to paleoenvironmental conditions in and around the lake. Physical properties of lake sediment can be used to interpret the extent and efficiency of weathering on the landscape, sediment transport within a catchment, and the presence of tephra (airborne volcanic glass fragments) horizons within the core (e.g. Hallett et al., 2001; Dahl et al., 2003; Larsen et al., 2012; Rosenbaum et al., 2012). Physical characteristics, including bulk sediment density and magnetic susceptibility (MS), of lake sediments in nonglaciated basins located near active volcanic centers are primarily influenced by erosional products from the landscape and the input of tephra into the lake basin from volcanic sources (e.g. Hallett et al., 2001). Whole core density and MS was measured at UM-LRC using a Geotek Multi-Sensor Core Logger (MSCL) after which core segments were split and core halves were photographed using a DMT CoreScan Color flatbed scanner.

The presence of iron oxides and ferromagnesian minerals in tephra can result in peaks in MS within the sediment cores if background values of MS are low enough (Berger et al., 1994). Tephra can also produce density anomalies, as the vitric material is typically more or less dense than erosional products and autochthonous OM (e.g. Larsen et al., 2012). Layers of tephra were identified visually with assistance from MS and density measurement. After confirming the presence of a tephra, layer thickness was measured and subsamples were collected for geochemical analysis by T. Thordarson in 2009. For each layer sampled tephra fragments were washed and sieved to remove OM and obtain the optimum size fraction (typically 100 μm to 250 μm fraction). Tephra fragments were then placed in probe plugs and polished with 6 μm and 1 μm diamond paste to expose fresh glass surfaces. The plugs were cleaned in an ultrasonic bath of deionized water before carbon coating. Samples were analyzed for chemical composition using a Cameca SX100 energy dispersive electron microprobe for Electron Microprobe Analysis (EMPA) at the NERC Tephra Analysis Unit at the University of Edinburgh. A using 5 μm to 8 μm beam size, 15 kV acceleration voltage, and a 2 nA beam-current were used. Beam size was reduced to the minimum possible without causing Na loss. International standards a99, VG2, BHVO2G and Lipari 1 were analyzed as unknowns at regular intervals as a quality check and to monitor for instrument drift. The uncertainty on the major element analysis is <1%.

4.3.3 Biological Proxies

Lacustrine and terrestrial primary productivity produces proxy signals that can be interpreted to discern changes in paleoclimatic and paleoenvironmental conditions influencing lake and catchment processes (e.g. Leng and Marshall, 2004; Wooller et al., 2008; Lennox et al., 2010; Larsen et al., 2011; 2012; Geirsdóttir et al., 2009a; 2013). Algae and terrestrial plants utilize carbon and nitrogen in their structures with characteristic chemical ratios (i.e. C:N) and isotopic compositions (i.e. $\delta^{13}C$, $\delta^{15}N$). When the living material dies a portion of the OM is buried in the sediment preserving the signal (i.e. %C, %N, %BSi). From this information it is possible to make inferences regarding the structure and stability of past ecosystems. Samples of total organic carbon (TOC), stable carbon isotopes ($\delta^{13}C$), total nitrogen (TN), and stable nitrogen isotopes ($\delta^{15}N$) were taken at 0.5 cm to 4.0 cm intervals from all core segments.

Samples of biogenic silica (BSi) were taken every 2.0 cm to 4.0 cm in the upper five sections of the core segments.

Sediment sampled for analysis of carbon and nitrogen were collected at UM-LRC and kept at 4 °C until they were freeze dried, weighed and sent to the University of California, Davis Stable Isotope Facility (SIF-UC Davis) for processing. An Elementar Vario EL Cube or Micro Cube elemental analyzer (Elementar Analysensysteme GmbH, Hanau, Germany) interfaced to a PDZ Europa 20-20 isotope ratio mass spectrometer (Sercon Ltd., Cheshire, UK) was used to process the samples. Freeze-dried samples were combusted at 1000 °C and N_2 and CO_2 gas were separated using a molecular sieve adsorption trap before entering the continuous-flow IRMS for $\delta^{13}C$ and $\delta^{15}N$ measurements. $\delta^{13}C$ values are expressed relative to Vienna Pee Dee Belemnite with a long-term standard deviation of 0.2‰ while $\delta^{15}N$ values are expressed relative to air with a long-term standard deviation of 0.3‰. Additional TC values were measured at the Institute of Earth Sciences (IES) at the University of Iceland. These samples were collected every 2.0 cm to 4.0 cm to compliment BSi measurements. Freeze-dried samples were run on a CM5200 Autosampler/Furnace (combusted to 950°C) and measured on a CM5014 CO_2 Coulometer v 3.0 with a detection limit of 0.05 weight-percent.

BSi was analyzed at the University of Illinois following methodologies by Mortlock and Froelich (1989), except for the use of 10% Na_2CO_3 during extraction. A Spectronic Genesys 5 spectrophotometer was used to measure the concentration of BSi, which was then converted to weight percent SiO_2 of dry sediments. The analytical precision of the BSi measurements was ±3%.

4.3.4 Temperature reconstruction

Chironomid (Diptera: Chironomidae, or non-biting midges) assemblages have been shown to respond quickly to climate change and have thus been used in paleolimnological studies to reconstruct low amplitude temperature changes via chironomid-based transfer functions (Eggermont and Heiri, 2012 and references therein). Studies have used chironomid assemblages in Icelandic lake sediment cores to reconstruct Holocene temperature (e.g. Caseldine et al., 2003; 2006; Axford et al., 2007; 2009; Langdon et al., 2008; 2010) despite relatively impoverished chironomid fauna compared to mainland Europe or North America (Hrafnsdóttir, 2005). For this study, Y. Axford (unpublished data) followed standard protocols for subfossil taxonomic analysis (Walker, 2001). Sediment samples were deflocculated in warm 5% KOH for 20 minutes, and rinsed on a 100 µm mesh sieve. Head capsules were picked from a Bogorov sorting tray under a 40x power dissecting microscope, then mounted on slides using Euparal. Square-root transformed species data were employed to model July air temperatures using the WA partial-least-squares (WA-PLS) transfer function developed by Langdon et al., (2008), which is based upon calibration data from lakes in northwestern and western Iceland. Temperatures were modeled using the software program C2 v 1.4.3 (Juggins, 2003).

4.3.5 Chronology

4.3.5.1 Tephrochronology

Tephra produced by volcanic eruptions can be transported hundreds of kilometers downwind until deposition. In lake and landscape studies tephra layers represent important stratigraphic markers as they offer chronological control. Horizons of basaltic and rhyolitic tephra of Icelandic origin are common in Icelandic lake sediments due to abundant Holocene volcanic activity (Thordarson and Larsen, 2007) providing a way to derive absolute dates within a sediment core. The permanent settlement of Iceland is inferred from written accounts to have occurred just after deposition of the Settlement tephra layer (Vö), observed in the Icelandic sediment record and Greenland ice core where it has been dated to 871±2 AD (Grönvold et al., 1995). Historical records after ca. 900 AD in addition to soil and lacustrine sequences for prehistoric eruptions (Larsen and Thorarinsson, 1977; Kirkbride and Dugmore, 2006; Jóhannsdóttir, 2007; Óladóttir et al., 2008; Larsen et al., 2011) have helped establish a secure tephrostratigraphy in Iceland.

4.3.5.2 Radiocarbon Dating

Two radiocarbon samples, one plant macrofossil and basal bulk sediments for humic acid extraction, were collected from the core. Radiocarbon samples were prepared by the Laboratory for AMS Radiocarbon Preparation and Research (NSRL), at the Institute of Arctic and Alpine Research at the University of Colorado, Boulder and measured at the University of California, Irvine.

4.4 Results and Proxy Interpretations

4.4.1 Development of Age Model

4.4.1.1 Tephrochronology

A Holocene tephrochronology for the sediment core was constructed from 18well-identified tephra layers. In total 108 tephra layers were observed within the core of which 107 were geochemically analyzed providing a good understanding of tephra disturbance frequency in south Iceland. The majority of tephra layers in Vestra Gíslholtsvatn are of basaltic composition and attributed to the East Volcanic Zone (EVZ). Horizons are predominantly sourced to the Katla, Hekla, and Grímsvötn volcanic systems (Fig. 3.1). The total thickness of tephra in the core is 59.3 cm accounting for 7.3% of the total sediment column.

Major element composition of 18 geochemically fingerprinted tephra layers allowed for their correlation to the historical eruptions: Katla 1918, Katla 1721, Katla 1500, Hekla 1104, Eldgjá (934-942 AD), Katla 920 and Vatnaöldur (Settlement) (871±2 AD); and the prehistoric eruptions: H-A (~2595 BP), H-B (~2842 BP), KE (~2962 BP), H3 (~3000 BP), KN (~3500 BP), SILK N4 (~3900 BP), H4 (~4260 BP), T-tephra (~5636 BP), SILK A9 (~7660 BP), H Bas (~8420 BP), and Saksunarvatn (~10.3 ka BP) (Thorarinsson, 1967; Larsen and Thorarinsson, 1977; Larsen, 1984, 2000; Thordarson et al., 2001; Jóhannsdóttir, 2007; Óladóttir et al., 2008; Jagan, 2010; Ólafsdóttir, 2010).

4.4.1.2 ^{14}C Results

One radiocarbon date of 6880±20 BP from a plant macrofossil was used in conjunction with the identified tephra horizons to create an age model for the core. Another radiocarbon sample (humic acid) was taken from the basal sediments but not used (See Table 4.1).

Table 4.1 Radiocarbon samples from VGHV08-1A-1B sediment core. The date produced from the humic acid sample was not used in the age model as it was younger than tephra horizons identified above the sample depth. As the sediments are basal in the core segment possible explanations for the anomalous age include suction of younger sediments during extraction, or contamination from the core catcher or by other means.

Sample no.	Core section	Depth in section (cm)	Sample Type	Chemical Fraction	$\delta^{13}C$	Fraction Modern	Radiocarbon Age (^{14}C BP)
*NSRL-16277	6	108-109	Bulk sediment	Humic Acids	-23.9‰	0.5284±0.0009	5,125±15
NSRL-16278	4	141	Plant macrofossil	Macrofossils	-27.9‰	0.4246±0.0009	6,880±20

*Not used in age model

4.4.1.3 Age Model

The age model for the Vestra Gíslholtsvatn sediment core was constructed by fitting control points (tephra and radiocarbon ages and their depths) with a smoothed spline using the CLAM code (Blaauw, 2010) (Fig. 4.4). Age model uncertainty is low for historic times and variable between the settlement (Vö: 871±2 AD) and Saksunarvatn (10,200±200 BP) tephra horizons due to uncertainties associated with tephra dating. We have no age constraints in the core prior to the Saksunarvatn tephra. Pre-10.3 ka sediment accumulation rates were modeled using the relationship between density and sedimentation rates from the age model controlled portion of the core for purposes of observing the impact of Saksunarvatn tephra deposition on the lake and catchment. All time and sediment accumulation rates before 10.3 ka should only be taken as relative. Modeled ages are presented as years before 1950 AD.

Figure 4.4 CLAM age model using a spline smoothing for the last 10.3 ka. The chronology is based on 18 unique geochemically dated tephra layers (blue triangles) and one radiocarbon date (red circle). Uncertainty in age is represented by the gray shading. See *4.3.5 Chronology* for discussion of age model derivation.

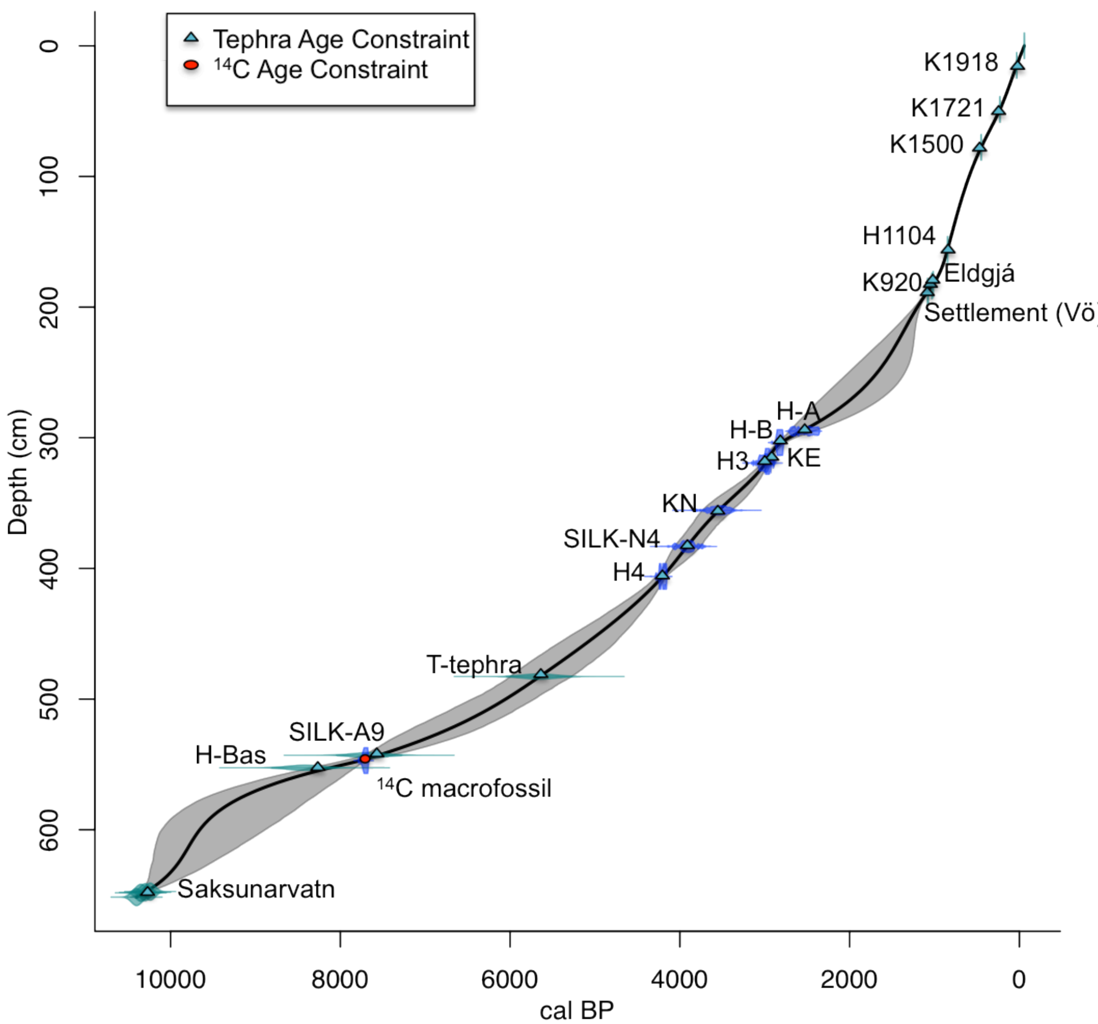

The CLAM code constructed an age-depth model (Fig. 4.4) and the resultant sediment accumulation rate (Fig. 4.5a). A lack of tie points in the early Holocene make it difficult to observe abrupt or short lived changes in sedimentation rates before 4.2 ka. A third of our tie points occur in the last 1100 years, and then reveal abrupt and changes in sediment accumulation rate after settlement. The lowest sedimentation rates (<0.2 mm a^{-1}) occur at ~8.8 ka following landscape restabilization after deposition of the Saksunarvatn tephra (~10.3 ka). Sediment accumulation rate then slowly increases to a plateau of 0.5 mm a^{-1} between 7.0 ka and 6.0 ka after which gradual increases are punctuated more abrupt escalations at 4.2 ka, 3.0 ka, 1.7 ka, 1.0 ka, and ~0.3ka reaching a maximum rate of 2.4 mm a^{-1} at 0.8 ka (Fig. 4.5a).

Figure 4.5 Physical proxy time series for Vestra Gislholtsvatn Holocene record a. sediment accumulation rate; b. magnetic suceptibility (MS); c. bulk sediment density; d. tephra frequency and thickness. Bold lines represent approximately 50 year running average superimposed on more highly resolved data. Vertical red lines indicate periods of transition in the core at 10.3 ka, 8.0 ka, 5.5 ka, 4.2 ka, and 1.1 ka.

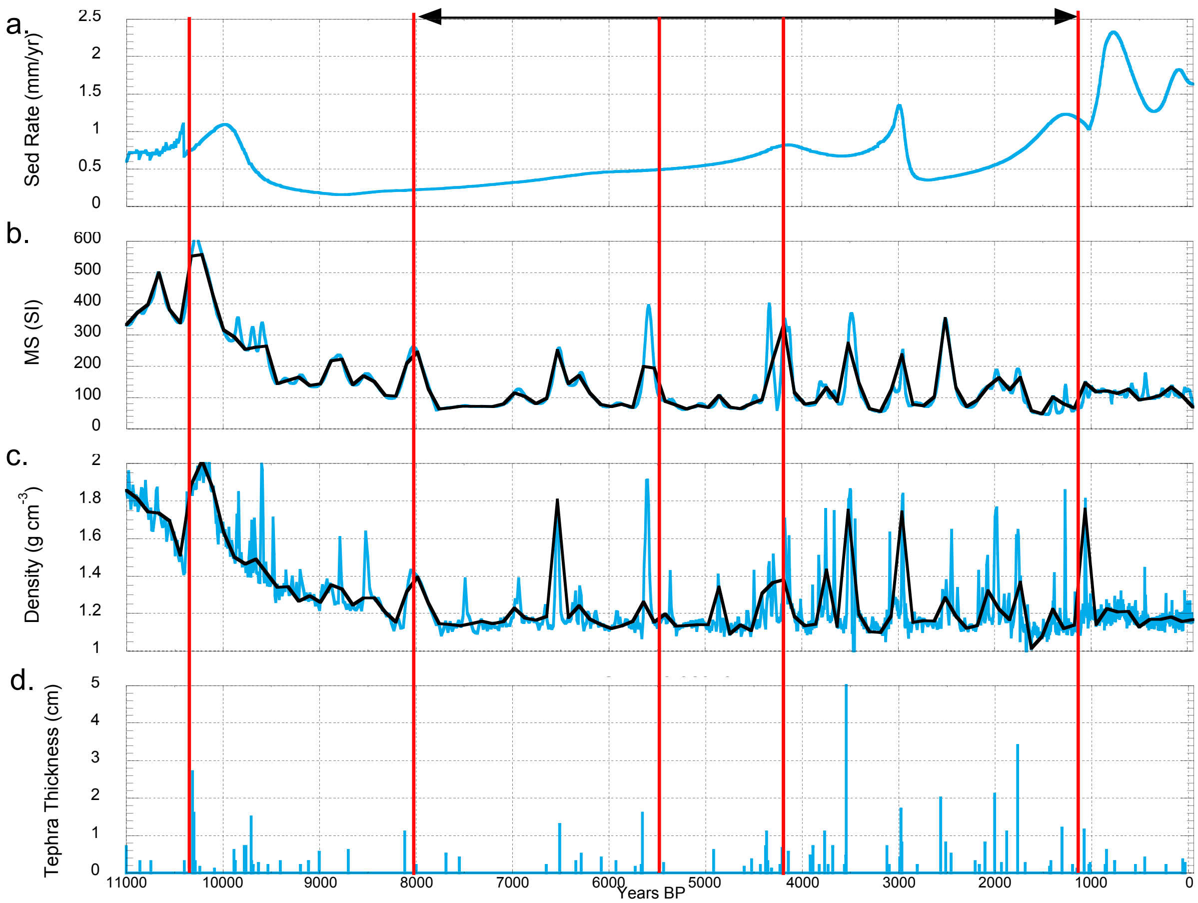

4.4.2 Physical Properties

The physical characteristics of lake sediment (density, MS, and sediment accumulation rate) predominantly reflect products of terrestrial erosion entering the basin. Elevated values indicate an increased minerogenic flux into the lake and/or greater catchment erosion. As the Vestra Gíslholtsvatn catchment is small and nonglaciated there is little erosion of fresh bedrock. Peaks in MS and density typically reflect the input of tephra rather than terrestrial erosion. Within the sediment cores most tephra horizons are <1 cm thick (Fig. 4.6a) and were deposited within 250 years of other tephra layers (Fig. 4.6b).

Figure 4.6 a. Histogram of tephra layer thickness for 11 ka to present; b. Histogram of tephra layer frequency for 11 ka to present

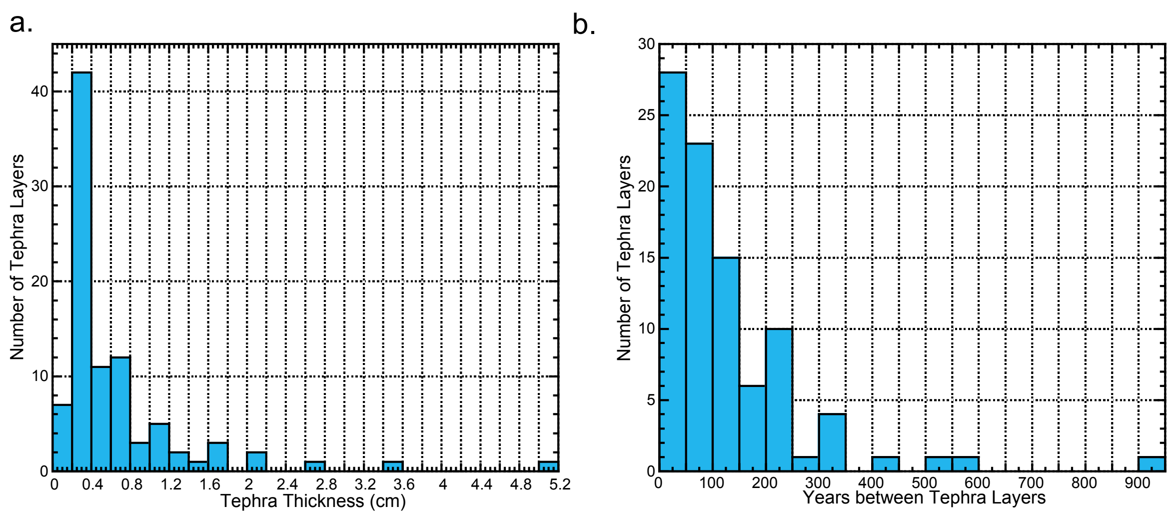

The structures of MS and density down-core variations are well correlated for the Holocene (Fig. 4.5, 4.7a) with peaks in both proxies commonly associated with tephra layers (Fig. 4.5). Values of MS and density are highest in the early Holocene decreasing until reaching a quasi-stable background state at ~8.3 ka. Perturbations in density are fairly short-lived generally lasting <100 years indicating a relatively robust lacustrine ecosystem capable of fast recovery from disturbance propagated by tephra fall in the catchment. Tephra horizons >1 cm in thickness coincide with the largest deviations from background conditions while abrupt increases in sediment accumulation rate correlate to both clusters of tephra horizons and thick tephra deposition events.

4.4.3 Organic Properties

BSi is an amorphous form of silica biogenically precipitated into the water column by a variety of aquatic organisms. In Icelandic lakes BSi dominantly come from diatoms, algae made of opal ($SiO_2 + nH_2O$) frustules (Conley, 2002). Plant and diatom growth depends heavily on the duration of the ice-free season and water temperature. Thus, lake productivity is a function of climate, nutrient availability, wind strength (which affects nutrient availability through upwelling), and water column characteristics (turbidity, pH, etc.) and BSi is used as a proxy for within lake primary productivity and springtime temperatures (Geirsdóttir et al., 2009a). The %BSi preserved in the sedimentary record depends on the mass of BSi produced, the fraction of BSi dissolved in the water column before burial, and the flux of non-diatom materials (primarily minerogenic sediments) into the lake.

A strong relationship between preservation potential and sediment accumulation rate exists so that when sedimentation rates are low diatom frustules remain in the water column longer and are more prone to dissolution (Ryves et al., 2006). Because of this, BSi can be treated as a first order approximation for primary productivity when sediment accumulation rate is relatively constant. We evaluate the dependency of %BSi on sediment accumulation rate between 8.3 ka and Settlement (~1.1 ka) (Fig. 4.7b) and

Figure 4.7 Bi-plot relationships between various physical and biological proxies between 8.4 ka and settlement. A. Density vs. MS; b. %BSi vs. sediment accumulation rate; c. MS vs. %BSi; d. Density vs. MS; e. %BSi vs. %TOC; f. Sediment accumulation rate vs. %TOC; g. MS vs. %TOC; h. Density vs. %TOC; i. C:N vs. %TOC; j. $\delta^{13}C$ vs. %TOC; k. C:N vs. $\delta^{13}C$; l. Sediment accumulation rate vs. $\delta^{15}N$

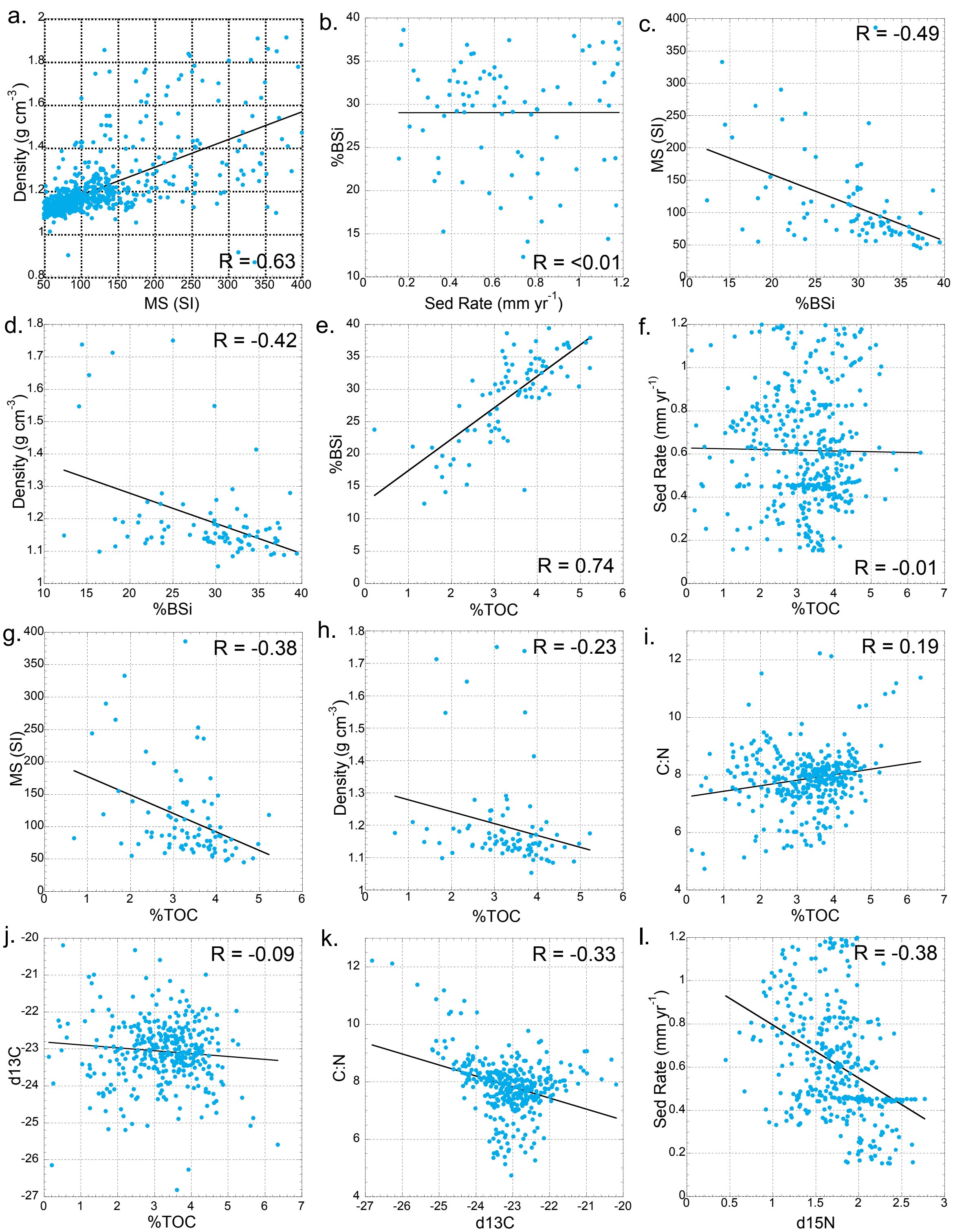

attain no correlation (R = <0.01), indicating sedimentation rate has no significant influence on diatom abundance during this time interval. However, bi-plots of MS and density with %BSi show strong negative correlations (Fig. 4.7c, d) signifying tephra deposition has some control on the diatom abundance preserved in the sediment record.

The proportion of carbon (%C) and nitrogen (%N) found in lake sediments is dependent on lacustrine primary productivity, erosion of terrestrial vegetation and soil, digenesis, and sedimentation rate (Meyers, 1997; Geirsdóttir et al., 2009a; Lennox et al., 2010; Larsen et al., 2012). As there is no primary calcium carbonate ($CaCO_3$) in the volcanic bedrock of Iceland (basalt) it can be assumed that %C represents exclusively organic carbon (total organic carbon, %TOC). %TOC, like %BSi is commonly considered a measure of primary productivity and thus a function of the same climate parameters. As %TOC has a strong positive correlation with %BSi (R = 0.74) (Fig. 4.7e) and no correlation with sediment accumulation rate (R = 0.01) (Fig. 4.7f) between 8.3 ka and Settlement, the proxy primarily represents changes in lacustrine primary productivity. However, negative correlations between %TOC and the physical proxies (Fig. 4.7g, h) indicate a relationship between tephra deposition and the abundance of carbon preserved in the lake sediment. %TOC has weak correlations with C:N and $\delta^{13}C$ (Fig. 4.7i, j) during this time period further supporting limited terrestrial input into the basin and an aquatically dominated ecosystem.

The contribution of terrestrial vegetation in lake sediment can be addressed using the ratio of carbon to nitrogen (C:N). C:N is an independent proxy determined by the relative proportion of terrestrial OM to aquatic OM in bulk sediment. Aquatic plants typically have a C:N value between 4 and 10, whereas terrestrial C:N is higher and more variable with most samples between 10 and 50 (Meyers, 1997; Meyers and Teranes, 2001). In Vestra Gíslholtsvatn the proportion of carbon and nitrogen in organic residuals is relatively constant once OM properties attain quasi-stabilization at ~8.4 ka indicating a predominant signal of aquatic biomass in sediment OM (Fig. 4.8b). The ratio of stable carbon isotopes ($\delta^{13}C$) is another independent proxy reflecting OM source. $\delta^{13}C$ is a proxy for carbon cycling as values are forced by the rate of dissolved inorganic carbon (DIC) uptake during photosynthesis and the DIC source (i.e. atmosphere, bedrock carbon, terrestrial vegetation, etc.) (Håkansson, 1985; Meyers and Teranes, 2001). Warmer temperatures increase the rate of DIC uptake and as there is preferential uptake of the lighter carbon isotope ^{12}C, $\delta^{13}C$ increases. Additionally, if the OM source changes, the $\delta^{13}C$ preserved in sediment will shift in the direction of the new source. As the volcanic bedrock (basalt) around Vestra Gíslholtsvatn is C poor, trends in $\delta^{13}C$ relate to either the rate of DIC uptake, which is influenced by air and water temperatures above the lake thermocline or the $\delta^{13}C$ of the OM source (Turney, 1999; Meyers and Teranes 2001). Between 8.3 ka and Settlement, $\delta^{13}C$ and C:N have a moderately strong negative correlation (R = -0.33) (Fig. 4.7k) implying $\delta^{13}C$ should be interpreted as a proxy for OM source rather than changes in DIC uptake.

Stable nitrogen isotopes, $\delta^{15}N$, provide a signal of ecosystem structure within lakes and their catchments representing the prevalence of littoral communities (Talbot and Laerdal, 2000; Lennox et al., 2010). Abundant littoral wetland vegetation increases the rate of dissolved inorganic nitrogen (DIN) uptake via the intensification of nitrification and denitrification in near shore sediment and soil indicating healthy communities of soil and sediment microbes and vegetation (Kling et al. 1992; Lennox et al. 2010; Janbu et al., 2011). Climate conditions less supportive of littoral ecosystems and/or increased soil erosion would thus decrease values of $\delta^{15}N$. $\delta^{15}N$ has a moderately significant negative correlation (R = -0.38) (Fig. 5.7l) with sediment accumulation rate between 8.4 ka and Settlement supporting a connection between terrestrial landscape stability and the success of soil microbial communities.

The small, low gradient catchment of Vestra Gíslholtsvatn provides relatively few erosional products to the lake basin so nearly all carbon entering the sediment is authigenic in origin (%TOC and C:N between 8.4 ka and settlement are 3.2 ± 1.0%; n = 417 and 7.9 ± 1.0; n = 364 respectively). Consequently, lacustrine primary productivity has a significant influence on the composition of DIC in the lake. We argue that the dominant control on OM $\delta^{13}C$ is related to changes in lacustrine primary productivity with terrestrial carbon affecting the signal only in periods of low within lake productivity. Terrestrial plants ($\delta^{13}C$: ~-26‰), aquatic algae ($\delta^{13}C$: ~-30‰) and aquatic plants ($\delta^{13}C$: -20‰ to -13‰) represent three distinct OM sources in Icelandic lakes (e.g. Meyers and Lallier-Veges, 1999; Wang and Wooller, 2006; Langdon et al., 2010). Vestra Gíslholtsvatn has a large littoral zone (Fig. 4.2c) where macrophytes are likely to grow. Thus, influence of the relatively heavy $\delta^{13}C$ of macrophytes on bulk sediment $\delta^{13}C$ is much greater than in deeper ultraoligotrophic lakes in Iceland (e.g. Haukadalsvatn [Geirsdóttir et al., 2013]) where terrestrial OM and phytoplankton dominate the signal. We interpret more negative $\delta^{13}C$ as a reflection of more allochtonous terrestrial plant sources while less negative $\delta^{13}C$ indicates increased contributions from autochthonous aquatic vegetation. Our interpretation is supported by low $\delta^{13}C$ typically coinciding with high C:N and low %BSi (Fig. 4.8).

All OM proxies achieve their Holocene background value by ~8.4 ka remaining relatively consistent until ~5.5 ka where large centennial scale changes are coupled with increased variability in all proxies that persists until ~1.1 ka. At ~1.1 ka %BSi, $\delta^{13}C$ and %TOC abruptly decrease while C:N increases. Proxies during the last 1000 years of the Holocene have a unique structure that corresponds to rapidly changing sediment accumulation rate indicating ecosystem modifications and landscape destabilization associated with Settlement (1078±2 BP). For this reason we isolate the data between 8.3 ka and Settlement for Principle Component Analysis (PCA) as it represents climate driven variability without an anthropogenic overprint.

4.4.4 Chironomid Paleotemperature Reconstruction

Chironomid temperature reconstructions support a cool early Holocene with gradual warming beginning after 10.3 ka reaching peak warmth by ~5.5 ka (Fig. 4.8f). After ~5.5 ka average July temperature is relatively warm with no dramatic deviations from the range of uncertainty. Low resolution in the midge data set likely masks Holocene climate variability that is better observed in the OM proxy records.

Figure 4.8 Time series data of OM proxies. a. %TOC; b. C:N; c. $\delta^{13}C$; d. $\delta^{15}N$; e. %BSi; f. July air temperature inferred from chironomid assemblages based upon a WA-PLS transfer function; g. Tephra layer thickness and frequency. Black lines represent an approximately 50 year smoothing overlaying higher resolution data. Vertical red lines indicate periods of transition in the core at 10.3 ka, 8.0 ka, 5.5 ka, 4.2 ka, and 1.1 ka.

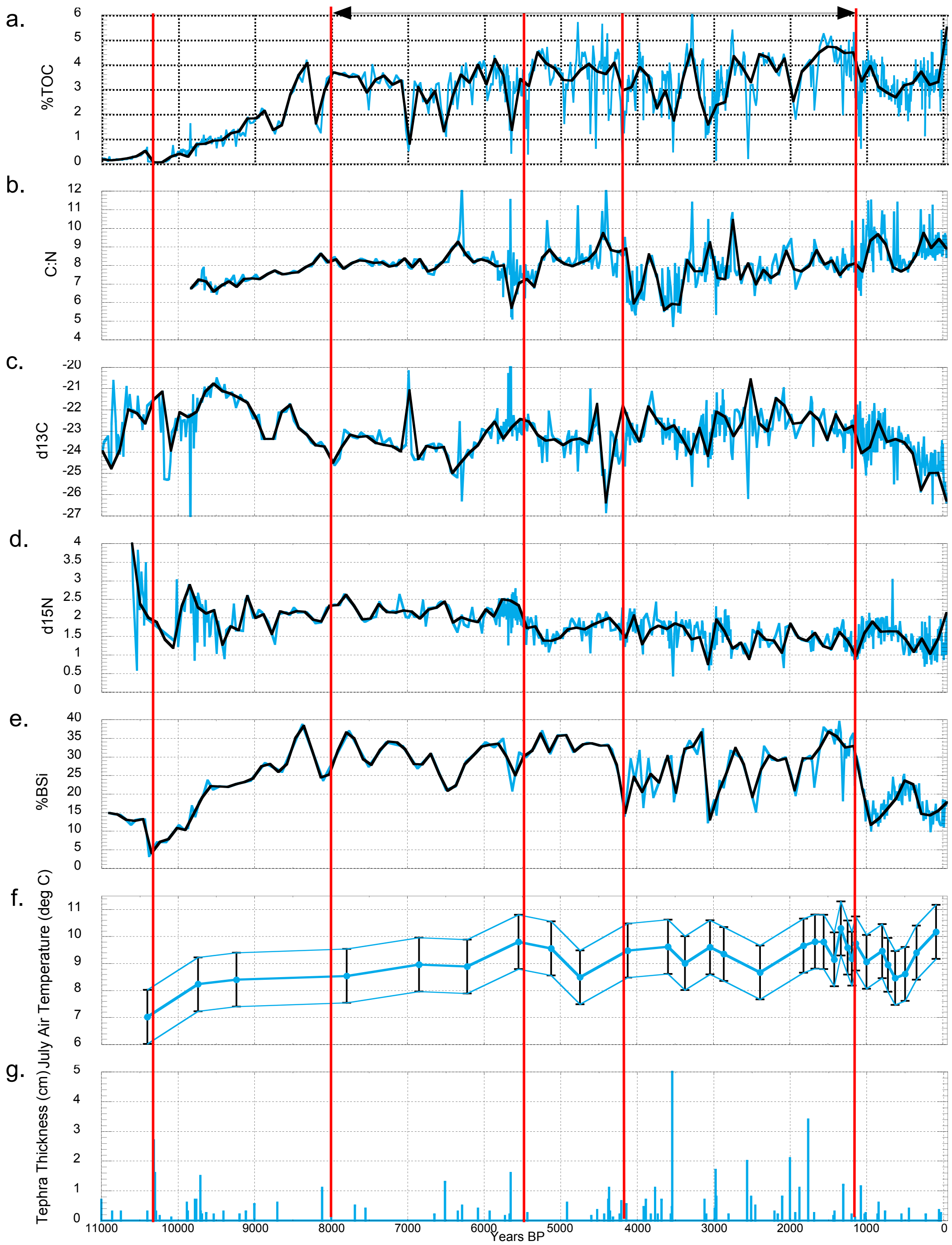

4.5 A Multi-proxy Compilation of Climate Change: 8.3 ka to Settlement (1078±2 BP)

4.5.1 Principle Component Analysis (PCA) of Resampled Proxy Time Series

To compare all OM and physical proxies from Vestra Gíslholtsvatn over the climate dominated portion of the Holocene we resampled %TOC, C:N, %BSi, $\delta^{13}C$, $\delta^{15}N$, MS and density using the Analyseries software (Paillard et al., 1996). As %BSi has the lowest temporal resolution we resampled all proxies between ~8.3 ka and ~1.1 ka at 20 year increments. These data were then used in a PCA. PCA is useful for identifying major gradients within complex multivariate datasets by reducing the datasets to latent variables through an indirect ordination technique (Janžekovič and Novak, 2012). As there are roughly linear relationships between variables (Fig. 4.5, 4.8) it is appropriate to perform a PCA (McCune and Grace, 2002).

PCA was performed using R, with each dataset scaled to unit variance. PC (Principle Component) 1 accounted for 36.3% of the variation in the data while PC 2 represented 21.4% of the variance (Table 4.2). As the other components each accounted for less than 15% of the variance they were disregarded. PC 1 in the PCA bi-plot represents the minerogenic influx and its influence on primary productivity while PC 2 indicates ecosystem structure and OM source (Fig. 4.9). Discrete data clouds distinguish periods identified in the time series with shifts along PC 2 between ~8.3 ka and Settlement separated by a transition at 5.5 ka (Fig. 4.10). Tephra disturbances also plot in separate clouds indicating unique ecosystem perturbations from tephra fall events.

Table 4.2 PCA summary and component loadings for VGHV multi-proxy record between 8.3 ka and settlement (1.1 ka)

	Comp 1	**Comp 2**	**Comp 3**	**Comp 4**	**Comp 5**	**Comp 6**	**Comp 7**
Standard Deviation	1.59	1.23	1.02	0.87	0.74	0.56	0.54
Proportion of Variance	0.363	0.214	0.149	0.108	0.079	0.045	0.041
Cumulative Proportion	0.363	0.577	0.727	0.835	0.914	0.959	1
Loadings							
%TOC	-0.454		-0.289	0.582	0.248	0.555	
C:N	-0.147	-0.497	-0.583	-0.15	-0.597		-0.103
%BSi	-0.499	-0.139	0.201	0.421		-0.692	-0.167
$\delta^{13}C$		0.069		0.165	-0.661	0.12	-0.194
$\delta^{15}N$		-0.494	0.684	0.189	-0.29	0.397	
MS	0.523		-0.178	0.333	0.163		-0.739
Density	0.491		-0.166	0.536	-0.168	-0.194	0.612

Component scores were used to produce succinct time series with PC 1 synthesizing physical proxies and OM productivity and PC 2 integrating biological proxies representative of ecosystem structure and OM source (Fig. 4.10). PC 1 is most significantly influenced by tephra perturbations while PC 2 indicates millennial scale changes consistent with non-linear climate evolution.

Figure 4.9 PCA bi-plot for resampled data between ~8.3 ka and ~1.1ka. Data clouds indicate transitions in ecosystem structure through the HTM and Neoglaciation and variability attributable to tephra disturbance. >90% of the appropriate data falls within the appropriate cluster.

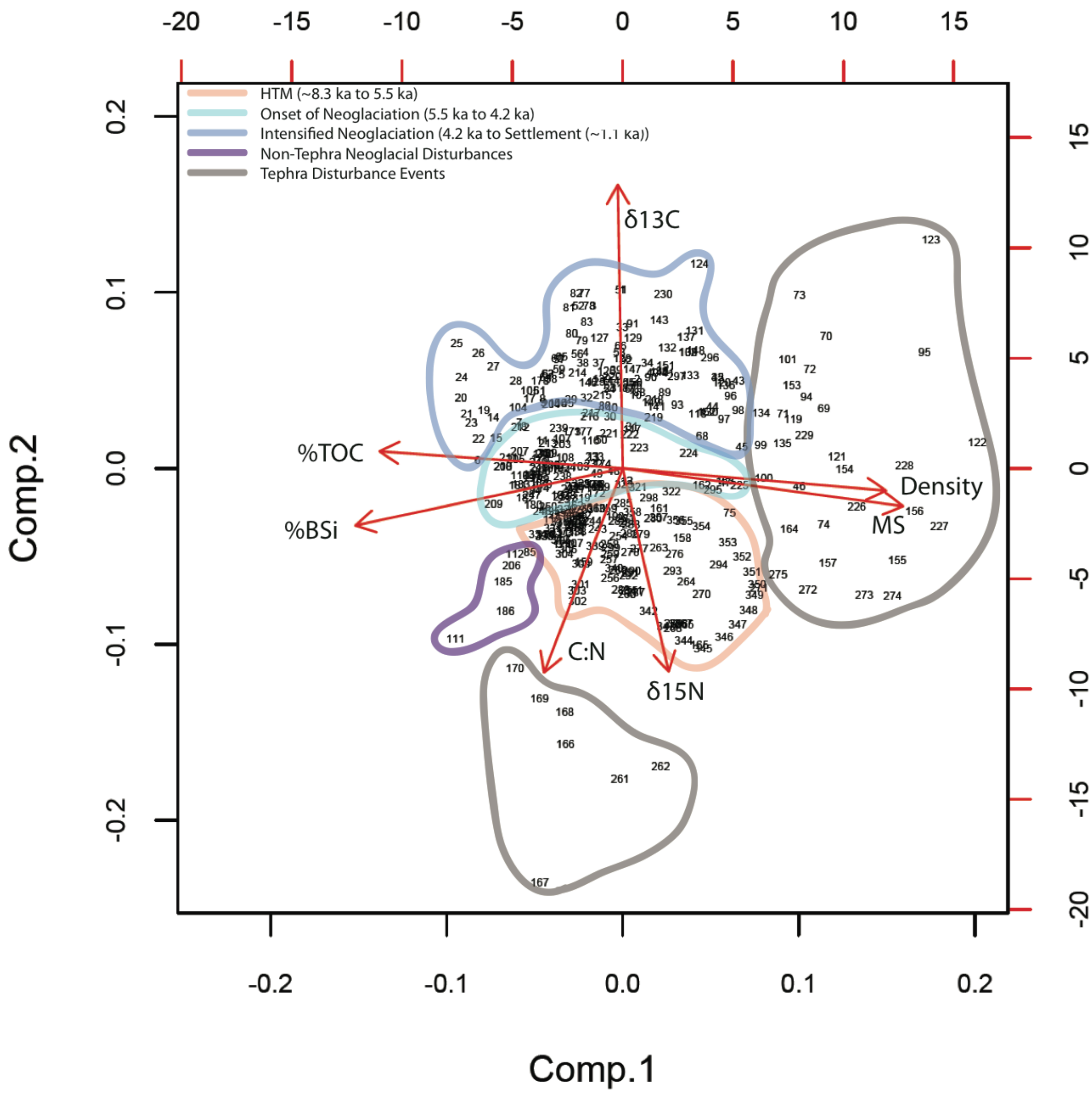

4.6 Climate and Ecosystem Reconstruction

4.6.1 Holocene climate and ecosystem development at Vestra Gíslholtsvatn

Multiple physical and OM proxies from Vestra Gíslholtsvatn sediment are used to reconstruct Holocene environmental conditions in south Iceland. As the lake catchment is nonglaciated the record reflects ecosystem development, which is closely tied to climate (e.g. Hallsdóttir, 1995; Hallsdóttir and Caseldine, 2005). General climate reconstructions for western and central Iceland have indicated synchronized non-linear responses to a simple insolation forcing (Geirsdóttir et al., 2013). We observe similar transitory periods in Vestra Gíslholtsvatn although with less dramatic changes suggesting that the climate of southern Iceland is more stable than its northwest and central counterparts because there is less variability in the surface current that flows along the south Icelandic coast (e.g. Malmberg and Kristmannsson, 1992).

4.6.2 Pre 10.3 ka: Transition from Deglaciation and Deposition of the Saksunarvatn Tephra

Prior to the eruption and deposition of the Saksunarvatn tephra deglacial sediment dominated the lacustrine system with little, albeit increasing primary productivity in the lake and catchment. In Vestra Gíslholtsvatn the Saksunarvatn tephra is comprised of three basaltic layers (see Fig. 4.3). These match horizons identified by Jóhannsdóttir (2007) to have been deposited between ~10.2 ka and ~10.4 ka and of the same geochemical composition as the Saksunarvatn tephra identified in the Faroe Islands (Mangerud et al, 1986). Deposition of this thick layer of tephra reduced the minimal primary productivity in and around the lake to near zero values (Fig. 4.8).

Before 10.3 ka $\delta^{13}C$ values suggest increasing aquatic primary productivity. The large decrease in $\delta^{13}C$ following the Saksunarvatn tephra can be attributed to a decrease in lacustrine primary productivity coupled with an influx of terrestrial carbon eroded from the catchment. Sedimentation rate is modeled to be relatively high due to elevated MS and density. Midge inferred summer temperature indicates a Holocene low after the Saksunarvatn tephra.

4.6.3 10.3 ka – 8.0 ka: Early Holocene Stabilization and Lake Ontogeny

The Saksunarvatn tephra horizon is followed by Holocene peaks in MS and density that likely correspond to an abrupt increase in sediment accumulation rate. Between ~10.0 ka and 9.5 ka sediment accumulation rate decreases to a Holocene low of ~0.2 mm a^{-1} while %BSi, $\delta^{13}C$, and temperature abruptly increase indicating some primary productivity within the lake ecosystem. However, %TOC increases more gradually in anticorrelation with MS and density. We interpret the interval between 10.3 ka and 8.0 ka to be a period of landscape and ecosystem stabilization within the lake and in its catchment as indicated by %BSi, %TOC, and $\delta^{15}N$. Relatively warm summer temperatures likely contributed to landscape and ecosystem development increasing primary productivity as the lake attained quasi-equilibrium after approximately two millennia. Landscape stabilization at this time was surprisingly slow and is likely explained by the distribution of residual inland ice in southern Iceland associated with deglaciation.

Physical and OM proxies do not reach a quasi-stable background state until ~8.0 ka. Abrupt, short-lived decreases in %TOC, $\delta^{13}C$, and %BSi coupled with increases in physical proxies shortly after establishment of environmental stability are attributed to the 8.2 ka cold event (e.g. Alley and Ágústsdóttir, 2005; Quillmann et al., 2012). Our record suggests these changes persisted for ~200 years, with negative deviations in %TOC, our highest resolution OM proxy, from 8260 BP to 8060 BP (Fig. 4.8). The expected signal of the 8.2 ka event in physical proxies is convoluted by a tephra deposition event from Hekla at ~8.1 ka (Fig. 4.8g). Low-resolution chironomid sampling is likely responsible for not capturing the 8.2 ka cold event.

4.6.4 8.0 ka – 5.5 ka: Holocene Thermal Maximum

PCA component score time series were used to interpret Holocene climate evolution between 8.0 ka and settlement. The Holocene Thermal Maximum (HTM) at Vestra Gíslholtsvatn is indicated by quasi-equilibrium of proxies following deposition of the Saksunarvatn tephra. After a mild 8.2 ka event %TOC and %BSi return to previous values by ~8.0 ka and all proxies suggest a productive lacustrine ecosystem and limited catchment erosion under a warm, stable climate. Decreasing values of PC 2 and a peak in PC 1 further support this assertion (4.10a, b). Values of $\delta^{15}N$ are relatively high and stable throughout the HTM while $\delta^{13}C$ is lower and %BSi higher than observations during lake formation supporting greater diatom productivity in addition to abundant communities of littoral aquatic vegetation. Aquatic productivity reaches a peak ~5.6 ka indicated by low C:N and heavy $\delta^{13}C$ and $\delta^{15}N$ (Fig. 4.8).

Midge-inferred summer temperatures support warmth throughout the HTM with heightened warming beginning ~6.1 ka and persisting to ~5.5 ka. Sediment accumulation rates were at a Holocene low in the early HTM, gradually increasing to

Figure 4.10 Time series of PCA component scores for resampled data. a. Component 1; b. Component 2; c. Tephra thickness and frequency between 8.3 ka and ~1.1 ka. Vertical red lines demarcate periods of transition in the proxy record at 5.5 ka and 4.2 ka.

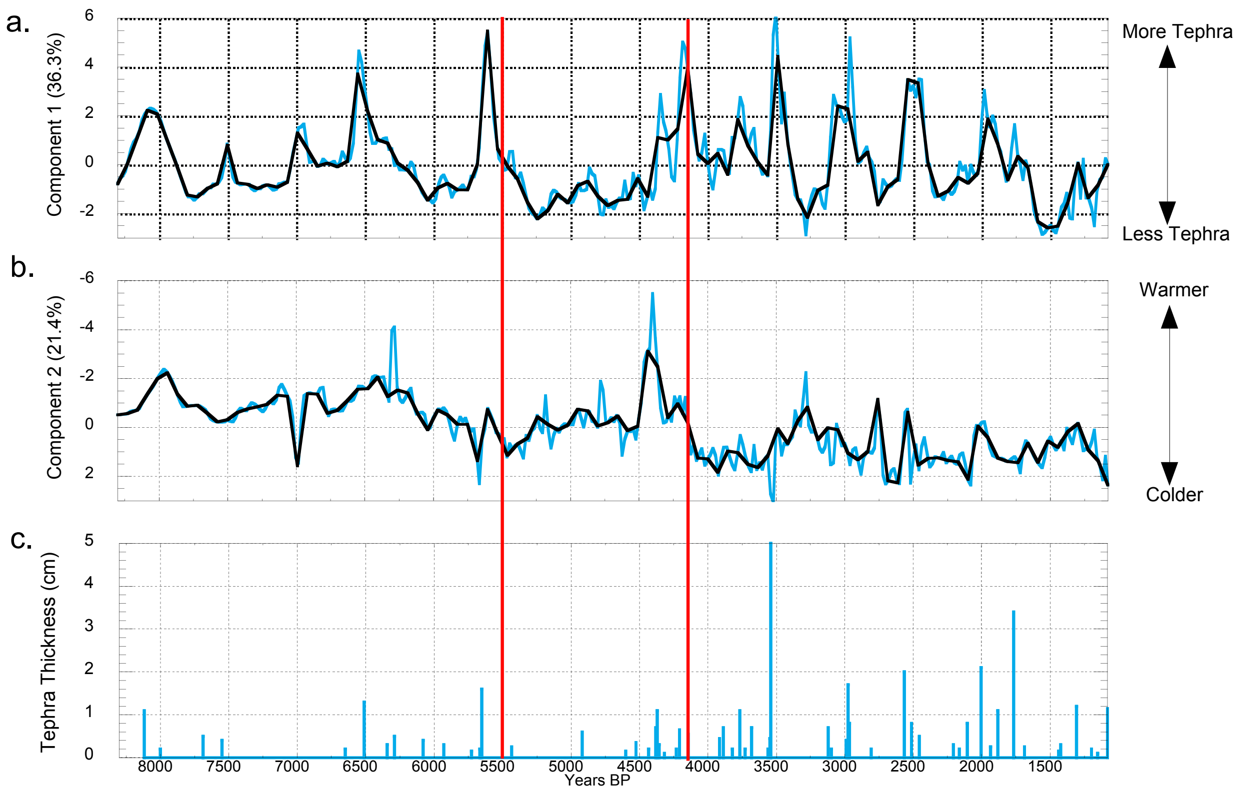

~0.5 mm a^{-1} by ~6.0 ka (Fig. 4.5). 7.5 ka to 6.5 ka was a time of few large volcanic eruptions. However, a cluster of tephra producing eruptions between 6.5 ka and 5.5 ka is associated with peaks in PC 1 and a gradual shift in PC 2 (Fig. 4.10). These signals support increased variability in the flux of minerogenic material entering the basin negatively influencing the signal of lacustrine primary productivity and a gradual shift in ecosystem communities during the last millennium of the HTM (Fig. 4.10).

4.6.5 5.5 ka: Onset of Neoglaciation

At ~5.5 ka %TOC, C:N, and sedimentation rate increase while $\delta^{13}C$ and $\delta^{15}N$ decrease for ~500 years indicating a cooling climate coupled with changes in ecosystem structure at Vestra Gíslholtsvatn (Fig. 4.5, 4.8). 5.5 ka marks the onset of an irreversible transition to a new quasi-equilibrium in both PC 1 and PC 2 (Fig. 4.9, 4.10). ~5 ka to 4.2 ka is a time in the proxy record dominated by volcanic activity. Biological proxies indicate numerous negative deviations in %TOC and $\delta^{13}C$ coupled with positive deviations in C:N, changes signifying increased erosion of terrestrial carbon and reduced aquatic productivity due to a combination of cooler temperatures and increased landscape disturbance from tephra remobilization. Midge summer temperature reconstructions indicate a possible decrease in summer temperatures supporting the onset of Neoglaciation after ~5.5 ka. Data in the PCA bi-plot permanently transitions along PC 2 from the HTM cluster to a new discrete cluster further supporting initiation of an irreversible change in ecosystem configuration associated with the onset of Neoglaciation in Iceland (Fig. 4.9).

4.6.6 4.2 ka – 1.1 ka: Intensification of Neoglaciation

Between ~4.2 ka and 1.1 ka OM proxies indicate periods of lake ecosystem disturbance occurring on decadal to centennial time scales. This variability is likely related to persistent cooling and numerous thick tephra fall events in the catchment. At ~4.3 ka sediment accumulation rate increases in conjunction with peaks in MS and density and a dense cluster of eruptions including the significant rhyolitic horizon, H4 (~4.2 ka). H4 (~4.2 ka) is an extensive rhyolitic tephra horizon coinciding with intensified Neoglaciation at Vestra Gíslholtsvatn. Our proxy record indicates dramatic short-lived decreases in %TOC, $\delta^{13}C$, and %BSi coupled with increases in C:N, MS, and density immediately after ~4.2 ka (Fig. 4.5, 4.8). Additionally component scores show an irreversible shift in PC 2 and increased variability in PC 1 (Fig. 4.10) indicative of a persistent change to a cooler and more variable climate state. This is supported by the transition into a discrete post-4.2 ka cluster on the PCA bi-plot that persists until at least Settlement (Fig. 4.9).

The high frequency of tephra deposition during the Neoglacial created numerous short-lived peaks in MS and density. However, physical proxies return to pre-tephra values within decades to centuries (Fig. 4.5). OM proxies prior to 4.2 ka and 1.1 ka show decreased %TOC and %BSi associated with nearly all substantial tephra horizons. These declines are often coupled with a shorter-lived depression of $\delta^{15}N$ and $\delta^{13}C$ and briefly elevated C:N. Significant changes in C:N are less common, supporting out interpretation that alterations to lacustrine ecosystem structure are represented in the proxy record rather than persistent catchment erosion. Notable thick tephra horizons deposited in Vestra Gíslholtsvatn during this time period include KN (~3.5 ka), KE (~3.0 ka), and H-A (~2.5 ka) (Fig. 4.3).

4.6.7 1.1 ka to Present: Anthropogenic Overprint of the Last Millennia

Between 1.1 ka and present physical proxies exhibit little variability and there is only one tephra layer >1 cm thick observed in the lake record. Despite this apparent stability in the physical proxy record OM proxies indicate significant changes (Fig. 4.5, 4.8). Holocene warmth in the chironomid record is succeeded by substantial cooling noted by a ~200 year peak in C:N coupled with declines in $\delta^{13}C$, and $\delta^{15}N$. Decreases in %TOC and %BSi are likely attributable to a dilution effect from an increase in sediment accumulation rate (Fig. 4.8). The initiation of this cool period is confounded by the settlement of Iceland (1078±2 BP), which is marked in the sediment record by the Settlement tephra (Vö) (Fig. 4.3). Ecosystem instability continued following Settlement with brief landscape recovery at ~1.0 ka suggesting warmth related to the Medieval Warm Period (MWP). However, intense landscape destabilization at ~0.9 ka, most likely brought on by agricultural practices convolutes the climate signal. Structure in the last 1000 years of the OM proxy record supports lake ecosystem stability between 0.7 ka and ~0.3 ka, with low values of C:N, steady $\delta^{13}C$, and relatively elevated $\delta^{15}N$ and %BSi. At ~0.3 ka proxies indicate lacustrine ecosystem instability that persists for the remainder of the Holocene with increasing values of C:N and %TOC, but decreasing %BSi and $\delta^{13}C$ (Fig. 4.5, 4.8).

Human settlement of Iceland at ~1.1 ka contributed to large ecosystem changes in the Vestra Gíslholtsvatn catchment. Settlers removed almost all trees near the vicinity of farms and woodlands were unable to reestablish due to the grazing of sheep; grass heath, dwarf shrub, and mires expanded at their expense (Hallsdóttir and Caseldine, 2005). Farming was practiced within the lake catchment so the above processes contributed to an abrupt increase in catchment erosion that persisted for centuries. Sediment accumulation rate reaches its Holocene maximum during the last millennia, peaking at 2.4 mm a^{-1} at 0.8 ka approximately 250 years after settlement. The lack of variability in physical proxies supports the input of organic rich soil and terrestrial vegetation rather than minerogenic eroded bedrock or tephra (Fig. 4.5).

Sustained depression of %BSi and %TOC in the late Holocene is related to dilution attributable to the dramatic increase in sedimentation rate. However, the structure within the reduced proportions is telling of complicated changes. Following Settlement, $\delta^{13}C$ has three stepwise decreases of 1.5‰ at 0.9 ka, 0.3 ka and in the last century of the Holocene. These are likely attributable to an increase in the terrestrial component preserved in the lake sediment due to increased soil erosion from intensified utilization of scrub vegetation and overgrazing (Dugmore and Buckland, 1991; Hallsdóttir and Caseldine, 2005; Arnalds, 2008b). Changes in $\delta^{13}C$ are closely coupled with deviations in other OM proxies with transient stabilization between 0.8 ka and 0.3 ka supporting quasi-equilibrium of the catchment and lakes ecosystems following the initial disturbance from settlement (Fig. 4.8).

4.7 Discussion and Conclusions

Much of the short-lived Holocene variability at Vestra Gíslholtsvatn can be attributed to tephra layers in the sediment core as %TOC and %BSi abruptly decreases after nearly all tephra horizons returning to previous values within decades. This indicates dilution and/or decreased primary productivity immediately after all tephra deposition events. The climate signal is best represented in the data between 8.0 ka and 1.1 ka. Longer-lived deviations from the quasi-background state at 5.5 ka and 4.2 ka reflect irreversible shifts in proxy records related to Holocene climate evolution in Iceland (Fig. 4.10). Time periods used in this study were selected using the multi-proxy and PCA time series (Fig. 4.5, 4.8, 4.10). Designations at 10.3 ka, 8.0 ka, and 1.1 ka were chosen using obvious changes in ecosystem structure, function and development associated with deposition of the Saksunarvatn tephra, the warm and stable conditions of the HTM, and settlement of Iceland, respectively. 5.5 ka and 4.2 ka were selected using discrete clusters on the PCA bi-plot and the PC 1 and PC 2 time series as they are periods when component scores achieved new quasi-equilibriums indicating irreversible transitions in lacustrine ecosystem structure and function (Fig. 4.9, 4.10).

The ontogeny of Vestra Gíslholtsvatn began after deglaciation in Iceland, only to be reset by deposition of the Saksunarvatn tephra as indicated by OM proxies. This signal is likely related to dilution from the tephra fall, continued erosion of remobilized ash and intense ecosystem destabilization. It has been previously shown that deposition of the Saksunarvatn tephra had drastic influence on vegetational succession around Torfadalsvatn, a lake in Northern Iceland (Björck et al., 1992) and that the tephra fall was followed by decades to centuries of landscape instability (Hallsdóttir and Caseldine, 2005).

After the Saksunarvatn tephra layers development of a successful ecosystem was relatively slow, taking ~2000 years. Decreasing trends of physical proxies coupled with increasing values of %TOC and %BSi between 10.3 ka and 8.4 ka suggest catchment stabilization occurred concurrently with increasing lacustrine primary productivity. The sluggish development of Vestra Gíslholtsvatn is probably associated with gradual soil development in the catchment and the build up of limiting nutrients in the lake. Relatively small and transient changes in proxies between ~8.3 ka and 8.0 ka support a mild 8.2 ka cold event, less significant than what is observed in western and central Iceland (e.g. Larsen et al., 2012; Geirsdóttir et al., 2013). However, low data resolution at this time period also hinders the observation of short-lived climate events. Following the 8.2 ka cold, event a warm and stable HTM persisted at Vestra Gíslholtsvatn from 8.0 ka to ~5.5 ka, timing similar to what is observed in other Icelandic lakes (Caseldine et al., 2006; Larsen et al., 2012; Geirsdóttir et al., 2013).

Pollen studies indicate the landscape surrounding Vestra Gíslholtsvatn has been well vegetated since at least ~5.6 ka (Hallsdóttir and Caseldine, 2005) explaining the relatively low sedimentation rate and low minerogenic contribution to lake sediment prior to and at this time period. However, the later half of the Holocene is notable in the pollen record as changes in climatic conditions associated with the onset of Neoglaciation contributed to a retrogressive succession towards more open birch forests and widespread mires and heathland across south Iceland (Hallsdóttir and Caseldine, 2005). Other Holocene lake records indicate the onset of Neoglaciation at ~5.5 ka with incremental cooling until amplification at ~4.2 ka (e.g. Geirsdóttir et al., 2013). The Vestra Gíslholtsvatn record observes a permanent shift in OM proxies most notably $\delta^{13}C$, $\delta^{15}N$, and C:N, and PC 2 at ~5.5 ka indicating a transition in ecosystem structure and function due to the Neoglacial climate state.

Neoglaciation is notable in the multi-proxy record with increased centennial scale variability related to tephra disturbances and changes in the climate system. Abrupt changes in the state of the system at ~4.2 ka indicated by a discrete cluster in the PCA bi-plot (Fig. 4.9), a permanent shift in PC 2, and increased variability in the PC 1 time series support intensification of Neoglaciation with a cooler and more variable climate in southern Iceland (Fig. 4.10). Other Icelandic lakes also produce an irreversible step-wise change in their multi-proxy records at ~4.2 ka indicative of more pronounced Neoglaciation (Larsen et al., 2012; Geirsdóttir et al., 2013). Another significance of the ~4.2 ka event is the widespread explosive rhyolitic eruption of Hekla depositing the H4 tephra. The event produced ~9 km^3 of tephra covering over 62,200 km^2 on land with at least 1 cm of vitric material (Larsen and Thorarinsson, 1977). Pollen records from Vestra Gíslholtsvatn following the H4 tephra layer indicate a decline in tree pollen and increased abundance of shrub and herb pollen (Hallsdóttir and Caseldine, 2005).

Using known tephra horizons as chronostratigraphic markers, Hallsdóttir and Caseldine (2005) analyzed pollen assemblages surrounding the tephra observing a birch pollen minimum before and after the KN tephra (~3.5 ka) interpreted to indicate a cooling climate in south and southwestern Iceland. Following the KE tephra (~2.9 ka) woodlands regenerated before diminishing again around the H-A tephra (~2.5 ka). These centennial scale changes in forest abundance reveal factors other than volcanic eruptions must have operated to reduce woodland cover, supporting our conclusion of Neoglacial climate variability in south Iceland.

A gradual increase in sediment accumulation rate suggests steady summer cooling in the Holocene. Raised values of sediment accumulation rate at 4.2 ka, 3.0 ka and 1.2 ka correspond to periods of enhanced tephra disturbance in the catchment. The abundance of tephra fall events in the sediment record further supports our assertion that the majority of minerogenic input into Vestra Gíslholtsvatn came from direct deposition and remobilization of tephra from the landscape. Throughout the Holocene, but most pronounced in the Neoglacial, OM proxies support two possible consequences of tephra fall in the lake basin; OM dilution and/or brief declines of lacustrine primary productivity. Decreased values of $\delta^{13}C$ following significant horizons suggest decreased landscape stability and erosion of terrestrial vegetation after substantial tephra fall events (Fig. 4.8). However, depressions of $\delta^{13}C$ are often shorter in length than deviations in %TOC and %BSi suggesting any influx of terrestrial OM was fleeting and increased sediment accumulation rate from the deposition of remobilized tephra dominated the signal. A transient decline in lake primary productivity immediately after tephra horizons is supported by short-lived declines in $\delta^{13}C$ and $\delta^{15}N$

and elevated C:N. This signal supports alteration of ecosystem structure due to a reduction in littoral communities after tephra fall events. Changes in $\delta^{13}C$, C:N, and $\delta^{15}N$ are often less persistent than deviations in %TOC, %BSi, MS and density supporting a longer period of increased sediment accumulation rate than decreased primary productivity. Hardardóttir (2001) observed continued deposition of remobilized tephra into Hestvatn, a lake within 10 km of Vestra Gíslholtsvatn, for many decades following the deposition of the KN (~3.5 ka) and H4 (~4.2 ka) tephra. This supports arguments for similar periods of elevated sedimentation within Vestra Gíslholtsvatn following explosive volcanic eruptions. For this reason we argue that transient increases in sediment accumulation rate coupled with shorter-lived decreases in lacustrine primary productivity produced variability in the multi-proxy record from Vestra Gíslholtsvatn following substantial tephra fall events.

Between 8.3 ka and Settlement (~1.1 ka) %BSi is interpreted as a dominant measure of primary productivity and an indicator of spring/summer temperature in Vestra Gíslholtsvatn (Fig. 4.8e) (Geirsdóttir et al., 2009a). However, the relationship between sediment accumulation rate, %BSi, and %TOC changes in the post-settlement interval as anthropogenic forcings override the signal. Significant centennial scale structure is observed in proxy signals from ~1.1 ka to present with changes attributable to both climate conditions and extensive land use following the settlement of Iceland. Elevated sediment accumulation rates after settlement are not coupled with increases in MS, density, or thick tephra layers indicating the erosion of organic rich soils. An increase in soil erosion and decline in aquatic productivity at ~0.3 ka can also be attributed to both climate and anthropogenic processes from intensification of the Little

Ice Age (LIA) (e.g. Larsen et al., 2011) and modern agricultural practices respectively (Fig. 4.5). The LIA is overshadowed by the signal of settlement making it difficult to precisely date the timing and duration of post-settlement climate events as represented in these lake sediments. A detailed study of the last 1500 years could help isolate and better explains the anthropogenic component in the last millennium of the proxy record.

At Vestra Gíslholtsvatn much of the short-term variability observed in the proxy record is associated with tephra deposition in the lake and catchment while centennial and millennial scale changes relate to climate. Lacustrine ontogeny dominates the first two thousand years of the proxy record between ~11.0 ka and 8.4 ka. The climate signal is most pronounced between 8.4 ka and 1.1 ka with the lake transitioning to an alternative quasi-stable ecosystem state at ~5.5 ka differentiating the HTM and Neoglaciation. The Neoglacial intensifies producing another irreversible change in ecosystem structure and function at 4.2 ka. Anthropogenic signals overprint the climate record following the settlement of Iceland at ~1.1 ka. In conclusion, when compared to other Icelandic lakes, OM and physical proxies in Vestra Gíslholtsvatn indicate less variability albeit similar timing of environmental changes during the Holocene (e.g. Caseldine et al., 2006; Larsen et al., 2011; 2012; Geirsdóttir et al., 2013).

CHAPTER 5: DECADAL TO MILLENNIAL LAKE AND CATCHMENT RESPONSES TO MAJOR TEPHRA FALLS IN ICELAND

Celene L. Christensen[1], Áslaug Geirsdóttir[2], Gifford H. Miller[1,2], Thorvaldur Thordarson[3], Darren J. Larsen[1,2]

1. INSTAAR and Department of Geological Sciences, University of Colorado at Boulder, Boulder, CO, USA

2. Institute of Earth Sciences, University of Iceland, Reykjavik, Iceland

3. School of GeoSciences, University of Edinburgh, Edinburgh, United Kingdom

5.1 Introduction

Tephra (clastic airborne volcanic glass) produced by explosive volcanic eruptions can be transported hundreds and sometimes thousands of kilometers downwind where it accumulates on the landscape. Air-fall tephra deposits are common in lake sediments in Iceland due to the abundance of active volcanic centers and frequent volcanism in the Holocene (Thordarson and Höskuldsson, 2008). For centuries tephra fall events have been noted at varying degrees to influence physical, chemical, and biological systems within depositional environments (e.g. Kirk, 1808; Forchhammer, 1822; Sharp, 1890; Larsen and Thorarinsson, 1977; Thorarinsson, 1979; Cook et al., 1981; Kennedy, 1981; Mack, 1981; del Moral and Grishin, 1999; Cronin et al., 2002; Long et al., 2011; Myers, 2011; Ayris and Delmelle, 2012). Frequent explosive volcanism in Iceland has resulted in widespread distribution of fine-grained tephra of common magma types across much of the island (Thordarson and Larsen, 2007; Thordarson and Höskuldsson, 2008). Although incomplete, most widespread tephra horizons have been geochemically characterized and mapped (e.g. Larsen and Thorarinsson, 1977; Thorarinsson, 1979; Róbertsdóttir et al., 1992; Larsen et al., 1999; Jóhannsdóttir, 2007; Óladóttir et al., 2008; Thordarson and Höskuldsson, 2008; Jagan, 2010; Lowe, 2011) indicating widespread tephra interaction with the depositional environment. Despite this longstanding observation, little work has been conducted on understanding the short- and long-term consequences associated with tephra disturbance on the Icelandic landscape.

Iceland sits in a thermally sensitive region of the northern North Atlantic, in an ideal location for high-resolution paleoenvironmental lake studies producing relatively high ratio of signal to noise. Iceland's maritime climate keeps the landmass relatively warm and wet with a strong regional climate gradient from the southwest to northeast, influenced by orography, latitude, and proximity of warm ocean currents. Additionally, our ability to produce well-dated lake sediment cores (e.g. Larsen et al., 2011; 2012; Geirsdóttir et al., 2009a; 2013) using tephrochronology, radiocarbon, and paleomagnetic secular variation (PSV) synchronization between lake and well dated marine sediment cores (e.g. Jóhannsdóttir et al., 2007; Jagan et al., 2010; Ólafsdóttir, 2010) make paleolimnology studies possible. Conspicuous tephra horizons allow us to identify time windows using modeled sediment accumulation rates. With this information changes in lake sediment proxies can be examined on sub-decadal scales before and after significant tephra fall events.

Previous studies have observed that the environmental consequences of tephra fall are not exclusively governed by the physical and/or chemical properties of the volcanic ejecta but also the unique characteristics of the receiving landscape, including its climate state and ecosystem structure (e.g. Ayris and Delmelle, 2012 and references therein). Logically, different environments are affected by tephra deposition on various temporal and spatial scales. While large eruptions produce the most substantial landscape disturbance, it is also important to understand how smaller, but recurrent eruptions may impact a landscape and its ecosystems. Climate plays the most important role in dictating the background state of high latitude ecosystems (e.g. Bigelow et al., 2003; Kaplan et al., 2003). Holocene climate in Iceland is notably variable with anomalous cold summers and abrupt climatic transitions superimposed on a trend of decreasing Northern Hemisphere summer insolation (e.g. Geirsdóttir et al., 2013). This variability is thought to be related to some combination of fluctuations in the ocean-atmosphere system, reduced solar irradiance, and regional and global explosive volcanism (e.g. Denton and Broecker, 2008, Wanner et al., 2008; 2011, Miller et al., 2012). However, agreement on the principle controls, length, and timing for these relatively short-term and often rapid transitory periods has not been reached.

In this study we focus on the influence of four large post-glacial, pre-settlement explosive Icelandic eruptions that produced large volumes of tephra that was widely distributed across the island; two of rhyolitic and two of basaltic composition. We utilize climate proxies preserved in lacustrine archives to observe the catchment response to tephra perturbations as well as changes in within-lake bioactivity. Our four lakes: Vestra Gíslholtsvatn (VGHV), Hvítárvatn (HVT), Haukadalsvatn (HAK), Torfadalsvatn (TORF)

(Fig. 5.1, Table 5.1) span an elevational range and north-south transect across Iceland.

We focus on sediment proxy records with sub-decadal to decadal resolution

Figure 5.1 Location map of lakes used in this study and volcanic sources of targeted tephra layers in Iceland (from Google Maps). Bathymetry of Torfadalsvatn (TORF) adapted from Axford et al., (2007); Hvítárvatn (HVT) unaltered from Black (2008); Vestra Gíslholtsvatn adapted from Rist (1975); Haukadalsvatn adapted from Geirsdóttir et al., (2009a). The Hekla (source of H3, H4, and T-tephra) and Katla (KN and Tv-5) volcanic sources in the southern portion of Iceland are marked with red triangles (Jóhannsdóttir, 2007, Jagan, 2010).

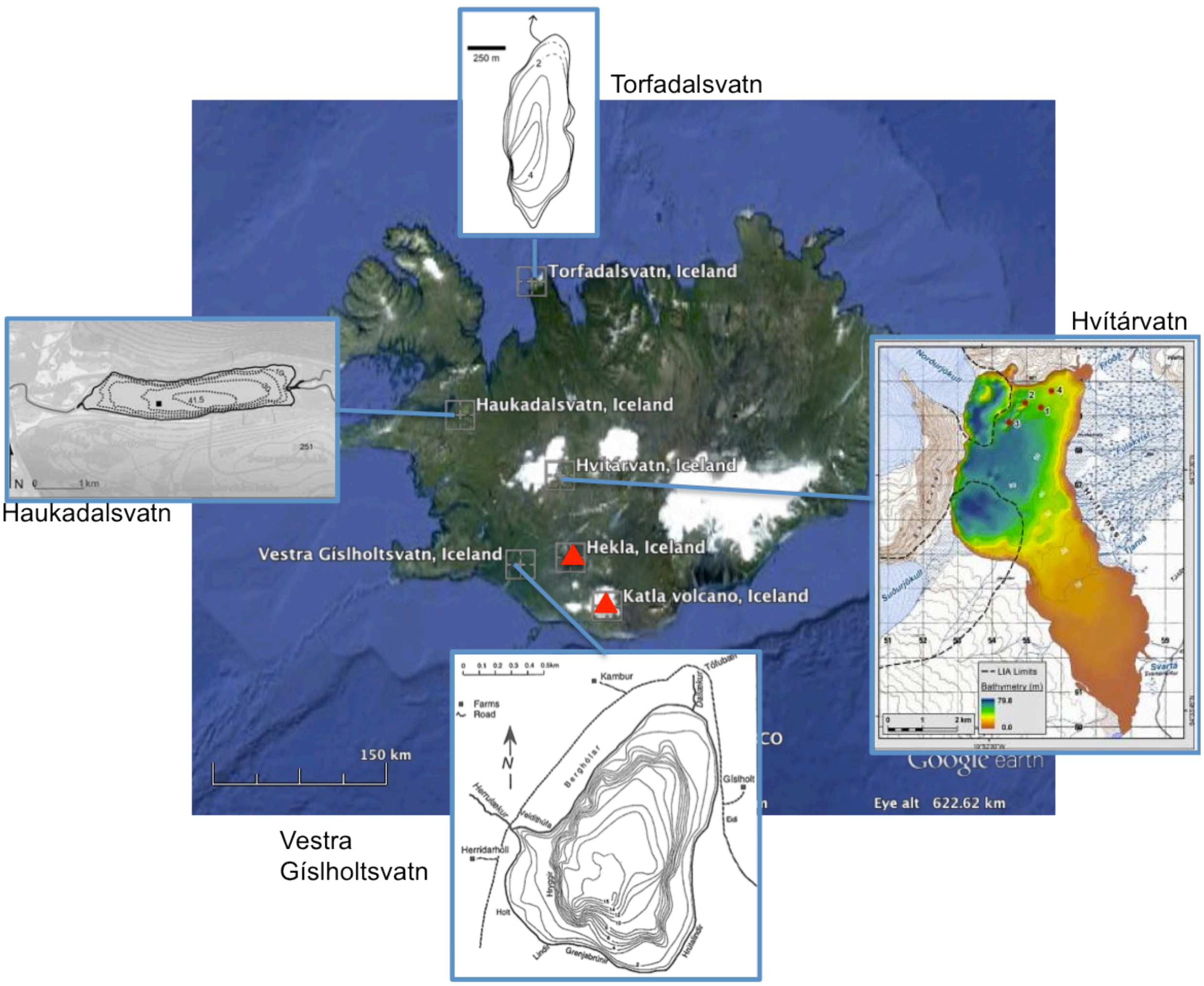

Table 5.1 Location of lakes and various environmental parameters

Lake	Location	Mean Annual Temp (°C)	Mean July Temp (°C)	Area (km^2)	Max Depth (m)	Catchment Size (km^2)	Elevation (m asl)	Type	Modern Vegetation	# Tephra in Holocene Sed Record	References
Vestra Gíslholtsvatn (VGHV)	63°57' N, 20°31' W	3.9 (1958 to 2004 AD)[1]	11.1 (1958 to 2004 AD)[1]	1.57	15	<5	52	Productive	Shrub heath and fens/mires where water can accumulate, forested before Settlement (871±2 AD)	108	Hardardóttir 1999; Hallsdóttir and Caseldine, 2005
Hvítárvatn (HVT)	64°37' N, 19°51' W	-0.9 (1966 to 2003 AD)[2]	7.3 (1965 to 2003 AD)[2]	28.9	83	820	422	Unproductive	Sedges and heath primarily in the Hvítárnes delta	>100	Black 2008; Larsen et al., 2011
Haukadalsvatn (HAK)	65°03' N, 21°28' W	3.4 (1830 to 1999 AD)[3]	10.0 (1830 to 1999 AD)[3]	3.3	42	172 (mostly lies 500 m a.s.l)	32	Unproductive	Forested before 1700s AD, currently sedges and grasses	40	Geirsdóttir et al., 2009
Torfadalsvatn (TORF)	66°04' N, 20°23' W	3.1 (1949 to 2001 AD)[4]	9.7 (1941 to 2003 AD)[4]	0.4	5.8	3.7	52	Productive	Dwarf-shrub heaths	<5	Rundgren 1997; Axford et al., 2007

[1]Hella, [2]Hveravellir, [3]Stykkishólmur, [4]Blönduós weather station data from http://www.vedur.is

surrounding four prominent tephra horizons (T-tephra, ~5650 BP; H4, ~4200 BP; KN, ~3500 BP; H3, ~3000 BP), two of which (T-tephra and H4) are observed in all four lakes while the other two (KN and H3) are only observed in VGHV and HVT.

Figure 5.2 Axes of tephra distribution for Hekla layers H3 and H4. Note the majority of the plume was transported northeast, away from the transect of lakes in our study. (Larsen and Eiriksson, 2008)

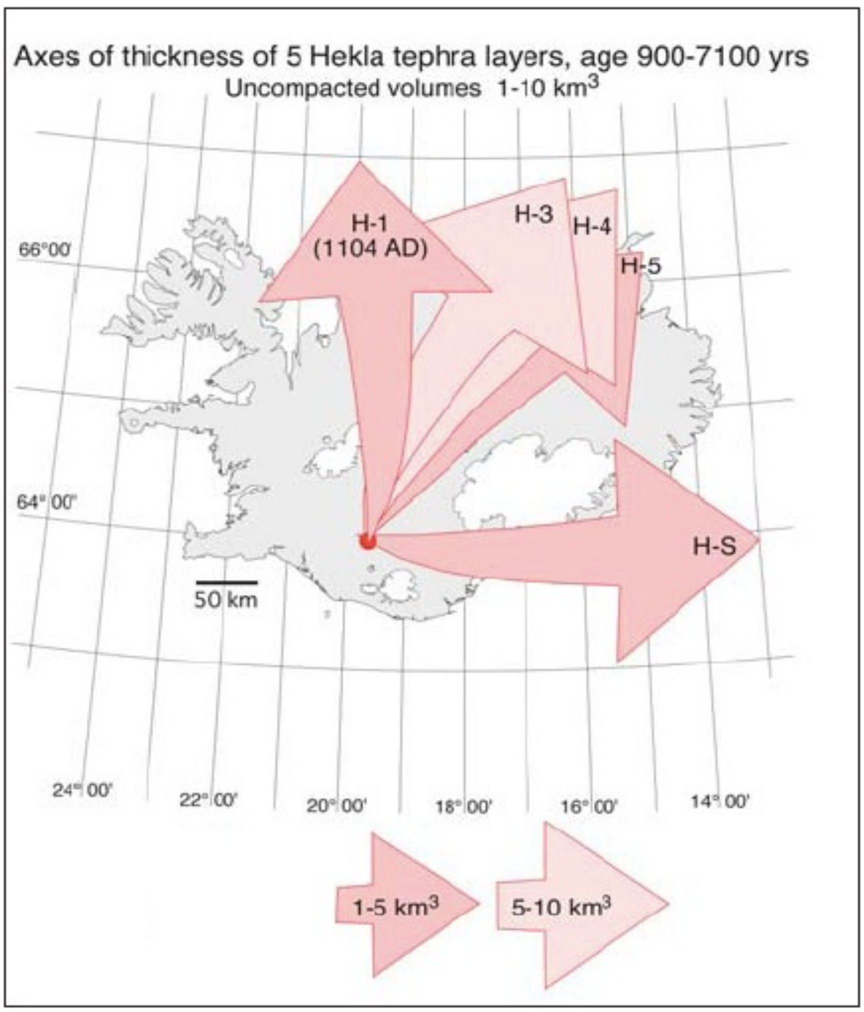

5.2 Site Descriptions

Of the four lakes used in this study VGHV sits most southerly, at a low elevtation (52 m asl) closest to the south coast of Iceland. HVT, the second most southern and most easterly lake is located at a relatively high elevation (422 m asl) in the central highlands. HAK is farthest west, located on the northwest coast at the lowest elevation (32 m asl) while TORF is the northernmost lake, positioned on the Skagi peninsula at a relatively low elevation (52 m asl) (Fig. 5.1). Table 5.1 lists summary information of lake locations, physical, and biological parameters. Of these lake VGHV and HVT are most proximal to the active volcanic centers of Iceland, and thus have the greatest probability of receiving tephra (See Fig. 5.1). Consistent with their location, they have the highest frequency of tephra layers in their Holocene sediment records. HAK and TORF are distal to tephra sources and only receive tephra from the largest eruptions and/or when wind and weather patterns are ideal for tephra delivery to their catchments.

5.2.1 Vestra Gíslholtsvatn (VGHV)

For a general location description of Vestra Gíslholtsvatn (VGHV) refer to Chapter 4.

5.2.2 Hvítárvatn (HVT)

Hvítárvatn (HVT 64°37 N, 19°51 W; 422 m asl) is an ultraoligotrophic lake located in the central highlands adjacent to the eastern margin of Langjökull (925 km^2) the second largest icecap in Iceland (See Fig. 5.1). The lake is relatively large with a surface area of 28.9 km^2 and maximum depth of 83 m. Its catchment is approximately 820 km^2 with two outlet glaciers and two melt-water streams on the north side of the lake acting as the primary sources of sediment input. Two other melt-water streams on northeastern shore also transport sediment into the lake creating the prograding Hvítárnes delta, an expansive wetland that is vegetated by sedges and heaths. Additional sediment is brought into the lake via aeolian processes (Black, 2008). Early Holocene basalt lava flows and late Pleistocene subglacial volcanics make up the bedrock surrounding the lake but are commonly overlain by alluvium and drift (Sinton et al., 2005). In this region soil packages are sparse, isolated to areas near stream channels or small, vegetated "islands" (Larsen et al., 2011). Soils are typically Andisols and prone to erosion due to low density and cohesion (Óskarsson et al., 2004; Arnalds, 2004; 2008). The ice-free season currently lasts about six months (from May to October) but drawn-out periods of ice cover and/or premature winter thaw can occur (Larsen et al., 2011; 2012).

5.2.3 Haukadalsvatn (HAK)

At the head of Hvammsfjördur in western Iceland resides Haukadalsvatn (HAK) (elevation 32 m asl), a coastal lake with a surface area of 3.3 km^2 (Fig. 5.1). The lake occupies an elongate bowl-shaped basin with a maximum depth of 42 m. It was inundated by the sea during deglaciation, becoming isolated ~10.6 ka. The glacially scoured bedrock basin is fed by a relatively large catchment (172 km^2) that predominantly resides >500 m asl. HAK is an ultraoligotrophic lake with little authigenic carbon production, lacking an extensive littoral zone where aquatic mosses can grow. Hence, macrophyte primary productivity has little influence on the carbon signals observed in the lake (Geirsdóttir et al., 2013). A large stream provides a high minerogenic sediment flux from the surrounding catchment, contributing a terrestrial carbon component to the lake sediment (Geirsdóttir et al., 2009a and b).

HAK lies outside the active volcanic zones of Iceland so any tephra layers observed in the Holocene lake record are from distal sources. Bedrock surrounding the lake is primarily Tertiary basalt and soils are most commonly Andisols, which retain organic carbon but lack cohesion, making them vulnerable to erosion from wind and water (Arnalds, 2004; 2008). Site names around HAK indicate a forested area at settlement time. However, historical accounts reveal removal of forests from the valley in which the lake sits before ~1700 AD. The valley is currently vegetated with grasses and sedges (Geirsdóttir et al., 2009a), species observed to preferentially grow in Iceland when forestland cannot reestablish (Hallsdóttir and Caseldine, 2005).

5.2.4 Torfadalsvatn (TORF)

Torfadalsvatn (TORF) (elevation 52 m asl) is a small (0.4 km^2), shallow (z_{max}= 5.8 m), coastal lake on the northern tip of the Skagi peninsula in north-central Iceland. The TORF catchment is also small (~4 km^2) with little topographic relief (See Fig. 5.1). There is minimal bedrock erosion and the lake receives a relatively low minerogenic sediment flux. TORF has an extensive littoral zone with macrophyte growth in the summer (Wang and Wooller, 2006). Compared to other lakes in this study TORF is relatively productive (Geirsdóttir et al., 2009a; Larsen et al., 2012) preserving signals of autochthonous carbon. At present a rocky plateau scattered with dwarf shrub surrounds the lake (Rundgren, 1995).

Previous studies (e.g. Björck et al., 1992; Rundgren, 1995; 1998; Rundgren and Ingólfsson, 1999) indicate that TORF and its catchment were deglaciated prior to deposition of the Vedde Ash ~12 ka (Mangerud et al., 1984). In the Holocene, changes in vegetation were somewhat coherent on the Skagi peninsula suggesting a climatic control of ecosystem structure in the region (Rundgren, 1995; 1998; Rundgren and Ingólfsson, 1999). Holocene temperature for TORF has been inferred from a previous lake sediment core using midge population changes. The study suggests summer temperature rose gradually following deglaciation, peaking at ~5 ka with the greatest warmth sustained until ~1 ka (Axford et al., 2007).

5.3 Factors Likely to Control the Environmental Impacts of Tephra Fall

Few studies on Icelandic tephra have emphasized the long-term landscape and ecosystem implications of tephra fall events (e.g. Kirkbride and Dugmore, 2003; Myers, 2011). The small body of research related to recent periods of tephra deposition in Iceland (i.e. Hekla, 1947; Eyjafjallajökull, 2010) has focused on tephrochronology (e.g. Thorarinsson, 1967; Haflidason et al., 2000; Yalcin et al., 2003; Wastegård, 2005), eruption comparisons (e.g. Thordarson and Höskuldsson, 2008; Davies et al., 2010), or anthropocentric concerns (e.g. Gudmundsson et al., 2008; Myers, 2011; Thorsteinsson et al., 2011; Karlsdóttir et al., 2012).

However, studies highlighting landscape and ecosystem impacts of tephra fall have been published subsequent to modern eruptions in other areas of the world (e.g. Mt. St. Helens, WA, USA 1980 [Cook et al., 1981; Mack, 1981; Kennedy, 1981; Schulte et al., 1985]; Volcan Hudson, Patagonia, Chile 1991 [Wilson et al., 2011]; Ruapehu, New Zealand 1995-1996 [Cronin et al., 1997], etc.). These studies generally focus on agricultural consequences of explosive volcanic eruptions including effects on crop yield, plant regrowth, and structural failure following tephra deposition. Findings indicate tephra fallout can abrade plant materials, inhibit photosynthesis, kill pollenating insects, increase soil albedo, reduce soil permeability and acidify soils. While most of these processes are short lived, with studies focusing on singular, isolated events, results offer insight into the immediate landscape impacts after tephra fall. On longer time scales others recognize that tephra rich soils (Andisols) develop relatively fast (Guicharnaud and Paton, 2006; Sigfusson et al., 2006) and readily store organic matter (OM) (e.g. Arnalds and Kimble, 2001; Óskarsson et al., 2004; Arnalds, 2008a, b; Sigfusson et al., 2008; Long et al., 2011). This suggests in certain instances tephra deposition may help soil quality, in turn influencing the complicated relationship between physical, biological, and chemical processes in an ecosystem setting.

No published studies have considered how Icelandic landscapes respond to the deposition of different tephra compositions (i.e. rhyolitic vs. basaltic). Throughout the Holocene volcanism in Iceland has produced large eruptions of tephra on both endmembers of the geochemical compositional spectrum (Thordarson and Larsen, 2007). Chemical reactivity of tephra upon exposure to environmental agents is likely influenced by the bulk chemical and mineralogical composition. Tephra composition is inherited from the magma and rocks from which the lithics are derived (Ayris and Delmelle, 2012). Rhyolitic tephra is lighter in color, higher in Si and lower in density than mafic basaltic tephra, which is more abundant in Mg, Fe, and S, contributing to its darker color and vulnerability to weathering processes (Sigfusson, 2008; Lowe, 2011). Thus, rhyolitic tephra is typically more mobile, traveling further and more readily redistributed on the landscape (Thorarinsson, 1979; Ayris and Delmelle, 2012).

5.4 Hypotheses

Based on literature reviews and our earlier work, we have developed six hypotheses that describe the controlling variables that predict how substantial tephra fall events are likely to influence within-lake and catchment processes.

(1) **Dependency on climate state.** The climate conditions preserved in lake proxy records are related to latitude, altitude, and the unique characteristics of individual sites. Low (high) elevation catchments are typically well (poorly) vegetated. Additionally, more southerly (northerly) sites have more robust (sensitive) plant communities. Thus, we hypothesis low elevation and/or more southerly sites in low relief landscapes are more resistant to disturbance from tephra fall than higher, colder, and/or greater relief landscapes.

(2) **Dependency on tephra composition.** We hypothesize rhyolitic tephra has a greater impact on depositional environments than basaltic tephra. Due to its low density, rhyolitic tephra is readily remobilized by wind, severing plants and potentially accumulating in dunes, smothering underlying vegetation. These impacts frequently lead to landscape instability and increased catchment soil erosion, retarding recolonization of plants (Lewontin, 1969). Furthermore, rhyolitic tephra acidifies soils and water sources stressing biological productivity. It also floats on lake surfaces, impacting light availability for aquatic bioactivity. Basaltic tephra has less impact on lacustrine environments and catchment stability as it weathers rapidly releasing nutrients that promote revegetation and in-lake bioactivity. It is also

more alkali and denser than rhyolitic tephra, sinking quickly in aquatic environments.

(3) **Temporal evolution of climate may transition a site from one sensitivity state to another.** We expect an amplification of tephra disturbance when coupled with a cooling climate through the Neoglacial. The degree of intensification will likely be site specific.

(4) **Season of eruption.** We anticipate the season of eruption to influence the extent of landscape perturbations, as plant communities are more sensitive during the spring and summer suggesting winter eruptions produce less significant signals.

(5) **Volume of tephra entering the basin and catchment.** We assume the larger the volume of tephra deposited the greater the impact, regardless of composition.

(6) **Interval of time between tephra deposition events at a site.** Lakes near active volcanic centers are more frequently affected by tephra fall events than distal lakes. We hypothesize lakes disrupted by multiple tephra depositions within a short period of time will experience a greater level of disturbance than lakes infrequently perturbed by tephra fall.

We anticipate our four lakes, located at different latitudes, altitudes, physiography and therefore a range of ecosystems, are likely to capture much of the hypothesized variability in landscape responses to tephra fall. Our four tephra deposition events include one in the Holocene Thermal Maximum (HTM), while the other three span the transition into the cooler summers of Neoglaciation, providing means to test the temporal evolution of catchment sensitivity to tephra perturbations.

5.5 Methods

The goal of this study was to obtain subdecadal to decadal resolution of physical and OM proxies representative of 200 years on either side of specific tephra horizons. This time window was selected to quantify the pre-eruptive state and evaluate the duration of the landscape and ecosystem perturbations from significant tephra fall events.

5.5.1 Sediment Cores and Samples

Twinned sediment cores were collected from HAK and HVT in 2003 using the DOSECC's GLAD-200 core rig (http://www.doesecc.org). For details of core collection, sampling and analysis of physical and biological proxies refer to Geirsdóttir et al., (2009a) and Larsen et al., (2011; 2012) respectively. Comprehensive descriptions of core collection and initial sample processing from the 2008 VGHV core are given in Chapter 4. An 8.5 m long sediment core was collected from TORF in February 2012 using an 11 cm diameter percussion coring system (Nesje, 1992). Physical proxies were measured at the University of Iceland using a GeoTek. Core sections were then split, photographed, packed and shipped to the University of Colorado Boulder for sampling of OM proxies.

Previous studies of all four lakes provide relatively high-resolution climate proxy data through the Holocene. However, additional samples of OM proxies were required to improve temporal resolution surrounding the tephra horizons of interest. Samples were taken at 0.5 to 1.0 cm resolution depending upon sediment accumulation rate from the VGHV, HVT, and HAK sediment cores at the Limnological Research Center at the University of Minnesota (LRC-UM) where the cores are in storage. Following collection, samples were kept at 4°C until they were freeze dried, subsamples weighed and sent to the University of California, Davis Stable Isotope Facility (SIF-UC Davis) for analysis C and N concentrations and their stable isotopes. An Elementar Vario EL Cube or Micro Cube elemental analyzer (Elementar Analysensysteme GmbH, Hanau, Germany) interfaced to a PDZ Europa 20-20 isotope ratio mass spectrometer (Sercon Ltd., Cheshire, UK) was used to measure stable carbon isotopes ($\delta^{13}C$) of each sample. Freeze-dried samples were combusted at 1000 °C and N_2 and CO_2 gas were separated using a molecular sieve adsorption trap before entering the continuous-flow IRMS for $\delta^{13}C$ measurements. $\delta^{13}C$ values have a long-term standard deviation of 0.2‰ and are expressed relative to Vienna Pee Dee Belemnite.

5.5.2 Age Models

Conspicuous basaltic and rhyolitic tephra horizons are useful for correlation between sediment cores and absolute dating when ages are available. All tephra horizons within the Holocene record were detected visually and subsampled for chemical composition in HAK (40 tephra layers) and VGHV (108 tephra layers), while over 100 tephra horizons were sampled in HVT (Jóhannsdóttir, 2007; Jagan, 2010; Thordarson, unpublished). In the 2012 TORF core <5 tephra layers were visually detectable of which 3 were subsampled for geochemical analysis. However, their composition has yet to be geochemically confirmed.

Age models for each core were constructed based on available dating constraints. We used previously derived age models for HAK (Geirsdóttir et al., 2013) and HVT (Larsen et al., 2011; 2012). Eighteen geochemically identified tephra horizons and one radiocarbon date were used to create an age model for the VGHV Holocene record. Chapter 4 contains a complete explanation of how the VGHV age model was derived. A preliminary TORF age model was constructed from 5 radiocarbon dates. While the age model for the TORF sediment core is the least well constrained, the two tephra types have been geochemically typed and we only need the relative sediment accumulation rates surrounding the tephra to define appropriate sampling windows.

Because the age models are smoothed they do not correctly express abrupt changes in sedimentation rate for the time scales in which we are interested. Following significant tephra horizons in the Icelandic lake Hestvatn, Hardardóttir (2001) observed transient increases in sedimentation accumulation rate constrained between identifiable tephra horizons. Due to the uncertainty surrounding changes in sediment accumulation rate post tephra deposition, we did not use the modeled sedimentation rate or calculated OM fluxes as reliable environmental proxies. However, it is noted that abrupt changes in sedimentation rate are observed following deposition of the rhyolitic tephra horizons, H3 and H4, in all lakes except TORF, where the age model is less well constrained. All lakes indicate no change in sediment accumulation rate following deposition of the basaltic tephra layers used in this study, T-tephra and KN (Larsen et al., 2011; 2012; Geirsdóttir et al., 2013).

5.5.3 Tephra Used to Evaluate Impacts

The T-tephra (~5650 BP; Ólafsdóttir, 2010), is a basaltic tephra erupted from the Hekla volcano (see Fig. 5.1) during the HTM and was positively identified in 3 lakes: VGHV (1.6 cm), HAK (0.4 cm), and HVT (0.5 cm) (Jóhannsdóttir, 2007, Jagan, 2010).

In TORF, a thick basaltic tephra layer (0.7 cm) was also determined to have been deposited during the HTM. However, preliminary age models indicate it is doubtful to be the T-tephra. Based on previous work in TORF the layer is most likely the Tv-5 horizon, a tephra erupted from the Katla volcano at ~6600 BP (Björck et al., 1992; Wastegård et al., 2001; Kristjánsdóttir et al., 2007). We decided to use the proxy signals in TORF surrounding the Tv-5 tephra as an analog for the T-tephra, as it is a relatively thick basaltic horizon deposited during the HTM. Use of the Tv-5 tephra and T-tephra enable us to compare the proxy responses to a substantial basaltic tephra deposition event in all four lakes during the same general time period.

Hekla 4 (H4: ~4200 BP; Dugmore et al., 1995) is a widespread rhyolitic tephra (Larsen and Thorarinsson, 1977) geochemically identified in two lakes; HVT (7.5 cm) and VGHV (0.65 cm) (Jóhannsdóttir, 2007: Jagan, 2010). A silicic tephra from a Hekla eruption deposited in HAK (0.90 cm) around 4.2 ka closely matches the geochemistry of what was identified as H4 in VGHV. Thus, we consider this tephra to indicate the H4 eruption is in HAK. In TORF, the H4 tephra (1.2 cm) was visually identified as a substantial rhyolitic layer within the appropriate time window in the preliminary radiocarbon based age model. This allowed us to sample around a tephra horizon deposited in not only all four lakes but also during a period of significant of climatic transition in Iceland (Larsen et al., 2012; Geirsdóttir et al., 2013).

The Hekla 3 (H3: ~3000 BP; Dugmore et al., 1995) and the Katla N (KN: ~3500 BP; Róbertsdóttir, 1992) tephra horizons were only geochemically identified in VGHV (0.4 cm and 5.0 cm respectively) and HVT (8.0 cm and 5.0 cm thick respectively) (Jóhannsdóttir, 2007; Jagan, 2010). H3 was chosen because it is the most substantial rhyolitic eruption of the Holocene (Larsen and Thorarinsson, 1977) and produced a strong signal of landscape disturbance in OM proxies in the HVT Holocene record (Larsen et al., 2011, Chapter 6). The KN tephra (Róbertsdóttir, 1992) was selected as it is the thickest tephra horizon in VGHV and one of the most substantial post-Saksunarvatn basaltic tephra layers in HVT. Table 5.2 lists the tephra horizons utilized in this study in each lake, the method used for identification, and geochemical composition when available.

5.5.4 Physical Proxies

Physical properties of lake sediment, magnetic susceptibility (MS) and bulk sediment density, were used to interpret the extent and efficiency of weathering on the landscape, sediment transport within a catchment, local glacial history when applicable, and identification of the presence of tephra in individual basins. Lakes draining glacial terrain provide opportunities to infer variability in glacial activity (Osborn et al., 2007) because glaciers produce prodigious quantities of sediment, which is transported via wind, water, and gravity until it is captured and preserved in lake basins. Studies have shown that glaciated basins produce more sediment and more efficient erosion than non-glaciated basins, regardless of basin size (Hallet et al., 1996). Increased abundance of the minerogenic component in glacial lake sediment is linked with increased glacial extent as greater clastic sedimentation is commonly interpreted to reflect enhanced production and erosion beneath an expanded body of ice (Nesje et al., 2000; Rosenbaum et al., 2012). However, changes in sediment availability and storage beneath alpine glaciers or changes in sediment from non-glacial sources can complicate the relationship between sediment yield and glacier extent (Leonard, 1997).

Table 5.2 Lakes found in, age, geochemical composition, and identification method of the H3, KN, H4 and T-tephra horizons used in this study. Tephra layers with varied composition are listed accordingly.

Lake	Tephra	Approx Age (BP)	Method of Identification	SiO_2	TiO_2	Al_2O_3	FeO	MnO	MgO	CaO	Na_2O	K_2O	P_2O_5	Total	Age Reference
VGHV	H3	3055±120	Geochemical[a]	71.84	0.19	13.93	3.07	0.11	0.13	2.04	4.91	2.57	0.02	98.83	Dugmore et al., 1995
				(0.51)	(0.01)	(0.35)	(0.12)	(0.01)	(0.01)	(0.08)	(0.12)	(0.10)	(0.01)	(1.03)	
				65.77	0.43	14.65	5.50	0.18	0.41	3.22	4.59	2.01	0.10	96.85	
				(0.97)	(0.21)	(0.66)	(1.19)	(0.02)	(0.19)	(0.60)	(0.39)	(0.12)	(0.04)	(2.09)	
HVT			Geochemical[b]	72.75	0.15	13.48	2.71	0.10	0.08	1.78	4.52	2.62	0.01	98.20	
				(1.30)	(0.06)	(0.56)	(0.58)	(0.02)	(0.06)	(0.36)	(0.23)	(0.19)	(0.01)	(0.85)	
				66.42	0.48	14.77	6.10	0.20	0.51	3.55	4.51	1.96	0.13	98.62	
				(2.13)	(0.13)	(0.54)	(1.11)	(0.03)	(0.19)	(0.57)	(0.23)	(0.26)	(0.07)	(0.74)	
				59.19	1.44	14.00	10.05	0.28	1.94	5.33	3.93	1.50	0.66	98.32	
				(1.32)	(0.19)	(0.80)	(0.78)	(0.03)	(0.48)	(0.44)	(0.34)	(0.15)	(0.12)	(0.88)	
				46.59	4.40	12.74	15.01	0.23	5.00	9.80	2.92	0.73	0.48	97.90	
				(0.57)	(0.16)	(0.31)	(0.64)	(0.01)	(0.24)	(0.31)	(0.18)	(0.07)	(0.02)	(0.57)	
VGHV	KN	3555±120	Geochemical[a]	46.50	4.49	12.77	14.89	0.22	5.25	10.08	2.92	0.69	0.45	98.26	Róbertsdóttir, 1992
				(0.48)	(0.16)	(0.32)	(0.38)	(0.01)	(0.17)	(0.17)	(0.12)	(0.04)	(0.04)	(0.72)	
HVT			Geochemical[a]	47.20	4.47	12.96	15.48	0.23	5.18	10.37	2.86	0.70	0.45	99.90	
				(0.40)	(0.08)	(0.42)	(0.23)	(0.03)	(0.25)	(0.17)	(0.11)	(0.05)	(0.03)	(0.77)	
? VGHV	H4	4275±10	Geochemical[a]	57.02	1.67	14.70	10.42	0.28	2.44	5.79	4.12	1.36	0.66	98.46	Dugmore et al., 1995
				(0.69)	(0.08)	(0.29)	(0.29)	(0.01)	(0.16)	(0.22)	(0.11)	(0.08)	(0.04)	(0.66)	
HVT			Geochemical[a]	74.21	0.13	13.29	2.19	0.09	0.06	1.42	4.43	2.81	0.02	98.66	
				(1.09)	(0.09)	(0.29)	(0.43)	(0.02)	(0.12)	(0.24)	(0.17)	(0.11)	(0.02)	(0.56)	
				58.44	1.43	14.83	10.20	0.25	2.02	5.69	4.12	1.41	0.68	99.07	
				(1.50)	(0.30)	(0.64)	(0.71)	(0.03)	(0.52)	(0.57)	(0.19)	(0.15)	(0.18)	(0.71)	
? HAK			Geochemical[c, d]	57.46	1.73	14.35	10.49	0.32	2.36	5.92	4.13	1.40	0.69	98.85	
				(0.71)	(0.05)	(0.32)	(0.26)	(0.02)	(0.14)	(0.23)	(0.13)	(0.11)	(0.04)	(0.17)	
TORF				Composition visually identified, layer confirmed with age model											
VGHV	T-Tephra	5657±200	Geochemical[a]	46.17	2.78	15.35	13.27	0.21	7.07	10.70	2.56	0.46	0.19	98.77	Ólafsdóttir et al., 2010
				(0.48)	(0.06)	(0.33)	(0.30)	(0.01)	(0.15)	(0.18)	(0.16)	(0.21)	(0.01)	(0.87)	
HVT			Geochemical[c]	45.70	2.68	15.56	13.29	0.19	7.26	10.87	2.51	0.40	0.27	98.72	
				(0.38)	(0.08)	(0.13)	(0.22)	(0.03)	(0.12)	(0.14)	(0.04)	(0.01)	(0.03)	(0.49)	
HAK			Geochemical[c]	45.84	2.66	15.71	13.32	0.20	7.30	10.89	2.56	0.39	0.21	99.08	
				(0.32)	(0.06)	(0.13)	(0.13)	(0.01)	(0.11)	(0.10)	(0.06)	(0.01)	(0.02)	(0.34)	
TORF	Tv-5	6000 ^{14}C		Composition visually identified, layer confirmed with age model											Björck et al., 1992

[a] Thordarson unpublished, see appendix; [b] Larsen et al., (2011); [c] Jóhannsdóttir (2007); [d] inferred using age modei

In Iceland this is relevant because glaciers still occupy a large area of the land mass but much of the terrestrial erosion occurs via aeolian processes (Óskarsson et al., 2004; Arnalds et al., 2012).

It is commonly assumed the minerogenic component of lake sediment varies inversely with the concentration of organic material as variations in erosively derived material rather than changes in lake productivity are thought to cause the observed differences in the abundance of these components (Dahl et al., 2003). This holds true unless abundant terrestrial OM is being eroded from the landscape or the lake has low primary productivity and is thus dominated by a signal of terrestrial carbon (e.g. Larsen et al., 2012; Geirsdóttir et al., 2009a; 2013). HAK and HVT are unproductive lakes so the proportion of OM preserved in the lake sediment is representative of terrestrial erosion and minerogenic input during periods of landscape destabilization. As VGHV and TORF are relatively productive, OM and erosive contributions to lake sediment are typically anticorrelated as minerogenic input dilutes and/or inhibits primary productivity (Table 5.1).

The influence of tephra on physical proxies depends upon the background values of MS and density observed in individual lakes. In lakes with relatively high productivity and low erosion the presence of iron oxides and ferromagnetic minerals in tephra results in peaks in MS and density within the sediment cores. Lakes with low productivity and high minerogenic input tephra layers may produce little or no change at basaltic tephra layers or negative anomalies across rhyolitic tephra layers (e.g. Geirsdóttir et al., 2009a; Larsen et al., 2012).

5.5.5 Biological Proxies

OM proxies used in the study include total organic carbon (%TOC), C:N, and $\delta^{13}C$. Lacustrine, terrestrial, and climate processes are represented by these proxies providing evidence of how tephra fall disturbs landscapes and ecosystems. Lake and catchment primary productivity create signals that can be interpreted for paleoclimatic and paleoenvironmental purposes (e.g. Leng and Marshall, 2004; Wooller et al., 2008; Lennox et al., 2010; Janbu et al., 2011; Larsen et al., 2011; 2012; Geirsdóttir et al., 2009a; 2013). Algae, aquatic macrophytes and terrestrial plants utilize carbon and nitrogen in their structures at characteristic chemical ratios (i.e. C:N) and isotopic compositions (i.e. $\delta^{13}C$). When the living material dies a portion of the OM is buried in the sediment preserving the signal (i.e. C:N, $\delta^{13}C$).

The abundance of carbon (%TOC) and nitrogen (%N) found in lake sediments is determined by lacustrine primary productivity, erosion of terrestrial vegetation and soils, and changes in the proportion of minerogenic input. %TOC is commonly considered a measure of primary productivity and dependent upon climate parameters. However, this only holds true in lakes where autochthonous primary productivity dominates the %TOC signal (Meyers 1997; Geirsdóttir et al., 2009a; Lennox et al., 2010; Janbu et al., 2011) such as in VGHV and TORF. In unproductive lakes (HVT and HAK), %TOC is strongly influenced by transient fluxes of aged soil carbon and often behaves more like a physical proxy (Larsen et al., 2012; Geirsdóttir et al., 2013).

The proportion of carbon derived from terrestrial vegetation relative to aquatic sources preserved in lake sediment can be deciphered using the ratio of carbon to nitrogen (C:N). Unlike %TOC, C:N is independent of sediment accumulation rate.

Aquatic plants typically have relatively low values of C:N, falling between 4 and 10, where as terrestrial C:N is higher with greater variability ranging from 10 to >50 (Meyers 1997; Meyers and Teranes, 2001). Unlike other OM and physical proxies, average C:N does not vary widely between lakes, generally falling between 6 and 8.5, with higher C:N reflecting increasing contribution from terrestrial carbon sources (See Table 5.3) (e.g. Wang and Wooller, 2006).

Another proxy independent of sediment accumulation rate is $\delta^{13}C$, the ratio of stable carbon isotopes. Like C:N, $\delta^{13}C$ reflects the source of carbon. Aquatic algae are typically most depleted in $\delta^{13}C$ (~-30‰), with terrestrial vegetation utilizing C4 photosynthetic pathways slightly heavier (~-26‰ [Wang and Wooller, 2006]), and aquatic macrophytes having the heaviest values (-20‰ to -13‰ [Wang and Wooller, 2006; Langdon et al., 2010]). From this we can assume more significant aquatic components in the carbon cycles of TORF and VGHV and greater terrestrial contribution to the lake sediment of HVT and HAK.

Table 5.3 Average proxy values before and after the deposition of each tephra of interest. Standard deviations are listed below each mean value in parenthesis.

VGHV	Pre %TOC	Post %TOC	Pre C:N	Post C:N	Pre d13C	Post d13C	Pre MS	Post MS	Pre Den	Post Den
T-tephra	3.27	2.79	7.94	7.60	-22.7	-22.5	86.6	181.0	1.14	1.30
	(0.63)	(0.85)	(0.33)	(1.03)	(0.54)	(1.45)	(28.4)	(111.8)	(0.03)	(0.24)
H4	3.41	2.66	8.56	6.77	-24.2	-23.2	224.3	205.3	1.25	1.29
	(1.16)	(0.91)	(0.69)	(1.32)	(0.73)	(0.74)	(204.0)	(106.2)	(0.11)	(0.16)
KN	3.19	3.08	6.71	6.95	-22.9	-23.4	109.7	208.2	1.20	1.30
	(0.75)	(1.11)	(0.89)	(1.16)	(0.39)	(0.50)	(33.3)	(110.9)	(0.12)	(0.29)
H3	2.26	2.71	8.15	7.56	-23.3	-22.4	99.4	130.8	1.21	1.26
	(0.99)	(0.82)	(0.73)	(0.54)	(0.80)	(0.51)	(30.4)	(62.9)	(0.10)	(0.21)
HVT										
T-tephra	0.39	0.35	6.82	7.87	-24.2	-24.8	260.7	237.8	1.73	1.70
	0.09	0.08	0.87	1.96	0.84	0.89	6.5	13.6	0.08	0.09
H4	0.31	0.50	5.98	7.32	-24.3	-25.7	415.0	301.2	1.85	1.96
	0.04	0.10	0.26	0.61	0.40	0.36	28.4	34.9	0.06	0.12
KN	0.34	0.26	6.45	6.50	-25.2	-25.6	391.1	454.0	2.04	2.13
	0.07	0.07	0.54	0.54	0.62	0.58	45.1	7.5	0.09	0.10
H3	0.32	0.80	6.01	8.59	-25.6	-25.9	414.7	344.9	1.98	1.94
	0.09	0.55	0.59	1.40	0.59	0.46	8.5	58.0	0.05	0.16
HAK										
T-tephra	0.83	0.86	8.82	8.33	-27.3	-27.3	669.8	611.1	1.64	1.66
	0.08	0.14	0.79	0.33	0.17	0.23	105.7	89.6	0.12	0.12
H4	0.82	0.81	8.75	8.44	-26.6	-27.5	736.7	805.1	1.65	1.75
	0.27	0.12	0.99	0.79	0.92	0.22	44.3	29.4	0.08	0.03
TORF										
T-tephra	7.18	6.89	8.33	8.70	-20.0	-18.8	50.2	47.9	1.18	1.24
	(0.75)	(1.28)	(0.48)	(0.65)	(0.60)	(0.90)	(7.2)	(7.3)	(0.02)	(0.02)
H4	7.12	7.28	7.62	8.23	-19.1	-19.4	36.8	32.6	1.22	1.20
	(0.89)	(1.24)	(0.24)	(0.63)	(0.52)	(0.80)	(2.8)	(7.6)	(0.05)	(0.08)

5.6 Results

Principle Component Analysis (PCA) is useful for identifying prominent gradients within complex multivariable datasets by diminishing them into latent variables through a technique of orthogonal transformation (Janžekovič and Novak, 2012). As there are relatively linear relationships (See Fig. A3.5, A3.6, A3.7, A3.8, A3.9, A3.10) between proxy variables we decided it was appropriate to conduct a PCA for each tephra deposition event in relevant lakes (McCune and Grace, 2002). The program R, was used to perform the PCAs with each data set scaled to unit variance.

To define the background state prior to perturbation we utilize subdecadal to decadally resolved proxy time series for the 200 years before each targeted tephra. We then compare the post-tephra time series to the background state to evaluate the magnitude and duration of disturbance from each tephra fall. In doing so we identify both short-lived and persistent changes in proxies following tephra deposition on the landscape. Time series are organized by tephra composition and placed in chronologic order with the older events described first.

5.6.1 PCA Results

After conducting a PCA for each tephra time window PCA bi-plots were made in order to identify periods of disturbance both before and after the tephra horizons of interest (Fig. 5.3, 5.4, 5.5, 5.6). Each PCA data point is given a sample number shown on the bi-plots, with number 1 indicating the oldest sample in the time series (~200 years before the tephra deposition event of interest) and the largest sample number signifying the most resent sample (~200 years after the tephra deposition event of interest). As each time series does not have the same number of samples due to variability in sedimentation rate and the availability of certain proxies, the sample number immediately after the targeted tephra horizon is denoted with a blue circle. Data clusters indicating disturbance following tephra layers are circled in brown.

PC 1 and 2 account for at least 70% of the observed variability within the data sets, allowing us to ignore the remaining components (Table 5.4). Component scores were calculated and used to produce succinct time series of PC 1 and 2 for each window surrounding targeted tephra deposition events (Fig. 5.7, 5.8). The two components do not always indicate the same processes between lakes but, the unproductive lakes, HAK and HVT, and the productive lakes, VGHV and TORF, eliciting similar responses respectively (Table 5.5).

5.6.2 Rhyolitic Tephra

5.6.2.1 Hekla 4 Layer (H4)

The Hekla layer, H4 (~4200 BP), came from one of the most significant rhyolitic eruptions of the Holocene in Iceland where approximately 9 km^3 of airborne ejecta was spread over 78,000 km^2 of land (Larsen and Thorarinsson, 1977; Dugmore et al., 1995). The H4 tephra horizon is followed by the most substantial and long-lasting proxy responses of our study. All 4 lakes yield a significant change in PC 1 (Fig. 5.7a) and subtle alteration in PC 2 (Fig. 5.7c) after tephra deposition. In the larger, unproductive lakes, HVT and HAK, PC 1 is dominated by the flux and source of OM from terrestrial erosion while PC 2 signifies variation in physical proxies. In the smaller, productive lakes, VGHV and TORF, PC 1 represents lacustrine primary productivity; a process that may also be dependent on the minerogenic flux whereas PC 2 denotes OM source which can also be considered a proxy of within lake productivity.

Table 5.4 PCA summary statistic for all lakes and eruptions expressing the proportion of variance for each component.

H4	Comp 1	Comp 2	Comp 3	Comp 4	Comp 5
VGHV	0.502	0.302	0.122	0.061	0.013
HVT	0.738	0.146	0.05	0.041	0.025
HAK	0.467	0.271	0.157	0.077	0.028
TORF	0.508	0.256	0.135	0.067	0.034
H3					
VGHV	0.484	0.295	0.121	0.060	0.040
HVT	0.702	0.196	0.072	0.017	0.013
T-tephra					
VGHV	0.450	0.306	0.169	0.045	0.029
HVT	0.476	0.256	0.173	0.054	0.041
HAK	0.513	0.257	0.149	0.060	0.021
TORF	0.433	0.284	0.183	0.063	0.038
KN					
VGHV	0.499	0.221	0.141	0.084	0.055
HVT	0.377	0.328	0.201	0.060	0.034

Table 5.5 PCA component interpretations for each lake and eruptions. Divided by productive (VGHV and TORF) and unproductive (HVT and HAK) lakes.

Tephra	Lakes	Age (BP)	Type	Unproductive Lakes (HVT and HAK)		Productive Lakes (VGHV and TORF)	
				Component 1	Component 2	Component 1	Component 2
H4	VGHV HVT HAK TORF	~4200	Rhyolitic	OM source and flux from terrestrial erosion	Physical proxies	Lacustrine primary productivity	OM source
H3	VGHV HVT	~3000	Rhyolitic	OM flux from terrestrial erosion	OM source	Lacustrine primary productivity	OM source
T-tephra	VGHV HVT HAK	~5650	Basaltic	Lacustrine primary productivity or landscape stability	OM source and minerogenic flux	Lacustrine primary productivity	Minerogenic flux and OM source
Tv-5	TORF	~6600					
KN	VGHV HVT	~3500	Basaltic	Lacustrine primary productivity or landscape stability	Minerogenic flux and OM source	Lacustrine primary productivity	OM source

The data point immediately post-H4 is an outlier in all PCA bi-plots (Fig. 5.3) with data clusters indicating change in primary productivity and landscape disturbance at every lake subsequent H4. Following deposition of the H4 tephra the lakes are disturbed for at least 75 years with unproductive lakes (HVT and HAK) attaining an irreversible shift to an alternative stable state within 50 years of the eruption as observed in PC 1 (Fig 5.3, 5.7a).

Prior to H4, the VGHV ecosystem has notable instability associated with a previous rhyolitic tephra horizon convoluting the H4 signal (Fig 5.7e). However, following all tephra layers in VGHV PC 1 and 2 both increase indicating a greater minerogenic flux coupled with reduced primary productivity in the lake basin (Fig 5.7a, c). Approximately 75 years after H4, PC 2 decreases to a quasi-stable state signifying recovery of lacustrine primary productivity to a balanced ecosystem state following multiple tephra perturbations (Fig 5.7a, c). Disturbance in TORF after deposition of the H4 tephra lasts for ~100 years, as indicated by an increase in the minerogenic component entering the basin and diminished primary productivity. After recovery from H4, OM proxies in TORF are more variable suggesting instability in the structure and function of the lacustrine ecosystem (Fig 5.7a).

Figure 5.3 PCA bi-plots for H4 tephra deposition event indicating component magnitude and direction for lake sediment proxies: %TOC, C:N, $\delta^{13}C$, MS, and density. Small/large numbers indicate data points early/late in the 400 year time series. Data point immediately after tephra horizon of interest is circled in blue. Periods of tephra disturbance are circled in brown. a. VGHV; b. HVT; c. HAK; d. TORF.

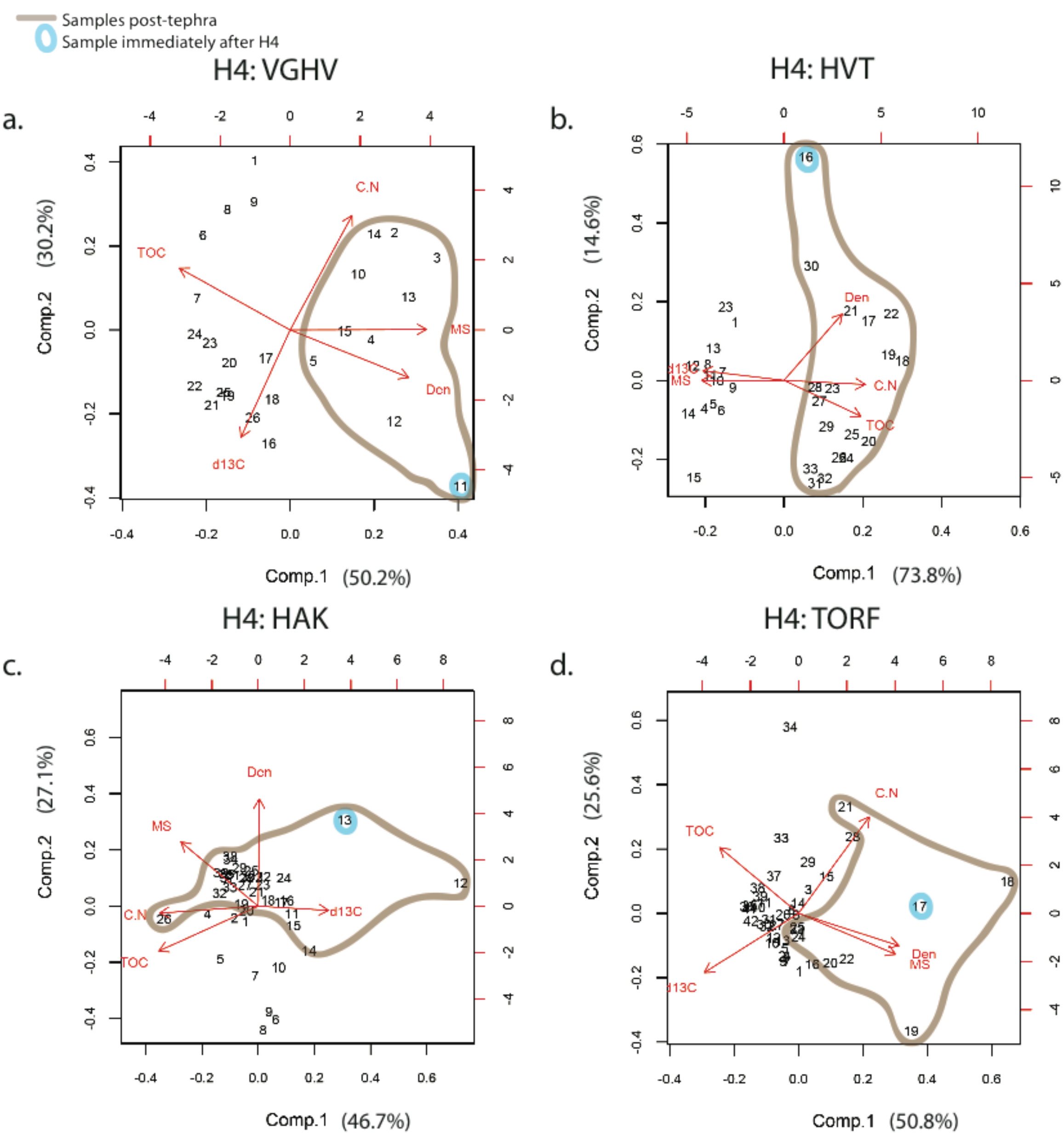

5.6.2.2 Hekla 3 Layer (H3)

The H3 tephra (~3000 BP) was erupted from Hekla during which approximately 12 km^3 of ejected material was released over 80,000 km^2. The eruption is considered the most severe Hekla eruption of the Holocene (Larsen and Thorarinsson, 1977; Dugmore et al., 1995). H3 is the thickest rhyolitic tephra layer in HVT (8 cm). In VGHV the H3 horizon is thin (0.4 cm) and thick basaltic tephra layers (>1 cm) follow within decades (Fig 5.7f). PC 1 and 2 of the PCAs represent the same processes as indicated during the H4 time series for both lakes, albeit with reversed signs, except for PC 2 in HVT which signifies OM source rather than physical proxies.

Figure 5.4 PCA bi-plots for H3 tephra deposition event indicating component magnitude and direction for lake sediment proxies: %TOC, C:N, $\delta^{13}C$, MS, and density. Small/large numbers indicate data points early/late in the 400 year time series. Data point immediately after tephra horizon of interest is circled in blue. Periods of tephra disturbance are circled in brown. a. VGHV; b. HVT.

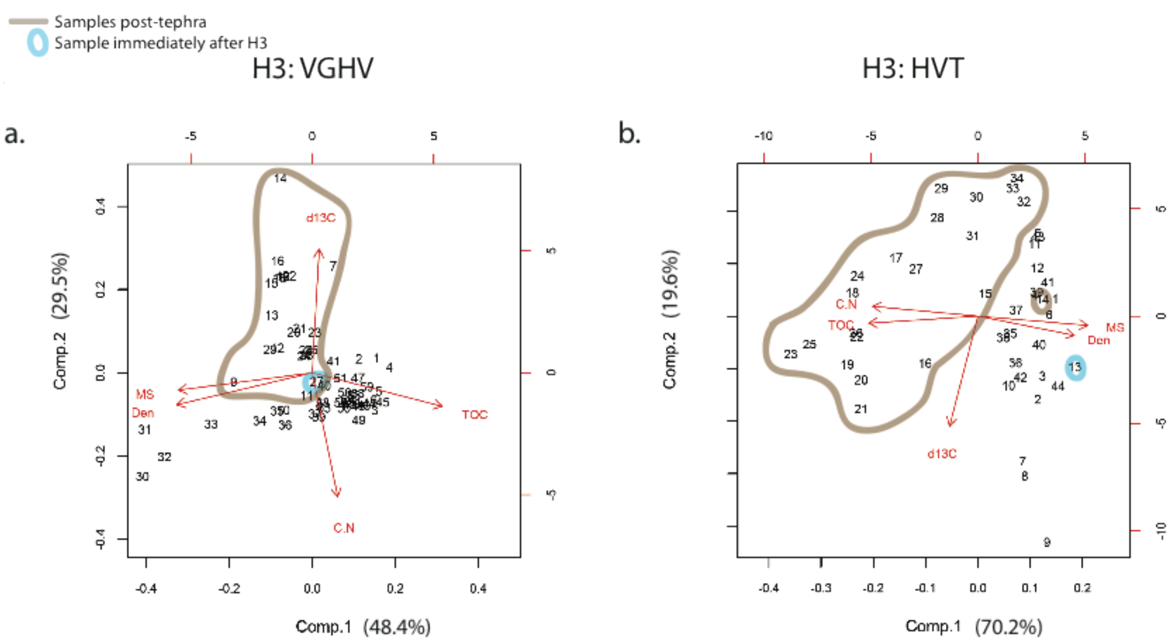

In VGHV significant disturbance related to a different rhyolitic tephra horizon approximately 150 years before H3, increasing the minerogenic sediment flux and depressing the lacustrine ecosystem to an alternative stable state that persisted until shortly after the H3 tephra horizon. Several decades after H3 two thick basaltic tephra layers are followed by a gradual decrease in the minerogenic component of the sediment attaining pre-disturbance stability within 100 years and improved lacustrine primary productivity extending for the remainder of the time window (Fig 5.7b, d).

In HVT a substantial influx of OM in to the basin occurs following deposition of the H3 tephra with elevated catchment erosion enduring for approximately 100 years (Fig 5.7b, d). PC 2 is controlled by fluctuations in $\delta^{13}C$, density, and %TOC indicating an increased abundance of terrestrial OM entering the lake (e.g. Meyers and Lallier-Vergès, 1999; Larsen et al., 2011) after H3 (Fig 5.4b).

5.6.3 Basaltic Tephra

5.6.3.1 T-tephra (VGHV, HVT, HAK) and Tv-5 (TORF) Layers

The T-tephra (~5650 BP) and Tv-5 (~6600 BP) tephra horizons are thick basaltic layers erupted from the Hekla and Katla volcanic systems respectively during HTM (Björck et al., 1992; Ólafsdóttir, 2010). During this time period all 4 lakes exhibit the most similar proxy relationships, with PC 1 indicating lacustrine primary productivity and PC 2 signifying predominantly OM source in less productive lakes and minerogenic flux in more productive lakes. PC 1 relates best to ecosystem structure and function while PC 2 represents catchment erosion and landscape instability.

Figure 5.5 PCA bi-plots for T-tephra deposition event indicating component magnitude and direction for lake sediment proxies: %TOC, C:N, $\delta^{13}C$, MS, and density. Small/large numbers indicate data points early/late in the 400 year time series. Data point immediately after tephra horizon of interest is circled in blue. Periods of tephra disturbance are circled in brown. a. VGHV; b. HVT; c. HAK; d. TORF.

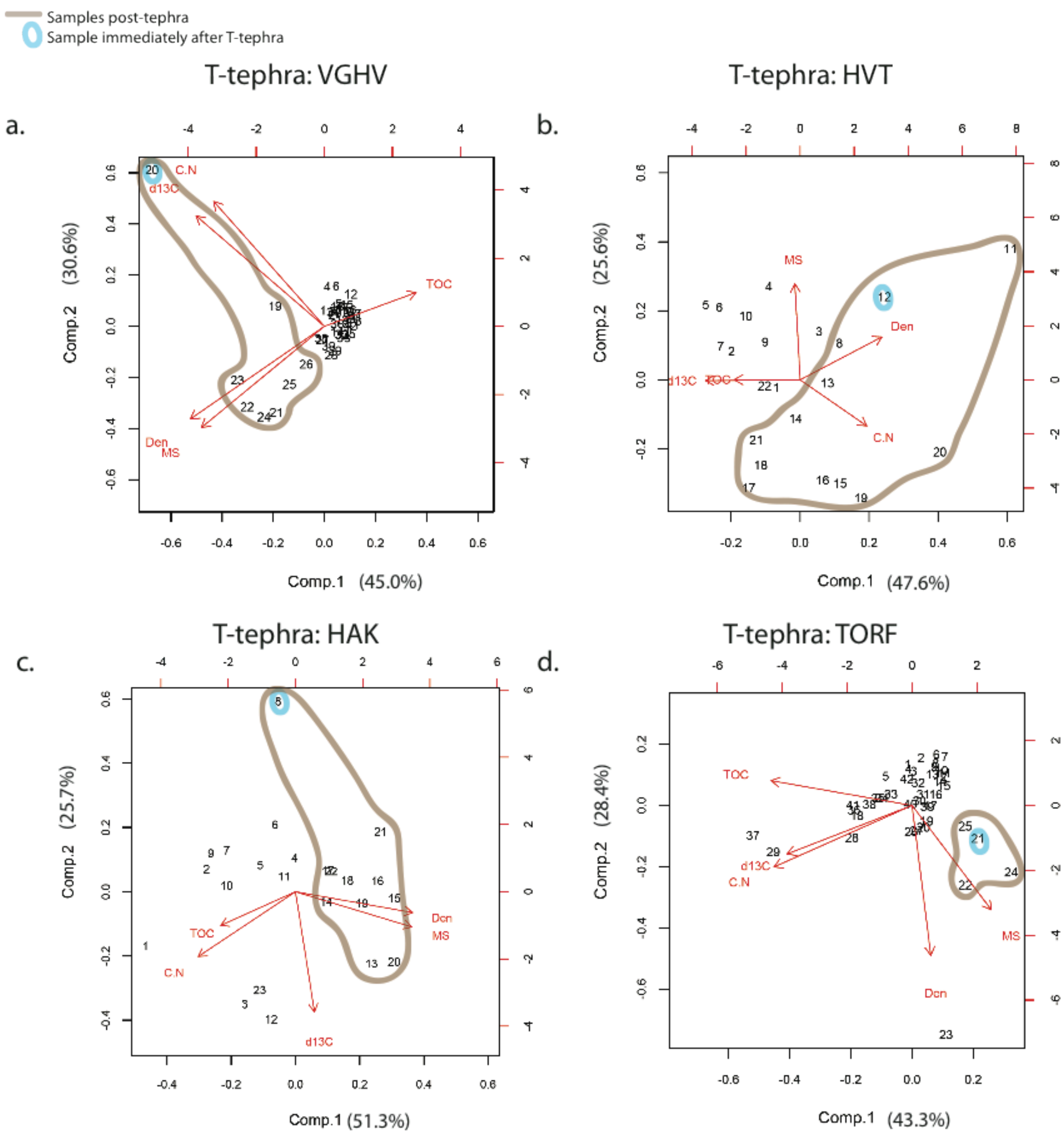

In the PCA bi-plots and time series for VGHV and TORF the T-tephra and Tv-5 horizons are followed by an outlier and data cloud signifying short-lived ecosystem disturbances as indicated by contracted lacustrine productivity and an increased minerogenic flux (Fig 5.5, 5.8a, c). These instabilities last for ~50 years in TORF and ~100 years and VGHV, with the temporal variability likely related to tephra layer thickness in each catchment and the timing of each eruption relative to the end of the HTM.

In HVT an eruption before the T-tephra is associated with early disturbance. However, following deposition of the T-tephra, the HVT ecosystem quickly returns to pre-eruption conditions in PC 1. HAK has no immediate change in PC 1 after the T-tephra horizon suggesting no changes to lacustrine productivity associated with tephra deposition. Both HVT and HAK experience an abrupt and persistent decline in PC 2 signifying a change in OM source that is coupled with elevated variance in PC 1 (Fig 5.8a, c).

5.6.3.2 Katla N Layer (KN)

The KN tephra layer erupted from the Katla volcano (KN: ~3500 BP from Róbertsdóttir et al., (1992)) during the Neoglacial (e.g. Larsen et al., 2012; Geirsdóttir et al., 2013) producing the thick basaltic tephra horizons in VGHV and HVT. The eruption occurred between H4 and H3 (Róbertsdóttir et al., 1992; Dugmore et al., 1995) at a period when the VGHV pollen record is marked by a substantial decrease in birch pollen abundance supporting decades to centuries of relatively cool and short summers (Hallsdóttir and Caseldine, 2005). PC 1 from the KN tephra PCAs indicates primary productivity in VGHV and HVT while PC 2 signifies OM source in VGHV and a combination of the minerogenic flux and OM source in HVT (Fig 5.6, 5.8b, d).

Prior to the eruption of KN, VGHV is relatively stable and productive with a deviation early in the time series controlled by the input of minerogenic material from another tephra fall event. After deposition of the KN tephra physical proxies increase creating a peak in PC 1 followed by a persistent decrease for the remainder of the time series (Fig 5.8b). PC 2 experiences a substantial decrease following KN denoting an influx of terrestrial OM into the basin. However, the PC 2 time series is overlain by a persistent decline suggesting a long-term decrease in lacustrine primary productivity and increasing terrestrial erosion in the catchment (Fig 5.8d).

Figure 5.6 PCA bi-plots for KN tephra deposition event indicating component magnitude and direction for lake sediment proxies: %TOC, C:N, $\delta^{13}C$, MS, and density. Small/large numbers indicate data points early/late in the 400 year time series. Data point immediately after tephra horizon of interest is circled in blue. Periods of tephra disturbance are circled in brown. a. VGHV; b. HVT.

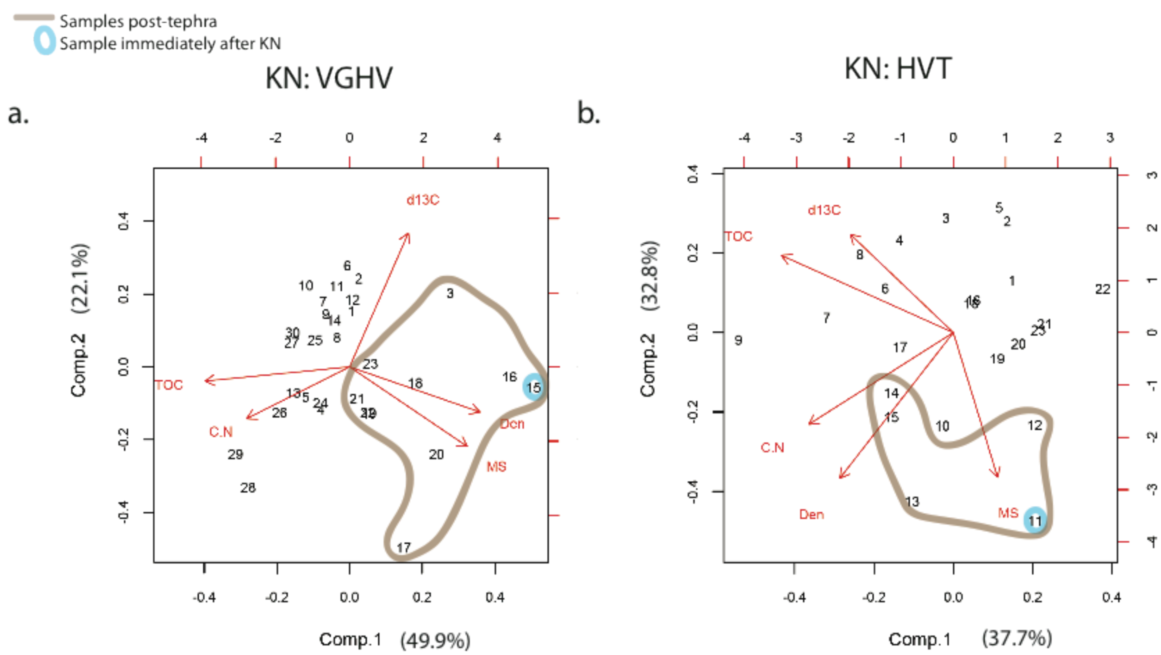

Figure 5.7 400 year PC time series, 200 years before and after tephra horizons of interest for Components 1 and 2 of rhyolitic eruptions H4 and H3 for all four lakes. a. and b. Component 1 before and after H4 and H3 respectively; c. and d. Component 2 before and after H4 and H3 respectively; e. and f. Tephra layer thickness and time of deposition of additional tephra horizons during targeted time windows surrounding H4 and H3, respectively.

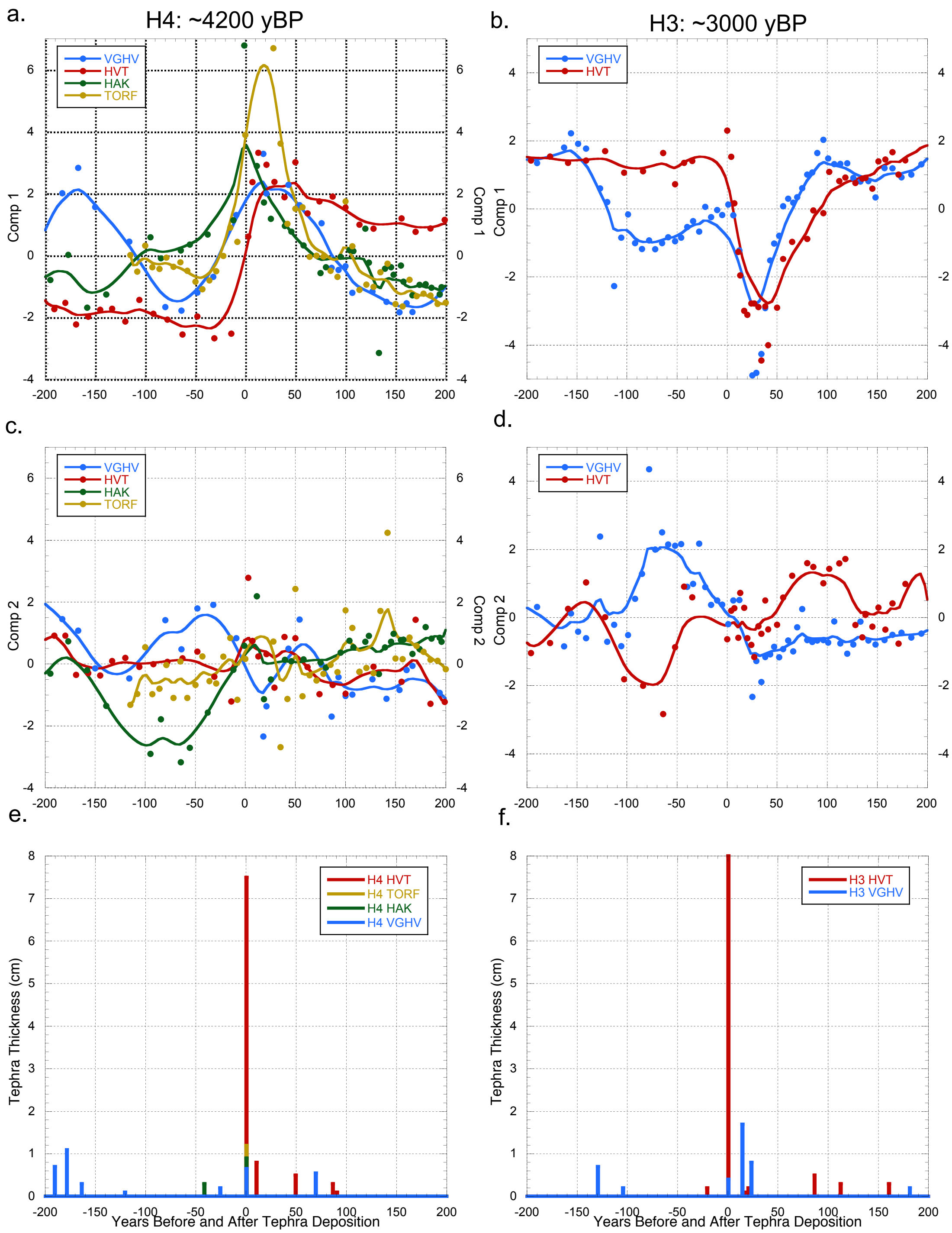

Figure 5.8 400 year PC time series, 200 years before and after tephra horizons of interest for Components 1 and 2 of rhyolitic eruptions T-tephra and KN for all four lakes. a. and b. Component 1 before and after T-tephra and KN respectively; c. and d. Component 2 before and after T-tephra and KN respectively; e. and f. Tephra layer thickness and time of deposition of additional tephra horizons during targeted time windows surrounding T-tephra and KN, respectively.

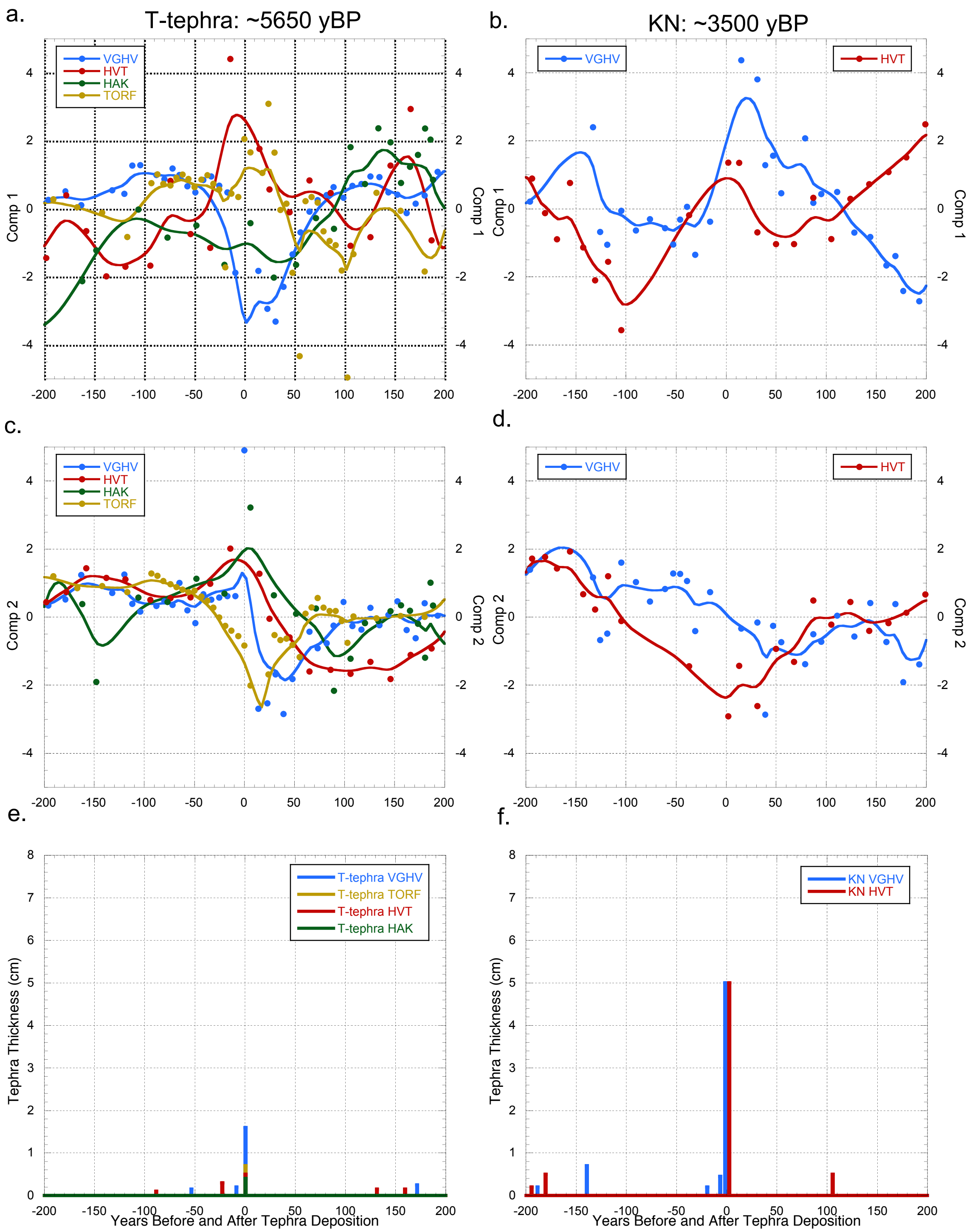

In HVT, the KN tephra produced component relationships more similar to the T-tephra time window. After deposition of the KN horizon PC 1 and 2 indicate a brief period of disturbance followed by a reduced minerogenic flux supporting increased lacustrine primary productivity and/or decreased catchment erosion (Fig 5.6b, 5.8b, d). The juxtaposition between responses to the KN tephra reveals regional variability in lacustrine environments that is dependent on complex relationships between the physical, chemical, and biological processes occurring in the lakes and catchments. Persistent trends observed throughout the time series are likely from a process not related to tephra deposition.

5.7 Discussion of Results

Tephra emission into lacustrine environments produces complex interactions between soil-plant-water systems (Ayris and Delmelle, 2012). A similar proxy response between lakes following comparable eruptions indicates uniformity in the disturbances evoked by tephra deposition following explosive volcanic eruptions. PCA bi-plots and PC time series show significant differences in component responses and relationships between rhyolitic and basaltic tephra fall. Rhyolitic tephra deposition events produce long-lived or irreversible changes in lake proxies signifying reduced primary productivity, landscape instability, and extensive erosion within the catchments. In contrast, basaltic tephra fall creates shorter-lived disturbances followed by a return to the pre-eruption ecosystem state and/or improved catchment stability and increased lacustrine primary productivity that typically persists beyond the time series.

The environmental effects of tephra fall on lacustrine environments are not solely governed by the physical or chemical properties of the tephra itself, but also the unique characteristics of each lake, its catchment, timing, and the duration of eruption and tephra deposition (Ayris and Delmelle, 2012). Modern observations indicate tephra abrades plants, inhibits photosynthesis, kills pollenating insects, increases soil albedo, reduces soil permeability and acidifies soils over short time scales (i.e. hours to months) (Cook et al., 1981; Mack, 1981; Kennedy, 1981; Schulte et al., 1985; Cronin et al., 1997; Wilson et al., 2011). Although, few have studied the long-term implications of tephra deposition, many note tephra rich soils (Andisols) support vegetation and that the deposition of tephra with certain properties may improve soil fertility (e.g. Gisladóttir et al., 2005; Arnalds, 2008a; Long et al., 2011; Ayris and Delmelle, 2012) and contribute limiting nutrients to lakes (Eicher and Rounsefell, 1957; Kurenkov, 1966; Telford et al., 2004).

5.7.1 Dependency on Climate State

We anticipated lake proxy responses to tephra perturbations to have some dependency on the climate state at individual catchments, because harsher climates support less diverse and often more sensitive ecosystems. When delicate ecosystems are pushed past a threshold following tephra fall, adverse climatic conditions can impede recovery back to the pre-eruptive state, producing an alternative equilibrium (i.e. H4 in HVT and HAK) (Lewontin, 1969). From our study we conclude that climate ultimately dictates disturbance length with more (less) persistent and greater (lower) magnitudes of disturbance observed after tephra fall in more sensitive (robust) lakes. Ecosystems are built around the interactions between species based on biological and physiochemical processes. These are dependent on the beneficial or restraining influences of temperature, nutrient availability, and water quality (Estes et al., 2011).

However, despite differences in ecosystem structure between the lakes and catchments used in this study (Tables 6.2 and 6.3) we observe similar multi-proxy responses amongst all lakes to different types of tephra perturbations (Fig 5.7, 5.8). This suggests consistent impacts of tephra fall in lacustrine environments independent of lake and catchment properties (Table 5.1). In general, all lakes produced significant departures in both physical and biological proxy time series following tephra deposition events (Fig 5.3, 5.4, 5.5, 5.6).

The most obvious permanent transition to an alternative ecosystem state occurs at HVT during the H4 time interval (Fig 5.3b, 5.7). Proxies suggest this transition was brought on by increased terrestrial erosion suppressing and likely debilitating primary productivity in the lake and catchment. HVT has the only glaciated catchment and is the highest elevation lake of our study sites (Table 5.1). Higher elevation lakes often have more sensitive ecosystems than lower lakes typically containing reduced biodiversity and closer proximity to biologic thresholds (e.g. Eggermont et al., 2010 and references within). Thus, the HVT catchment is most susceptible to perturbations and the ecosystem is more likely to transition to an alternative stable state following a significant disturbance. Additionally, of the lakes in this study, physical and biological processes in HVT are most closely linked to climate state. Thus the climate signal in the proxies is most apparent in the HVT sediment record.

HAK also undergoes an irreversible transition after H4 with component scores indicating heightened catchment erosion while the more productive lakes (VGHV and TORF) experienced transient decreases in primary productivity. The later is likely from a temporary influx of minerogenic material into the lake associated with tephra deposition and remobilization within the low gradient catchments. Between lakes the HAK catchment has the steepest slopes (Fig 5.1) providing a large region for erosion directly linked to the lake basin contributing to a long signal of disturbance after deposition of the H4 tephra.

Following a tephra horizon, contrasting proxy signals between lakes can have the same implications because climate, lacustrine ecosystems, and lake and catchment geomorphology direct the observed response. In unproductive lakes tephra input is associated with increases, decreases, or no change in physical proxies subsequent tephra layers while in relatively productive lakes both density and MS consistently peak at tephra horizons regardless of composition (Fig 5.3, 5.4, 5.5, 5.6). The high minerogenic background states of HVT and HAK suggest more abundant terrestrial erosion than VGHV and TORF (Table 5.3). This is because the prevalent organic material preserved in the sediments of VGHV and TORF is not diluted indicating abundant autochthonous primary productivity.

From our observations we determine that lake altitude, relative size and depth, and catchment size greatly influence sediment proxy signals with the most ecologically sensitive lake producing the most extreme responses to tephra fall. However, despite differences in climate state all lakes display some measure of disturbance following significant tephra deposition. This consistency is likely related to controlling parameters other than local climate.

5.7.2 Dependency on Tephra Composition

We expected to observe distinct differences in multi-proxy responses between rhyolitic and basaltic tephra deposition. Most lakes had different responses in physical and OM proxies to the two tephra compositions. This was most notable in HVT, our most sensitive lake, and least apparent in VGHV, the lake with the greatest proxy variability. Biological and physical proxy responses in the two unproductive lakes, HVT and HAK, suggest prolonged landscape disturbance with a reduction in terrestrial vegetation cover, increased erosion, and depression of aquatic primary productivity following deposition of the thick rhyolitic tephra layers. This behavior is still apparent but less dramatic in the productive lakes VGHV and TORF. Following thick basaltic tephra layers all lakes indicate short-lived landscape and ecosystem disturbances followed by either heightened aquatic primary productivity or no change from the pre-tephra background state.

The rapid weathering of tephra results in high concentrations of Al, Si, and Fe in tephra rich Andisols. Climate and tephra composition both contribute to the rate of weathering and soil characteristic with faster rates observed in more humid climates (Arnalds, 2008a). Basaltic tephra has a mafic composition characterized by high Fe, Ca, and Mg and low K and Na with 45 to 55% SiO_2 while rhyolitic tephra is felsic in composition with 65 to 75% SiO_2, low Fe and Ca, and high K and N. High dissolution rates of basaltic tephra releases an abundance of cations that maintain soil pH (Guichararnaud and Paton, 2005; Arnalds, 2008a) after tephra fall. In places such as Iceland where the eruption of basaltic tephra is frequent (Larsen and Eiriksson, 2008) soils are buffered by weathering of newly deposited materials (Arnalds, 2008a). The abundance of basaltic tephra fall events has thus made mafic tephra the main component in Icelandic soils (Arnalds et al., 2012). Meanwhile, rhyolitic tephra weathers more slowly with less abundance cations and greater release of water-soluble mineral acids resulting in soil and surface water acidification (Ayris and Delmelle, 2012). Soils dominated by more silicious parent materials also maintain vitric characteristics for longer periods of time contributing to reduced cohesion and great variability in soil fertility (Arnalds, 2008a, b). Reduced photosynthesis, plant decay, and soil erosion are all consequences of environmental acidification (Kilian et al., 2006; Ayris and Delmelle, 2012). While plant communities living in and around the lakes of this study (Table 5.1) are adapted to the relatively acidic soils of Iceland abrupt changes in the background soil pH and physical abrasion can produce long-lived damage to catchment vegetation.

We observe improved aquatic primary productivity in most lakes within ~100 years of basaltic tephra fall but no change or decreased lacustrine productivity following rhyolitic tephra deposition events (See Table 5.2 for geochemistry of primary tephra layers in this study). Tephra can be a direct source of nutrients for phytoplankton especially in lake systems limited in essential nutrients (Eicher and Rounsefell 1957; Kurenkov 1966). In small lakes diatom productivity and speciation is sensitive to periodic perturbations created by volcanic eruptions (Abella 1988; Barker et al. 2000). Studies have indicated increases in diatom abundance or adjustments in speciation following deposition of tephra layers attributing changes to shifting siliceous/non-siliceous primary productivity related to alterations in water column Si/P ratios. Additionally, cohesive tephra deposits on lake bottom sediments may limit certain species of diatoms by creating impermeable barriers that inhibit nutrient exchange across the water-sediment interface reducing benthic P recycling (Barker et al. 2000; Telford et al. 2004). As we have no high-resolution diatom or biogenic silica data for out time windows it is impossible to make definitive statements about changes in algal communities. However, our data suggests smaller lakes and catchments are more likely to have a signal of improved aquatic primary productivity within ~100 years of basaltic tephra layers while rhyolitic tephra appears to be detrimental to the landscape skewing stable isotope and C:N signals toward terrestrial sources.

While all tephra deposition events indicate landscape disturbance, tephra composition is important in controlling the temporal response of lacustrine ecosystems. Silicic (rhyolitic) explosive eruptions are associated with lower density tephra and a larger proportion (up to a factor of 10) of fine tephra as compared to basaltic eruptions (Rose and Durant, 2009). Tephra grain size and density are important properties controlling tephra residence time in the atmosphere, water bodies, and to a certain extent on soil surfaces. Thus, fine-grained particles are more likely to remain suspended in a fluid, traveling further distances and more readily remobilizing (e.g. Bonadonna et al., 1998; Wilson et al., 2011). Coarse tephra can be deposited within days, hours, or minutes while fine tephra may take weeks, months or even years to be removed from the atmosphere (Ayris and Delmelle, 2012). In this study, for purposes of our age models and time series we approach tephra deposition as an instantaneous event but recognize this assumption is not entirely true. However, it can be inferred that fine-grained rhyolitic tephra is more likely to travel further, remain in the atmosphere longer, and more easily remobilize on a landscape than coarser grained and denser basaltic tephra.

Wind erosion, resuspension of tephra, and secondary tephra fallout events are often a dominant process on a post-eruptive landscape for a prolonged period of time (Wilson et al., 2011; Ayris and Delmelle, 2012). Redeposition of a primary tephra layer into thicker consolidated deposits has been observed to occur between a few weeks and multiple years following an eruption. Aeolian mobilization of the unusually fine grained andesitic tephra deposited in 2010 by the Eyjafjallajökull volcano created episodes of poor air quality in Reykjavík, Iceland, ~100 km away, that were considered of equal or greater significance to air quality than the initial tephra fallout (Davies et al., 2010; Karlsdóttir et al., 2012; Thorsteinsson et al., 2012). This supports significant redeposition of the thick rhyolitic tephra layers H3 and H4 occurring for an extended period of time after initial deposition contributing to extensive landscape destabilization and erosion over broad areas. While the basaltic tephra layers examined in this study also experienced some remobilization it is unlikely to have been of the same magnitude as the rhyolitic tephra as the disturbances in the proxy record were shorter lived.

Our observations indicate that of the large tephra deposition events analyzed for this study, the rhyolitic tephra horizons, H3 and H4, are associated with more significant impacts on terrestrial and lacustrine ecosystems than the basaltic tephra layers, KN and T-tephra. This supports ecosystem disturbances related to tephra fall events have strong dependency on tephra composition with the more acidic and mobile rhyolitic tephra devastating landscapes to a greater degree and for longer periods of time than basaltic tephra.

5.7.3 Temporal Evolution of Climate and Ecosystem Sensitivity

We predicted an amplification in the extent of disturbance produced by individual tephra fall events as climate progressed from warmth of the HTM in the early Holocene to the cooler summers of late Holocene Neoglaciation. Both rhyolitic tephra deposition events take place at the same timing as significant Holocene cooling. Neoglaciation began in Iceland ~5.5 ka, intensifying at ~4.2 ka continuing into the present (Larsen et al., 2012; Geirsdóttir et al., 2013). Thus, H4 (~4.2 ka) marks the beginning of a strengthened Neoglacial period while H3 (~3 ka) occurs well into the Neoglacial at a time of icecap expansion (Larsen et al., 2011; 2012; Geirsdóttir et al., 2013). The Neoglacial was a time of cold and short summers, where windy conditions and changes in vegetational communities greatly contributed to soil erosion across Iceland (Gudmundsson, 1997; Hallsdóttir and Caseldine, 2005; Geirsdóttir et al., 2009a, Larsen et al., 2012). The transition into heightened Neoglaciation is marked by a change in proxy relationships after the H4 eruption in the unproductive lakes, HVT and HAK (6.2). This shift in proxy values indicates a greater component of terrestrial carbon preserved in the sediment suggesting increased landscape instability. It is important to recognize that at this time sedimentation rate abruptly increases in both lakes altering the carbon flux which make %TOC post-H4 an unreliable proxy for lacustrine primary productivity (Larsen et al., 2012; Geirsdóttir et al., 2009a; 2013). VGHV and TORF meanwhile show short-lived disturbances from the H4 tephra horizon in which neither lake was pushed over a critical ecosystem threshold thus both returned quickly to pre-tephra conditions.

The rhyolitic H3 tephra erupted during the Neoglacial with proxy signals in HVT eliciting similar responses to what was observed post-H4 (Fig. 5.7). Meanwhile, VGHV did not react to H3 as the tephra was extremely thin. Several decades after H3, fallout of thick basaltic tephra layers is followed by proxy signals supporting improved aquatic primary productivity. As the Neoglacial was highly variable at VGHV (Chapter 4) it is not surprising that the time windows surrounding targeted rhyolitic tephra horizons do not indicate exceptionally cold temperatures.

The HTM is well represented in the Icelandic lake records. It began in Iceland at ~7.9 ka transitioning into Neoglaciation between 6.0 ka and 5.5 ka (Caseldine et al., 2006; Larsen et al., 2012; Geirsdóttir et al., 2013; Chapter 4). The T-tephra (~5650 BP) (Ólafsdóttir, 2010) and Tv-5 tephra (6.6 ka) (Björck et al., 1992; Kristjánsdóttir et al., 2007) erupted during this time of relative warmth, low sedimentation rates, and high autogenic production. Langjökull was absent from the HVT catchment and proxy relationships indicate HVT and HAK were behaving in similar manners (Geirsdóttir et al., 2013). Proxy associations in VGHV and TORF meanwhile reveal stable catchments and productive lacustrine ecosystems (Axford et al., 2007; Chapter 4). Thus, the lakes and their responses to the basaltic tephra perturbations from the T-tephra and Tv-5 were most similar during the HTM with the tephra fallout doing little to destabilize ecosystem structure and function.

The other basaltic tephra of our study, KN (~3.5 ka) (Róbertsdóttir, 1992) was erupted during Neoglaciation. In VGHV, Neoglacial cooling overrides any ecosystem benefit from fallout of the basaltic tephra. After recovering from the initial tephra disturbance proxies in VGHV show an increase in %TOC and C:N coupled with a long-term decrease in $\delta^{13}C$ (Fig 5.6). The delayed response and extended duration cannot be attributed to any tephra layers. Proxies suggest an influx of terrestrial carbon into the basin in collaboration with reduced aquatic primary productivity, signals attributable to persistent cooling in the catchment throughout the time series window. HVT indicates a different multi-proxy signal after deposition of the KN tephra with a decreasing trend of %TOC and C:N supporting increased aquatic primary productivity and/or decreased terrestrial erosion. This suggests despite the relatively cool summers of the Neoglacial period deposition of a thick basaltic tephra improved ecosystem structure and function in HVT while doing little to directly benefit or damage ecosystem processes in VGHV.

Our results allow us to assert that Neoglaciation does have a substantial effect on the response of lakes to tephra fall events. The most stable terrestrial and lacustrine ecosystems are associated with greatly lessened landscape disturbance and faster recovery from tephra perturbations in all time periods. As the intensity of Neoglaciation varied between locations responses to tephra fall are as expected and variable between study sites.

5.7.4 Season of Eruption

The season of eruption likely has great influence on the extent of disturbance to lacustrine and terrestrial ecosystems from tephra deposits on a landscape as tephra, regardless of composition, is highly abrasive killing most surface vegetation via smothering, abrasion, or acidification of the soil pore water (Cook et al., 1981; Mack, 1981; Kennedy, 1981; Cronin et al., 1997; Wilson et al., 2011; Payne et al., 2013). Volcanic ash contains many chemical species including but not limited to F, SO_4, Ca, Mg, Na, K, Al, Fe, Mn, Zn, etc. that can leach into soil with often negative effects on microorganisms, soil pH, salinity, nutrient availability and the solubility of heavy metals in soils making it difficult for plants to grow or reestablish once destroyed (Witham et al., 2005; Aryis and Delmelle, 2012). This process is normally short lived, lasting days to months following tephra deposition (Myers 2011). We cannot observe those time scales with our sediment records but substantial tephra fall at sensitive times in vegetational and lake seasonal cycles, such as early in the growing season, could initiate positive feedbacks weakening ecosystems extending disturbances to temporal scales relevant for our purposes.

5.7.5 Volume of Tephra Entering the Basin and Catchment

We anticipated thicker (thinner) tephra deposits to be associated with longer (shorter) and more (less) significant ecosystem perturbations due to increased initial disturbance to plant communities and greater (reduced) probability of remobilization and secondary deposition events. Latitude has no direct bearing on the properties of each lake (Table 5.1) but proximity to the active tephra producing volcanic centers greatly influences responses to tephra fall in PCA bi-plots and PC time series. The Hekla and Katla volcanoes from which the T-tephra, H4, and H3 tephra horizons and Tv-5 and KN tephra horizons originated respectively (Jóhannsdóttir, 2007; Jagan, 2010) are located in south Iceland in the Eastern Volcanic Zone (EVZ) (Thordarson and Larsen, 2007). Tephra plumes typically blow north and east from these eruptive centers due to the prevailing wind directions in Iceland (Lacasse et al., 1998; Carn et al., 2008) so the northwestern lakes of our study only capture the largest and most widespread events. Previous studies have shown that most tephra layers are not widely dispersed and the same tephra layers are often not represented in even the most proximal lakes (Jóhannsdóttir 2007; Larsen and Eiríksson, 2008; Jagan 2010).

The most prominent physical impact of tephra comes from mobile ash damaging and detaching vegetation exposing bare soil. Wind and water are the primary erosive processes removing tephra from vegetative surfaces (Arnalds et al., 2012) with the surface roughness of vegetation greatly affecting particle retention and abrasion (Cook et al., 1981). When soils are stripped of vegetation terrestrial plants must reestablish quickly or erosion will initiate a positive feedback. Additional disturbances from the remobilization of tephra, other tephra fall events and/or changes to climate make plant regrowth difficult instigating rapid removal and transport of soil over potentially long distances (Óskarsson et al., 2004). Gisladóttir et al, (2005) observed aeolian processes near Langjökull were most effective where the proportion of loose materials was high and surfaces relatively flat. The increase in %TOC and C:N and change in $\delta^{13}C$ in HVT following the rhyolitic tephra layers (Fig 5.3b, 5.4b) is most likely from widespread soil erosion and aeolian transport in the region during the cold and windy Neoglacial. The smaller and less persistent changes observed at the other lakes is probably related to more abundant catchment vegetation making it difficult for tephra perturbations to permanently destabilize the landscape.

Tephra deposition on the soil surface can be devastating to plant and soil microbial communities. First tephra lacks organic carbon and nitrogen thus, complete burial of vegetation under a thick deposit limits the ability of nutrients to enter the soil surface and increases erosion via abrasion. Eroded material then contains a significant minerogenic component from the tephra diluting OM (del Moral and Grishin, 1999). This dilution explains the decrease in %TOC in nearly all lakes immediately following rhyolitic and basaltic tephra horizons. The HVT system is the anomalous as %TOC increases following the rhyolitic eruptions due to the substantial input of soil carbon (Larsen et al., 2012).

The residence time of tephra on soil is controlled by the intensity of aeolian or fluvial erosion, deposit cementation and stabilization by emergent vegetation. The erodibility of tephra deposits is partially dictated by particle size distribution as finer rhyolitic tephra may be more easily entrained by wind and surface runoff (Stout, 2004). However, a caveat is that fine grained tephra can stabilize a deposit via cementing but that phenomena was not supported by our study and likely varies greatly between locations. Plant regrowth also helps to stabilize fresh tephra deposits. After the 1980 eruption of Mt. St. Helens in Washington, USA and the 2010 eruption of the Eyjafjallajökull volcano in Iceland it was observed that most herb and shrub species persevered through tephra deposits up to 40 to 45 mm thick (Aryis and Demelle, 2012). A similar process likely explains the lack of disturbance or rapid recovery following thin secondary tephra horizons in VGHV and HVT.

Little information or consensus is available regarding the effect of tephra fall on wetland vegetation. Some studies have linked vegetation change to tephra deposition events (Dwyer and Mitchell, 1997; Edwards and Craigie, 1998) while others suggest limited disturbance (Hotes et al., 2006; Payne et al., 2013). A pollen record from VGHV indicates transitions in vegetation assemblages in both lacustrine and terrestrial ecosystems post-H4 (Hallsdóttir and Caseldine, 2005). Theses changes are likely a response to catchment destabilization from tephra deposition and the cooler and more variable summer temperatures of the Neoglacial climate. No clear change or transition appears subsequent H3 agreeing with observations in the proxy record. On both sides of the KN tephra horizon, low birch pollen is pronounced supporting our proxy evidence that climate was relatively cool at this time around VGHV (Hallsdóttir and Caseldine, 2005).

While the initial effects of tephra fall directly into water bodies are short-lived, erosion from the surrounding catchment in the following weeks, months or even years can result in sustained impacts on the turbidity of lake water. Transient increases in turbidity due to the presence of suspended particles in the water column have been shown to reduce light penetration and impact photosynthetic activity (Grobbelaar 1985; Dokulil, 1994). Subsequent the 1980 eruption of Mt. St. Helens lakes distal to the volcano indicated an increase in turbidity after which the tephra formed a well-consolidated mat overlying lake bottom sediments (Lee, 1996). Increased water column turbidity probably accounts for immediate changes in C:N and %TOC following tephra deposition. In TORF, C:N increases while %TOC and $\delta^{13}C$ decreases post-H4 suggesting reduced aquatic productivity coupled with an influx of terrestrial OM and minerogenic material. Variability in the post-H4 signal suggests a period of tephra remobilization extending for decades (Fig 5.7). As TORF is small and shallow (Table 5.1) increased water column turbidity would alter ecosystem structure and function until mobile sediment was removed from the catchment. In larger lakes suspended sediment is less important and changes in C:N are more likely related to modifications in sediment source rather than within lake primary productivity.

As HVT is the only glaciated catchment in our study additional complications can arise during tephra emission events as tephra deposition on snow and ice can reduce albedo enhancing ablation rates (Brock et al., 2007) unless the tephra layer is thick enough to produce an insulative rather than ablative effect. On Eyjafjallajökull, a glacier in southern Iceland Kirkbride and Dugmore (2003) determined a tephra thickness of 15 to 40 mm from the 1947 Hekla eruption reduced the relative ablation rate of underlying glacier ice by 50 to 75% respectively. Meanwhile thin tephra layers produce the opposite effect and increase ablation. This was apparent after the 2010 Eyjafjallajökull eruption as Mýrdalsjökull, the glacier covering Katla, was blanketed with a thick tephra layer insulating the ice but Torfajökull and Tindfjallajökull, small glaciers near the eruptive center, were only covered with thin tephra and ice loss accelerated until older insulative layers were exposed (Gudmundsson et al., 2011). In 2010 and 2011 thin layers of tephra on Langjökull also contributed to ablation rates greater than anything observed since measurements began (Pálsson et al., 2012). In HVT, tephra fall likely had positive or negative effects on glacier mass, with both scenarios potentially increasing the abundance of glacially derived sediment in the lacustrine record. Significant icecap expansion of Langjökull is implied in the proxy record at 4.2 ka and 2.9 ka corresponding the thick, light colored H4 and H3 tephra horizons respectively (Larsen et al., 2012). No glacier response is observed following fallout of the thick basaltic T-tephra or KN tephra layers. However, they are dark colored likely producing different albedo effects on the ice surface.

The thickness of tephra horizons is important relative to the length and extent of disturbance. However, layer thickness appears to be less significant than tephra composition, climate state, and site properties in determining the multi-decadal impact of substantial tephra deposition events. All tephra fall events influence lake and catchment ecosystem stability with thicker deposits producing longer signals of perturbation.

5.7.6 Interval of Time Between Tephra Deposition Events

We expected secondary tephra layers in targeted time windows to alter the signals associated with deposition of the tephra horizons of interest. Due to their proximity to the active volcanic centers of Iceland VGHV and HVT contain not only the tephra horizons of interest but numerous other layers. A lack of signal or unpredictable changes in some proxies at certain time periods can be explained using the variability between lake ecosystems and presence of additional tephra layers. The best examples of the later occur in the H3 and H4 PC time series for VGHV (Fig 5.7). In the H4 time series a basaltic tephra layer ~75 years after the H4 tephra horizon (Fig 5.7e) initiates an increase in %TOC, decrease in C:N and increase in $\delta^{13}C$, signals representative of high aquatic primary productivity. This suggests the basaltic tephra layer reset the system following the tephra disturbance from the rhyolitic H4 tephra. Additionally, a rhyolitic eruption early in the H3 time series (Fig 5.7f) is followed by low %TOC, high C:N, and low $\delta^{13}C$, an indication of instability in catchment ecosystems. Proxy responses subsequent H3 do not indicate prolonged disturbance to the system possibly related to the deposition of two thick basaltic tephra layers shortly after H3 improving ecosystem productivity (Fig 5.7b, d).

VGHV often has layers comparable in thickness to the targeted horizon within the 400 year time window while additional layers in HVT are relatively thin. Because of this, disturbances from auxiliary tephra horizons are inconsequential in HVT and prevalent in VGHV often overprinting any sign of perturbation from the tephra horizon of interest. Hence, VGHV has considerably more variability in its proxy signals than the other lakes. However, the rapid response times in VGHV and TORF, the most comparable lake in this study, suggest VGHV is no more adapted to tephra disturbances than lakes distal to the active volcanic centers. This indicates that the abundance of tephra fall events within a short period of time is not associated with improved ecosystem reliance but rather additional disturbances.

5.8 Conclusions

By conducting this study we are able to reach several conclusions allowing us to predict lacustrine ecosystem responses to large tephra deposition events. High-resolution multi-proxy records from the lakes in our study indicate all substantial tephra deposition events, regardless of geochemistry produce responses that persist for decades to centuries. Between the two tephra geochemical endmembers represented rhyolitic tephra was more disruptive to the landscape than basaltic tephra, with basaltic tephra sometimes appearing to improve lake and catchment productivity. Complicated relationships between physical, biological, and chemical processes including but not limited to; the contribution of limited nutrients to the lake and catchment, reduced remobilization of tephra post eruption, and improving landscape stability through soil development and plant growth likely explain this phenomenon. Tephra was most effective at producing long-lived disturbances in large unproductive lakes when climate conditions had shifted from relatively warm to relatively cool. Smaller lakes with greater background primary productivity and relatively thick, well-vegetated soils mantling low-relief catchments were able to return to pre-eruption ecosystem stability within 100 years of significant tephra fall events. Our observations indicate rhyolitic tephra deposition on relatively steep slopes with thin soils during episodes of decreasing summer temperatures have the highest probability of producing sustained transitions into less ecologically productive states.

CHAPTER 6: LONG TERM PROXY RESPONSE TO RHYOLITIC TEPHRA PERTURBATIONS IN HVÍTÁRVATN

6.1 Physical Setting

For a general location description of Hvítárvatn (HVT) refer to Chapter 5 (See Fig. 6.1).

Figure 6.1 a. Topographic location map of Hvítárvatn and its position in Iceland (gridlines on map are 1 km^2 scale). Multibeam survey results (Geirsdóttir et al., 2008) have been superimposed on the lake. Note the Hvítárnes delta on the eastern shoreline. b. Bathymetric map of Hvítárvatn obtained from a multibeam survey, cooler/warmer colors indicate deeper/shallower water depth. c. Location relative to Langjökull and approximate catchment size. Images unaltered from Geirsdóttir et al., (2008); Larsen et al., (2011); (2012).

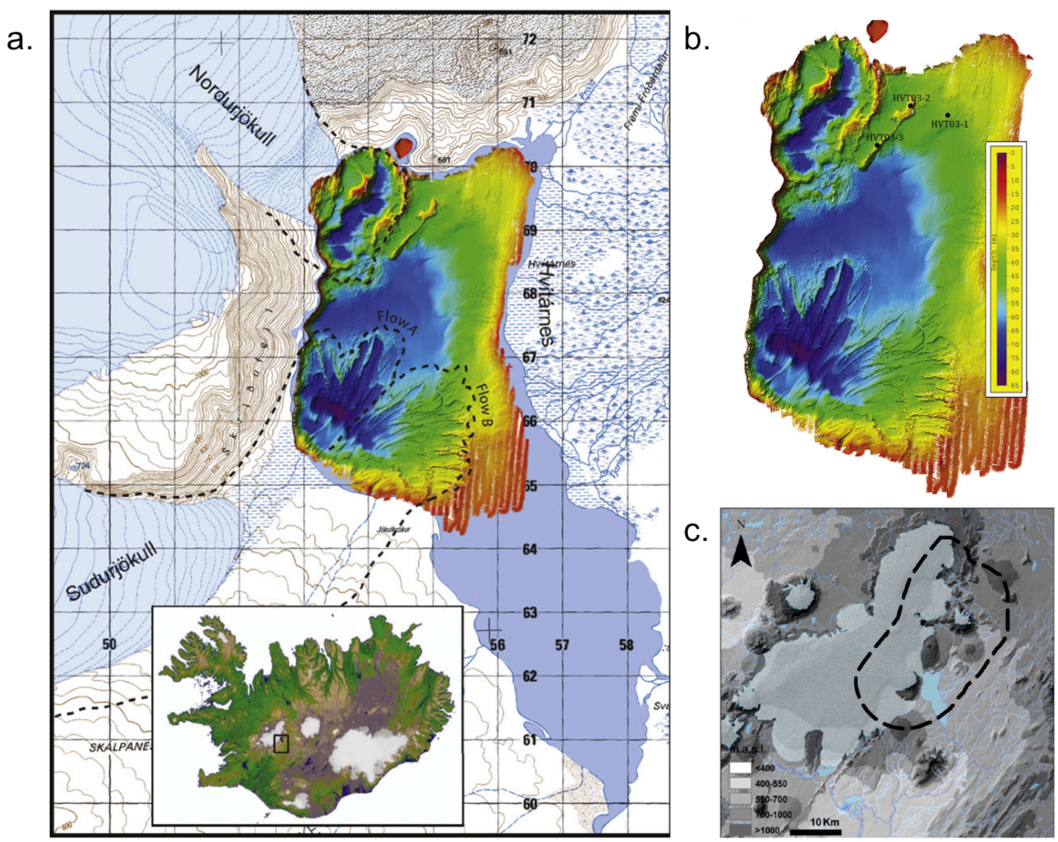

6.2 Aims and Objectives

Hekla 3 (H3) and Hekla 4 (H4) are the most substantial rhyolitic tephra horizons within the HVT sediment cores. H3 (~3000 BP from Larsen et al., 2011) is considered the most severe eruption of the Hekla volcano during the Holocene producing ~12 km^3 of ejected material while H4 (~4260 BP from Dugmore et al., (1995)) produced ~9 km^3 of tephra (Larsen and Thorarinsson, 1977). Eruptions of this magnitude occur in Iceland with a frequency on the order of 10^3 to 10^5 years (Thordarson and Larsen, 2007) and thus H3 and H4 are anomalously large and unique in the Holocene. The time following H3 and H4 at HVT is notable for significant periods of paleoenvironmental variability in the Holocene record with long lasting changes in both physical and organic matter (OM) proxies (Larsen et al., 2011; 2012). As HVT is a high elevation lake in a fragile landscape after deposition of these significant rhyolitic tephra layers we anticipate the large and sustained disturbances in the proxy record to suggest changes in landscape stability and ecosystem structure in the lake and catchment.

As we desired to eventually compare the multi-proxy responses between lakes following substantial tephra fall events it was important to determine disturbance longevity and how each was expressed in the proxy record for HVT, the most “sensitive” lake in our selected array. In answering these questions we hoped to attain a better understanding of an appropriate time window for high-resolution sampling around targeted tephra horizons. We chose to examine 1000 year time series, 500 years on either side of the tephra horizons, for significant physical and OM proxy to compare the response of H3 and H4 in the proxy record. The data is decadal to multi-decadal in resolution providing a high-resolution look at paleoenvironmental conditions before and after tephra deposition. For this review we asked three questions. 1. Are the responses to each tephra anomalous, or do other perturbations within these time frames produce changes of equal or greater magnitude? 2. How quickly does HVT return to pre-eruption proxy values, if it returns at all? 3. Do H3 and H4 exhibit similar responses in proxy signals and their magnitudes?

6.3 Methods

For detailed descriptions of age model development, sampling, and sample processing of physical and OM proxies and tephra horizons in HVT refer to Larsen et al., (2011; 2012).

6.4 Results

Time series data of %TOC and C:N show nearly the same signals before and after the tephra horizons of interest (Fig. 6.2 a, b). In HVT, %TOC has been shown to represent the influx of terrestrial carbon eroded from the landscape rather than in lake primary productivity (Larsen et al., 2011, 2012). C:N meanwhile tells the relative abundance of terrestrial versus aquatic OM preserved in the lake sediment (Meyers and Teranes, 2001). %TOC and C:N in the 300 years before H4 is fairly constant, with values of approximately 0.3% and 6 respectively. A gradual decreasing trend is evident in the initial 200 years of the time series. However, this appears to be within the range of natural variability and C:N is constant indicating no change in the relative proportions of terrestrial erosion and aquatic productivity. The 500 years prior to H3 also have low

Figure 6.2 1000 year time series of biological and physical proxies in HVT surrounding rhyolitic tephra horizons, H3 and H4. Solid red circles represent H3 while open circles represent H4. Solid black lines signify a 10% smoothing through the data. a. %TOC; b. C:N; c. $\delta^{13}C$; d. MS; e. Density

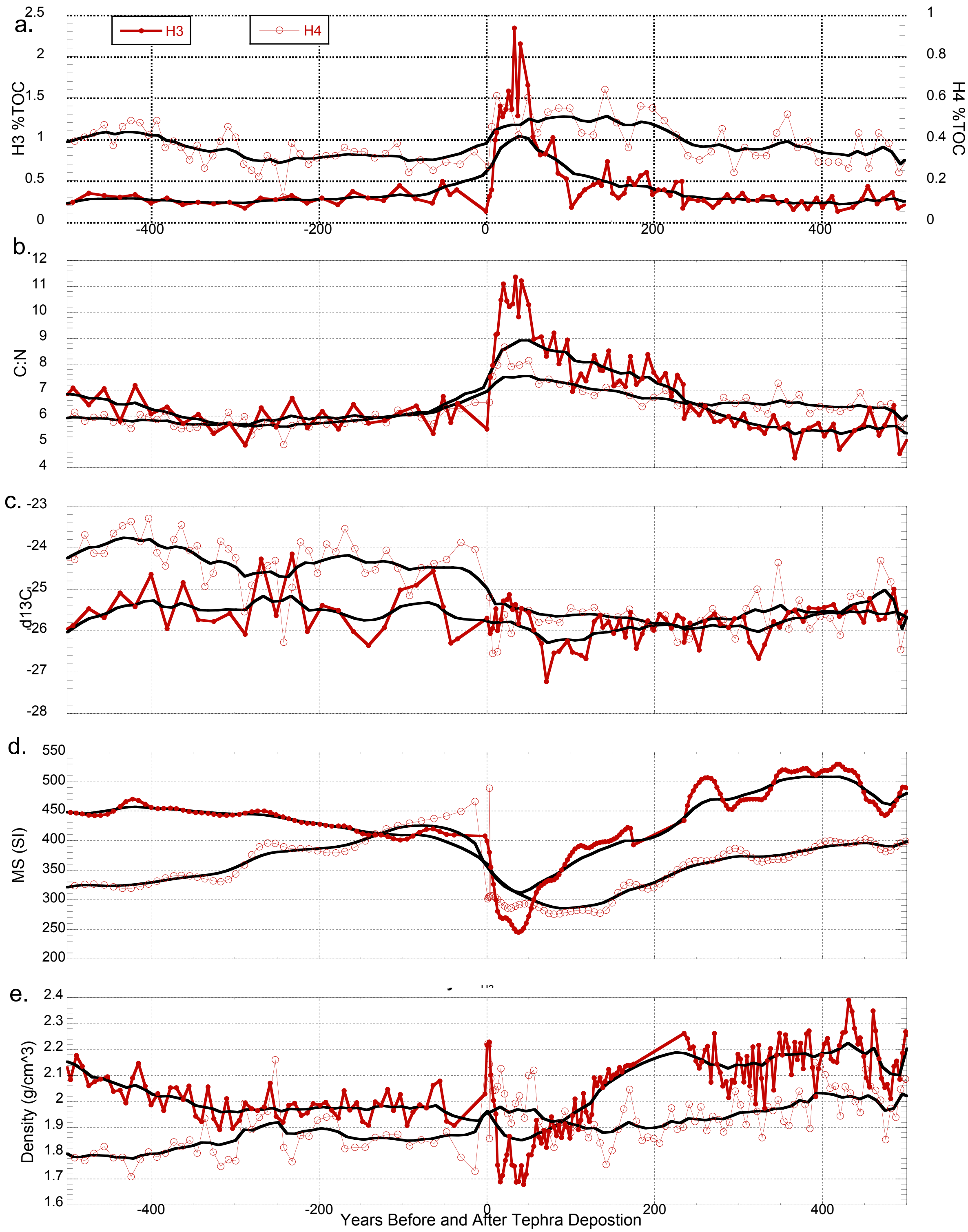

values of %TOC and relatively stable C:N (0.3% and 6 respectively) with slightly more variability in the data than observed in the H4 time series.

On a first order, both H3 and H4 time series show a remarkable increases in %TOC and C:N immediately after the tephra horizons. While the responses following H3 are significantly greater in magnitude than those after H4, elevated proxy signals in the H4 time series extend for a substantially longer period of time. After H4, %TOC is elevated for over 200 years before returning to pre-eruption values within approximately 250 years. C:N peaks immediately after H4 and is followed by a gradual decline with elevated values extending for the remainder of the time series. Meanwhile, increased %TOC persists for approximately 50 years after H3 before experiencing a two-stage decline back to pre-tephra values. The first stage extends ~50 years with %TOC returning to elevated levels similar to those observed after H4. This is followed by a gradual decline over 150 years returning %TOC to pre-tephra values within 250 years of H3. C:N also displays a two-step decrease at the same transition times as %TOC attaining below pre-eruption values with 250 years of H3.

Stable carbon isotopes ($\delta^{13}C$) in HVT indicate variations in the proportion of terrestrial OM washing into the lake rather than changes in lacustrine primary productivity or nutrient availability (e.g. Langdon et al., 2010; Larsen et al., 2011; 2012). $\delta^{13}C$ values are fairly consistent prior to the H3 and H4 tephra horizons (Fig. 6.2c). An abrupt negative shift of ~1.5‰ to a new average occurs after H4 persisting for the remainder of the time series. No significant change occurs immediately post-H3 however a decrease of ~1‰ over ~50 years corresponds with the initial decline in C:N and %TOC from the extremely elevated post-H3 values. After this dip $\delta^{13}C$ slowly returns to pre-H3 values over the remainder of the time series.

HVT has a glaciated catchment thus, MS and density are assumed to increase (decrease) with increasing (decreasing) glacial erosion (e.g. Leonard, 1997; Dahl et al., 2003; Rosenbaum et al., 2012). However, rhyolitic tephra can less dense than the minerogenic material eroded from bedrock so an abrupt influx of rhyolitic tephra produces transient low values of MS and density. Physical proxies then increase if soil and bedrock erosion is persistent. MS and density have a gradual increasing trend in the 500 years before H4 (Fig. 6.2d, e). Immediately after the H4 tephra horizon MS has an abrupt negative anomaly persisting for ~150 years while density has a short-lived positive anomaly lasting ~50 years. These deviations are followed by gradual increasing trends for the remainder of the time series. The H3 time series produces similar trends, however initial values of MS and density are both considerably higher than in the H4 time series indicating increased landscape erosion. Prior to the H3 tephra horizon both MS and density have fairly stable values with a gradual decreasing trend. After the tephra, MS abruptly decreases for 50 years before rapidly increasing for the remainder of the time series. Density experiences a brief positive anomaly followed by a negative anomaly that coincides with the negative deviation in MS. Density then rapidly increases stabilizing at a new high value after 200 years and remaining there for the duration of the time series.

6.5 Discussion

The changes observed within these 1000 year time windows are anomalous and persist for hundreds of years following the tephra horizons of interest indicating significant landscape destabilization and probable changes to ecosystem structure and function. Both rhyolitic tephra horizons are associated with similar changes in all proxy values except $\delta^{13}C$. However, this can be attributed to lake sediment irreversibly dominated by the soil endmember of $\delta^{13}C$ (See Fig. 6.3) after H4. While it is unlikely that the tephra perturbation alone produced these long-lived responses it is reasonable to infer that the landscape disturbance initiated by tephra deposition pushed the lake ecosystem past a threshold allowing significant destabilization and change to occur. This was likely amplified by the intensification of Neoglaciation (~4.2 ka) after H4 (Larsen et al., 2012; Geirsdóttir et al., 2013).

Figure 6.3 Bi-plots of soil organic matter properties in the Hvítárvatn catchment; a. $\delta^{13}C$ vs. %TOC; b. C:N vs. %TOC; c. C:N vs. δ^{13}

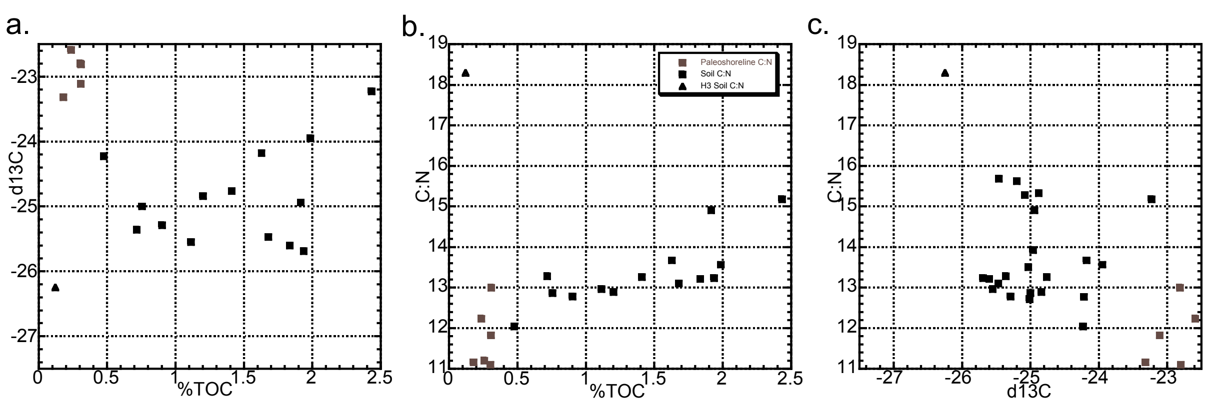

6.6 Conclusions

Rhyolitic tephra deposition events in HVT were followed by significant changes in both physical and OM lake sediment proxy values. Prior to the eruptions of interest proxy values were relatively stable and after the tephra layers most change occurred within 200 years. Thus, it can be assumed that in less sensitive lacustrine ecosystems 400 year windows, 200 years before and after tephra fall, will adequately capture changes directly attributed to tephra perturbations in lakes and their catchments.

CHAPTER 7: FINAL CONCLUSIONS AND FUTURE WORK

This thesis presents high-resolution records of environmental change in southern and western Iceland through the completion of two independent studies. The work conducted in Chapter 4 provides a high-resolution Holocene record of ecosystem development, variability, and change from climatic, volcanic, and anthropogenic perturbations at Vestra Gíslholtsvatn, a lake in southern Iceland. The Holocene record indicates an unproductive lake with a high influx of minerogenic material following deglaciation. As lake ontogeny slowly began lacustrine ecosystem development was reset by deposition of the Saksunarvatn tephra at ~10.3 ka. The lake then took approximately two millennia to establish a stable ecosystem structure supporting onset of the Holocene Thermal Maximum (HTM) at ~8.0 ka and a lack of early Holocene warmth observed in other lacustrine records from Iceland (Caseldine et al., 2006; Langdon et al., 2010; Larsen et al., 2012; Geirsdóttir et al., 2009b; 2013). The 8.2 ka cold event (e.g. Alley and Ágústsdóttir, 2005; Quillmann et al., 2012) was relatively mild but, prompted ~200 years of decreased ecosystem productivity and increased terrestrial erosion. The HTM was a relatively stable period at Vestra Gíslholtsvatn with high lacustrine primary productivity and a little indication of catchment instability. A slow transition in the proxy record began at ~6 ka attaining an alternative quasi-stable ecosystem state by ~5.5 ka indicating onset of Neoglaciation. Neoglaciation intensified at ~4.2 ka and persisted for the remainder of the Holocene with an abrupt cooling in the late Holocene culminating at ~0.7 ka. A strong signal of settlement by people is indicated in the multi-proxy record obstructing the climate signal for the last ~1.1 ka.

Throughout the Holocene numerous tephra deposition events create brief disturbances in lacustrine productivity and increase terrestrial erosion with the greatest perturbations occurring following the onset and intensification of Neoglaciation. Principle Component Analysis (PCA) was useful in discerning climate driven transitions in the multi-proxy record between ~8.3 ka and ~1.1 ka, a time period where proxy signals are dominated by climate rather than ecosystem, volcanic, or anthropogenic influences.

As Vestra Gíslholtsvatn observes similar timing of climate events observed at other Icelandic lakes in the mid-Holocene (Larsen et al., 2012; Geirsdóttir et al., 2013) it also likely recorded some climate signal over the last 1.1 ka, a period of extensive climate driven changes in Iceland including the Medieval Warm Period (MWP) and Little Ice Age (LIA). Further study using high-resolution multi-proxy records and PCA focusing on the last 1500 years may help separate the anthropogenic and climate signals to tell a story of human-landscape interactions during a period of substantially changing climate. Additionally, such work may help refine knowledge of LIA impacts in southern Iceland not directly related to glacial advance.

The studies produced in Chapters 5 and 6 use high-resolution multi-proxy sampling around prominent tephra horizons observed in an array of lake sediment records to discern alterations to ecosystem structure and function following substantial tephra deposition events. Findings indicate relatively coherent changes between lakes to perturbation from similar compositions of tephra and eruption events despite different morphological and ecosystem parameters. In general, thick rhyolitic tephra horizons produced longer lasting and more substantial disturbances than sizable basaltic tephra layers. Large, deep, unproductive lakes were more (less) sensitive to rhyolitic (basaltic) tephra disturbance than small, shallow, productive lakes. Climate appeared to greatly influence the response characteristic and length of tephra perturbations with intensified disturbance during Neoglaciation. The input of additional tephra horizons within the 400 year time windows also produced competing disturbances, which in some lakes overprinted proxy signals from the tephra horizons of interest. In summary, different types of eruptions produced vastly different multi-proxy signals albeit somewhat similar responses between diverse lake and catchment ecosystems.

Based on the results of this study further investigation is warranted to better understand the temporal extent and ecological influences of tephra fall in lacustrine systems. Additional data including but not limited to high-resolution sampling of biogenic silica, diatom assemblages, and/or pollen assemblages before and after tephra deposition events would improve the robustness of our results and offer more information as to the mechanisms behind observed variability. Ultrahigh-resolution multi-proxy analysis of additional correlative tephra horizons and/or adding more lakes to the array would also increase the strength of the conclusions. High-resolution analysis surrounding the tephra horizon H5, a rhyolitic layer deposited ~7 ka during the HTM (Larsen and Thorarinsson, 1977) would also be useful to further test the dependence on tephra type and climate. Jóhannsdóttir (2007) and Jagan (2010) have synthesized observations of known tephra horizons in lake sediment records and correlated many tephra layers between lake cores making it possible to strategically select the most ideal additional tephra horizons and the lakes in which to obtain them.

Due to constraints on time and the scope of this thesis ultrahigh-resolution samples surrounding the rhyolitic tephra horizon H1104, from an eruption of Hekla in

1104 AD (Larsen and Thorarinsson, 1977), have been collected from VGHV, HVT, and TORF and analyzed but not interpreted. Additionally, proxy data from samples surrounding the coupled rhyolitic and basaltic, Settlement tephra (Vö) are also available from VGHV, HVT, and HAK. Analysis of these layers could provide an intriguing look at the post settlement environment and the influence of human interaction with the landscape.

Improved spatial and temporal extent is needed to fully understand the complex processes mitigating lacustrine ecosystem structure and function after tephra fall events in Iceland during post-glacial times. The studies of this thesis are in part an extension of work completed by others in that we utilized pre-existing sediment cores, samples, and data. As new lake sediment cores are collected in Iceland, and high-resolution Holocene records are interpreted and added to the literature, external forcings such as explosive volcanism will hold an important role in explaining short-lived variability in lake and catchment processes. Consequently, establishment of unique tephra deposition events as simple mechanisms for spatially consistent environmental change across Iceland is an ongoing process that requires further study. Such work would better resolve the temporal influence of tephra fall events on ecosystem stability that may not be possible to observe in modern studies due to decadal scale disturbances. Increasing knowledge of the impacts and interactions of explosive volcanism with the environment will continue to hold precedence for current and future inhabitants of Iceland and anyone residing in other active volcanic regions of the world.

REFERENCES

Abella, S.E.B., 1988, THE EFFECT OF THE MT MAZAMA ASHFALL ON THE PLANKTONIC DIATOM COMMUNITY OF LAKE WASHINGTON. Limnology and Oceanography, 33: 1376-1385.

Alley, R.B. and Ágústsdóttir, A.M., 2005, The 8k event: cause and consequences of a major Holocene abrupt climate change. Quaternary Science Reviews, 24: 1123-1149.

Andrews, J.T., Hardardóttir, J., Stoner, J.S., Mann, M.E., Kristjánsdóttir, G.B. and Koc, N., 2003, Decadal to millennial-scale periodicities in North Iceland shelf sediments over the last 12000 cal yr: long-term North Atlantic oceanographic variability and solar forcing. Earth and Planetary Science Letters, 210: 453-465.

Arnalds, O. and Kimble, J., 2001, Andisols of deserts in Iceland. Soil Science Society of America Journal, 65: 1778-1786.

Arnalds, O., 2004, Volcanic soils of Iceland. Catena, 56.

Arnalds, O., 2008a, Andosols. Springer.

Arnalds, O., 2008b, Soils of Iceland. Jökull, 58.

Arnalds, O., Gisladóttir, F.O. and Orradóttir, B., 2012, Determination of aeolian transport rates of volcanic soils in Iceland. Geomorphology, 167.

Axford, Y., Miller, G.H., Geirsdóttir, A. and Langdon, P.G., 2007, Holocene temperature history of northern Iceland inferred from subfossil midges. Quaternary Science Reviews, 26: 3344-3358.

Axford, Y., Geirsdóttir, A., Miller, G.H. and Langdon, P.G., 2009, Climate of the Little Ice Age and the past 2000 years in northeast Iceland inferred from chironomids and other lake sediment proxies. Journal of Paleolimnology, 41: 7-24.

Ayris, P.M. and Delmelle, P., 2012, The immediate environmental effects of tephra emission. Bulletin of Volcanology, 74: 1905-1936.

Barker, P., Telford, R., Merdaci, O., Williamson, D., Taieb, M., Vincens, A. and Gibert, E., 2000, The sensitivity of a Tanzanian crater lake to catastrophic tephra input and four millennia of climate change. Holocene, 10: 303-310.

Beierle, B. and Bond, J., 2002, Density-induced settling of tephra through organic lake sediments. Journal of Paleolimnology, 28: 433-440.

Berger, G.W., Pillans, B.J. and Palmer, A.S., 1994, TEST OF THERMOLUMINESCENCE DATING OF LOESS FROM NEW-ZEALAND AND ALASKA. Quaternary Science Reviews, 13: 309-333.

Bigelow, N.H., Brubaker, L.B., Edwards, M.E., Harrison, S.P., Prentice, I.C., Anderson, P.M., Andreev, A.A., Bartlein, P.J., Christensen, T.R., Cramer, W., Kaplan, J.O., Lozhkin, A.V., Matveyeva, N.V., Murray, D.F., McGuire, A.D., Razzhivin, V.Y., Ritchie, J.C., Smith, B., Walker, D.A., Gajewski, K., Wolf, V., Holmqvist, B.H., Igarashi, Y., Kremenetskii, K., Paus, A., Pisaric, M.F.J. and Volkova, V.S., 2003, Climate change and Arctic ecosystems: 1. Vegetation changes north of 55 degrees N between the last glacial maximum, mid-Holocene, and present. Journal of Geophysical Research-Atmospheres, 108.

Björck, S., Ingólfsson, O., Haflidason, H., Hallsdóttir, M. and Anderson, N.J., 1992, LAKE TORFADALSVATN - A HIGH-RESOLUTION RECORD OF THE NORTH-ATLANTIC ASH ZONE-I AND THE LAST GLACIAL-INTERGLACIAL ENVIRONMENTAL-CHANGES IN ICELAND. Boreas, 21: 15-22.

Blaauw, M., 2010, Methods and code for 'classical' age-modelling of radiocarbon sequences. Quaternary Geochronology, 5: 512-518.

Black, J., Miller, G., Geirsdóttir, A., Manley, W. and Bjornsson, H., 2004, Sediment thickness and Holocene erosion rates derived from a seismic survey of Hvítárvatn, central Iceland. Jökull, 54: 37-56.

Black, J.L., 2008, Holocene Climate Change in South-Central Iceland: a multiproxy lacustrine record from glacial lake Hvítárvatn, University of Colorado, Boulder, Boulder, 348.

Bonadonna, C., Ernst, G.G.J. and Sparks, R.S.J., 1998, Thickness variations and volume estimates of tephra fall deposits: the importance of particle Reynolds number. Journal of Volcanology and Geothermal Research, 81: 173-187.

Bond, G., Kromer, B., Beer, J., Muscheler, R., Evans, M.N., Showers, W., Hoffmann, S., Lotti-Bond, R., Hajdas, I. and Bonani, G., 2001, Persistent solar influence on north Atlantic climate during the Holocene. Science, 294: 2130-2136.

Brock, B., Rivera, A., Casassa, G., Bown, F. and Acuna, C., 2007, The surface energy balance of an active ice-covered volcano: Vilarrica Volcano, Southern Chile. Annals of Glaciology, 45: 104-114.

Bromwich, D.H., Bai, L.H. and Bjarnason, G.G., 2005, High-resolution regional climate simulations over Iceland using Polar MM5. Monthly Weather Review, 133: 3527-3547.

Carn, S.A., Prata, A.J. and Karlsdóttir, S., 2008, Circumpolar transport of a volcanic cloud from Hekla (Iceland). Journal of Geophysical Research-Atmospheres, 113.

Caseldine, C., Geirsdóttir, A. and Langdon, P., 2003, Efstadalsvatn - a multi-proxy study of a Holocene lacustrine sequence from NW Iceland. Journal of Paleolimnology, 30: 55-73.

Caseldine, C., Langdon, P. and Holmes, N., 2006, Early Holocene climate variability and the timing and extent of the Holocene thermal maximum (HTM) in northern Iceland. Quaternary Science Reviews, 25: 2314-2331.

Conley, D.J., 2002, Terrestrial ecosystems and the global biogeochemical silica cycle. Global Biogeochemical Cycles, 16.

Cook, R.J., Barron, J.C., Papendick, R.I. and Williams III, G.J., 1981, Impacts on Agriculture of the Mount St. Helens Eruption. Science, 211: 16-22.

Cronin, S.J., Hedley, M.J., Smith, G. and Neall, V.E., 1997, Impact of Ruapehu ash fall on soil and pasture nutrient status 1, Oct 1995 eruptions. Journal of New Zealand Agricultural Resources, 40: 383-395.

Dahl, S.O., Bakke, J., Lie, O. and Nesje, A., 2003, Reconstruction of former glacier equilibrium-line altitudes based on proglacial sites: an evaluation of approaches and selection of sites. Quaternary Science Reviews, 22.

Davies, S.M., Larsen, G., Wastegård, S., Turney, C.S.M., Hall, V.A., Coyle, L. and Thordarson, T., 2010, Widespread dispersal of Icelandic tephra: how does the Eyjafjöll eruption of 2010 compare to past Icelandic events? Journal of Quaternary Science, 25: 605-611.

Davies, S.M., Abbott, P.M., Pearce, N.J.G., Wastegård, S. and Blockley, S.P.E., 2012, Integrating the INTIMATE records using tephrochronology: rising to the challenge. Quaternary Science Reviews, 36: 11-27.

del Moral, R. and Grishin, S.Y., 1999, Volcanic Disturbances and Ecosystem Recovery. In: Walker, L.R. (ed.), Ecosystems of Disturbed Ground. Elsevier, New York, 136-150.

Denton, G.H. and Broecker, W.S., 2008, Wobbly ocean conveyor circulation during the Holocene? Quaternary Science Reviews, 27: 1939-1950.

Dokulil, M.T., 1994, ENVIRONMENTAL-CONTROL OF PHYTOPLANKTON PRODUCTIVITY IN TURBULENT TURBID SYSTEMS. Hydrobiologia, 289: 65-72.

Dugmore, A. and Buckland, P., 1991, Tephrochronology and late Holocene soil erosion in south Iceland. In: Maizels, J.K. and Caseldine, C. (eds.), Environmental Change in Iceland: Past and Present. Kluwer Academic Publishers, Dordrecht, 147-159.

Dugmore, A.J., Cook, G.T., Shore, J.S., Newton, A.J., Edwards, K.J. and Larsen, G., 1995, Radiocarbon dating tephra layers in Britain and Iceland. Radiocarbon, 37: 379-388.

Dwyer, R.B. and Mitchell, F.J.G., 1997, Investigation of the environmental impact of remote volcanic activity on North Mayo, Ireland, during the mid-Holocene. Holocene, 7: 113-118.

Edwards, K.J. and Craigie, R., 1998, Palynological and vegetational changes associated with the deposition of Saksunarvatn Ash in the Faroe Islands. Frothskaparrit, 46: 245-258.

Eggermont, H., Verschuren, D., Audenaert, L., Lens, L., Russell, J., Klaassen, G. and Heiri, O., 2010, Limnological and ecological sensitivity of Rwenzori mountain lakes to climate warming. Hydrobiologia, 648: 123-142.

Eggermont, H. and Heiri, O., 2012, The chironomid-temperature relationship: expression in nature and palaeoenvironmental implications. Biological Reviews, 87: 430-456.

Eicher, G.J. and Rounsefell, G.A., 1957, Effects of lake fertilization by volcanic activity on abundance of salmon. Limnol and Oceanogr, 1: 70-76.

Forchhammer, 1822, LXXXVII: Account of a volcanic eruptions in Iceland. The Philosophical Magazine and Journal, 59: 428-432.

Freiligrath, F., 1876, Iceland-Moss Tea. University Press: Welch, Bigelow and Co., Boston 266 p.

Geirsdóttir, A., Miller, G.H., Wattrus, N.J., Bjornsson, H. and Thors, K., 2008, Stabilization of glaciers terminating in closed water bodies: evidence and broader implications. Geophysical Research Letters, 35.

Geirsdóttir, A., Miller, G.H., Axford, Y. and Ólafsdóttir, S., 2009a, Holocene and latest Pleistocene climate and glacier fluctuations in Iceland. Quaternary Science Reviews, 28: 2107-2118.

Geirsdóttir, A., Miller, G.H., Thordarson, T. and Ólafsdóttir, K.B., 2009b, A 2000 year record of climate variations reconstructed from Haukadalsvatn, West Iceland. Journal of Paleolimnology, 41: 95-115.

Geirsdóttir, Á., Miller, G.H., Larsen, D.J. and Ólafsdóttir, S., 2013, Abrupt

Holocene climate transitions in the northern North Atlantic region recorded by synchronized lacustrine records in Iceland. Quaternary Science Reviews, 70: 48-62.

Giraudeau, J., Jennings, A.E. and Andrews, J.T., 2004, Timing and mechanisms of surface and intermediate water circulation changes in the Nordic Seas over the last 10,000 cal years: a view from the North Iceland shelf. Quaternary Science Reviews, 23: 2127-2139.

Gisladóttir, F.O., Arnalds, O. and Gisladóttir, G., 2005, The effect of landscape and retreating glaciers on wind erosion in south Iceland. Land Degradation & Development, 16: 177-187.

Glew, J., 1991, Miniature gravity corer for recovering short sediment cores. Journal of Paleolimnology, 5: 285-287.

Grobbelaar, J.U., 1985, PHYTOPLANKTON PRODUCTIVITY IN TURBID WATERS. Journal of Plankton Research, 7: 653-663.

Grönvold, K., Óskarsson, N., Johnsen, S.J., Clausen, H.B., Hammer, C.U., Bond, G. and Bard, E., 1995, ASH LAYERS FROM ICELAND IN THE GREENLAND GRIP ICE CORE CORRELATED WITH OCEANIC AND LAND SEDIMENTS. Earth and Planetary Science Letters, 135: 149-155.

Gudmundsson, H.J., 1997, A review of the Holocene environmental history of Iceland. Quaternary Science Reviews, 16: 81-92.

Gudmundsson, M.T., 2005, Subglacial volcanic activity in Iceland. In: Caseldine, C., Russell, A., Hardardóttir, J. and Knudsen, O. (eds.), Iceland- Modern Processes and Past Environments. Elsevier, New York, 127-151.

Gudmundsson, M.T., Larsen, G., Höskuldsson, A. and Gylfason, A.G., 2008, Volcanic hazards in Iceland. Jökull, 58: 251-268.

Gudmundsson, S., Bjornsson, H., Magnusson, E., Berthier, E., Pálsson, F., Gudmundsson, M.T., Hognadottir, T. and Dall, J., 2011, Response of Eyjafjallajökull, Torfajökull and Tindfjallajökull ice caps in Iceland to regional warming, deduced by remote sensing. Polar Research, 30.

Guicharnaud, R. and Paton, G.I., 2006, An evaluation of acid deposition on cation leaching and weathering rates of an Andosol and a Cambisol. Journal of Geochemical Exploration, 88.

Haflidason, H., Eiríksson, J. and Van Kreveld, S., 2000, The tephrochronology of Iceland and the North Atlantic region during the Middle and Late Quaternary: a review. Journal of Quaternary Science, 15: 3-22.

Håkansson, S., 1985, A review of various factors influencing the stable carbon isotope ratio or organic lake sediments by the changes from glacial to post-glacial environmental conditions. Quaternary Science Reviews, 4: 135-146.

Hallet, B., Hunter, L. and Bogen, J., 1996, Rates of erosion and sediment evacuation by glaciers: A review of field data and their implications. Global and Planetary Change, 12.

Hallett, D.J., Mathewes, R.W. and Foit, F.F., 2001, Mid-Holocene Glacier Peak and Mount St. Helens we tephra layers detected in lake sediments from southern British Columbia using high-resolution techniques. Quaternary Research, 55.

Hallsdóttir, M., 1995, On the pre-settlement history of Icelandic vegetation. Buvisindi, 9: 17-29.

Hallsdóttir, M. and Caseldine, C.J., 2005, The Holocene vegetation history of Iceland, state-of-the-art and future research. In: Caseldine, C., Russell, A., Hardardóttir, J. and Knudsen, O. (eds.), Iceland- Modern Processes and Past Environments. Elsevier, San Diego, 319-334.

Hannesdóttir, H., Geirsdóttir, A., Miller, G.H., Manley, W. and Wattrus, N., 2009, Deglacial and Holocene sediment distribution in Hestvatn, South Iceland, derived from a seismic and multibeam survey. Jökull, 59: 67-88.

Hardardóttir, J., 1999, Late Weichelian and Holocene Environmental History of South and West Iceland as Interpreted from Studies of Lake and Terrestrial Sediments, University of Colorado, Boulder, Boulder

Hardardóttir, J., Geirsdóttir, A. and Sveinbjornsdóttir, A.E., 2001, Seismostratigraphy and sediment studies of Lake Hestvatn, southern Iceland: implications for the deglacial history of the region. Journal of Quaternary Science, 16: 167-179.

Hotes, S., Poschlod, P. and Takahashi, H., 2006, Effects of volcanic activity on mire development: case studies from Hokkaido, northern Japan. Holocene, 16: 561-573.

Hrafnsdóttir, T., 2005, Chironomida of Iceland. The Zoology of Iceland, University of Copenhagen, 169.

Imsland, P., 1989, Study Models for Volcanic Hazards in Iceland. In: Latter, J.H. (ed.), Volcanic Hazards: Assessment and Monitoring. Springer-Verlag, New York, 36-56.

Jagan, A., 2010, Tephra stratigraphy and geochemistry from three Icelandic lake cores: a new method for determining source volcano of tephra layers, University of

Edinburgh, Edinburgh

Janbu, A.D., Paasche, O. and Talbot, M.R., 2011, Paleoclimate changes inferred from stable isotopes and magnetic properties of organic-rich lake sediments in Arctic Norway. Journal of Paleolimnology, 46: 29-44.

Janžekovič, F. and Novak, T., 2012, PCA – A Powerful Method for Analyze Ecological Niches. Principal Component Analysis - Multidisciplinary Applications.

Jóhannsdóttir, G.E., 2007, Mid Holocene to late glacial tephrochronology West Iceland as revealed in three lacustrine environments, University of Iceland, Reykjavik

Jóhannesson, H. and Sæmundsson, K., 1998, *Geological map of Iceland, 1:500.000. Bedrock geology* (Icelandic Institute of Natural History and Iceland Geodetic Survey, Reykjavík

Juggins, S., 2003. C2 User Guide: Software for Ecological and Palaeoecological Data Analysis and Visualization. University of Newcastle, Newcastle upon Tyne, UK.

Kaplan, J.O., Bigelow, N.H., Prentice, I.C., Harrison, S.P., Bartlein, P.J., Christensen, T.R., Cramer, W., Matveyeva, N.V., McGuire, A.D., Murray, D.F., Razzhivin, V.Y., Smith, B., Walker, D.A., Anderson, P.M., Andreev, A.A., Brubaker, L.B., Edwards, M.E. and Lozhkin, A.V., 2003, Climate change and Arctic ecosystems: 2. Modeling, paleodata-model comparisons, and future projections. Journal of Geophysical Research-Atmospheres, 108.

Karlsdóttir, S.n., Gylfason, A.g.s.G., Höskuldsson, A.r., Brandsdóttir, B.s., Ilyinskaya, E., Gudmundsson, M.s.T. and Högnadótti, o.r.s., 2012, The 2010 Eyjafjallajökull eruption, Iceland. Icelandic Meteorological Office, Montreal.

Kaufman, D.S., Ager, T.A., Anderson, N.J., Anderson, P.M., Andrews, J.T., Bartlein, P.T., Brubaker, L.B., Coats, L.L., Cwynar, L.C., Duvall, M.L., Dyke, A.S., Edwards, M.E., Eisner, W.R., Gajewski, K., Geirsdóttir, A., Hu, F.S., Jennings, A.E., Kaplan, M.R., Kerwin, M.W., Lozhkin, A.V., MacDonald, G.M., Miller, G.H., Mock, C.J., Oswald, W.W., Otto-Bliesner, B.L., Porinchu, D.F., Ruhland, K., Smol, J.P., Steig, E.J. and Wolfe, B.B., 2004, Holocene thermal maximum in the western Arctic (0-180 degrees W) (vol 23, pg 529, 2003). Quaternary Science Reviews, 23: 2059-2060.

Kennedy, R.A., 1980, ASH FROM MT ST-HELENS. Nature, 287: 581-581.

Kilian, R., Biester, H., Behrmann, J., Baeza, O., Fesq-Martin, M., Hohner, M., Schimpf, D., Friedmann, A. and Mangini, A., 2006, Millennium-scale volcanic impact on a superhumid and pristine ecosystem. Geology, 34: 609-612.

Kirk, W., 1808, The fiery museum or the burning mountains, accounts of those dreadful eruptions which have so frequently broke out at mounts Vesuvius and Ætna: with a circumstantial narrative of their eruptions in one of which, (at Vesuvius) the town of Ottaniano was nearly reduced to ashes: with every particular relative to those great volcanoes which have so astonished the surrounding nations, and the world. Sussex Press, Lewes.

Kirkbride, M.P. and Dugmore, A.J., 2003, Glaciological response to distal tephra fallout from the 1947 eruption of Hekla, south Iceland. Journal of Glaciology, 49: 420-428.

Kirkbride, M.P. and Dugmore, A.J., 2006, Responses of mountain Iee caps in central Iceland to Holocene climate change. Quaternary Science Reviews, 25: 1692-1707.

Kling, G.W., Fry, B. and Obrien, W.J., 1992, STABLE ISOTOPES AND PLANKTONIC TROPHIC STRUCTURE IN ARCTIC LAKES. Ecology, 73: 561-566.

Knudsen, K.L. and Eiríksson, J., 2002, Application of tephrochronology to the timing and correlation of palaeoceanographic events recorded in Holocene and Late Glacial shelf sediments off North Iceland. Marine Geology, 191: 165-188.

Kristjánsdóttir, G.B., Stoner, J.S., Jennings, A.E., Andrews, J.T. and Gronvold, K., 2007, Geochemistry of Holocene cryptotephras from the north Iceland shelf (MD99-2269): intercalibration with radiocarbon and palaeomagnetic chronostratigraphies. Holocene, 17: 155-176.

Kurenkov, II, 1966, INFLUENCE OF VOLCANIC ASHFALL ON BIOLOGICAL PROCESSES IN A LAKE. Limnology and Oceanography, 11: 426-&.

Lacasse, C., Carey, S. and Sigurdsson, H., 1998, Volcanogenic sedimentation in the Iceland Basin: influence of subaerial and subglacial eruptions. Journal of Volcanology and Geothermal Research, 83: 47-73.

Langdon, P.G., Holmes, N. and Caseldine, C.J., 2008, Environmental controls on modern chironomid faunas from NW Iceland and implications for reconstructing climate change. Journal of Paleolimnology, 40: 273-293.

Langdon, P.G., Leng, M.J., Holmes, N. and Caseldine, C.J., 2010, Lacustrine evidence of early-Holocene environmental change in northern Iceland: a multiproxy palaeoecology and stable isotope study. Holocene, 20: 205-214.

Larsen, D.J., Miller, G.H., Geirsdóttir, A. and Thordarson, T., 2011, A 3000-year varved record of glacier activity and climate change from the proglacial lake Hvítárvatn, Iceland. Quaternary Science Reviews, 30: 2715-2731.

Larsen, D.J., Miller, G.H., Geirsdóttir, A. and Ólafsdóttir, S., 2012, Non-linear Holocene climate evolution in the North Atlantic: a high-resolution, multi-proxy record of glacier activity and environmental change from Hvítárvatn, central Iceland. Quaternary Science Reviews, 39: 14-25.

Larsen, G. and Thorarinsson, S., 1977, H4 and other Hekla Tephra Layers. Jökull, 27: 28-46.

Larsen, G., 1984, RECENT VOLCANIC HISTORY OF THE VEIDIVOTN FISSURE SWARM, SOUTHERN ICELAND - AN APPROACH TO VOLCANIC RISK ASSESSMENT. Journal of Volcanology and Geothermal Research, 22: 33-58.

Larsen, G., Dugmore, A. and Newton, A., 1999, Geochemistry of historical-age silicic tephras in Iceland. Holocene, 9: 463-471.

Larsen, G., 2000, Holocene eruptions within the Katla volcanic system, south Iceland: Characteristics and environmental impact Jökull, 49: 1-28.

Larsen, G. and Eiríksson, J., 2008, Late Quaternary terrestrial tephrochronology of Iceland - frequency of explosive eruptions, type and volume of tephra deposits. Journal of Quaternary Science, 23: 109-120.

Lee, D.B., 1996, Effects of the eruptions of Mount St. Helens on physical, chemical, and biological characteristics of surface water, ground water, and precipitation in the Western United States, Water Supply Paper 2438.

Leng, M.J. and Marshall, J.D., 2004, Palaeoclimate interpretation of stable isotope data from lake sediment archives. Quaternary Science Reviews, 23: 811-831.

Lennox, B., Spooner, I., Jull, T. and Patterson, W.P., 2010, Post-glacial climate change and its effect on a shallow dimictic lake in Nova Scotia, Canada. Journal of Paleolimnology, 43: 15-27.

Leonard, E.M., 1997, The relationship between glacial activity and sediment production: Evidence from a 4450-year varve record of neoglacial sedimentation in Hector Lake, Alberta, Canada. Journal of Paleolimnology, 17.

Lewontin, R.C., 1969, THE MEANING OF STABILITY. Brookhaven Symposia in Biology, 22: 13-24.

Logemann, K. and Harms, I., 2006, High resolution modelling of the North Icelandic Irminger Current (NIIC). Ocean Science, 2: 291-304.

Long, C.J., Power, M.J. and Bartlein, P.J., 2011, The effects of fire and tephra deposition on forest vegetation in the Central Cascades, Oregon. Quaternary Research, 75: 151-158.

Lowe, D.J., 2011, Tephrochronology and its application: A review. Quaternary

Geochronology, 6: 107-153.

Mack, R.N., 1981, INITIAL EFFECTS OF ASHFALL FROM MOUNT ST-HELENS ON VEGETATION IN EASTERN WASHINGTON AND ADJACENT IDAHO. Science, 213: 537-539.

Malmberg, S.-A. and Kristmannsson, S.S., 1992, Hydrographic conditions in Icelandic waters, 1980-1989. ICES Marine Science Symposia, 195: 76-92.

Mangerud, J., Furnes, H. and Johansen, J., 1986, A 9000-YEAR-OLD ASH BED ON THE FAROE ISLANDS. Quaternary Research, 26: 262-265.

Mayewski, P.A., Rohling, E.E., Stager, J.C., Karlen, W., Maasch, K.A., Meeker, L.D., Meyerson, E.A., Gasse, F., van Kreveld, S., Holmgren, K., Lee-Thorp, J., Rosqvist, G., Rack, F., Staubwasser, M., Schneider, R.R. and Steig, E.J., 2004, Holocene climate variability. Quaternary Research, 62: 243-255.

McCune, B. and Grace, J.B., 2002, Analysis of Ecological Communities. MjM Software Designs, Gleneden, OR 304 p.

Meyers, P.A., 1997, Organic geochemical proxies of paleoceanographic, paleolimnologic, and paleoclimatic processes. Organic Geochemistry, 27.

Meyers, P.A. and Teranes, J.L., 2001, Sediment organic matter. In: Last, W.M. and Smol, J.P. (eds.), Tracking Environmental Change Using Lake Sediment: Physical and Geochemical Methods. Kluwer Academic, Dordrecht, 239-269.

Miller, G.H., Geirsdóttir, A., Zhong, Y.F., Larsen, D.J., Otto-Bliesner, B.L., Holland, M.M., Bailey, D.A., Refsnider, K.A., Lehman, S.J., Southon, J.R., Anderson, C., Bjornsson, H. and Thordarson, T., 2012, Abrupt onset of the Little Ice Age triggered by volcanism and sustained by sea-ice/ocean feedbacks. Geophysical Research Letters, 39.

Mortlock, R.A. and Froelich, P.N., 1989, A SIMPLE METHOD FOR THE RAPID-DETERMINATION OF BIOGENIC OPAL IN PELAGIC MARINE-SEDIMENTS. Deep-Sea Research Part a-Oceanographic Research Papers, 36.

Myers, N.J., 2011, Volcanogenic Sulfate and Fluoride deposition: Effects on organic and mineral soil gas fluxes and chemistry, University of York, 246.

Nesje, A., 1992, A PISTON CORER FOR LACUSTRINE AND MARINE-SEDIMENTS. Arctic and Alpine Research, 24: 257-259.

Nesje, A., Dahl, S.O., Andersson, C. and Matthews, J.A., 2000, The lacustrine sedimentary sequence in Sygneskardvatnet, western Norway: a continuous, high-resolution record of the Jostedalsbreen ice cap during the Holocene.

Quaternary Science Reviews, 19.

Óladóttir, B.A., Sigmarsson, O., Larsen, G. and Thordarson, T., 2008, Katla volcano, Iceland: magma composition, dynamics and eruption frequency as recorded by Holocene tephra layers. Bulletin of Volcanology, 70: 475-493.

Ólafsdóttir, R. and Gudmundsson, H.J., 2002, Holocene land degradation and climatic change in northeastern Iceland. Holocene, 12: 159-167.

Ólafsdóttir S., Geirsdóttir Á., Miller G.H., Stoner J.S. and Channell J.E.T. 2013. Synchronizing Holocene lacustrine and marine sediment records using paleomagnetic secular variation. Geology.

Ólafsdóttir, S., 2010, Holocene Marine and Lacustrine Paleoclimate and Paleomagnetic Records from Iceland: Land-Sea Correlations, University of Iceland, Reykjavik

Ólafsdóttir, S., Jennings, A.E., Geirsdottir, A., Andrews, J. and Miller, G.H., 2010, Holocene variability of the North Atlantic Irminger current on the south- and northwest shelf of Iceland. Marine Micropaleontology, 77: 101-118.

Osborn, G., Menounos, B., Koch, J., Clague, J.J. and Vallis, V., 2007, Multi-proxy record of Holocene glacial history of the Spearhead and Fitzsimmons ranges, southern Coast Mountains, British Columbia. Quaternary Science Reviews, 26.

Óskarsson, H., Arnalds, O., Gudmundsson, J. and Gudbergsson, G., 2004, Organic carbon in Icelandic Andosols: geographical variation and impact of erosion. Catena, 56.

Payne, R.J., Edwards, K.J. and Blackford, J.J., 2013, Volcanic impacts on the Holocene vegetation history of Britain and Ireland? A review and meta-analysis of the pollen evidence. Vegetation History and Archaeobotany, 22: 153-164.

Pálsson, F., Guðmundsson, S., Björnsson, H., Berthier, E., Eyjólfur, M., Guðmundsson, S. and Haraldsson, H.H., 2012, Mass and volume changes of Langjokull ice cap, Iceland,1890 to 2009, deduced from old maps, satellite images and in situ mass balance measurements Jökull: 81-96.

Quillmann, U., Marchitto, T.M., Jennings, A.E., Andrews, J.T. and Friestad, B.F., 2012, Cooling and freshening at 8.2 ka on the NW Iceland Shelf recorded in paired delta O-18 and Mg/Ca measurements of the benthic foraminifer Cibicides lobatulus. Quaternary Research, 78: 528-539.

Rist, S., 1975, Stöðuvötn (e. Lakes), Report, Icelandic National Energy Authority report, Reykjakvik

Róbertsdóttir, B.G., Year, Forsoguleg gjoskulog fra Kotlu, adur nefnd ‘Katla

5000' Geoscience Society of Iceland Spring Meeting Reyjakvik, 8-9

Rose, W.I. and Durant, A.J., 2009, Fine ash content of explosive eruptions. Journal of Volcanology and Geothermal Research, 186: 32-39.

Rosenbaum, J.G., Reynolds, R.L. and Colman, S.M., 2012, Fingerprinting of glacial silt in lake sediments yields continuous records of alpine glaciation (35-15ka), western USA. Quaternary Research, 78.

Rousse, S., Kissel, C., Laj, C., Eiriksson, J. and Knudsen, K.L., 2006, Holocene centennial to millennial-scale climatic variability: Evidence from high-resolution magnetic analyses of the last 10 cal kyr off North Iceland (core MD99-2275). Earth and Planetary Science Letters, 242: 390-405.

Rundgren, M., 1995, Biostratigraphic evidence of the Allerod-Younger Dryas-Preboreal oscillation in northern Iceland. Quaternary Research, 44: 405-416.

Rundgren, M., 1998, Early Holocene Vegetation of Northern Iceland: Pollen and plant macrofossil evidence from the Skagi peninsula. The Holocene, 8: 553-564.

Rundgren, M. and Ingolfsson, O., 1999, Plant survival in Iceland during periods of glaciation? Journal of Biogeography, 26: 387-396.

Ryves, D.B., Battarbee, R.W., Juggins, S., Fritz, S.C. and Anderson, N.J., 2006, Physical and chemical predictors of diatom dissolution in freshwater and saline lake sediments in North America and West Greenland. Limnology and Oceanography, 51.

Schulte, P.J., Teskey, R.O., Hinckley, T.M., Stevens, R.G. and Leslie, D.A., 1985, THE EFFECT OF TEPHRA DEPOSITION AND PLANTING TREATMENT ON SOIL OXYGEN LEVELS AND WATER RELATIONS OF NEWLY PLANTED SEEDLINGS. Forest Science, 31: 109-116.

Sharp, B., 1890, An Account of the Vincelonian Volcano. Proceedings of the Academy of Natural Sciences of Philadelphia, 42: 289-295.

Sicre, M.-A., Jacob, J., Ezat, U., Rousse, S., Kissel, C., Yiou, P., Eiriksson, J., Knudsen, K.L., Jansen, E. and Turon, J.-L., 2008, Decadal variability of sea surface temperatures off North Iceland over the last 2000 years. Earth and Planetary Science Letters, 268: 137-142.

Sigfusson, B., Gislason, S.R. and Paton, G.I., 2006, The effect of soil solution chemistry on the weathering rate of a Histic Andosol. Journal of Geochemical Exploration, 88.

Sigfusson, B., Gislason, S.R. and Paton, G.I., 2008, Pedogenesis and weathering rates of a Histic Andosol in Iceland: Field and experimental soil solution study. Geoderma, 144.

Sinton, J., Grönvold, K. and Saemundsson, K., 2005, Postglacial eruptive history of the Western Volcanic Zone, Iceland. Geochemistry Geophysics Geosystems, 6.

Stout, J.E., 2004, A method for establishing the critical threshold for aeolian transport in the field. Earth Surface Processes and Landforms, 29: 1195-1207.

Talbot, M.R. and Laerdal, T., 2000, The Late Pleistocene-Holocene palaeolimnology of Lake Victoria, East Africa, based upon elemental and isotopic analyses of sedimentary organic matter. Journal of Paleolimnology, 23.

Telford, R.J., Barker, P., Metcalfe, S. and Newton, A., 2004, Lacustrine responses to tephra deposition: examples from Mexico. Quaternary Science Reviews, 23: 2337-2353.

Thorarinsson, S., 1967, The eruptions of Hekla in historical times In: Einarsson, T., Kjartansson G., and Thorarinsson S. (ed.), The eruption of Hekla 1947- 48. Society Scientific Islandica Reykjavík 1-177.

Thorarinsson, S., 1979, On the Damage Caused by Volcanic Eruptions with Special Reference to Tephra and Gases. In: Sheets, P.D. and Grayson, D.K. (eds.), Volcanic Activity and Human Ecology. Academic Press, Inc, New York, 125-159.

Thordarson, T., Miller, D.J., Larsen, G., Self, S. and Sigurdsson, H., 2001, New estimates of sulfur degassing and atmospheric mass-loading by the 934 AD Eldgja eruption, Iceland. Journal of Volcanology and Geothermal Research, 108: 33-54.

Thordarson, T. and Larsen, G., 2007, Volcanism in Iceland in historical time: Volcano types, eruption styles and eruptive history. Journal of Geodynamics, 43: 118-152.

Thordarson, T. and Höskuldsson, A., 2008, Postglacial volcanism in Iceland. Jökull, 58: 197-228.

Thorsteinsson, T., Gisladóttir, G., Bullard, J. and McTainsh, G., 2011, Dust storm contributions to airborne particulate matter in Reykjavik, Iceland. Atmospheric Environment, 45: 5924-5933.

Turney, C.S.M., 1999, Lacustrine bulk organic delta C-13 in the British Isles during the last glacial-Holocene transition (14-9 ka C-14 BP). Arctic Antarctic and Alpine Research, 31.

Walker, I.R., 2001. Midges: Chironomidae and related Diptera, In: Smol, J.P., Birks, H.J.B., Last, W.M. (Eds.), Tracking Environmental Change Using Lake

Sediments. Volume 4: Zoological Indicators. Kluwer, Dordrecht, The Netherlands, pp. 43-66.

Wang, Y. and Wooller, M.J., 2006, The stable isotopic (C and N) composition of modern plants and lichens from northern Iceland: with ecological and paleoenvironmental implications. Jökull, 56: 27-38.

Wanner, H., Beer, J., Buetikofer, J., Crowley, T.J., Cubasch, U., Flueckiger, J., Goosse, H., Grosjean, M., Joos, F., Kaplan, J.O., Kuettel, M., Mueller, S.A., Prentice, I.C., Solomina, O., Stocker, T.F., Tarasov, P., Wagner, M. and Widmann, M., 2008, Mid- to Late Holocene climate change: an overview. Quaternary Science Reviews, 27: 1791-1828.

Wanner, H., Solomina, O., Grosjean, M., Ritz, S.P. and Jetel, M., 2011, Structure and origin of Holocene cold events. Quaternary Science Reviews, 30: 3109-3123.

Wastegård, S., Björck, S., Grauert, M. and Hannon, G.E., 2001, The Mjauvotn tephra and other Holocene tephra horizons from the Faroe Islands: a link between the Icelandic source region, the Nordic Seas, and the European continent. Holocene, 11: 101-109.

Wastegård, S., 2005, Late Quaternary tephrochronology of Sweden: a review. Quaternary International, 130: 49-62.

Wilson, T.M., Cole, W.J., Stewart, C., Cronin, S.J. and Johnston, D.M., 2011, Ash storms: impacts of wind-remobilised volcanic ash on rural communities and agriculture following the 1991 Hudson eruptions, southern Patagonia, Chile. Bull Volcanol: 223-229.

Witham, C.S., Oppenheimer, C. and Horwell, C.J., 2005, Volcanic ash-leachates: a review and recommendations for sampling methods. Journal of Volcanology and Geothermal Research, 141: 299-326.

Wolfe, C.J., Bjarnason, I.T., VanDecar, J.C. and Solomon, S.C., 1997, Seismic structure of the Iceland mantle plume. Nature, 385: 245-247.

Wooller, M., Wang, Y. and Axford, Y., 2008, A multiple stable isotope record of Late Quaternary limnological changes and chironomid paleoecology from northeastern Iceland. Journal of Paleolimnology, 40: 63-77.

Wright, H.E., 1967, A SQUARE-ROD PISTON SAMPLER FOR LAKE SEDIMENTS. Journal of Sedimentary Petrology, 37: 975-976.

Yalcin, K., Wake, C.P. and Germani, M.S., 2003, A 100-year record of North Pacific volcanism in an ice core from Eclipse Icefield, Yukon Territory, Canada. Journal of Geophysical Research-Atmospheres, 108.

APPENDIX 1: MULTI-PROXY DATA FROM VESTRA GÍSLHOLTSVATN

Core VGHV08-1A-1B from Vestra Gíslholtsvatn

Physical and organic matter proxies used to produce the Holocene record of environmental change. See Fig 4.2 (core images), 4.5 (physical proxy time series), and 4.8 (biological time series). Years before present (BP) relative to 1950 unless otherwise indicated.

Age BP	%TOC	%N	C:N	%BSi	$\delta^{13}C$	$\delta^{15}N$	Depth in Core cm	Sed Rate mm/yr	Age BP	MS SI	Den g/cm^3	Age BP	MS SI	Den g/cm^3
-58							0	1.63	-57	69	1.17	4250	70	1.16
-54	5.49			17.71			0.65	1.63	-54	77	1.15	4257	61	1.16
-52	5.49						0.9	1.63	-51	83	1.16	4295	209	1.51
-51	5.36	0.6	8.92		-26.28	2.13	1.15	1.63	-48	90	1.15	4302	226	1.27
-48	4.96	0.59	8.45		-26.37	1.03	1.65	1.63	-45	94	1.20	4309	254	1.19
-45	4.4	0.49	9.07		-25.97	1.6	2.15	1.63	-41	99	1.17	4316	295	1.19
-42	5.22						2.65	1.63	-38	104	1.15	4323	344	1.33
-40	5.22			16.81			2.9	1.64	-35	108	1.18	4330	386	1.29
-39	5.01	0.52	9.58		-25.96	1.54	3.15	1.64	-32	113	1.17	4337	400	1.47
-36	4.82	0.51	9.54		-25.79	1.3	3.65	1.64	-29	117	1.20	4345	373	1.44
-33	4.59	0.47	9.68		-25.45	1.22	4.15	1.64	-26	120	1.26	4352	318	1.29
-30	4.71						4.65	1.64	-23	122	1.22	4359	257	1.28
-28	4.71			18.1			4.9	1.64	-20	123	1.22	4367	203	1.21
-27	4.49	0.5	8.94		-25.89	1.03	5.15	1.64	-17	124	1.17	4374	164	1.12
-24	4.26	0.47	9.04		-25.79	1.2	5.65	1.65	-14	123	1.17	4381	136	1.14
-20	3.79	0.41	9.23		-25.63	1.31	6.15	1.65	-11	123	1.17	4389	118	1.17
-17	4.22						6.65	1.65	-8	124	1.15	4396	106	1.22
-16	4.22			11.27			6.9	1.65	-5	126	1.22	4404	98	1.21
-14	4.13	0.45	9.1		-25.33	0.89	7.15	1.66	-2	126	1.26	4411	93	1.31
-11	3.82	0.4	9.48		-24.85	1.2	7.65	1.66	1	125	1.23	4419	88	1.24
-8	4.25	0.44	9.6		-25.04	1.14	8.15	1.66	4	123	1.21	4426	84	1.18
-5	4.47						8.65	1.67	7	121	1.25	4434	83	1.14
-4	4.47			18.31			8.9	1.67	10	120	1.22	4442	84	1.13
-2	3.73	0.43	8.62		-23.67	1.03	9.15	1.67	13	119	1.21	4449	85	1.16
1	3.35	0.39	8.64		-23.76	1.28	9.65	1.68	16	121	1.15	4457	89	1.16
4	2.77	0.32	8.59		-23.98	1.18	10.15	1.68	19	124	1.19	4465	94	1.12
7	2.66						10.65	1.69	22	127	1.22	4473	101	1.13
8	2.66			11.57			10.9	1.69	24	130	1.25	4480	106	1.16
9	3.02	0.35	8.54		-23.49	1.01	11.15	1.69	27	130	1.32	4488	107	1.23
12	2.95	0.33	8.95		-24.02	1.41	11.65	1.70	30	126	1.21	4496	102	1.43
15	5.36	0.35	9.19		-23.78	1.57	12.15	1.70	33	122	1.21	4504	94	1.17
18	2.85						12.65	1.71	36	118	1.18	4512	86	1.14
20	2.85			11.58			12.9	1.71	39	113	1.15	4520	81	1.12
21	3	0.34	8.92		-24.89	1.4	13.15	1.72	42	111	1.16	4528	78	1.08
24	2.81	0.32	8.78		-24.66	1.94	13.65	1.72	44	109	1.11	4536	77	1.11
27	2.77	0.3	9.3		-24.63	1.64	14.15	1.73	47	108	1.19	4544	77	1.14
30	2.13	0.24	9.05		-24.65	1.67	14.65	1.74	50	107	1.20	4552	77	1.17
33	2.77						15.15	1.75	53	106	1.11	4560	77	1.21
34	2.77			11.93			15.4	1.75	56	106	1.19	4569	75	1.21
36	2.73	0.31	8.88		-24.58	1.67	15.65	1.75	58		1.19	4577	72	1.12
38	3.22	0.37	8.69		-24.46	1.74	16.15	1.76	61	107	1.18	4585	70	1.13
41	3.17	0.35	9.14		-24.66	1.69	16.65	1.77	64	105	1.18	4593	68	1.11
44	3.38						17.15	1.77	67	105	1.20	4602	66	1.14
46	3.38			12.73			17.4	1.78	70	104	1.18	4610	65	1.12
47	3.53	0.38	9.27		-24.62	1.64	17.65	1.78	72	103	1.16	4618	64	1.10
50	3.53	0.37	9.52		-24.83	1.63	18.15	1.79	75	102	1.16	4627	64	1.08
53	3.63	0.37	9.73		-24.04	1.41	18.65	1.79	78	101	1.14	4635	64	1.14
55	3.09						19.15	1.80	81	101	1.13	4644	65	1.12
57	3.09			15.5			19.4	1.80	83	101	1.12	4652	65	1.17
58	3.48	0.37	9.43		-24.98	1.5	19.65	1.80	86	103	1.12	4661	65	1.18
61	3.43	0.35	9.72		-24.95	1.67	20.15	1.81	89	105	1.14	4669	66	1.12
64	3.3	0.38	8.68		-24.64	1.42	20.65	1.81	92	106	1.13	4678	66	1.10
68	3.79			14.2			21.15	1.81	94	109	1.20	4686	66	1.15
69	3.4	0.39	8.63		-25.05	1.03	21.4	1.81	97	110	1.16	4695	66	1.13

Core VGHV08-1A-1B from Vestra Gíslholtsvatn
Physical and organic matter proxies (continued).

Age BP	%TOC	%N	C:N	%BSi	$\delta^{13}C$	$\delta^{15}N$	Depth in Core cm	Sed Rate mm/yr	Age BP	MS SI	Den g/cm^3	Age BP	MS SI	Den g/cm^3
72	3.5	0.39	8.95		-24.84	0.83	22.15	1.82	100	110	1.14	4704	66	1.13
75	3.64	0.41	8.94		-24.78	0.91	22.65	1.82	103	111	1.17	4713	66	1.13
79	3.36			13.03			23.4	1.82	105	111	1.18	4721	66	1.11
80	3.52	0.4	8.7		-24.76	1.38	23.65	1.82	108	110	1.21	4730	66	1.14
86	3.57	0.41	8.64		-25.1	1.18	24.65	1.82	111	110	1.18	4739	68	1.11
88	3.77						25.15	1.82	114	108	1.21	4748	69	1.09
90	3.6		9.6	17.07			25.4	1.82	116	107	1.17	4757	69	1.11
91	3.62	0.42	8.59		-24.83	0.91	25.65	1.82	119	107	1.16	4766	71	1.12
94	3.35	0.39	8.59		-24.09	1.26	26.15	1.82	122	107	1.10	4775	71	1.14
97	3.21	0.39	8.3		-23.97	1.41	26.65	1.82	125	108	1.16	4784	72	1.15
99	3						27.15	1.82	128	109	1.18	4793	73	1.16
101	3			14.89			27.4	1.82	130	111	1.18	4802	75	1.08
102	3.51	0.41	8.6		-23.94	0.87	27.65	1.82	133	113	1.18	4811	79	1.16
105	2.96	0.34	8.79		-24.42	1.26	28.15	1.82	136	116	1.14	4820	84	1.17
108	3.05	0.36	8.46		-24.43	1.02	28.65	1.81	139	118	1.14	4829	91	1.14
110	3.46						29.15	1.81	142	122	1.17	4838	100	1.10
112	3.46			14.71			29.4	1.81	145	125	1.13	4847	106	1.17
113	3.48	0.39	8.85		-24.87	1.2	29.65	1.81	147	128	1.18	4857	106	1.33
116	2.89	0.31	9.38		-24.35	1.03	30.15	1.81	150	131	1.17	4866	101	1.41
119	3.04	0.34	9.01		-24.12	1.07	30.65	1.80	153	134	1.18	4875	94	1.14
122	3.27						31.15	1.80	156	136	1.14	4885	87	1.11
123	3.27			12.04			31.4	1.79	159	137	1.26	4894	82	1.14
124	3.1	0.36	8.62		-24.1	1.4	31.65	1.79	162	137	1.17	4903	77	1.15
127	3.36	0.4	8.47		-25.04	1.11	32.15	1.79	165	134	1.19	4913	74	1.15
130	4.46	0.4	11.21		-26.4	1.11	32.65	1.78	168	132	1.16	4922	72	1.16
133	3.61						33.15	1.77	171	128	1.18	4932	70	1.11
134	3.61			15.18			33.4	1.77	174	125	1.17	4941	69	1.13
136	3.62	0.42	8.57		-25.11	1.12	33.65	1.76	177	120	1.20	4951	68	1.10
144	4.48						35.15	1.76	180	116	1.14	4961	67	1.12
146	4.48			12.38			35.4	1.74	183	113	1.19	4970	68	1.14
147	3.71	0.41	9.16		-24.97	0.77	35.65	1.73	186	110	1.15	4980	69	1.12
150	3.47	0.39	8.77		-24.07	0.9	36.15	1.73	190	108	1.16	4990	70	1.13
153	2.95	0.32	9.25		-24.07	1.2	36.65	1.72	193	106	1.19	4999	72	1.15
156	3.18						37.15	1.71	196	105	1.19	5009	75	1.14
157	3.18			9.99			37.4	1.70	199	104	1.19	5019	77	1.15
159	3.17	0.37	8.61		-24.43	0.9	37.65	1.70	202	103	1.16	5029	78	1.17
162	3.63	0.4	8.99		-24.5	1.16	38.15	1.69	206	104	1.18	5039	80	1.15
165	2.8	0.3	9.38		-24.91	1.01	38.65	1.68	209	104	1.17	5048	80	1.16
168	3.17						39.15	1.68	212	106	1.16	5058	80	1.16
169	3.17			14.69			39.4	1.66	215	108	1.18	5068	78	1.16
171	2.25	0.21	10.71		-25.06	2.03	39.65	1.66	219	109	1.30	5078	75	1.15
174	3.59	0.38	9.41		-24.82	1.1	40.15	1.65	222	109	1.28	5088	73	1.11
177	2.72	0.29	9.24		-25.09	1.31	40.65	1.64	226	108	1.14	5098	72	1.16
180	3.55						41.15	1.63	229	108	1.18	5109	70	1.13
181	3.55			15.3			41.4	1.62	233	108	1.11	5119	70	1.14
183	3.41	0.37	9.22		-24.84	1.55	41.65	1.62	236	110	1.17	5129	68	1.16
186	3.4	0.38	8.88		-25	1.12	42.15	1.61	240	114	1.13	5139	68	1.13
189	3.02	0.35	8.54		-24.85	1.38	42.65	1.60	243	116	1.15	5149	68	1.16
192	4.13						43.15	1.59	247	121	1.19	5160	67	1.14
194	4.13			15.31			43.4	1.58	250	124	1.19	5170	65	1.15
195	3.49	0.4	8.8		-24.58	1.04	43.65	1.57	254	127	1.14	5180	64	1.14
199	3.47	0.39	8.88		-24.58	1.39	44.15	1.56	258	127	1.19	5191	63	1.13
202	3.22	0.37	8.73		-24.59	1.38	44.65	1.55	261	126	1.11	5201	62	1.15
205	3.72						45.15	1.54	265	121	1.17	5211	62	1.13
207	3.72			18.05			45.4	1.53	269	117	1.17	5222	61	1.14
208	3.36	0.38	8.77		-24.16	0.78	45.65	1.52	273	112	1.15	5232	61	1.13
212	3.13	0.35	8.83		-24.57	1.71	46.15	1.52	276	108	1.15	5243	63	1.13
215	3.26	0.39	8.42		-24.3	0.87	46.65	1.50	280	106	1.19	5253	65	1.13
218	2.75						47.15	1.49	284	104	1.17	5264	66	1.12
220	2.75			13.49			47.4	1.48	288	103	1.14	5275	68	1.12
222	3.07	0.35	8.85		-24.43	1.49	47.65	1.47	292	102	1.11	5285	71	1.13
225	2.28	0.27	8.42		-24.74	1.28	48.15	1.47	295	101	1.16	5296	73	1.09
229	1.13	0.14	8.35		-25.08	1.86	48.65	1.45	299	100	1.17	5307	77	1.14
232	3.47						49.15	1.45	303	102	1.12	5317	82	1.13
234	3.47			14.34			49.4	1.43	307	104	1.18	5328	87	1.16
236	3.34	0.36	9.32		-24.92	0.71	49.65	1.42	311	105	1.14	5339	92	1.18
239	3.8	0.4	9.44		-24.03	0.91	50.15	1.42	315	106	1.18	5350	94	1.23
243	4.26	0.42	10.14		-23.31	0.95	50.65	1.40	319	104	1.17	5361	94	1.42
246	3.29						51.15	1.40	323	103	1.14	5372	91	1.20
248	3.29			13.03			51.4	1.39	327	102	1.16	5383	89	1.17

Core VGHV08-1A-1B from Vestra Gíslholtsvatn
Physical and organic matter proxies (continued).

Age BP	%TOC	%N	C:N	%BSi	$\delta^{13}C$	$\delta^{15}N$	Depth in Core cm	Sed Rate mm/yr	Age BP	MS SI	Den g/cm^3	Age BP	MS SI	Den g/cm^3
250	3.98	0.42	9.48		-23.67	0.93	51.65	1.38	330	100	1.14	5394	89	1.15
253	3.53	0.4	8.73		-24.69	1.25	52.15	1.38	334	98	1.15	5405	88	1.15
257	3.6	0.4	8.94		-24.63	1.16	52.65	1.37	338	97	1.17	5416	88	1.20
261	3.39						53.15	1.36	342	96	1.13	5427	90	1.17
263	3.39			17.72			53.4	1.35	346	96	1.12	5438	91	1.19
264	3.83	0.41	9.35		-23.8	1.1	53.65	1.35	350	96	1.13	5449	93	1.17
268	2.21	0.26	8.45		-24.55	1.87	54.15	1.34	354	97	1.15	5460	96	1.15
272	3.18	0.36	8.73		-24.54	1.42	54.65	1.34	358	97	1.13	5471	100	1.15
278	3.49			14.62			55.4	1.33	362	97	1.17	5483	108	1.15
285	4.13	0.38	10.97		-25.86	1.16	56.4	1.32	366	96	1.15	5494	119	1.12
293	3.12			15.26			57.4	1.31	370	97	1.16	5505	137	1.14
300	3.63	0.41	8.82		-24.47	1.47	58.4	1.30	374		1.12	5517	161	1.14
308	3.27			22.64			59.4	1.29	378	96	1.17	5528	194	1.15
316	3.5	0.41	8.57		-23.56	1.27	60.4	1.28	382	96	1.14	5539	238	1.15
324	3.38			16.32			61.4	1.28	386	97	1.16	5551	290	1.19
332	3.68	0.42	8.67		-24.59	1.41	62.4	1.27	389	97	1.17	5562	342	1.25
340	3.54			20.62			63.4	1.27	393	98	1.15	5574	381	1.41
347	3.33	0.39	8.56		-24.29	1.08	64.4	1.27	397	98	1.17	5585	395	1.78
355	4.17			22.2			65.4	1.27	401	100	1.12	5597	379	1.91
363	3.5	0.41	8.48		-24.03	1.25	66.4	1.27	405	103	1.14	5608	340	1.91
371	3.71			20.55			67.4	1.27	409	107	1.18	5620	287	1.62
379	3.42	0.4	8.66		-23.74	1.08	68.4	1.27	413	114	1.19	5632	232	1.45
387	3.16			22.63			69.4	1.28	416	123	1.13	5643	185	1.18
395	3.27	0.4	8.19		-24.06	1.46	70.4	1.28	420	135	1.18	5655	147	1.07
402	3.27			21.3			71.4	1.29	424	149	1.18	5667	121	1.12
410	2.97	0.36	8.16		-23.98	1.55	72.4	1.30	428	161	1.19	5679	102	1.14
418	2.53			22.54			73.4	1.31	432	171	1.23	5691	90	1.12
425	3.25	0.4	8.21		-23.55	1.08	74.4	1.32	435	176	1.29	5702	81	1.18
433	2.09			18.25			75.4	1.33	439	173	1.19	5714	75	1.15
440	2.79	0.34	8.17		-23.54	1	76.4	1.35	443	163	1.44	5726	70	1.10
455	1.73	0.23	7.66		-23.2	1.34	78.4	1.36	446	149	1.21	5738	68	1.13
462	2.73			22.92			79.4	1.40	450	136	1.14	5750	68	1.16
469	2.73	0.34	7.99		-23.77	1.28	80.4	1.42	454	125	1.14	5762	68	1.12
476	3.41			23.44			81.4	1.44	457	119	1.18	5774	68	1.13
483	2.17	0.28	7.77		-23.34	1.54	82.4	1.46	461	113	1.20	5787	70	1.13
490	3.13			19.85			83.4	1.48	464	109	1.21	5799	72	1.16
494	3.24	0.4	8.07		-23.54	1.18	83.9	1.50	468	104	1.16	5811	74	1.16
504	3.15			25.18			85.4	1.50	471	102	1.14	5823	74	1.17
510	3.1	0.37	8.29		-23.54	1.02	86.4	1.54	475	98	1.14	5836	75	1.14
517	3.25			24.4			87.4	1.56	478	96	1.18	5848	77	1.14
523	3.28	0.4	8.27		-23.6	1.21	88.4	1.58	482	94	1.17	5860	78	1.13
529	3.04			17.27			89.4	1.60	485	93	1.13	5873	80	1.14
536	2.96	0.37	7.97		-23.26	1.44	90.4	1.62	488	92	1.14	5885	82	1.18
542	2.38			18.39			91.4	1.64	492	91	1.15	5898	83	1.15
548	2.83	0.37	7.67		-23.11	1.63	92.4	1.66	495	91	1.13	5911	83	1.21
554	2.93			22.56			93.4	1.68	498	91	1.13	5923	80	1.21
560	2.09	0.25	8.52		-23.5	1.88	94.4	1.70	502	92	1.13	5936	78	1.15
566	2.47			21.88			95.4	1.72	505	93	1.17	5949	75	1.13
572	2.87	0.37	7.83		-22.81	1.6	96.4	1.75	508	95	1.15	5962	73	1.13
578	1.93			18.4			97.4	1.77	511	97	1.15	5974	71	1.12
583	2.81	0.33	8.43		-23.08	1.37	98.4	1.79	514	101	1.14	5987	71	1.12
589	2.28			18.87			99.4	1.81	518	104	1.17	6000	71	1.11
595	3.36	0.3	11.37		-25.28	1.63	100.4	1.83	521	107	1.21	6013	70	1.12
600	2.79			20.54			101.4	1.85	524	112	1.18	6027	70	1.13
606	2.82	0.34	8.29		-23.93	1.58	102.4	1.87	527	115	1.16	6040	71	1.11
611	2.64			18.68			103.4	1.89	530	119	1.16	6053	71	1.14
616	2.66	0.33	8.02		-23.37	1.77	104.4	1.91	533	122	1.14	6066	74	1.14
622	2.51			18.97			105.4	1.93	536	123	1.20	6080	76	1.13
624	2.41	0.3	8.09		-23.65	1.73	105.9	1.95	539	122	1.26	6093	79	1.15
628	2.79	0.27	7.88		-23.94	1.73	106.65	1.96	542	119	1.25	6106	84	1.13
632	3.18			21.72			107.4	1.98	545	116	1.16	6120	88	1.17
637	3.52	0.32	10.85		-25.47	1.71	108.4	1.99	548	114	1.17	6134	94	1.21
642	2.88			22.14			109.4	2.01	551	114	1.15	6147	98	1.19
647	3.18	0.4	7.99		-23.41	1.54	110.4	2.03	554	115	1.16	6161	101	1.15
652	3.11			24.41			111.4	2.05	557	117	1.22	6175	107	1.16
657	3.03	0.4	7.65		-22.87	3.02	112.4	2.07	560	120	1.21	6189	111	1.12
662	3			20.71			113.4	2.08	563	124	1.19	6203	117	1.19
667	3.12	0.39	8.05		-23.62	1.4	114.4	2.10	566	128	1.19	6217	126	1.21
672	2.54			18.59			115.4	2.12	569	132	1.23	6231	135	1.15
677	2.83	0.35	8.13		-23.7	1.64	116.4	2.14	572	138	1.23	6245	148	1.14

Core VGHV08-1A-1B from Vestra Gíslholtsvatn

Physical and organic matter proxies (continued).

Age BP	%TOC	%N	C:N	%BSi	$\delta^{13}C$	$\delta^{15}N$	Depth in Core cm	Sed Rate mm/yr	Age BP	MS SI	Den g/cm^3	Age BP	MS SI	Den g/cm^3
681	2.62			19.7			117.4	2.15	574	142	1.19	6259	161	1.11
695	2.77	0.33	8.35		-23.25	1.72	120.4	2.17	577	143	1.21	6273	174	1.16
700	2.72			18.75			121.4	2.21	580	142	1.21	6288	180	1.29
704	2.6	0.31	8.51		-22.81	1.62	122.4	2.22	583	137	1.22	6302	175	1.34
709	2.94			20.47			123.4	2.24	586	132	1.19	6317	164	1.15
716	3.11	0.38	8.29		-23.04	1.56	124.9	2.25	588	126	1.16	6331	153	1.17
722	3.03	0.35	8.7		-23.5	1.61	126.4	2.26	591	122	1.20	6346	144	1.31
727	2.85			14.41			127.4	2.28	594	121	1.16	6361	140	1.21
731	2.9	0.32	9.15		-23.52	2.02	128.4	2.29	596	121	1.20	6376	138	1.25
735	3.25			16.89			129.4	2.29	599	122	1.17	6391	138	1.17
740	3.36	0.36	9.38		-23.48	2.01	130.4	2.30	602	123	1.14	6406	139	1.16
744	3.09			15.2			131.4	2.31	604	126	1.25	6421	144	1.18
748	3.2	0.35	9.15		-23.58	1.84	132.4	2.31	607	127	1.22	6436	153	1.15
752	3.21			15.63			133.4	2.31	610	128	1.21	6451	169	1.15
757	3.15	0.32	9.69		-21.97	1.61	134.4	2.32	612	127	1.20	6467	192	1.16
761	2.71			13.46			135.4	2.32	615	125	1.23	6482	218	1.17
765	2.83	0.26	10.69		-23.81	1.39	136.4	2.33	617	121	1.21	6497	244	1.21
769	3.95			18.15			137.4	2.33	620	116	1.17	6513	258	1.43
774	3.06	0.31	10.01		-22.16	1.96	138.4	2.33	623	111	1.16	6529	254	1.78
778	3.79			15.95			139.4	2.33	625	108	1.14	6545	233	1.72
782	3.71	0.37	9.93		-22.48	1.92	140.4	2.32	628	106	1.13	6560	203	1.29
786	4.05			17.16			141.4	2.32	630	104	1.18	6576	171	1.14
789	3.99	0.41	9.73		-23.39	1.87	142.15	2.31	633	102	1.18	6592	144	1.12
792	4.28	0.39	10.9		-23.29	1.99	142.9	2.31	635	102	1.16	6609	123	1.13
794	4.07			16.18			143.4	2.31	638	102	1.16	6625	109	1.12
802	3.37	0.39	9.92	17.07	-23.36	1.98	145.2	2.30	640	101	1.17	6641	99	1.17
806	3	0.36	8.32		-23.41	1.31	146.2	2.29	643	101	1.19	6658	92	1.24
810	2.72			16			147.2	2.28	645	102	1.17	6674	87	1.18
814	2.71	0.31	8.71		-22.2	1.95	148.2	2.27	647	102	1.19	6691	83	1.14
818	2.71			12.53			149.2	2.26	650	103	1.18	6708	81	1.14
823	2.99	0.34	8.76		-23.17	1.86	150.2	2.25	652	105	1.20	6724	80	1.12
827	3.08			13.65			151.2	2.24	655	108	1.18	6741	80	1.15
831	3.06	0.34	9.08		-23.3	1.54	152.2	2.23	657	110	1.20	6758	80	1.16
835	3.06			12.98			153.2	2.22	659	112	1.21	6775	82	1.16
839	3.09	0.33	9.47		-22.1	1.48	154.2	2.21	662	115	1.23	6793	84	1.18
843	2.92	0.31	9.55	11.48	-23.07	1.69	155.2	2.19	664	116	1.24	6810	87	1.17
846	2.91						155.7	2.18	667	117	1.21	6827	90	1.15
848	3.53	0.36	9.69		-22.45	1.98	156.2	2.17	669	118	1.27	6845	95	1.17
852	3.2			14.72			157.2	2.16	671	119	1.24	6863	101	1.18
856	2.98	0.32	9.24		-23.96	1.95	158.2	2.14	674	118	1.23	6880	110	1.15
861	3.6			13.83			159.2	2.11	676	118	1.20	6898	118	1.15
865	3.48						160.2	2.08	678	117	1.20	6916	125	1.25
867	3.48			12.35			160.7	2.05	681	115	1.25	6934	127	1.38
869	3.75	0.39	9.73		-23.1	1.86	161.2	2.04	683	114	1.19	6952	125	1.26
874	4.01	0.41	9.71		-23.46	1.96	162.2	2.01	685	113	1.22	6971	119	1.27
879	3.87			15.78			163.2	1.97	687	112	1.23	6989	109	1.18
883	3.92	0.4	9.8		-23.97	1.71	164.2	1.92	690	111	1.32	7008	101	1.17
888	3.84			14.92			165.2	1.88	692	110	1.19	7026	94	1.13
891	4.05	0.4	9.73		-22.18	1.86	165.7	1.84	694	109	1.20	7045	88	1.14
894	4.17	0.42	10.03		-21.73	1.74	166.2	1.82	696	109	1.19	7064	83	1.13
899	3.69			14.78			167.2	1.78	699	109	1.18	7083	81	1.17
905	3.65	0.4	9.32		-22.48	1.59	168.2	1.73	701	110	1.22	7102	77	1.13
910	3.82	0.48	7.68	17.93	-23.95	1.19	169.2	1.68	703	110	1.17	7121	75	1.17
916	3.55	0.4	8.95		-22.29	1.85	170.2	1.63	705	111	1.20	7141	73	1.11
919	4.08	0.41	9.84		-22.1	1.89	170.7	1.59	708	113	1.22	7160	72	1.13
923	3.66	0.43	8.28	14.31	-22.46	1.52	171.2	1.56	710	113	1.21	7180	71	1.12
929	4.09	0.42	9.77		-23.45	1.55	172.2	1.53	712	115	1.23	7199	71	1.15
936	4.34	0.38	11.49	10.14	-24.57	1.72	173.2	1.48	714	116	1.22	7219	71	1.12
943	3.95	0.4	9.42		-23.87	1.79	174.2	1.43	716	117	1.26	7239	71	1.14
950	3.95	0.4	9.5	13.82	-23.95	1.84	175.2	1.38	719	116	1.26	7259	71	1.11
954	4.13	0.41	9.97		-23.64	1.97	175.7	1.34	721	115	1.27	7280	72	1.15
958	3.71	0.42	8.73		-23.93	1.57	176.2	1.32	723	114	1.22	7300	72	1.12
962	3.59	0.37	9.67		-22.26	2.11	176.7	1.30	725	113	1.21	7320	72	1.17
966	3.53	0.37	9.61		-22.98	1.48	177.2	1.28	727	113	1.20	7341	71	1.15
971	3.83						177.7	1.25	730	113	1.19	7362	71	1.09
975	4.53	0.4	11.44		-24.35	1.73	178.2	1.23	732	114	1.22	7382	71	1.10
979	3.86	0.39	9.97		-22.58	1.9	178.7	1.21	734	115	1.18	7403	72	1.11
984	3.82	0.4	9.97		-23.94	1.71	179.2	1.19	736	116	1.20	7425	72	1.14
988	3.88			18.05			179.7	1.17	738	116	1.25	7446	72	1.18
993	4.06	0.4	10.13		-24.67	1.8	180.2	1.15	740	116	1.20	7467	73	1.20

Core VGHV08-1A-1B from Vestra Gíslholtsvatn
Physical and organic matter proxies (continued).

Age BP	%TOC	%N	C:N	%BSi	$\delta^{13}C$	$\delta^{15}N$	Depth in Core cm	Sed Rate mm/yr	Age BP	MS SI	Den g/cm^3	Age BP	MS SI	Den g/cm^3
998	4.02	0.4	10.11		-22.71	1.88	180.7	1.12	743	115	1.20	7489	74	1.39
1003	4.01	0.43	9.35		-25.06	1.58	181.2	1.11	745	116	1.16	7510	73	1.18
1008	4.14			12.88			181.7	1.08	747	117	1.25	7532	72	1.13
1013	2.87	0.33	8.57		-24.51	1.38	182.2	1.07	749	118	1.23	7554	72	1.16
1024	3.26	0.33	8.26		-24.24	1.59	183.2	1.05	751	120	1.20	7576	70	1.13
1029	3.11			20.95			183.7	1.03	753	120	1.29	7598	69	1.14
1035	3.93	0.46	8.64		-22.89	1.35	184.2	1.04	756	120	1.26	7621	68	1.11
1040	4.13	0.4	10.45		-24.15	1.96	184.7	1.05	758	118	1.21	7643	67	1.15
1046	3.82	0.42	7.95		-22.43	1.19	185.2	1.06	760	117	1.18	7667	67	1.10
1052	2.99			21.45			185.7	1.07	762	116	1.16	7690	66	1.15
1057	2.44	0.26	7.34		-22.88	2.02	186.2	1.08	764	116	1.18	7714	65	1.11
1063	3.53	0.39	9.16		-24.06	1.74	186.7	1.09	766	117	1.21	7738	65	1.08
1069	0.62	0.1	6.42		-23.47	1.45	187.2	1.10	768	117	1.21	7763	63	1.15
1079	3.45	0.35	8.04		-21.64	1.18	189.2	1.11	771	118	1.19	7789	60	1.14
1084	2.9			26.18			189.7	1.12	773	115	1.21	7947	206	1.36
1090	2.87	0.42	6.69		-22.46	1.06	190.2	1.12	775	112	1.19	7974	236	1.39
1096	1.12	0.14	8.16		-22.25	1.8	190.7	1.13	777	109	1.21	8001	255	1.41
1101	2.49	0.33	7.49		-23.51	1.44	191.2	1.14	779	104	1.19	8027	262	1.42
1112	2.21	0.3	7.42		-23.27	0.92	192.2	1.14	781	100	1.15	8054	252	1.43
1117	3.05	0.39	7.76		-21.8	1.38	192.7	1.15	784	93	1.20	8080	228	1.37
1123	4.09	0.6	6.85		-22.26	0.9	193.2	1.15	786	82	1.17	8106	198	1.28
1128	3.83			30.07			193.7	1.16	792	93	1.22	8131	166	1.13
1133	4.23	0.55	7.67		-22.59	0.97	194.2	1.16	794	101	1.16	8156	139	1.12
1144	2.67	0.32	8.21		-23.29	1.1	195.2	1.17	795	108	1.14	8181	119	1.17
1149	3.22			22.48			195.7	1.18	797	112	1.19	8206	105	1.16
1154	3.78	0.49	7.67		-22.8	1.16	196.2	1.18	800	114	1.23	8230	98	1.11
1159	3.61	0.44	8.15		-22.28	0.89	196.7	1.18	802	116	1.21	8254	96	1.15
1164	5.27	0.59	9.01		-22.88	1.23	197.2	1.19	804	117	1.19	8278	97	1.20
1169	4.46			36.25			197.7	1.19	806	118	1.20	8302	101	1.18
1174	4.5	0.51	8.9		-22.83	1.02	198.2	1.19	808	119	1.18	8325	108	1.21
1179	4.55	0.54	8.49		-22.5	1.2	198.7	1.20	811	119	1.22	8348	116	1.22
1184	4.68	0.45	10.36		-24.73	0.99	199.2	1.20	813	120	1.25	8371	125	1.26
1193	4.31	0.52	8.35		-22.54	1.09	200.2	1.21	815	119	1.22	8393	134	1.28
1198	3.35	0.42	7.93		-23.16	1.61	200.7	1.21	817	120	1.21	8415	143	1.27
1207	3.96			34.77			201.7	1.21	819	120	1.15	8437	152	1.29
1217	3.5	0.43	8.06		-22.85	1.26	202.7	1.22	822	120	1.19	8459	161	1.29
1226	4.97			30.43			203.7	1.22	824	120	1.21	8480	171	1.33
1235	4.21	0.54	7.77		-23.08	1.45	204.7	1.22	826	120	1.22	8501	176	1.50
1244	4.1			32.54			205.7	1.23	828	120	1.17	8522	176	1.63
1253	3.57	0.44	8.06		-23.02	1.11	206.7	1.23	831	119	1.19	8543	169	1.29
1262	3.72			29.85			207.7	1.23	833	120	1.22	8563	160	1.22
1271	4.57	0.55	8.29		-22.7	1.12	208.7	1.23	835	120	1.19	8583	151	1.26
1280	4.55	0.53	8.57	33.4	-23.8	1.66	209.7	1.23	837	121	1.23	8603	143	1.23
1288	4.29	0.53	8.09		-22.9	1.23	210.7	1.23	840	121	1.27	8623	140	1.22
1297	3.11	0.39	7.98	23.75	-23.99	1.86	211.7	1.23	842	121	1.21	8642	139	1.23
1306	1.98	0.22	8.88	18.31	-23.29	1.93	212.7	1.22	844	120	1.15	8661	142	1.25
1331	4.74	0.64	7.37	36.43	-23.04	1.67	215.7	1.22	846	119	1.14	8680	148	1.22
1352	4.27	0.56	7.58	39.42	-22.95	1.61	218.2	1.21	849	120	1.19	8699	158	1.24
1378	4.05	0.48	8.43	34.71	-23.24	1.72	221.2	1.19	851	121	1.15	8718	171	1.23
1395	4.7	0.59	7.96	37.21	-22.08	1.55	223.2	1.16	853	121	1.16	8736	189	1.26
1412	4.12	0.54	7.65	33.6	-23.1	1.7	225.2	1.15	856	121	1.17	8754	209	1.26
1461	5.13	0.61	8.4	37.19	-22.77	1.14	230.7	1.12	858	123	1.15	8772	226	1.37
1507	4.72	0.6	7.8	36.75	-23.45	1.55	235.7	1.06	860	123	1.12	8789	235	1.61
1556	5.23	0.65	8.09	37.92	-21.97	1.24	240.7	1.00	863	123	1.14	8806	236	1.25
1610	4.7	0.57	8.22	31.98	-22.46	1.33	245.7	0.93	865	125	1.22	8824	231	1.26
1680	2.17	0.23	9.37	21.99	-22.29	1.58	251.7	0.86	868	125	1.18	8840	225	1.25
1693	3.96	0.5	7.99		-23.7	1.13	252.7	0.78	870	125	1.20	8857	223	1.29
1706	3.87	0.45	8.67	28.8	-21.69	1.63	253.7	0.77	873	125	1.20	8874	219	1.34
1719	3.11	0.37	8.33		-21.41	1.11	254.7	0.76	875	126	1.16	8890	212	1.36
1732	4.19	0.52	8.1	30.26	-22.06	1.35	255.7	0.75	878	126	1.17	8906	200	1.31
1840	3.74	0.48	7.71	28.86	-22.57	1.4	263.2	0.73	880	126	1.21	8922	186	1.38
1922	1.79	0.27	6.75	19.72	-23.33	1.55	268.2	0.64	883	126	1.21	8938	171	1.34
1979	3.09	0.33	9.42	25.01	-22.23	1.81	271.4	0.59	885	126	1.19	8953	160	1.29
2056	4.12	0.47	8.81	29.84	-22.88	1.74	275.4	0.56	888	125	1.17	8968	152	1.35
2076	4.4	0.49	9.07		-20.99	0.67	276.4	0.52	891	126	1.19	8983	146	1.30
2139	3.55	0.47	7.51	29.07	-22.49	1.83	279.4	0.51	893	123	1.24	8998	141	1.22
2183	3.76	0.44	8.59		-21.44	1.52	281.4	0.49	896	121	1.24	9013	138	1.25
2229	4.28	0.53	8	29.23	-22.93	1.32	283.4	0.47	899	118	1.18	9027	135	1.26
2253	4.02	0.58	7.04		-22.89	1.31	284.4	0.46	902	117	1.17	9042	134	1.24
2277	4.45	0.61	7.27		-23.67	1.22	285.4	0.45	904	115	1.19	9056	134	1.30

Core VGHV08-1A-1B from Vestra Gíslholtsvatn

Physical and organic matter proxies (continued).

Age BP	%TOC	%N	C:N	%BSi	$\delta^{13}C$	$\delta^{15}N$	Depth in Core cm	Sed Rate mm/yr	Age BP	MS SI	Den g/cm^3	Age BP	MS SI	Den g/cm^3
2301	4.07	0.53	7.88		-22.49	1.38	286.4	0.44	907	115	1.16	9070	134	1.27
2326	4.2	0.65	7.21		-23.04	1.42	287.4	0.44	910	116	1.15	9084	135	1.27
2339	3.97			32.77			287.9	0.43	913	117	1.14	9097	137	1.30
2352	4.46	0.57	7.87		-22.47	1.4	288.4	0.43	916	119	1.14	9111	140	1.27
2378	4.3	0.59	7.33		-21.96	1.68	289.4	0.42	919	121	1.21	9124	143	1.29
2391	4.39	0.52	8.45		-22.15	1.21	289.9	0.42	922	122	1.18	9137	148	1.30
2404	4.4	0.55	8.06		-22.74	1.87	290.4	0.41	926	122	1.15	9150	155	1.27
2431	2.62	0.39	7.51		-23.75	1.58	291.4	0.41	929	123	1.19	9163	162	1.32
2445	2.36			15.26			291.9	0.40	932	121	1.21	9175	169	1.35
2459	2.56	0.4	6.4		-22.33	1.61	292.4	0.40	935	120	1.15	9188	172	1.38
2487	3.18	0.44	8.03		-23.2	1.67	293.4	0.40	939		1.17	9200	172	1.43
2515	3.15	0.39	8.09		-20.59	0.96	294.4	0.39	942	117	1.16	9212	166	1.27
2544	0.21	0.02		23.79	-26.15		295.4	0.38	946	117	1.17	9224	161	1.28
2589	4.32	0.55	7.89		-21.92	1.3	298.9	0.38	949	118	1.13	9236	155	1.36
2604	4.49	0.59	7.55		-21.91	1.04	299.4	0.37	953	118	1.16	9247	149	1.30
2634	3.59	0.55	7.04	29.76	-22.84	1.31	300.4	0.37	957	120	1.18	9259	146	1.31
2664	4.11	0.53	7.77		-22.13	1.32	301.4	0.36	960	120	1.17	9270	144	1.33
2693	4.03	0.54	7.47		-21.99	1.16	302.4	0.35	964	121	1.19	9281	145	1.40
2722	3.58	0.46	7.75		-22.02	1.22	303.4	0.35	968	122	1.17	9292	145	1.35
2749	5.38	0.5	10.81		-24.32	1.16	304.4	0.36	972	122	1.17	9303	147	1.30
2768	4.87	0.47	10.42		-23.97	0.92	305.15	0.36	976	124	1.19	9314	151	1.30
2774	3.93	0.51	7.68	31.63	-23.13	1.66	305.4	0.37	980	125	1.19	9325	154	1.34
2792	3.85	0.48	7.96		-22.4	1.54	305.65	0.37	984	128	1.22	9335	159	1.34
2797	3.55	0.47	7.53		-22.64	1.87	306.15	0.38	989	130	1.23	9346	160	1.43
2803	3.15	0.43	7.38		-22.6	2.04	306.4	0.38	993	134	1.18	9356	161	1.32
2814	2.70	0.37	7.32		-22.65	2.03	306.8	0.39	997	135	1.18	9366	159	1.35
2819	3.77	0.47	8.10		-22.77	1.44	307.15	0.40	1002	133	1.24	9376	156	1.32
2824	3.28	0.43	7.67		-22.36	1.69	307.4	0.40	1006	126	1.30	9386	153	1.30
2833	3.27	0.43	7.54		-22.34	1.85	307.65	0.41	1011	118	1.17	9396	149	1.31
2837	3.21	0.40	7.94		-23.18	1.51	308.15	0.42	1016	109	1.25	9406	146	1.34
2842	2.16	0.30	7.28		-22.29	2.20	308.4	0.43	1021	104	1.18	9415	145	1.28
2850	2.97	0.41	7.24		-22.64	2.16	308.65	0.44	1025	101	1.15	9425	144	1.31
2854	3	0.41	7.24		-23.48	1.65	309.15	0.46	1030	102	1.13	9434	144	1.35
2858	2.61	0.35	7.48		-22.86	1.62	309.4	0.47	1035	106	1.18	9443	144	1.31
2862	2.91			21.80			309.65	0.48	1040	115	1.18	9452	146	1.26
2866	2.41	0.31	7.86		-21.59	1.52	309.9	0.49	1045	125	1.25	9461	150	1.30
2873	2.94	0.38	7.69		-21.55	1.53	310.15	0.51	1049	137	1.37	9470	156	1.52
2879	2.77	0.33	8.39		-21.08	1.35	310.65	0.54	1054	147	1.50	9479	163	1.71
2885	3.29	0.42	7.83		-22.60	1.72	311.15	0.57	1058	149	1.81	9488	171	1.40
2888	3.46	0.43	8.04		-22.65	1.82	311.65	0.59	1063	142	1.56	9497	179	1.38
2891	3.42	0.45	7.63		-22.133	1.65	311.9	0.61	1067	129	1.21	9505	188	1.36
2897	3.93	0.49	8.00		-21.85	1.63	312.15	0.63	1072	115	1.19	9514	198	1.35
2902	3.65	0.47	7.75		-22.10	1.98	312.65	0.67	1076	102	1.15	9522	210	1.35
2907	3.24	0.44	7.40		-22.44	1.88	313.15	0.70	1081	93	1.19	9530	225	1.38
2912	3.37	0.47	7.22		-22.76	1.89	313.65	0.74	1085	87	1.25	9539	242	1.35
2917	2.89	0.37	7.70		-23.18	1.87	314.15	0.78	1090	81	1.18	9547	260	1.40
2919	2.93			23.56			314.65	0.82	1094	76	1.21	9555	277	1.47
2922	2.73	0.36	7.49		-22.81	1.80	314.9	0.84	1098	72	1.16	9563	289	1.37
2926	2.76	0.38	7.34		-22.25	1.81	315.15	0.87	1103	69	1.13	9571	300	1.37
2930	2.55	0.35	7.36		-22.43	1.85	315.65	0.92	1107	67	1.10	9579	314	1.41
2934	2.60	0.37	7.10		-22.49	1.8	316.15	0.96	1111	68	1.09	9586	328	1.71
2937	3.76	0.46	8.17		-22.45	1.67	316.65	1.00	1116	68	1.14	9594	338	1.96
2939	2.03	0.29	6.92		-22.42	1.98	316.9	1.02	1120	68	1.15	9602	335	2.00
2943	2.57	0.35	7.28		-22.63	1.97	317.15	1.06	1124	67	1.21	9609	321	1.67
2947	2.46	0.33	7.37		-22.37	1.85	317.65	1.11	1129	65	1.26	9617	299	1.36
2949	2.36	0.30	7.91		-22.41	1.85	318.15	1.14	1133	63	1.11	9624	278	1.37
2951	1.76	0.22	7.82		-21.94	1.70	318.4	1.16	1137	62	1.13	9632	261	1.37
2956	1.29	0.16	7.93		-21.23	1.29	318.65	1.19	1141	61	1.10	9639	252	1.42
2958	3.7			14.43			319.15	1.22	1145	62	1.12	9647	249	1.41
2960	0.65	0.09	7.47		-22.32	1.50	319.4	1.24	1150	65	1.14	9654	253	1.42
2964	0.13	0.02	5.39		-23.21	2.29	319.65	1.27	1154	69	1.11	9661	261	1.49
2977	2.74	0.33	8.24		-23.25	1.26	322.9	1.33	1158	70	1.19	9668	281	1.61
2980	1.85	0.23	8.05		-22.11	1.74	323.15	1.34	1162	71	1.20	9675	296	1.70
2982	2.86	0.34	8.44		-22.80	1.20	323.4	1.34	1166	70	1.31	9683	311	1.45
2988	2.86	0.34	8.35		-22.05	1.16	323.65	1.34	1170	67	1.17	9690	323	1.42
2990	2.41			18.28			324.2	1.34	1175	63	1.11	9697	324	1.45
2993	2.49	0.31	7.94		-23.08	1.84	324.4	1.34	1179	60	1.11	9704	316	1.69
2999	2.44	0.31	7.85		-23.26	1.78	324.65	1.33	1183	58	1.11	9711	301	1.40
3004	2.13	0.27	7.77		-23.15	1.64	325.15	1.31	1187	56	1.10	9718	285	1.49
3010	2.45	0.29	8.57		-22.91	1.21	325.65	1.29	1191	56	1.10	9725	272	1.58

Core VGHV08-1A-1B from Vestra Gíslholtsvatn
Physical and organic matter proxies (continued).

Age BP	%TOC	%N	C:N	%BSi	$\delta^{13}C$	$\delta^{15}N$	Depth in Core cm	Sed Rate mm/yr	Age BP	MS SI	Den g/cm^3	Age BP	MS SI	Den g/cm^3
3013	3	0.34	8.73		-22.26	1.24	326.15	1.26	1195	57	1.09	9732	261	1.50
3016	1.91	0.22	8.78		-24.09	1.32	326.4	1.25	1199	60	1.09	9738	255	1.43
3022	1.89	0.22	8.55		-22.934	1.22	326.65	1.23	1203	62	1.11	9745	252	1.40
3028	1.94	0.23	8.40		-23.078	0.75	327.15	1.18	1207	66	1.14	9752	251	1.45
3035	1.61	0.19	8.53		-24.281	0.89	327.65	1.15	1211	70	1.12	9759	252	1.47
3041	1.61	0.19	8.59		-24.195	1.00	328.15	1.10	1216	74	1.14	9766	253	1.42
3044	2.27	0.24	9.27		-23.1	1.57	328.65	1.08	1220	75	1.14	9773	254	1.47
3047	1.79	0.21	8.69		-24.16	1.31	328.9	1.07	1224	74	1.15	9780	257	1.46
3054	1.49	0.17	8.95		-24.20	0.61	329.15	1.05	1228	73	1.14	9786	261	1.46
3060	1.26	0.14	8.81		-23.75	1.05	329.65	1.04	1232	72	1.17	9793	266	1.47
3067	1.68	0.16	10.44		-24.68	0.78	330.15	1.02	1236	74	1.16	9800	274	1.45
3071	1.37			12.33			330.65	1.01	1240	78	1.09	9807	284	1.48
3074	1.19	0.15	8.08		-23.71	0.76	330.9	1.00	1244	85	1.10	9814	297	1.52
3081	1.24	0.16	7.57		-23.43	0.86	331.15	0.99	1248	96	1.12	9821	312	1.49
3088	1.53	0.19	8.05		-21.59	1.10	331.65	0.98	1252	109	1.09	9827	327	1.50
3095	1.32	0.18	7.50		-21.97	1.24	332.15	0.96	1256	124	1.15	9834	342	1.70
3102	1.04	0.15	7.15		-23.41	1.29	332.8	0.95	1260	135	1.21	9841	353	1.84
3105	1.82	0.20	9.19		-23.97	1.58	333.15	0.94	1265	139	1.55	9848	355	1.55
3109	2.67	0.37	7.16		-22.74	1.62	333.4	0.93	1269	132	1.85	9855	348	1.73
3116	2.44	0.27	8.89		-24.09	1.57	333.65	0.93	1273	117	1.20	9862	334	1.63
3131	4.21	0.53	7.91		-22.24	1.46	334.4	0.91	1277	100	1.14	9869	318	1.50
3135	3.97			37.43			335.15	0.89	1281	86	1.15	9876	305	1.47
3139	3.92	0.51	7.71		-22.49	1.83	335.4	0.89	1285	75	1.10	9883	294	1.50
3146	4.14	0.54	7.65		-23.14	1.89	335.65	0.88	1289	67	1.14	9890	288	1.52
3154	3.90	0.52	7.48		-22.31	1.67	336.15	0.87	1293	62	1.11	9897	283	1.50
3181	2.68	0.34	7.85		-22.82	1.48	336.65	0.86	1298	59	1.14	9904	281	1.56
3212	3.9			30.82			338.4	0.83	1302	56	1.13	9911	281	1.59
3212		0.55	7.08		-24.02	1.87	340.4	0.80	1306	55	1.11	9919	280	1.55
3228	3.8	0.56	6.84		-23.72	1.75	340.4	0.80	1310	54	1.15	9926	282	1.51
3244	4.17	0.54	7.71		-23.33	1.78	341.4	0.79	1314	54	1.16	9933	282	1.57
3261	4.28	0.53	8.11		-23.13	1.45	342.4	0.78	1319	53	1.20	9940	285	1.66
3277	6.35	0.56	11.38		-25.59	1.11	343.4	0.76	1323	52	1.22	9948	287	1.56
3294	4.4	0.5	8.83		-24.08	1.77	344.4	0.75	1327	51	1.15	9955	290	1.55
3310	4.14	0.53	8.64	34.3	-23.81	1.93	346.4	0.74	1331	50	1.09	9963	294	1.58
3327	3.95	0.55	7.14		-23.03	1.73	346.4	0.74	1336	51	1.13	9970	298	1.56
3344	4.82	0.58	8.31		-23.89	1.77	347.4	0.73	1340	50	1.15	9978	303	1.64
3360	4.39	0.53	8.3		-24.16	1.91	348.4	0.72	1344	51	1.12	9986	308	1.64
3369	4	0.51	7.84		-22.9	1.54	349.4	0.71	1349	52	1.11	9993	313	1.62
3377	3.79	0.48	7.84		-23.59	1.66	349.9	0.71	1353	54	1.09	10001	320	1.68
3394	3.66	0.52	7.03		-23	1.77	350.4	0.71	1357	57	1.10	10009	325	1.65
3411	3.1	0.42	7.19	29.83	-23.55	1.93	352.4	0.70	1362	61	1.11	10017	331	1.63
3427	2.64	0.48	5.46		-23.41	1.8	352.4	0.70	1366	67	1.11	10025	339	1.67
3444	2.97	0.49	6.03		-23.52	1.77	353.4	0.69	1370	75	1.12	10033	344	1.69
3452	3.62	0.46	7.88		-22.82	1.65	354.4	0.69	1375	84	1.17	10041	350	1.72
3460	2.84	0.51	5.51		-23.51	1.47	354.9	0.69	1379	92	1.41	10049	356	1.57
3477			7.43		-24.32	1.22	355.4	0.68	1384	98	1.28	10058	363	1.63
3485	2.97	0.4	7.52		-22.98	2.15	356.4	0.68	1388	102	1.15	10066	371	1.72
3493	2.09	0.34	6.1		-22.98	1.75	356.9	0.68	1393	103	1.26	10074	381	1.69
3501	2.22	0.28	8.07		-23.85	1.84	357.4	0.68	1397	99	1.19	10083	393	1.77
3509	1.86	0.33	5.72		-22.48	1.56	357.9	0.68	1402	92	1.15	10092	405	1.81
3517	1.65			17.98			358.4	0.68	1407	83	1.15	10100	417	1.87
3525	0.48	0.1	4.73		-23.04	0.45	358.9	0.68	1411	73	1.17	10109	431	1.86
3548	3.22			30.22			365.8	0.67	1416	65	1.11	10118	444	1.85
3556	3.58	0.53	6.76		-22.74	1.88	365.9	0.67	1421	59	1.14	10127	456	1.87
3571	4.04	0.55	7.34		-23.39	1.2	366.7	0.67	1425	55	1.10	10136	469	1.93
3579	1.82	0.24	7.7		-22.65	1.9	367.4	0.67	1430	51	1.09	10146	481	2.00
3587	3.61	0.63	5.76		-22.78	1.4	367.9	0.67	1435	49	1.10	10155	494	1.94
3594	3.67	0.47	7.85		-22.42	1.7	368.4	0.67	1440	47	1.07	10164	506	1.95
3602	3.71	0.66	5.64		-23.1	1.66	368.9	0.67	1444	46	1.09	10174	516	1.94
3616	3.21	0.56	5.72		-23.31	1.75	369.4	0.67	1449	45	1.13	10184	526	2.01
3624	2.73			29.12			370.4	0.67	1454	45	1.06	10193	534	1.98
3631	3.58	0.57	6.33		-22.86	1.8	370.9	0.67	1459	45	1.15	10203	543	1.90
3645	3.37	0.61	5.54		-22.66	1.9	371.4	0.67	1464	45	1.13	10213	552	1.98
3660	3.65	0.54	6.77		-23.6	1.57	372.4	0.68	1469	46	1.08	10224	562	2.02
3667	3.73	0.48	7.78		-23.3	1.58	373.4	0.68	1474	47	1.08	10234	574	1.95
3674	1.88	0.32	5.86		-22.42	1.88	373.9	0.68	1479	48	1.10	10244	586	1.91
3695	3.02			23.99			374.9	0.68	1484	48	1.13	10255	598	1.92
3736	2.2	0.29	7.49		-22.4	1.95	378.4	0.69	1489	48	1.12	10265	605	1.98
3749	2.56	0.35	7.4		-22.65	2.41	378.9	0.70	1494	48	1.16	10276	608	1.87
3782	2.05			19.18			381.2	0.71	1499	47	1.12	10287	607	1.87

Core VGHV08-1A-1B from Vestra Gíslholtsvatn
Physical and organic matter proxies (continued).

Age BP	%TOC	%N	C:N	%BSi	$\delta^{13}C$	$\delta^{15}N$	Depth in Core cm	Sed Rate mm/yr
3801	3.42	0.4	8.51		-21.16	1.55	382.4	0.71
3846	3.58			29.44			386.7	0.73
3871	2.86	0.36	8.05		-22.27	2.11	387.4	0.73
3908	3.77	0.61	6.15		-23.19	1.98	389.4	0.74
3914	1.78			16.44			392.4	0.75
3920	4.32	0.69	6.24		-23.28	1.04	393	0.75
3932	4.11	0.63	6.54		-22.98	1.37	393.4	0.75
3938	3.79	0.47	8.01		-23.46	1.94	394.4	0.76
3944	3.71	0.6	6.22		-23.38	1.87	394.9	0.76
3956	4.48	0.67	6.7		-23.49	1.45	395.4	0.76
3962	3.78			31.61			396.4	0.77
3968	4.85	0.68	7.1		-23.5	1.78	396.9	0.77
3980	3.89	0.63	6.18		-23.45	1.66	397.4	0.77
3992	3.6	0.61	5.92		-23.38	1.65	398.4	0.78
3998	3.66	0.46	7.88		-22.73	1.66	399.4	0.78
4005	3.61	0.62	5.86		-23.14	1.82	399.9	0.79
4017	2.15	0.4	5.35		-23.52	1.61	400.4	0.79
4023	2.37			23.66			401.4	0.79
4029	2.73	0.49	5.55		-23.43	2.22	401.9	0.80
4053	3.75	0.56	6.68		-23.26	1.65	403.4	0.80
4059	3.31	0.43	7.65		-22.66	2.14	404.4	0.81
4066	3.25	0.58	5.58		-23.12	1.91	404.9	0.81
4078	2.91	0.52	6.02		-22.71	1.79	405.4	0.81
4084	2.91			29.38			406.4	0.82
4090	3.12	0.53	5.93		-23.63	2.23	406.9	0.82
4109	3.54	0.57	6.16		-22.66	1.9	407.4	0.82
4116	2.51	0.41	6.07		-23.21	1.74	408.9	0.82
4122	3.37	0.43	7.78		-22.49	1.85	409.4	0.82
4128	2.73	0.45	6.04		-22.15	1.36	409.9	0.82
4138	2.04	0.24	8.36		-23.41	1.57	410.4	0.82
4141					-23.12		411.15	0.82
4158	2.09	0.22	9.48		-24.63	1.24	411.9	0.82
4161	1.86			14.1			412.65	0.82
4168	1.25	0.15	8.61		-24.6	1.56	412.9	0.82
4188	2.62	0.31	8.49		-22.04	2.04	413.4	0.82
4191	0.25	0.05			-23.93	2.25	414.9	0.81
4215	2.54	0.29	8.66		-24.31	1.42	416.3	0.81
4229	2.88			24.46			417.4	0.80
4236	4.43	0.51	8.7		-24.54	1.83	418	0.80
4251	4.6	0.52	8.79		-24.22	1.75	418.4	0.80
4265	4.24	0.57	7.4		-23.42	1.8	419.9	0.79
4280	4.48	0.55	8.07		-24.18	1.68	420.4	0.79
4312	3.6	0.48	7.48		-23.22	1.67	421.4	0.78
4327	3.27			31.93			423.9	0.76
4343	2	0.23	8.88		-23.03	1.65	424.6	0.76
4358	2.16	0.23	9.19		-24.82	1.99	426.4	0.74
4372	1.75	0.19	9.09		-25.17	1.99	428.4	0.73
4388	5.22			33.27			429.1	0.73
4404	3.61	0.3	12.22		-26.82	2.15	429.6	0.72
4420	4.28	0.45	9.41		-24.85	1.96	430.6	0.71
4437	2.81	0.3	9.42		-25.08	1.99	432.3	0.70
4453	5.61	0.52	10.88		-25.08	1.74	432.6	0.70
4470	3.85			33			433.6	0.69
4486	4.12	0.5	8.22		-23.18	2.08	434.6	0.68
4503	3.89	0.49	7.87		-23.09	2.11	435.6	0.68
4520	3.69	0.46	8.01		-21.72	2.03	436.6	0.67
4537	0.62	0.07	8.73		-22.69	1.75	437.8	0.66
4555	4.21			33.48			438.6	0.66
4572	4.73	0.58	8.23		-22.85	1.79	439.6	0.65
4590	3.53	0.45	7.83		-23.45	1.9	440.6	0.65
4607	1.22	0.13	9.06		-21.05	1.07	442.2	0.64
4625	4.07	0.5	8.2		-23.15	1.71	442.6	0.63
4643	3.42			33.81			443.6	0.63
4661	4.19	0.5	8.41		-24	1.53	444.6	0.62
4680	4.49	0.54	8.35		-23.47	1.64	445.6	0.62
4698	4.33	0.54	8.1		-23.54	1.88	446.6	0.61
4717	4.48	0.52	8.6		-23.65	1.39	447.6	0.61
4735	3.81			33			448.6	0.60
4754	4.06	0.5	8.08		-23.34	1.98	449.6	0.60
4773	5.68	0.51	11.18		-24.87	1.79	450.6	0.59

Age BP	MS SI	Den g/cm^3
1505	47	1.07
1510	48	1.09
1515	48	1.08
1521	48	1.09
1526	48	1.10
1531	49	1.09
1537	50	1.09
1542	50	1.09
1548	50	1.12
1553	50	1.07
1559	51	1.09
1565	52	1.13
1570	52	1.10
1576	51	1.09
1582	52	1.14
1588	52	1.15
1594	52	1.10
1600	53	1.12
1606	54	1.08
1612	56	1.08
1618	58	1.01
1624	61	1.10
1630	64	1.10
1636	69	1.11
1642	73	1.15
1649	70	1.15
1655	80	1.24
1661	83	1.17
1668	83	0.90
1674	84	1.11
1681	84	1.14
1688	88	1.10
1694	92	1.11
1701	101	1.11
1708	113	1.14
1715	127	1.18
1722	144	1.17
1729	161	1.40
1736	175	1.05
1743	184	1.44
1750	189	1.61
1757	191	1.64
1765	189	1.55
1772	182	1.62
1779	171	1.40
1787	157	1.23
1794	142	1.20
1802	128	1.16
1810	119	1.13
1817	114	1.14
1825	115	1.07
1833	118	1.18
1841	124	1.16
1849	130	1.30
1857	134	1.26
1865	137	1.16
1873	136	1.17
1882	133	1.15
1890	130	1.18
1898	127	1.30
1907	124	1.23
1949	155	1.14
1957	169	1.29
1966	181	1.52
1976	188	1.76
1985	186	1.75
1994	175	1.71
2003	161	1.45
2013	146	1.19
2022	135	1.15

Age BP	MS SI	Den g/cm^3
10298	601	1.89
10309	589	1.89
10320	573	1.83
10331	552	1.89
10342	527	1.87
10353	496	1.82
10364	463	1.80
10375	428	1.84
10386	397	1.55
10397	374	1.42
10408	357	1.41
10419	347	1.45
10430	342	1.50
10441	338	1.51
10452	339	1.48
10463	339	1.51
10474	342	1.59
10485	345	1.58
10496	350	1.51
10507	356	1.63
10518	361	1.63
10529	368	1.60
10540	374	1.63
10551	380	1.70
10562	385	1.67
10573	391	1.63
10584	399	1.59
10595	409	1.71
10606	421	1.71
10617	437	1.67
10628	453	1.66
10639	471	1.68
10650	488	1.73
10661	498	1.73
10672	499	1.76
10683	489	1.87
10694	472	1.85
10705	452	1.73
10716	435	1.69
10727	422	1.64
10738	414	1.65
10749	408	1.76
10760	403	1.73
10771	399	1.71
10782	396	1.76
10793	390	1.80
10804	382	1.90
10815	375	1.79
10826	370	1.78
10836	369	1.86
10847	372	1.87
10858	374	1.81
10869	376	1.77
10880	374	1.75
10891	370	1.82
10902	364	1.83
10913	359	1.78
10924		1.83
10935	347	1.88
10946	342	1.81
10957	336	1.76
10968	333	1.88
10979	331	1.96
10990	331	1.82
11001	332	1.86

Core VGHV08-1A-1B from Vestra Gíslholtsvatn
Physical and organic matter proxies (continued).

Age BP	%TOC	%N	C:N	%BSi	$\delta^{13}C$	$\delta^{15}N$	Depth in Core cm	Sed Rate mm/yr	Age BP	MS SI	Den g/cm^3
4792	4.2	0.5	8.39		-22.99	1.73	451.6	0.59	2032	129	1.16
4811	3.73	0.46	8.18		-23.31	1.83	452.6	0.59	2041	129	1.17
4830	2.49			31.35			453.6	0.58	2051	132	1.17
4850	3.23	0.41	7.95		-23.28	1.97	454.6	0.58	2061	135	1.19
4869	4.07	0.5	8.1		-24.06	1.89	455.6	0.57	2071	135	1.51
4889	3.56	0.43	8.38		-23.01	1.64	456.6	0.57	2080	133	1.46
4908	3.01	0.37	8.24		-23.29	1.72	457.6	0.57	2091	130	1.17
4928	3.19			35.91			459.1	0.56	2101	127	1.15
4948	1.62	0.2	8.07		-24.24	1.71	459.6	0.56	2111	125	1.17
4968	3.64	0.45	8.14		-23.63	1.45	460.6	0.55	2121	121	1.33
4988	3.52	0.43	8.17		-23.6	1.5	461.6	0.55	2132	117	1.18
5008	3.82	0.46	8.39		-23.45	1.46	462.6	0.55	2142	111	1.14
5028	3.85			35.84			463.6	0.54	2153	106	1.20
5049	3.78	0.45	8.3		-23.38	1.62	464.6	0.54	2163	100	1.43
5069	3.98	0.48	8.32		-23.44	1.32	465.6	0.54	2174	93	1.14
5090	3.48	0.42	8.21		-23.32	1.55	466.6	0.54	2185	87	1.14
5110	3.36	0.39	8.62		-23.17	1.41	467.6	0.53	2196	81	1.11
5131	3.17			30.94			468.6	0.53	2207	77	1.12
5152	3.83	0.42	9.03		-22.08	1.09	469.6	0.53	2218	73	1.11
5173	4.68	0.45	10.38		-24.41	1.67	470.6	0.52	2229	71	1.13
5194	3.84	0.44	8.67		-23.24	1.24	471.6	0.52	2240	69	1.14
5215	4.37	0.53	8.31		-23.35	1.41	472.6	0.52	2252	68	1.14
5236	4.62	0.6	8.43	36.91	-24.46	1.3	473.6	0.52	2263	69	1.13
5257	4.38	0.54	8.14		-23.36	1.55	474.6	0.51	2275	68	1.11
5278	4.55	0.57	8.03		-23.7	1.46	475.6	0.51	2286	70	1.12
5300	4.48	0.61	7.54		-23.18	1.57	476.6	0.51	2298	72	1.12
5321	4.31	0.57	7.64		-23.06	2.04	477.6	0.51	2310	73	1.17
5343	3.76	0.64	6.8	32.48	-22.68	1.28	478.6	0.51	2322	76	1.11
5364	4.2	0.55	7.72		-22.62	1.85	479.6	0.50	2334	79	1.13
5386	3.71	0.51	7.34		-22.7	1.99	480.6	0.50	2346	84	1.11
5407	3.58	0.5	7.24		-22.65	1.88	481.6	0.50	2358	91	1.13
5424	0.39	0.39	7.62		-22.23	1.69	482.6	0.50	2370	100	1.17
5429	2.53	0.33	7.65		-22.77	2.01	483.35	0.50	2383	111	1.33
5435	1.67	0.23	7.23		-22.97	1.83	483.8	0.49	2395	125	1.18
5445	1.43	0.19	7.43		-22.76	1.3	483.85	0.49	2408	142	1.20
5451				29.94			484.35	0.49	2421	163	1.19
5456	3.3	0.41	8		-22.73	1.72	484.6	0.49	2434	188	1.23
5462	3.12	0.5	6.28		-22.41	1.61	484.85	0.49	2446	216	1.64
5467	2.88	0.39	7.42		-22.46	2.02	485.1	0.49	2459	249	1.31
5473	3.33	0.43	8.03		-22.96	2.02	485.35	0.49	2473	285	1.14
5478	3.09	0.43	7.24		-22.96	2.03	485.6	0.49	2486	320	1.23
5489	3.77	0.5	7.47		-22.54	1.77	485.85	0.49	2499	346	1.37
5495	3.16	0.42	7.52		-23.13	1.85	486.35	0.49	2513	352	1.28
5500	2.74	0.37	7.34		-23.15	1.92	486.6	0.49	2526	334	1.29
5511	2.75	0.37	7.43		-23.09	1.82	486.85	0.49	2540	298	1.32
5517	3.03	0.42	7.42		-22.97	2.03	487.35	0.49	2554	253	1.12
5522	3.42	0.43	7.95		-22.5	1.92	487.6	0.49	2567	208	1.17
5535	3.36	0.46	7.31		-22.66	2.21	487.85	0.49	2581	169	1.13
5539	3.31	0.49	7.04		-22.92	1.98	488.45	0.49	2596	139	1.12
5539				31.15			488.6	0.49	2610	116	1.16
5544	2.88	0.4	7.24		-23.03	2.32	488.6	0.49	2624	101	1.16
5555	3.04	0.42	7.18		-22.88	2.07	488.85	0.49	2638	90	1.12
5561	3.46	0.52	6.49		-23.15	1.83	489.35	0.48	2652	83	1.15
5566	3.84	0.47	8.26		-23.42	2.12	489.6	0.48	2666	77	1.15
5577	3.17	0.42	7.58		-22.76	2.56	489.85	0.48	2680	74	1.15
5583	2.93	0.44	7.01		-22.88	1.96	490.35	0.48	2694	71	1.13
5588	2.96	0.39	7.6		-22.91	2.77	490.6	0.48	2707	71	1.15
5599	2.83	0.39	7.3		-22.72	2.44	490.85	0.48	2720	71	1.16
5605	2.89	0.42	6.95		-22.54	2.01	491.35	0.48	2733	73	1.17
5610	3.28	0.38	8.65		-22.29	2.65	491.6	0.48	2746	75	1.10
5621	2.38	0.31	7.75		-22.54	2.66	491.85	0.48	2758	78	1.17
5627	1.55	0.33	5.13	20.96	-23.2	1.77	492.35	0.48	2770	80	1.17
5632	1.42	0.2	6.97		-22.94	2.61	492.6	0.48	2782	82	1.18
5644	0.43	0.08	5.26		-22.39	1.61	492.85	0.48	2793		1.16
5652	2.03	0.18	11.53		-15.79	2.48	495.3	0.48	2803	82	1.12
5658	3.28	0.44	7.55		-22.82	2.02	495.35	0.48	2813	84	1.15
5664	1.36	0.16	8.29		-20.99	2.37	495.6	0.48	2822	83	1.15
5675	3.52	0.44	8.01		-22.52	2.11	495.9	0.48	2831	83	1.20
5680	2.47	0.37	8.78		-20.32	1.28	496.35	0.48	2840	81	1.20
5686	3.72	0.46	8.01		-22.74	2.51	496.6	0.48	2848	77	1.15

Core VGHV08-1A-1B from Vestra Gíslholtsvatn
Physical and organic matter proxies (continued).

Age BP	%TOC	%N	C:N	%BSi	$\delta^{13}C$	$\delta^{15}N$	Depth in Core cm	Sed Rate mm/yr	Age BP	MS SI	Den g/cm^3
5697	3.98	0.51	7.78		-22.69	2.28	496.85	0.48	2855	75	1.15
5703	3.87	0.54	7.29		-23.13	1.98	497.35	0.48	2863		1.10
5708	3.76	0.48	7.8		-22.48	2.34	497.6	0.48	2869	73	1.12
5719	2.51	0.34	7.42		-22.87	2.15	497.85	0.47	2876	73	1.13
5725	3.47	0.47	7.62		-22.83	2.08	498.35	0.47	2882	73	1.15
5731	2.85	0.37	7.75		-23.02	2.51	498.7	0.47	2888	75	1.14
5742	3.97	0.49	8.07		-22.61	2.05	498.85	0.47	2893	79	1.07
5747	3.25	0.57	6.34	34.89	-23.45	2.09	499.35	0.47	2898	83	1.11
5753	3.63	0.47	7.74		-23.17	2.39	499.6	0.47	2903	88	1.16
5764	3.49	0.45	7.79		-22.82	2.42	499.85	0.47	2908	93	1.17
5770	3.17	0.44	7.35		-23.23	2.06	500.35	0.47	2913	99	1.17
5776	3.29	0.44	7.56		-22.8	2.39	500.6	0.47	2917	106	1.20
5787	2.93	0.38	7.63		-23.27	2.38	500.85	0.47	2921	114	1.25
5793	3.28	0.46	7.22		-23.25	1.78	501.35	0.47	2925	127	1.13
5798	3.49	0.46	7.61		-23.35	2.5	501.6	0.47	2929	144	1.14
5810	3.79	0.49	7.68		-23.08	2.31	501.85	0.47	2933	165	1.21
5815	3.68	0.52	7.24		-23.57	2	502.35	0.47	2937	190	1.28
5821	3.86	0.47	8.2		-21.97	2.14	502.6	0.47	2940	213	1.33
5838	3.43	0.46	7.94		-22.44	1.83	502.85	0.47	2944	232	1.56
5862	4.34			32.59			503.6	0.47	2948	246	1.84
5885	3.18	0.36	8.73		-22.65	2.15	504.6	0.47	2951	251	1.75
5908	3.2	0.38	8.33		-23.33	2.24	505.6	0.47	2955	248	1.83
5932	2.88	0.35	8.15		-23.07	2.24	507.5	0.46	2959	236	1.74
5956	2.55	0.3	8.4		-23.03	2.27	507.6	0.46	2962	218	1.68
5980	3.86			33.91			508.6	0.46	2966	198	1.32
6004	4.14	0.49	8.41		-22.95	2.01	509.6	0.46	2970	178	1.24
6028	3.85	0.46	8.32		-22.9	1.6	510.6	0.46	2975	159	1.21
6053	4.09	0.49	8.33		-23.51	1.9	511.6	0.46	2979	144	1.20
6078	4	0.48	8.32		-23.67	1.88	512.6	0.45	2984	133	1.21
6104	3.49			31.09			513.7	0.45	2988	126	1.18
6129	3.67	0.45	8.11		-23.55	1.94	514.6	0.45	2993	122	1.20
6155	2.38	0.29	8.28		-24.26	2.27	515.6	0.45	2998	121	1.19
6181	3.2	0.38	8.41		-24.12	2.03	516.6	0.44	3003	120	1.26
6208	3.32	0.38	8.72		-23.9	1.75	517.6	0.44	3008	119	1.22
6235	4.04			28.65			518.6	0.44	3013	118	1.24
6262	3.09	0.36	8.55		-24.36	1.82	519.6	0.43	3018	118	1.27
6290	3.92	0.32	12.12		-26.27	2.06	520.6	0.43	3023	119	1.25
6318	3.12	0.32	9.77		-22.58	1.86	521.6	0.42	3028	121	1.28
6347	2.21	0.24	9.13		-25.19	1.62	523.5	0.42	3034	123	1.27
6376	3.31			22.03			523.6	0.41	3039	127	1.26
6405	2.39	0.27	8.99		-25.03	1.86	524.6	0.41	3045	131	1.30
6435	3.65	0.41	8.82		-24.89	2.19	525.6	0.40	3050	135	1.26
6465	3.16	0.39	8.18		-24.2	2.33	526.6	0.40	3056	136	1.24
6496	1.1			21.12			527.6	0.39	3062	134	1.24
6559	2.17	0.27	8.15		-23.66	2.44	529.1	0.39	3068	128	1.23
6591	3.24	0.4	8.02		-23.61	2.39	530.6	0.38	3073	119	1.15
6624	3.18	0.4	8		-23.97	2.27	531.6	0.37	3079	110	1.31
6657	2.46	0.33	7.48		-23.6	2.28	533.4	0.37	3085	101	1.63
6691	3.02			30.76			533.6	0.36	3091	92	1.28
6725	2.03	0.27	7.56		-23.68	2.26	534.6	0.36	3098	83	1.12
6761	2.6	0.33	7.91		-23.73	1.79	535.6	0.35	3104	77	1.14
6796	2.5	0.32	7.85		-24.35	2.47	536.6	0.35	3110	70	1.12
6832	3.25	0.39	8.29		-24.3	2.01	537.6	0.34	3116	68	1.21
6869	3.06			26.97			538.6	0.33	3123	66	1.12
6907	3.31	0.4	8.32		-24.37	2.03	539.6	0.33	3129	63	1.05
6945	1.71	0.22	7.82		-24.08	2.17	540.6	0.32	3135	60	1.17
6984	0.52	0.07	7.9		-20.19	2	541.6	0.32	3142	58	1.13
7023	1.37	0.16	8.29		-23.66	2.02	542.6	0.31	3149	57	1.14
7063	3.33			32.86			543.6	0.31	3155	57	1.11
7104	3.37	0.41	8.29		-23.94	2.62	544.6	0.30	3162	56	1.09
7146	3.56	0.45	7.96		-23.75	2.13	545.6	0.30	3169	55	1.10
7188	3.22	0.39	8.15		-23.78	2.19	546.6	0.29	3175	55	1.10
7231	3.04	0.38	7.94		-23.35	2.15	547.6	0.29	3182	55	1.10
7275	3.28			33.93			548.6	0.28	3189	55	1.12
7320	3.65	0.44	8.22		-23.61	2.24	549.6	0.28	3196	54	1.11
7365	3.23	0.4	8.03		-22.97	2.43	550.6	0.27	3203	55	1.11
7411	3.31	0.4	8.33		-23.59	2.03	551.6	0.27	3210	56	1.13
7458	3.98	0.5	7.96		-23.25	2	552.6	0.26	3217	56	1.14
7506	2.18			27.42			553.6	0.26	3224	56	1.12
7555	3.68	0.44	8.28		-23.22	1.89	555.5	0.25	3231	56	1.15

Core VGHV08-1A-1B from Vestra Gíslholtsvatn
Physical and organic matter proxies (continued).

Age BP	%TOC	%N	C:N	%BSi	$\delta^{13}C$	$\delta^{15}N$	Depth in Core cm	Sed Rate mm/yr	Age BP	MS SI	Den g/cm^3
7604	3.37	0.4	8.35		-23.08	1.99	555.6	0.25	3238	57	1.14
7656	3.55	0.43	8.21		-23.35	2.19	556.6	0.24	3245	58	1.10
7688							557.6	0.24	3252	59	1.12
7709	3.62	0.44	8.16		-23.29	2.36	558.2	0.24	3259	59	1.16
7766	3.46			36.91			558.6	0.24	3267	60	1.18
7826	3.67	0.47	7.81		-22.94	2.63	559.6	0.23	3274	61	1.13
7889	3.58	0.45	7.96		-24.27	2.34	560.6	0.23	3281	62	1.12
7954	3.69	0.44	8.44		-24.61	2.36	561.6	0.22	3289	63	1.11
8000							562.6	0.22	3296	65	1.10
8056	3.42	0.42	8.15		-23.91	2.27	563.3	0.22	3303	68	1.12
8104	2.54			23.72			564.15	0.21	3311	70	1.10
8136	1.25	0.14	8.63		-23.53	1.87	565.6	0.21	3318	73	1.10
8199	1.63	0.2	8.34		-23.68	1.85	565.9	0.21	3325	78	1.12
8260	3.07	0.39	7.94		-23.54	2.01	566.9	0.21	3333	83	1.15
8319	4.16	0.53	7.93		-23.14	2.15	567.9	0.20	3340	88	1.17
8376	3.29			38.63			568.9	0.20	3348	92	1.16
8432	3.58	0.47	7.63		-22.82	2.14	569.9	0.19	3355	95	1.12
8486	2.95	0.38	7.69		-22.49	2.27	570.9	0.19	3363	99	1.16
8538	2.74	0.36	7.57		-21.73	2.08	571.9	0.18	3370	102	1.14
8589	2.07	0.27	7.52		-22.08	2.15	572.9	0.17	3378	105	1.17
8639	1.55			26.01			573.9	0.16	3385	114	1.19
8686	1.7	0.22	7.57		-22.13	2.1	574.9	0.16	3393	123	1.16
8733	1.2	0.16	7.71		-23.37	1.3	576.2	0.16	3400	136	1.21
8821	1.82	0.24	7.55		-23.38	1.88	576.9	0.16	3408	152	1.19
8863	2.1			28.33			578.9	0.16	3415	172	1.18
8904	2.21	0.3	7.31		-23.38	2.15	579.9	0.17	3423	196	1.21
8943	1.85	0.25	7.25		-22.24	2.21	580.9	0.17	3430	225	1.23
8981	1.81	0.24	7.49		-22.4	2.01	581.9	0.17	3438	256	1.40
9018	1.65	0.22	7.34		-22.4	2	583.5	0.18	3445	287	1.70
9053	1.62			23.59			583.9	0.18	3453	314	0.92
9087	1.85	0.26	7.2		-21.69	2.59	584.9	0.19	3460	336	0.87
9120	1.11	0.16	7.15		-21.56	2.47	586.6	0.20	3468	353	1.13
9152	1.24	0.17	7.47		-21.55	1.64	586.9	0.20	3475	365	1.10
9183	1.12	0.16	7.19		-21.31	1.66	587.9	0.21	3482	369	1.54
9213	1.37			22.85			589.3	0.22	3490	366	1.85
9241	0.71	0.1	6.85		-21.87	1.66	589.9	0.22	3497	354	1.86
9269	1.36	0.18	7.45		-21.42	2.36	590.9	0.23	3505	331	1.81
9295	1.29	0.18	7.26		-21.19	1.79	591.9	0.23	3512	301	1.81
9320	1.18	0.17	7.13		-21.25	1.75	592.9	0.24	3519	265	1.71
9345	1.03			21.96			593.9	0.25	3527	227	1.35
9368	1.33	0.18	7.27		-21.43	1.66	594.9	0.26	3534	192	1.20
9391	0.85	0.12	6.92		-20.84	0.91	595.9	0.26	3541	162	1.12
9413	0.71	0.1	6.99		-21.16	1.2	597.5	0.28	3549	137	1.18
9434	1.1	0.16	6.9		-21.05	1.44	597.9	0.28	3556	119	1.15
9454	0.95			22.08			598.9	0.29	3563	104	1.10
9473	1.03	0.15	6.79		-20.75	1.89	599.9	0.30	3571	93	1.13
9492	0.64	0.1	6.48		-20.52	1.05	600.9	0.31	3578	86	1.13
9510	1	0.15	6.87		-20.83	1.59	601.9	0.32	3585	81	1.12
9527	0.92	0.14	6.63		-20.77	2.21	602.9	0.33	3592	79	1.14
9543	0.92			21.25			604.2	0.35	3599	78	1.17
9559	0.81	0.12	6.57		-20.92	1.98	604.9	0.36	3606	78	1.13
9574	1.08	0.15	7.07		-21.39	1.57	605.9	0.37	3613	78	1.16
9589	1.05	0.15	6.89		-21.23	1.5	606.9	0.38	3620	82	1.12
9603	1	0.14	6.96		-20.93	2.08	607.9	0.40	3628	86	1.13
9616	0.99			23.66			608.9	0.41	3635	93	1.13
9629	0.91	0.13	7.06		-21.36	1.9	609.9	0.43	3642	102	1.16
9632							610.9	0.44	3649	110	1.24
9642	0.77	0.11	7.34		-21.34	2.45	611.1	0.45	3655	117	1.43
9654	0.87	0.13	6.71		-20.96	1.25	611.9	0.46	3662	120	1.74
9666	1.13	0.14	7.87		-21.21	2.13	612.9	0.48	3669	117	1.26
9677	0.87			19.45			613.9	0.49	3676	111	1.22
9688	0.96	0.12	7.69		-21.61	2.34	614.9	0.51	3683	105	1.19
9699	0.86	0.12	7.14		-21.5	2.24	615.9	0.53	3690	101	1.17
9729	0.78			17.64			617.9	0.57	3697	98	1.17
9739	0.68	0.09	7.19		-22.02	2.65	619.9	0.62	3704	99	1.15
9749	0.82	0.12	7.03		-21.49	1.36	620.9	0.64	3710	101	1.18
9758	0.82	0.12	6.99		-21.93	1.83	621.9	0.66	3717	105	1.18
9767	0.32	0.04			-23.01	2.56	623.3	0.70	3724	112	1.17
9777	0.69			13.95			623.9	0.71	3731	119	1.21
9786	0.64	0.09			-22.22	0.87	625.3	0.76	3737	127	1.30

Core VGHV08-1A-1B from Vestra Gíslholtsvatn

Physical and organic matter proxies (continued).

Age BP	%TOC	%N	C:N	%BSi	$\delta^{13}C$	$\delta^{15}N$	Depth in Core cm	Sed Rate mm/yr	Age BP	MS SI	Den g/cm^3
9795	0.66	0.08			-23.78	1.83	625.9	0.77	3744	135	1.55
9804	0.54	0.08			-21.32	2.47	626.9	0.79	3751	139	1.75
9813	0.65	0.09			-22.58	2.63	627.9	0.82	3757	140	1.50
9822	0.62			16.7			628.9	0.84	3764	139	1.22
9832	0.68	0.1	6.75		-22.21	2.15	629.9	0.87	3771	137	1.23
9841	1.59	0.09			-27.12	2.74	630.9	0.90	3777	137	1.21
9851	0.54	0.08			-22.29		631.9	0.92	3784	139	1.19
9861	0.53	0.08			-22.23	2.88	632.9	0.95	3790	143	1.19
9871	0.27			10.85			633.9	0.97	3797	148	1.22
9881	0.5	0.07			-22.56	2.65	635.1	1.00	3803	150	1.29
9902	0.37	0.05			-23.24	2.6	636.4	1.03	3810	147	1.27
9913	0.54	0.08			-22.48	2.19	637.9	1.05	3816	140	1.44
9925	0.51			10.36			638.9	1.06	3823	128	1.51
9937	0.56	0.08			-22.54	2.32	639.9	1.07	3829	116	1.17
9949	0.39	0.06			-22.51	2.36	640.9	1.08	3836	104	1.18
9962	0.55	0.05			-23.44		641.9	1.09	3842	93	1.15
9975	0.38	0.05			-22.34		642.9	1.09	3849	87	1.13
9989	0.41			11.53			643.9	1.09	3855	82	1.15
10003	0.48	0.07			-22.37	1.24	644.9	1.09	3861	79	1.14
10018	0.35	0.05			-22.94	3.01	645.9	1.08	3868	77	1.13
10033	0.29	0.04			-22.43	1.67	646.9	1.07	3874	77	1.14
10049	0.3	0.04			-22.84	1.38	647.9	1.06	3880	77	1.20
10066	0.71			9.45			648.9	1.05	3886	76	1.35
10083	0.29	0.04			-23.08		649.9	1.03	3893	76	1.12
10101	0.25	0.03			-24.43		651.1	1.00	3899	76	1.16
10120	0.15	0.02			-25.26		651.9	0.99	3905	75	1.09
10139	0.12	0.01			-25.31		652.9	0.97	3911	75	1.14
10160	0.07			7			653.9	0.95	3918	74	1.10
10181	0.12	0.01			-25.27		654.9	0.92	3924	75	1.15
10203	0.05	0			-21.16		655.9	0.90	3930	75	1.13
10226	0.06	0			-23.02		656.9	0.87	3936	75	1.11
10250	0.05	0			-21.32		658.5	0.83	3942	76	1.09
10275	0.03			6.99			658.9	0.82	3949	76	1.13
10303	0.04	0			-21.47		660.9	0.77	3955	77	1.10
10367	0.08						663.5	0.74	3961	78	1.12
10380	0.08			3.31			664.9	0.70	3967	79	1.14
10394	0.08	0					665.4	0.69	3973	81	1.13
10405	0.64	0.08			-21.81	1.98	666.2	0.67	3979	83	1.12
10411	0.57	0.08			-22.09	1.97	666.9	1.10	3985	86	1.14
10422	0.52	0.07			-22.6	3.47	667.9	1.06	3991	89	1.16
10432	0.5			13.11			668.9	0.97	3997	92	1.17
10443	0.5	0.08			-22.47	1.82	669.9	0.98	4003	93	1.22
10454	0.48	0.07			-22.26	2.56	670.9	0.91	4010	95	1.27
10466	0.39	0.06			-22.9	2.7	671.9	0.85	4016	95	1.18
10478	0.36	0.05			-22.38	3.22	672.9	0.89	4022	93	1.20
10490	0.32			13.2			673.9	0.80	4028	92	1.19
10503	0.32	0.04			-22.37	2.24	674.9	0.85	4034	91	1.19
10515	0.32	0.05			-21.82	3.47	675.9	0.79	4040	91	1.11
10527	0.32	0.05			-21.39	3.8	676.9	0.82	4046	92	1.12
10540	0.3	0.04			-22.16	0.6	677.9	0.80	4052	94	1.11
10554	0.25			12.97			678.9	0.77	4058	97	1.15
10577	0.26	0.03					680.9	0.77	4064	102	1.15
10591	0.28	0.04			-22.01	2.89	681.9	0.84	4071	109	1.16
10603	0.19	0.04			-22.34	4.02	682.9	0.75	4077	118	1.19
10617	0.19			11.75			683.9	0.79	4083	129	1.22
10631	0.22	0.04			-21.31		684.9	0.72	4089	144	1.22
10646	0.22	0.03					685.9	0.72	4095	164	1.22
10660	0.2	0.03			-22.07		686.9	0.68	4101	190	1.25
10673	0.17	0.03			-20.93		687.9	0.71	4108	220	1.23
10687	0.17			13.21			688.9	0.76	4114	255	1.23
10702	0.17	0.03			-22.14		689.9	0.70	4120	289	1.27
10716	0.19	0.02			-24.17		690.9	0.70	4126	315	1.43
10730	0.14	0.02			-22.62		691.9	0.72	4133	324	1.61
10758	0.15	0.02			-24.07		693.7	0.63	4139	321	1.28
10761				14.38			693.9	0.71	4145	313	1.25
10775	0.17	0.03			-23.35		694.9	0.69	4152	313	1.38
10788	0.13	0.02			-23.19		695.9	0.71	4158	320	1.47
10802	0.17	0.02			-24.16		696.9	0.74	4164	333	1.55
10816	0.15	0.02			-22.54		697.9	0.72	4171	345	1.63
10830				14.52			698.9	0.73	4177	350	1.70

Core VGHV08-1A-1B from Vestra Gíslholtsvatn
Physical and organic matter proxies (continued).

Age BP	%TOC	%N	C:N	%BSi	$\delta^{13}C$	$\delta^{15}N$	Depth in Core cm	Sed Rate mm/yr	Age BP	MS SI	Den g/cm^3
10844	0.15	0.03			-20.64		699.9	0.72	4184	343	1.33
10870	0.12	0.02			-22.67		701.6	0.64	4190	323	1.41
10874	0.13	0.01			-24.72		701.9	0.72	4197	292	1.33
10887	0.14	0.02			-24.48		702.9	0.73	4203	255	1.24
10898	0.25	0.03			-24.43		703.65	0.74	4210	215	1.25
10901				14.87			703.9	0.72	4217	176	1.18
10915	0.1	0.01			-23.25		704.9	0.72	4223	144	1.16
10954	0.19						707.7	0.72	4230	117	1.18
10970	0.2	0.02			-23.54		708.7	0.72	4237	96	1.15
10986	0.16	0.02			-23.96		709.7	0.65	4244	80	1.16

Core VGHV08-1A-1B
Tie-points used for VGHV08-1A-1B age model. See Figure 4.4 for VGHV08-1A-1B age model.

Tephra Name	^{14}C Age	BP	Error	Depth (cm)	Modeled Age (BP)
K1918		32	1	15	32
K1721		229	1	48.7	229
K1500		450	1	77.7	450
H1104		846	1	155.8	846
E934-40		1016	1	182.5	1016
K920		1030	1	183.8	1030
SL872		1078	2	189.1	1078
H-A	2450		44	298.1	2565
H-B	2740		20	306.8	2806
KE	2850		10	322.9	2975
H3	2879		34	324.2	2988
KN	3300		100	365.4	3541
SILK N4	3600		66	393	3915
H4	3826		12	416.3	4207
H T-layer		5657	200	495.3	5651
SILK A9		7660	200	555.5	7550
14C	6880		20	559.6	7766
H-Bas		8420	200	565.6	8117
G 10ka 1		10240	60	660.4	10287
G 10ka 2		10300	60	660.9	10300
G 10ka 3		10350	60	662.9	10313
G 10ka 4		10400	60	666.2	10402

Core VGHV08-1A-1B

Chironomid distribution used by Y. Axford to infer mean July air temperatures at Vestra Gíslholtsvatn. See Figure 4.8 for chironomid inferred summer temperature time series.

Age (BP)	Depth in Core (cm)	July air T (°C)	Heterotrissocladius (cold)	Dicrotendipes (warm)	heads/g
87	24.9	10.17	37.39	0.00	22.37
344	63.9	9.40	39.72	2.84	27.33
494	83.9	8.61	38.18	0.00	38.81
624	105.9	8.46	56.74	0.00	42.12
716	124.9	8.95	21.05	0.00	29.56
792	142.9	9.46	33.73	0.00	18.93
998	180.7	9.06	25.66	0.00	24.06
1140	194.7	9.74	27.93	3.60	55.20
1187	199.7	9.18	29.84	1.05	39.30
1244	205.7	9.59	25.27	2.15	60.00
1331	215.7	10.30	21.26	11.49	42.57
1417	225.2	9.15	32.80	5.38	47.45
1556	240.7	9.80	20.61	7.63	42.72
1670	250.7	9.81	19.42	9.71	48.13
1820	262.7	9.66	26.79	12.50	38.28
2391	289.9	8.67	31.29	1.23	40.56
2862	309.9	9.35	42.98	3.51	28.50
3044	328.9	9.60	32.69	2.56	24.05
3369	349.9	9.01	52.98	0.60	40.82
3594	368.9	9.62	38.92	4.86	46.25
4122	409.9	9.48	25.32	3.80	63.71
4744	449.1	8.49	53.11	1.69	62.77
5120	469.1	9.56	46.26	0.00	48.91
5549	489.1	9.80	42.62	1.64	46.51
6221	519.1	8.89	58.76	2.06	84.07
6850	539.1	8.96	65.00	0.00	117.65
7796	560.1	8.54	71.03	0.00	208.82
9237	594.4	8.40	62.86	0.00	140.00
9739	620.9	8.23	64.71	0.00	83.57
10402	666.9	7.02	0.00	0.00	20.86

Core VGHV08-1A-1B

Tephra layer thickness and depth in core from visual identification, modeled age from CLAM age model and tephra age, volcanic system, and formation determined from geochemical analysis by T. Thordarson. Data used in Fig. 4.5, 4.6, 4.8, and 4.10. NA indicates sample was not analyzed.

Layer #	Depth	Modeled Age	Tephra Age BP(^{14}C Age)	Thickness (cm)	Volcanic System	Formation
1	15.0	32	32	0.25	Katla	K1918
2	19.0	55	72	0.35	Bárdarbunga-Veiðivötn Hekla	B-V basalt H1878 contamination (mixed)
3	48.5	229	229	0.20	Katla	K1721
4	77.7	450	450	0.40	Katla	K1500
5	92.3	547	534?	0.20	Bárdarbunga-Veiðivötn Hekla Katla	B-V basalt H rhyolite, dacite, basalt K1416?

Core VGHV08-1A-1B

Tephra layer identification in Vestra Gíslholtsvatn sediment record (continued).

Layer #	Depth	Modeled Age	Tephra Age BP (^{14}C Age)	Thickness (cm)	Volcanic System	Formation
6	135.8	763	792?	0.30	Hekla	H1158?
7	155.8	846	846	0.60	Hekla	H1104
8	158.9	859	889?	0.20	WVZ Hekla	basalt H basalt, dacite
9	182.5	1016	1016	0.25	Katla	E934
10	183.8	1030	1030	0.20	Katla	K920
11	188.2 188.5	1078	1079	0.25 1.15	Bárdarbunga-Veiđivötn Torfajökull	Settlement Layer (basalt) Settlement Layer (basalt, icelandite, rhyolite)
12	196.1	1153	1089?	0.10	Grímsvötn? Katla	G basalt K 9th century (860 AD)
13	200.6	1197	1114?	0.20	Hekla	H basalt
14	212.9	1307	1180?	1.20	Katla	K basalt
15	226.4	1422	1253?	0.30	Katla	K1190?
16	227.9	1436		0.15	Hekla Bárdarbunga-Veiđivötn	H basalt B-V basalt
17	252.2	1687		0.25	Katla	K basalt
18	258.1	1765		3.40	Katla	K rhyolite, basalt
19	265.7	1880		1.10	Katla	K basalt
20	268.8	1933		0.25	Katla	K basalt
21	272.6	2002		2.10	Katla	K basalt
22	277.8	2105		0.80	Katla	K basalt
23	280.5	2163		0.20	Katla Hekla	K basalt, unu rhyolite H dacite
24	282.5	2208		0.30	Katla	K basalt
25	292.3	2456		0.50	Veiđivötn Katla	B-V basalt K basalt
26	294.3	2512		0.80	Katla	K basalt
27	296.8	2565	(2450 ± 44)	2.00	Hekla	H-A
28	306.8	2806	(2740 ± 20)	0.20	Hekla Grímsvötn?	H-B G? basalt
29	320.3	2966		0.80	Katla	K basalt
30	321.2	2975	(2850 ± 10)	1.70	Katla	KE?
31	324.2	2988	(2879 ± 34)	0.40	Hekla	H3
32	332.8	3097		0.20	Hekla	H basalt, icelandite
33	334.4	3120		0.70	Katla	K basalt
34	360.4	3541	(3300 ± 100)	5.00	Katla	KN, K unu rhyolite
35	365.8	3547	(3515 ± 55)	0.45	Hekla	HS
36	366.7	3561		0.20	Katla	K basalt (SILK like?)
37	374.9	3681		0.70	Katla	K basalt
38	378.4	3729		0.20	Katla	K basalt
39	381.2	3766		1.10	Katla	K basalt
40	385.4	3821		0.20	Hekla	H rhyolite, dacite, icelandite, basalt
41	386.7	3887		0.70	Katla	K basalt
42	392.7	3915	(~3600)	0.45	Katla	SILK N4
43	411.6	4144		0.55	Hekla	H basalt, icelandite
44	416.3	4207	(3826 ± 12)	0.65	Askja Hekla	Askja basalt? H4?
45	418.0	4231		0.20	Hekla Katla	H basalt K basalt, SILK-like
46	423.9	4317		0.10	Katla	K basalt
47	426.4	4355		0.30	Hekla	H basalt
48	427.3	4369		1.10	Hekla	H F-layer
49	429.1	4380	~4440	0.70	Katla	K basalt
50	432.3	4432	(4140 or 4840)	0.20	Katla	K basalt, icelandite, SILK N2 or N1?
51	437.8	4524		0.35	Katla	K basalt
52	442.2	4600		0.15	Grímsvötn Hekla	G basalt H unu rhyolite?
53	459.1	4918		0.60	Katla	K basalt, rhyolite
54	483.8	5433		0.25	Katla	K basalt
55	493.7	5651	5657	1.60	Hekla	H T-layer, intermediate, dacite
56	495.9	5665		0.20	Katla	K SILK?

Core VGHV08-1A-1B

Tephra layer identification in Vestra Gíslholtsvatn sediment record (continued).

Layer #	Depth	Modeled Age	Tephra Age BP (^{14}C Age)	Thickness (cm)	Volcanic System	Formation
57	498.7	5727		0.15	North Volcanic Zone? Katla	Askja? K basalt
58	507.5	5929		0.30	Katla North Volcanic Zone?	K basalt Askja?
59	513.7	6081		0.40	Hekla Bárdarbunga-Veiđivötn	H basalt B-V basalt
60	521.6	6290		0.50	NA	NA
61	523.5	6344		0.30	Bárdarbunga-Veiđivötn	B-V basalt
62	529.1	6511		1.30	Katla?	K basalt, rhyolite
63	533.4	6650		0.20	Katla Bárdarbunga-Veiđivötn	K basalt B-V basalt
64	555.5	7550	7360	0.40	Katla	K GJ-SILK
65	555.8	7688	7660?	0.50	Hekla Grímsvötn Katla	H basalt G basalt K GJ-SILK A9?
66	563.3	8000		0.20	Reykjanes Volcanic Belt? Katla	? K basalt, unu rhyolite
67	564.5	8117	8420?	1.10	Hekla	H basalt, intermediate
68	576.2	8701		0.60	Katla	K basalt
69	583.5	9003		0.55	Katla	K unu rhyolite, basalt
70	586.6	9111		0.30	Katla or Hekla Grímsvötn	K or H basalt G basalt
71	589.3	9195		0.20	Hekla Grímsvötn	H basalt G basalt
72	597.5	9404		0.30	Katla	K basalt
73	604.2	9532		0.20	Hekla	H basalt
74	611.1	9632	9400?	0.25	Bárdarbunga-Veiđivötn	B-V basalt
75	615.9	9688		0.20	Hekla	H basalt
76	617.4	9704		0.30	Grímsvötn Hekla	G basalt H basalt
77	617.9	9709		1.50	Katla	K basalt
78	623.3	9762		0.70	Grímsvötn Katla	G basalt K basalt
79	625.3	9780		0.70	Katla	K basalt
80	635.1	9873		0.30	West Volcanic Zone Grímsvötn Hekla	? G? H basalt
81	636.4	9886		0.60	Grímsvötn Hekla	G basalt H basalt
82	651.1	10087		0.10	Bárdarbunga-Veiđivötn Grímsvötn Hekla	B-V basalt G H basalt
83	658.5	10240		0.15	Bárdarbunga-Veiđivötn Grímsvötn	B-V basalt G 10ka series
84	660.1	10287	10240?	0.30	Grímsvötn	G 10ka series
85	660.9	10300	10300?	1.60	Grímsvötn	G 10ka series
86	662.7	10313	10350?	0.30	Grímsvötn	G 10ka series
87	663.5	10402	10400?	2.70	Bárdarbunga-Veiđivötn Grímsvötn Hekla	? G 10ka series H basalt
88	693.7	10746		0.30	Hekla	H basalt
89	701.6	10860		0.30	Hekla	H basalt
90 90	711.5	11001		0.70	Hekla Grímsvötn	H basalt G basalt
91 91	717.8	11112		0.30	Hekla Katla	H basalt K rhyolite
92 92	720.3	11143		0.10	Hekla Grímsvötn	H basalt G basalt
93	722.6	11175		0.20	Hekla	H basalt
94 94	729.1	11285		0.10	Hekla Kverkfjöll?	H basalt Kv-?

Core VGHV08-1A-1B
Tephra layer identification in Vestra Gíslholtsvatn sediment record (continued).

Layer #	Depth	Modeled Age	Tephra Age BP	Thickness (cm)	Volcanic System	Formation
95	733.1	11350		0.10	Hekla	H basalt
96	741.9	11486		0.10	Hekla	H basalt
97	744.9	11532		0.10	Hekla	H basalt
97					Katla	K intermediate, rhyolite
98	758.5	11735		0.10	Hekla	H basalt
99	768.4	11888		0.10	Grímsvötn	G basalt
99					Hekla	H basalt
100	778.9	12052		0.10	Hekla	H basalt
101	780.4	12067		0.10	Hekla	H basalt
102	788.2	12191		0.10	Hekla	H basalt
102					Grímsvötn	G basalt
103	792.1	12253		0.10	Hekla	H basalt
104	795.1	12300		0.20	Hekla	H basalt
104					Katla	K intermediate, rhyolite
105	801.0	12392		0.20	Hekla	H basalt
106	805.2	12520		0.40	Hekla	H basalt
107	809.6	12535		0.30	Hekla	H basalt
107					Katla	K intermediate, rhyolite
108	810.6	12526		0.10	Hekla	H basalt
108					Grímsvötn	G basalt

Core VGHV08-1A-1B
Physical and organic matter proxies resampled at 20 year resolution with Analyseries between ~8.3 ka and ~1.1 ka by Á. Geirsdóttir for Principle Component Analysis (PCA). Results of PCA displayed in Fig. 4.9 and 4.10)

Age yBP	%TOC	%N	C:N	%Bsi	$\delta^{13}C$	$\delta^{15}N$	Age yBP	MS	Density	Sed Rate (yr/cm)
1079	3.51	0.35	8.04	23.78	-21.64	1.18	1081	93.27	1.17	6.12
1099	2.15	0.29	7.51	27.50	-22.92	1.39	1101	71.20	1.15	6.11
1119	3.25	0.46	7.33	29.26	-22.45	1.05	1121	67.04	1.17	6.09
1139	3.44	0.44	7.89	26.12	-22.91	1.04	1141	62.61	1.12	6.06
1159	4.13	0.50	8.33	29.31	-22.73	1.10	1161	69.25	1.19	6.02
1179	4.55	0.50	9.22	35.87	-23.31	1.07	1181	59.57	1.11	5.96
1199	3.87	0.45	8.17	35.07	-23.01	1.38	1201	61.68	1.11	5.89
1219	4.11	0.45	7.99	32.13	-22.92	1.33	1221	73.41	1.14	5.81
1239	4.19	0.51	7.87	31.78	-23.05	1.35	1241	83.20	1.12	5.72
1259	3.80	0.48	8.14	30.73	-22.91	1.12	1261	128.89	1.37	5.64
1279	4.48	0.54	8.36	31.69	-23.22	1.38	1281	88.68	1.16	5.58
1299	2.91	0.36	8.33	22.87	-23.53	1.77	1301	57.54	1.13	5.54
1319	3.44	0.44	8.08	27.56	-23.16	1.80	1321	52.33	1.17	5.50
1339	4.55	0.61	7.46	37.46	-23.01	1.65	1341	50.99	1.12	5.49
1359	4.21	0.54	7.82	38.12	-23.03	1.64	1361	62.32	1.10	5.50
1379	4.19	0.51	8.28	35.52	-23.02	1.68	1381	93.14	1.24	5.52
1399	4.50	0.57	7.89	36.07	-22.43	1.60	1401	91.37	1.18	5.56
1419	4.28	0.55	7.77	34.16	-23.04	1.62	1421	59.58	1.12	5.61
1439	4.68	0.58	8.07	35.55	-22.92	1.40	1441	47.04	1.10	5.69
1459	5.04	0.60	8.33	36.90	-22.82	1.20	1461	45.27	1.11	5.80
1479	4.97	0.61	8.16	37.02	-23.03	1.30	1481	47.71	1.11	5.90
1499	4.79	0.61	7.90	36.83	-23.33	1.47	1501	47.45	1.11	6.00
1519	4.85	0.61	7.88	37.03	-23.09	1.48	1521	48.15	1.09	6.12
1539	5.06	0.63	8.00	37.51	-22.49	1.35	1541	49.87	1.10	6.24
1559	5.17	0.64	8.10	37.46	-22.05	1.26	1561	51.24	1.10	6.37
1579	5.00	0.62	8.15	35.45	-22.18	1.28	1581	51.71	1.12	6.51
1599	4.80	0.59	8.20	33.24	-22.36	1.31	1601	53.40	1.10	6.65
1619	4.36	0.53	8.38	30.77	-22.44	1.36	1622	59.95	1.07	6.79
1639	3.64	0.43	8.71	27.92	-22.39	1.43	1642	70.45	1.13	6.93
1659	2.91	0.34	9.04	25.07	-22.34	1.50	1662	81.59	1.12	7.04

Core VGHV08-1A-1B
Resampled proxy data (continued).

Age BP	%TOC	%N	C:N	%Bsi	$\delta^{13}C$	$\delta^{15}N$	Age BP	MS	Density	Sed Rate (yr/cm)
1679	2.58	0.28	9.08	22.93	-22.50	1.51	1682	85.60	1.11	7.18
1699	3.85	0.46	8.36	26.78	-22.72	1.36	1702	103.15	1.12	7.29
1719	3.47	0.41	8.34	29.49	-21.58	1.26	1722	143.11	1.22	7.40
1739	4.15	0.51	8.08	30.15	-22.08	1.35	1742	180.81	1.34	7.50
1760	4.08	0.51	8.00	29.92	-22.19	1.36	1762	188.62	1.60	7.65
1780	3.99	0.50	7.93	29.66	-22.28	1.37	1782	165.87	1.39	7.79
1800	3.91	0.50	7.86	29.40	-22.37	1.38	1802	130.09	1.17	7.86
1820	3.83	0.49	7.79	29.14	-22.47	1.39	1822	115.46	1.11	7.89
1840	3.70	0.48	7.69	28.72	-22.57	1.40	1842	124.52	1.20	7.86
1860	3.27	0.44	7.48	26.83	-22.74	1.43	1862	135.12	1.22	7.79
1880	2.80	0.38	7.24	24.60	-22.93	1.47	1882	132.97	1.16	7.69
1900	2.32	0.33	7.01	22.37	-23.11	1.51	1902	126.39	1.25	7.54
1920	1.91	0.28	6.86	20.34	-23.27	1.55	1922	134.93	1.21	7.45
1940	2.19	0.28	7.59	21.21	-23.01	1.62	1942	149.91	1.16	7.41
1960	2.65	0.31	8.53	23.07	-22.62	1.71	1962	174.64	1.38	7.27
1980	3.08	0.33	9.30	24.86	-22.30	1.79	1982	185.12	1.73	7.08
2000	3.37	0.36	9.25	26.20	-22.40	1.79	2002	162.81	1.53	6.89
2020	3.63	0.40	9.10	27.46	-22.56	1.77	2022	136.66	1.17	6.74
2040	3.90	0.44	8.94	28.71	-22.73	1.76	2042	129.90	1.17	6.54
2060	4.17	0.47	8.88	29.71	-22.50	1.55	2062	134.38	1.25	6.38
2080	4.32	0.48	8.93	29.64	-21.22	0.82	2082	132.38	1.40	6.22
2100	4.08	0.48	8.47	29.45	-21.53	1.08	2102	127.00	1.16	6.11
2120	3.81	0.48	7.97	29.26	-22.00	1.44	2122	120.71	1.26	6.01
2140	3.59	0.47	7.64	29.10	-22.37	1.76	2142	111.36	1.17	5.87
2160	3.65	0.46	8.03	29.10	-22.03	1.70	2162	100.50	1.30	5.75
2180	3.75	0.44	8.47	29.14	-21.59	1.56	2182	88.62	1.15	5.63
2200	3.95	0.47	8.37	29.17	-21.94	1.46	2202	78.86	1.12	5.52
2220	4.18	0.51	8.11	29.21	-22.59	1.37	2222	72.41	1.12	5.41
2240	4.16	0.55	7.55	29.51	-22.91	1.32	2242	68.98	1.14	5.30
2260	4.15	0.59	7.12	30.15	-23.08	1.29	2262	68.56	1.13	5.24
2280	4.36	0.60	7.37	30.80	-23.45	1.25	2282	69.34	1.11	5.17
2300	4.13	0.55	7.75	31.44	-22.71	1.35	2302	72.30	1.14	5.08
2320	4.16	0.61	7.38	32.08	-22.87	1.41	2322	76.05	1.13	5.00
2340	4.12	0.61	7.58	32.35	-22.77	1.41	2342	82.59	1.12	4.93
2360	4.41	0.58	7.69	29.68	-22.35	1.47	2362	94.32	1.14	4.85
2380	4.33	0.58	7.70	26.38	-22.04	1.57	2382	111.05	1.26	4.78
2400	4.34	0.53	8.17	23.08	-22.49	1.55	2402	134.67	1.20	4.71
2420	3.34	0.47	7.72	19.78	-23.28	1.72	2422	166.06	1.20	4.60
2440	2.47	0.39	7.13	16.52	-23.36	1.59	2442	207.61	1.42	4.54
2460	2.60	0.40	6.67	16.35	-22.54	1.61	2462	257.58	1.33	4.49
2480	3.02	0.43	7.64	18.07	-22.93	1.65	2482	309.46	1.19	4.42
2500	3.17	0.42	8.06	19.79	-22.14	1.40	2502	345.71	1.33	4.37
2520	2.57	0.34	8.07	21.51	-21.54	1.01	2522	337.78	1.29	4.34
2540	0.79	0.11	8.02	23.22	-24.93	1.06	2542	289.36	1.28	4.31
2560	1.68	0.18	7.97	24.68	-24.81	1.16	2562	224.34	1.15	4.28
2580	3.51	0.41	7.91	26.01	-22.93	1.25	2582	167.56	1.13	4.25
2600	4.41	0.57	7.63	27.33	-21.93	1.16	2602	128.59	1.13	4.23
2620	4.01	0.57	7.26	28.66	-22.35	1.16	2622	103.15	1.16	4.22
2640	3.71	0.55	7.22	29.53	-22.69	1.30	2642	87.97	1.13	4.21
2660	4.02	0.53	7.65	28.94	-22.27	1.32	2663	78.72	1.15	4.18
2680	4.07	0.53	7.60	28.24	-22.06	1.25	2683	73.46	1.14	4.17
2700	3.92	0.52	7.55	27.54	-22.00	1.18	2703	71.01	1.14	4.17
2720	3.75	0.48	7.95	26.85	-22.10	1.21	2723	71.61	1.16	4.15
2740	4.79	0.48	9.89	26.15	-23.40	1.19	2743	74.58	1.14	4.15
2760	5.06	0.48	10.47	25.45	-24.15	1.05	2763	78.71	1.16	4.15
2780	3.95	0.50	7.90	24.75	-23.04	1.50	2783	81.63	1.17	4.15
2800	3.35	0.46	7.51	24.06	-22.57	1.82	2803	82.47	1.14	4.15
2820	3.23	0.42	7.66	23.36	-22.58	1.79	2823	83.23	1.16	4.16
2840	2.83	0.38	7.47	22.66	-22.55	1.89	2843	79.40	1.19	4.17
2860	2.75	0.36	7.58	22.01	-22.54	1.73	2863	73.97	1.13	4.20
2880	3.05	0.37	7.98	22.26	-21.74	1.53	2883	74.22	1.13	4.21

Core VGHV08-1A-1B
Resampled proxy data (continued).

Age BP	%TOC	%N	C:N	%Bsi	$\delta^{13}C$	$\delta^{15}N$	Age BP	MS	Density	Sed Rate (yr/cm)
2900	3.57	0.46	7.67	22.88	-22.14	1.78	2903	88.00	1.13	4.31
2920	2.90	0.40	7.44	23.06	-22.75	1.85	2923	123.84	1.18	4.57
2940	2.59	0.36	7.42	19.32	-22.47	1.86	2943	219.39	1.41	5.13
2960	1.23	0.15	6.94	15.37	-22.29	1.72	2963	213.18	1.63	5.82
2980	2.44	0.26	8.09	16.72	-22.83	1.49	2983	138.51	1.21	6.34
3000	2.37	0.31	8.01	17.72	-23.01	1.64	3003	120.03	1.22	6.91
3020	2.10	0.25	8.59	16.29	-23.12	1.21	3023	119.55	1.26	7.51
3040	1.76	0.21	8.71	14.83	-23.86	1.02	3043	129.55	1.27	8.03
3060	1.47	0.16	9.32	13.36	-24.15	0.90	3063	131.12	1.24	8.69
3080	1.32	0.16	7.93	14.86	-23.36	0.84	3083	104.14	1.35	9.25
3101	1.59	0.18	7.70	22.51	-22.65	1.28	3103	78.09	1.17	9.84
3121	3.09	0.35	8.37	30.34	-23.35	1.56	3123	65.49	1.14	10.32
3141	4.04	0.52	7.70	36.48	-22.60	1.70	3143	58.23	1.13	10.79
3161	3.60	0.50	7.58	35.55	-22.49	1.67	3163	55.90	1.10	11.08
3181	2.89	0.38	7.75	33.83	-22.79	1.53	3183	54.94	1.10	11.40
3201	3.45	0.45	7.34	32.12	-23.48	1.68	3203	55.03	1.12	11.52
3221	3.85	0.55	6.96	31.07	-23.88	1.82	3223	56.02	1.13	11.50
3241	4.07	0.55	7.53	31.70	-23.48	1.76	3243	57.72	1.13	11.34
3261	4.56	0.53	8.62	32.41	-23.37	1.53	3263	59.64	1.15	11.16
3281	5.68	0.54	10.43	33.12	-25.01	1.26	3283	62.30	1.13	10.97
3301	4.32	0.51	8.75	33.83	-24.08	1.76	3303	67.65	1.11	10.73
3321	4.04	0.54	7.70	33.98	-23.45	1.84	3323	76.70	1.11	10.47
3341	4.56	0.57	8.04	33.12	-23.57	1.75	3343	89.29	1.16	10.24
3361	4.33	0.54	8.14	32.24	-23.88	1.82	3363	98.90	1.14	10.12
3381	3.78	0.50	7.58	31.35	-23.32	1.64	3383	111.95	1.17	9.94
3401	3.43	0.49	7.11	30.47	-23.19	1.80	3403	143.20	1.19	9.75
3421	2.84	0.45	6.11	29.17	-23.48	1.88	3423	199.67	1.20	9.55
3441	2.98	0.49	6.25	26.97	-23.45	1.78	3443	277.82	1.43	9.36
3461	3.06	0.49	6.40	24.73	-23.34	1.55	3463	341.54	0.99	9.09
3481	2.85	0.43	7.20	22.50	-23.76	1.52	3483	366.27	1.38	8.86
3501	2.09	0.32	6.75	20.26	-23.25	1.82	3503	332.95	1.84	8.69
3521	1.20	0.22	5.08	19.18	-22.79	1.03	3523	244.45	1.64	8.58
3541	2.35	0.26	5.84	25.68	-22.92	0.98	3543	156.59	1.18	8.49
3561	3.72	0.50	6.98	30.07	-22.91	1.65	3563	105.39	1.14	8.62
3581	2.99	0.44	6.96	29.81	-22.94	1.54	3583	83.06	1.13	8.91
3601	3.62	0.58	6.29	29.52	-22.82	1.63	3603	78.11	1.15	10.36
3621	3.12	0.58	5.97	29.22	-23.18	1.74	3623	84.01	1.14	12.50
3641	3.46	0.58	5.88	28.22	-22.78	1.84	3643	103.43	1.16	13.10
3661	3.54	0.55	6.90	26.78	-23.30	1.67	3663	117.55	1.48	14.95
3681	2.33	0.35	6.10	25.34	-22.54	1.82	3683	105.41	1.21	17.38
3701	2.87	0.31	6.60	23.95	-22.41	1.91	3704	99.61	1.16	19.36
3721	2.50	0.30	7.13	22.81	-22.41	1.93	3724	111.72	1.18	21.23
3741	2.36	0.31	7.45	21.71	-22.47	2.04	3744	133.06	1.40	22.74
3761	2.37	0.35	7.68	20.60	-22.40	2.28	3764	138.69	1.45	23.72
3781	2.24	0.38	8.11	19.60	-21.83	1.96	3784	139.86	1.21	24.39
3801	3.25	0.40	8.45	21.46	-21.30	1.64	3804	147.71	1.24	24.99
3821	3.49	0.39	8.37	24.67	-21.42	1.67	3824	126.19	1.39	25.50
3841	3.54	0.38	8.24	27.87	-21.74	1.83	3844	93.29	1.16	26.13
3861	3.15	0.37	8.10	27.49	-22.06	1.99	3864	78.77	1.14	26.71
3881	3.11	0.40	7.47	23.67	-22.44	2.09	3884	76.47	1.21	27.37
3901	3.51	0.53	6.47	19.85	-22.93	2.02	3904	75.39	1.14	27.88
3921	3.59	0.66	6.33	17.90	-23.21	1.43	3924	74.70	1.13	28.48
3941	3.89	0.58	6.87	23.43	-23.27	1.64	3944	75.83	1.11	29.03
3961	4.33	0.66	6.86	29.55	-23.48	1.61	3964	78.65	1.12	29.58
3981	3.97	0.65	6.21	29.78	-23.46	1.70	3984	85.50	1.13	30.02
4001	3.51	0.56	6.46	27.17	-23.10	1.69	4004	93.29	1.19	29.01
4021	2.47	0.47	5.48	24.62	-23.43	1.77	4024	92.94	1.21	25.50
4041	3.25	0.51	6.18	24.88	-23.37	2.04	4044	92.07	1.15	23.55
4061	3.37	0.52	6.48	26.75	-23.03	1.88	4064	102.53	1.14	21.48
4081	2.99	0.54	5.95	28.60	-22.98	1.89	4084	133.16	1.19	19.74
4101	3.35	0.54	6.07	27.01	-23.23	2.10	4104	203.73	1.23	17.74

Core VGHV08-1A-1B
Resampled proxy data (continued).

Age BP	%TOC	%N	C:N	%Bsi	$\delta^{13}C$	$\delta^{15}N$	Age BP	MS	Density	Sed Rate (yr/cm)
4121	2.90	0.47	6.70	23.05	-22.73	1.80	4124	299.91	1.30	15.71
4141	2.13	0.31	8.49	19.08	-23.21	1.48	4144	316.66	1.39	14.03
4161	1.76	0.21	9.02	15.32	-24.46	1.35	4164	332.00	1.47	12.08
4181	1.93	0.21	8.53	16.37	-23.38	1.75	4184	336.36	1.54	10.64
4201	1.24	0.15	8.58	19.41	-23.85	2.02	4204	249.91	1.31	9.38
4221	2.70	0.30	8.67	22.46	-24.33	1.55	4224	143.48	1.19	8.76
4241	4.38	0.49	8.73	24.96	-24.45	1.77	4244	81.80	1.16	8.40
4261	4.38	0.54	7.84	26.50	-23.86	1.77	4264	89.59	1.19	8.37
4281	4.36	0.56	7.94	28.03	-23.94	1.72	4284	166.43	1.36	8.40
4301	3.89	0.52	7.65	29.55	-23.66	1.68	4304	237.99	1.37	8.47
4321	3.36	0.44	7.96	31.07	-23.20	1.67	4324	347.08	1.25	8.78
4341	2.28	0.29	8.81	32.12	-23.13	1.66	4344	365.39	1.41	9.35
4361	2.02	0.23	9.14	32.56	-24.54	1.91	4364	224.93	1.27	10.26
4381	3.71	0.21	10.15	33.00	-25.46	2.01	4384	131.28	1.15	10.75
4401	4.06	0.27	11.57	33.24	-26.43	2.11	4404	98.64	1.21	11.06
4422	3.92	0.40	9.64	33.18	-25.36	2.02	4424	85.81	1.24	11.58
4442	3.80	0.35	10.00	33.11	-25.05	1.95	4444	84.59	1.14	11.97
4462	4.72	0.50	10.08	33.05	-24.78	1.80	4464	94.08	1.15	12.47
4482	4.02	0.51	8.54	33.03	-23.68	1.97	4484	105.31	1.16	12.87
4502	3.91	0.50	7.94	33.14	-23.08	2.10	4504	93.74	1.28	13.24
4522	3.11	0.45	8.18	33.26	-22.12	2.04	4524	79.84	1.12	13.59
4542	1.81	0.17	8.62	33.37	-22.57	1.81	4544	77.01	1.12	13.92
4562	4.36	0.34	8.36	33.48	-22.78	1.77	4564	75.75	1.19	14.20
4582	4.08	0.53	8.00	33.56	-23.04	1.82	4584	70.18	1.14	14.40
4602	2.11	0.34	8.66	33.63	-22.39	1.60	4604	65.84	1.12	14.67
4622	3.32	0.31	8.38	33.70	-22.24	1.38	4624	64.04	1.10	14.94
4642	3.62	0.50	8.31	33.78	-23.44	1.66	4644	64.75	1.13	15.19
4662	4.14	0.50	8.39	33.70	-23.86	1.56	4664	65.47	1.16	15.84
4682	4.43	0.53	8.29	33.52	-23.59	1.62	4684	66.00	1.12	16.16
4702	4.38	0.53	8.26	33.35	-23.54	1.79	4704	66.00	1.13	16.41
4722	4.27	0.52	8.50	33.17	-23.61	1.50	4724	66.11	1.12	16.55
4742	3.91	0.51	8.23	32.97	-23.48	1.68	4745	68.44	1.12	16.66
4762	4.73	0.50	9.60	32.65	-23.70	1.92	4765	70.30	1.11	16.72
4782	4.99	0.51	9.67	32.30	-24.30	1.79	4785	72.07	1.15	16.72
4802	3.96	0.49	8.26	31.95	-23.14	1.76	4805	76.48	1.13	16.67
4822	3.03	0.45	8.10	31.61	-23.30	1.84	4825	87.90	1.16	16.58
4842	2.93	0.42	7.99	31.63	-23.29	1.92	4845	103.34	1.13	16.43
4862	3.74	0.44	8.06	32.52	-23.58	1.94	4865	101.27	1.32	16.26
4882	3.74	0.48	8.29	33.45	-23.62	1.81	4885	87.59	1.17	16.10
4902	3.20	0.41	8.28	34.38	-23.14	1.67	4905	76.95	1.14	15.92
4922	3.10	0.34	8.17	35.31	-23.51	1.72	4925	71.51	1.15	15.69
4942	2.17	0.25	8.09	35.90	-23.98	1.71	4945	68.64	1.12	15.51
4962	2.98	0.29	8.12	35.89	-23.96	1.61	4965	67.62	1.12	15.37
4982	3.56	0.44	8.17	35.88	-23.62	1.47	4985	69.54	1.13	15.14
5002	3.72	0.44	8.33	35.86	-23.53	1.48	5005	73.68	1.14	14.95
5022	3.84	0.46	8.36	35.85	-23.43	1.49	5025	77.62	1.15	14.71
5042	3.81	0.46	8.32	35.49	-23.40	1.57	5045	79.91	1.16	14.49
5062	3.90	0.46	8.31	34.55	-23.40	1.52	5065	78.47	1.16	14.20
5082	3.67	0.46	8.25	33.61	-23.39	1.40	5085	73.77	1.14	14.02
5102	3.41	0.42	8.49	32.66	-23.27	1.50	5105	70.89	1.14	13.75
5122	3.25	0.40	8.75	31.71	-22.98	1.37	5125	68.91	1.14	13.38
5142	3.52	0.41	8.96	31.26	-22.47	1.22	5145	67.92	1.14	13.14
5162	4.24	0.43	9.79	32.30	-22.72	1.22	5165	66.01	1.15	12.87
5182	4.32	0.45	9.50	33.43	-24.04	1.55	5185	63.55	1.14	12.64
5202	4.05	0.46	8.50	34.57	-23.33	1.31	5205	62.06	1.14	12.44
5222	4.45	0.53	8.36	35.71	-23.54	1.38	5225	61.15	1.14	12.20
5242	4.54	0.58	8.32	36.65	-24.19	1.34	5245	63.42	1.13	12.17
5262	4.43	0.55	8.11	36.13	-23.53	1.50	5265	66.37	1.12	12.12
5282	4.53	0.57	7.90	35.30	-23.60	1.48	5285	70.71	1.12	12.09
5302	4.45	0.60	7.59	34.48	-23.27	1.55	5305	76.52	1.11	12.07
5322	4.25	0.58	7.48	33.65	-23.08	1.88	5325	85.66	1.14	12.07

Core VGHV08-1A-1B
Resampled proxy data (continued).

Age BP	%TOC	%N	C:N	%Bsi	$\delta^{13}C$	$\delta^{15}N$	Age BP	MS	Density	Sed Rate (yr/cm)
5342	3.88	0.61	7.01	32.82	-22.79	1.57	5345	92.88	1.18	12.09
5362	4.09	0.59	7.57	32.20	-22.64	1.60	5365	92.66	1.32	12.13
5382	3.81	0.53	7.39	31.74	-22.67	1.92	5385	89.28	1.20	12.17
5402	3.48	0.51	7.29	31.27	-22.68	1.94	5405	88.22	1.15	12.25
5422	1.62	0.45	7.53	30.80	-22.43	1.79	5425	89.52	1.18	12.34
5442	1.78	0.26	7.48	30.33	-22.83	1.74	5445	92.41	1.18	12.44
5462	3.08	0.37	7.37	30.03	-22.62	1.58	5465	98.08	1.16	12.55
5482	3.40	0.43	7.43	30.27	-22.81	1.99	5485	110.75	1.15	12.74
5502	2.87	0.43	7.41	30.54	-22.99	1.85	5505	138.35	1.13	12.85
5522	3.24	0.40	7.63	30.82	-22.85	1.92	5525	187.17	1.14	12.97
5542	3.12	0.45	7.19	30.99	-22.80	2.12	5545	265.50	1.16	13.04
5562	3.45	0.45	7.47	29.36	-23.07	2.07	5565	350.97	1.23	13.16
5582	3.06	0.44	7.42	27.05	-22.96	2.28	5585	388.46	1.53	13.27
5602	2.96	0.40	7.64	24.74	-22.74	2.48	5605	348.12	1.88	13.53
5622	2.16	0.35	6.92	22.42	-22.54	2.51	5625	262.46	1.70	13.78
5642	1.06	0.19	7.49	21.86	-22.57	2.10	5645	179.10	1.33	13.98
5662	2.37	0.24	8.20	24.14	-19.99	2.17	5665	125.51	1.10	14.09
5682	3.32	0.35	8.19	26.46	-21.72	1.99	5685	95.87	1.13	14.21
5702	3.80	0.50	7.63	28.78	-22.80	2.29	5705	79.63	1.15	14.44
5722	3.00	0.42	7.61	31.09	-22.74	2.20	5725	70.79	1.13	14.62
5742	3.50	0.44	7.48	33.41	-22.89	2.25	5745	68.03	1.13	15.02
5763	3.45	0.49	7.63	34.72	-23.08	2.31	5765	68.01	1.14	15.23
5783	3.13	0.43	7.51	34.34	-23.04	2.29	5786	69.79	1.13	15.45
5803	3.59	0.44	7.58	33.94	-23.27	2.25	5806	73.00	1.15	15.60
5823	3.73	0.49	7.97	33.55	-22.76	2.18	5826	74.30	1.16	15.72
5843	3.65	0.46	8.06	33.15	-22.36	1.92	5846	76.48	1.14	15.84
5863	4.11	0.43	8.39	32.75	-22.52	1.94	5866	78.90	1.14	16.03
5883	3.38	0.39	8.64	32.73	-22.61	2.08	5886	81.85	1.15	16.25
5903	3.19	0.37	8.40	32.95	-23.00	2.19	5906	82.86	1.16	16.39
5923	3.00	0.37	8.21	33.18	-23.23	2.24	5926	79.72	1.20	16.60
5943	2.73	0.35	8.28	33.40	-23.07	2.24	5946	75.86	1.16	16.84
5963	2.93	0.32	8.40	33.62	-23.03	2.26	5966	72.39	1.13	17.05
5983	3.83	0.38	8.41	33.83	-23.00	2.17	5986	71.00	1.12	17.18
6003	4.08	0.45	8.40	33.59	-22.96	2.06	6006	70.54	1.11	17.38
6023	3.93	0.48	8.34	33.14	-22.92	1.84	6026	70.15	1.12	17.59
6043	3.99	0.47	8.32	32.68	-23.11	1.68	6046	71.01	1.12	17.75
6063	4.05	0.49	8.32	32.23	-23.51	1.87	6066	73.74	1.14	17.87
6083	3.90	0.48	8.29	31.78	-23.64	1.88	6086	77.41	1.14	18.06
6103	3.57	0.47	8.21	31.32	-23.63	1.90	6106	83.69	1.14	18.26
6123	3.60	0.46	8.14	30.91	-23.58	1.92	6126	90.55	1.16	18.44
6143	2.99	0.42	8.21	30.53	-23.76	2.01	6146	97.46	1.20	18.62
6163	2.64	0.31	8.33	30.16	-24.19	2.21	6166	103.23	1.17	18.80
6183	3.16	0.35	8.46	29.79	-24.14	2.09	6186	110.28	1.15	18.97
6203	3.31	0.38	8.67	29.42	-23.99	1.90	6206	119.14	1.16	19.14
6223	3.72	0.38	8.67	29.04	-23.97	1.76	6226	131.91	1.19	19.30
6243	3.76	0.37	8.60	28.62	-24.14	1.78	6246	148.88	1.15	19.46
6263	3.25	0.36	9.10	27.77	-24.34	1.81	6266	167.35	1.12	19.61
6283	3.70	0.35	11.36	26.83	-25.35	1.92	6286	177.99	1.20	19.75
6303	3.55	0.32	10.85	25.89	-25.35	2.02	6306	171.72	1.31	19.83
6323	2.96	0.32	9.63	24.96	-23.18	1.89	6326	157.02	1.19	19.94
6343	2.40	0.28	9.21	24.02	-24.24	1.73	6346	144.81	1.22	20.08
6363	2.82	0.25	9.09	23.08	-25.16	1.65	6366	139.41	1.25	20.21
6383	3.07	0.25	9.04	22.20	-25.11	1.73	6386	138.04	1.23	20.33
6403	2.57	0.26	8.98	21.90	-25.05	1.81	6406	139.69	1.17	20.45
6423	3.15	0.31	8.88	21.75	-24.98	1.96	6426	147.23	1.17	20.57
6443	3.51	0.40	8.60	21.59	-24.82	2.16	6446	164.06	1.16	20.69
6463	3.11	0.40	8.23	21.44	-24.40	2.28	6466	191.41	1.15	20.80
6483	1.96	0.38	8.17	21.29	-24.13	2.34	6486	225.24	1.17	20.91
6503	1.24	0.35	8.17	21.21	-24.02	2.36	6506	251.75	1.23	21.01
6523	1.56	0.32	8.16	21.98	-23.90	2.39	6526	253.31	1.52	21.09
6543	1.90	0.30	8.16	22.97	-23.79	2.41	6546	229.20	1.75	21.13

Core VGHV08-1A-1B
Resampled proxy data (continued).

Age BP	%TOC	%N	C:N	%Bsi	$\delta^{13}C$	$\delta^{15}N$	Age BP	MS	Density	Sed Rate (yr/cm)
6563	2.32	0.28	8.13	23.96	-23.68	2.43	6566	190.49	1.42	21.17
6583	2.97	0.33	8.05	24.95	-23.63	2.42	6586	153.87	1.16	21.23
6603	3.22	0.40	8.01	25.94	-23.68	2.38	6606	126.82	1.12	21.26
6623	3.14	0.40	7.95	26.92	-23.88	2.31	6626	108.65	1.13	21.31
6643	2.76	0.38	7.66	27.91	-23.83	2.27	6646	96.92	1.16	21.36
6663	2.58	0.34	7.49	28.90	-23.63	2.28	6666	89.41	1.22	21.39
6683	2.89	0.31	7.52	29.89	-23.62	2.28	6686	84.17	1.18	21.44
6703	2.66	0.30	7.54	30.61	-23.65	2.27	6706	81.29	1.14	21.47
6723	2.16	0.28	7.59	30.29	-23.67	2.26	6726	80.09	1.13	21.51
6743	2.32	0.28	7.76	29.86	-23.70	2.15	6746	80.00	1.14	21.56
6763	2.57	0.32	7.89	29.44	-23.73	1.89	6766	81.00	1.16	21.59
6783	2.54	0.33	7.87	29.01	-24.00	2.03	6786	83.29	1.16	21.63
6803	2.66	0.32	7.97	28.59	-24.30	2.38	6806	86.38	1.17	21.66
6823	3.07	0.35	8.21	28.16	-24.32	2.25	6827	90.14	1.16	21.70
6843	3.19	0.39	8.30	27.74	-24.31	2.03	6847	95.61	1.16	21.72
6863	3.09	0.39	8.30	27.31	-24.32	2.02	6867	103.08	1.18	21.75
6883	3.15	0.40	8.31	27.14	-24.34	2.02	6887	112.89	1.16	21.75
6903	3.24	0.40	8.29	27.70	-24.36	2.03	6907	121.33	1.16	21.76
6923	2.62	0.37	8.07	28.31	-24.30	2.05	6927	126.14	1.26	21.77
6943	1.80	0.27	7.85	28.92	-24.14	2.13	6947	125.49	1.35	21.80
6963	1.15	0.19	7.87	29.52	-22.96	2.13	6967	120.19	1.27	21.81
6983	0.65	0.11	7.94	30.13	-20.99	2.05	6987	110.50	1.24	21.83
7003	0.94	0.09	8.12	30.74	-21.27	2.00	7007	101.62	1.18	21.84
7023	1.45	0.14	8.28	31.34	-23.03	2.01	7027	93.94	1.16	21.85
7043	2.37	0.20	8.29	31.95	-23.71	2.10	7047	87.64	1.14	21.86
7063	3.22	0.25	8.29	32.56	-23.77	2.24	7067	82.92	1.14	21.87
7083	3.35	0.31	8.29	32.91	-23.84	2.39	7087	80.11	1.16	21.89
7104	3.38	0.37	8.26	33.01	-23.91	2.54	7107	76.57	1.15	21.91
7124	3.46	0.42	8.12	33.11	-23.89	2.51	7127	74.42	1.16	21.92
7144	3.53	0.43	7.99	33.21	-23.79	2.28	7147	72.71	1.13	21.93
7164	3.42	0.44	8.05	33.31	-23.76	2.14	7167	71.66	1.12	21.95
7184	3.26	0.41	8.13	33.41	-23.77	2.17	7187	71.01	1.13	21.96
7204	3.15	0.39	8.06	33.51	-23.70	2.18	7207	71.00	1.14	21.97
7224	3.07	0.39	7.97	33.61	-23.50	2.17	7227	71.00	1.13	21.98
7244	3.11	0.39	7.99	33.72	-23.37	2.16	7247	71.00	1.13	22.00
7264	3.22	0.40	8.05	33.82	-23.42	2.17	7267	71.38	1.12	22.02
7284	3.35	0.41	8.11	33.87	-23.48	2.19	7287	71.99	1.14	22.02
7304	3.52	0.43	8.18	33.43	-23.54	2.21	7307	72.00	1.13	22.02
7324	3.60	0.44	8.19	32.87	-23.58	2.23	7327	71.66	1.15	22.04
7344	3.43	0.43	8.11	32.30	-23.38	2.29	7347	71.02	1.15	22.06
7364	3.26	0.41	8.06	31.74	-23.10	2.38	7367	71.00	1.11	22.06
7384	3.26	0.40	8.17	31.18	-23.12	2.36	7387	71.27	1.10	22.07
7404	3.30	0.40	8.29	30.61	-23.39	2.19	7407	71.96	1.10	22.09
7424	3.49	0.41	8.21	30.05	-23.54	2.04	7427	72.00	1.13	22.11
7444	3.78	0.45	8.05	29.49	-23.41	2.02	7447	72.15	1.16	22.11
7464	3.74	0.49	7.99	28.93	-23.28	2.00	7467	73.00	1.19	22.11
7484	3.01	0.49	8.05	28.36	-23.24	1.98	7487	73.76	1.27	22.12
7504	2.37	0.48	8.12	27.80	-23.24	1.96	7507	73.14	1.32	22.14
7524	2.73	0.47	8.18	27.68	-23.23	1.94	7527	72.25	1.17	22.15
7544	3.34	0.46	8.25	28.38	-23.23	1.92	7547	71.98	1.14	22.15
7564	3.62	0.45	8.29	29.11	-23.21	1.90	7567	70.80	1.15	22.16
7584	3.50	0.43	8.32	29.84	-23.16	1.93	7587	69.49	1.13	22.18
7604	3.39	0.41	8.34	30.57	-23.10	1.97	7607	68.60	1.14	22.19
7624	3.44	0.41	8.29	31.30	-23.14	2.02	7627	67.71	1.12	22.19
7644	3.51	0.42	8.23	32.03	-23.25	2.10	7647	67.04	1.14	22.20
7664	3.56	0.43	8.20	32.76	-23.33	2.18	7667	66.88	1.13	22.21
7684	3.59	0.44	8.18	33.49	-23.33	2.24	7687	66.12	1.12	22.22
7704	3.61	0.44	8.16	34.22	-23.30	2.31	7707	65.29	1.14	22.23
7724	3.58	0.44	8.11	34.95	-23.27	2.37	7727	65.00	1.11	22.23
7744	3.52	0.45	8.05	35.68	-23.21	2.41	7747	64.25	1.09	22.25
7764	3.48	0.45	7.99	36.41	-23.15	2.46	7767	62.46	1.13	22.25

Core VGHV08-1A-1B
Resampled proxy data (continued).

Age BP	%TOC	%N	C:N	%Bsi	$\delta^{13}C$	$\delta^{15}N$	Age BP	MS	Density	Sed Rate (yr/cm)
7784	3.52	0.46	7.93	36.64	-23.09	2.51	7787	62.03	1.14	22.25
7804	3.59	0.46	7.87	35.89	-23.03	2.55	7807	77.04	1.15	22.25
7824	3.66	0.47	7.82	35.11	-22.97	2.60	7827	95.54	1.18	22.25
7844	3.64	0.47	7.86	34.33	-23.15	2.60	7847	114.04	1.20	22.25
7864	3.62	0.46	7.91	33.55	-23.57	2.51	7868	132.54	1.23	22.25
7884	3.59	0.46	7.96	32.77	-23.99	2.42	7888	151.04	1.26	22.26
7904	3.61	0.45	8.09	31.99	-24.30	2.35	7908	169.54	1.28	22.26
7924	3.64	0.45	8.24	31.21	-24.41	2.35	7928	188.04	1.31	22.26
7944	3.67	0.44	8.38	30.43	-24.51	2.35	7948	207.06	1.34	22.26
7964	3.66	0.44	8.40	29.65	-24.58	2.36	7968	228.76	1.36	22.27
7984	3.61	0.43	8.34	28.87	-24.46	2.34	7988	245.58	1.39	22.28
8004	3.56	0.43	8.29	28.09	-24.32	2.33	8008	256.66	1.40	22.30
8024	3.50	0.43	8.23	27.31	-24.19	2.31	8028	260.36	1.41	22.30
8044	3.45	0.42	8.18	26.53	-24.05	2.29	8048	254.15	1.42	22.31
8064	3.27	0.42	8.22	25.75	-23.92	2.27	8068	239.36	1.42	22.32
8084	2.90	0.36	8.34	24.97	-23.82	2.19	8088	219.07	1.38	22.34
8104	2.48	0.30	8.46	24.19	-23.72	2.09	8108	195.57	1.32	22.35
8124	1.72	0.23	8.58	24.16	-23.63	1.99	8128	170.39	1.22	22.36
8144	1.30	0.16	8.58	25.25	-23.55	1.89	8148	147.91	1.13	22.37
8164	1.42	0.16	8.49	26.34	-23.58	1.86	8168	129.57	1.13	22.39
8184	1.54	0.17	8.39	27.44	-23.62	1.86	8188	115.25	1.16	22.41
8204	1.77	0.19	8.28	28.53	-23.67	1.85	8208	104.92	1.16	22.43
8224	2.23	0.24	8.15	29.63	-23.64	1.88	8228	98.95	1.14	22.43
8244	2.70	0.30	8.02	30.72	-23.60	1.94	8248	96.56	1.12	22.43
8264	3.15	0.36	7.94	31.82	-23.55	1.99	8268	96.58	1.15	22.44
8284	3.52	0.41	7.93	32.92	-23.43	2.04	8288	98.65	1.19	22.47
8304	3.89	0.46	7.93	34.01	-23.30	2.09	8308	102.86	1.19	22.49

APPENDIX 2: HIGH RESOLUTION MULTI-PROXY DATA SURROUNDING TARGETED TEPHRA HORIZONS

Vestra Gíslholtsvatn

Multi-proxy data for rhyolitic eruptions H4 and H3 used for Principle Component Analysis (PCA)

VGHV H4						
Years Before and After Tephra	%TOC	C:N	$\delta^{13}C$	Years Before and After Tephra	MS	Den
-218.00	4.28	9.41	-24.85	-207.00	164.00	1.12
-183.00	1.75	9.09	-25.17	-199.00	203.00	1.21
-167.00	2.16	9.19	-24.82	-190.00	257.00	1.28
-150.00	2.00	8.88	-23.03	-182.00	318.00	1.29
-116.00	3.60	7.48	-23.22	-174.00	373.00	1.44
-80.00	4.48	8.07	-24.18	-166.00	400.00	1.47
-64.00	4.24	7.40	-23.42	-158.00	386.00	1.29
-48.00	4.60	8.79	-24.22	-150.00	344.00	1.33
-32.00	4.43	8.70	-24.54	-141.00	295.00	1.19
-9.00	2.54	8.66	-24.31	-133.00	254.00	1.19
18.00	0.25	5.53	-23.93	-125.00	226.00	1.27
21.00	2.62	8.49	-22.04	-118.00	209.00	1.51
43.00	1.25	8.61	-24.60	-75.00	61.00	1.16
54.00	2.09	9.48	-24.63	-67.00	70.00	1.16
76.00	2.04	8.36	-23.41	-60.00	80.00	1.16
86.00	2.73	6.04	-22.15	-52.00	96.00	1.15
93.00	3.37	7.78	-22.49	-45.00	117.00	1.18
100.00	2.51	6.07	-23.21	-37.00	144.00	1.16
107.00	3.54	6.16	-22.66	-29.00	176.00	1.18
127.00	3.12	5.93	-23.63	-22.00	215.00	1.25
141.00	2.91	6.02	-22.71	-15.00	255.00	1.24
154.00	3.25	5.58	-23.12	-7.00	292.00	1.33
161.00	3.31	7.65	-22.66	0.00	323.00	1.41
167.00	3.75	6.68	-23.26	8.00	343.00	1.33
194.00	2.73	5.55	-23.43	15.00	350.00	1.70
206.00	2.15	5.35	-23.52	22.00	345.00	1.63
219.00	3.61	5.86	-23.14	29.00	333.00	1.55
				37.00	320.00	1.47
				44.00	313.00	1.38
				51.00	313.00	1.25
				58.00	321.00	1.28
				65.00	324.00	1.61
				72.00	315.00	1.43
				79.00	289.00	1.27
				86.00	255.00	1.23
				93.00	220.00	1.23
				100.00	190.00	1.25
				106.00	164.00	1.22
				113.00	144.00	1.22
				120.00	129.00	1.22
				127.00	118.00	1.19
				134.00	109.00	1.16
				140.00	102.00	1.15
				147.00	97.00	1.15
				154.00	94.00	1.11
				160.00	92.00	1.12
				167.00	91.00	1.11
				174.00	91.00	1.19
				180.00	92.00	1.19
				187.00	93.00	1.20
				193.00	95.00	1.18
				200.00	95.00	1.27

VGHV H3						
Years Before and After Tephra	%TOC	C:N	$\delta^{13}C$	Years Before and After Tephra	MS	Den
-221.00	3.90	7.08	-24.02	-201.00	55.00	1.10
-190.00	2.68	7.85	-22.82	-194.00	55.00	1.10
-163.00	3.90	7.48	-22.30	-187.00	56.00	1.09
-156.00	4.14	7.65	-23.14	-181.00	57.00	1.11
-149.00	3.92	7.71	-22.49	-174.00	57.00	1.14
-141.00	4.21	7.91	-22.24	-167.00	58.00	1.13
-127.00	2.44	8.89	-24.09	-161.00	60.00	1.17
-120.00	2.67	7.16	-22.74	-154.00	63.00	1.05
-113.00	1.04	7.15	-23.41	-148.00	66.00	1.12
-106.00	1.32	7.50	-21.97	-141.00	68.00	1.21
-99.00	1.53	8.05	-21.59	-135.00	70.00	1.12
-92.00	1.24	7.57	-23.43	-129.00	77.00	1.14
-85.00	1.19	8.08	-23.71	-123.00	83.00	1.12
-78.00	1.68	10.44	-24.68	-116.00	92.00	1.28
-72.00	1.26	8.81	-23.74	-110.00	101.00	1.63
-65.00	1.49	8.95	-24.20	-104.00	110.00	1.31
-59.00	1.79	8.69	-24.16	-98.00	119.00	1.15
-52.00	1.61	8.59	-24.19	-92.00	128.00	1.23
-46.00	1.61	8.53	-24.28	-86.00	134.00	1.24
-40.00	1.94	8.40	-23.08	-80.00	136.00	1.24
-34.00	1.89	8.55	-22.93	-74.00	135.00	1.26
-28.00	1.91	8.78	-24.09	-69.00	131.00	1.30
-22.00	2.45	8.57	-22.91	-63.00	127.00	1.26
-16.00	2.13	7.77	-23.15	-57.00	123.00	1.27
-10.00	2.44	7.85	-23.26	-52.00	121.00	1.28
-5.00	2.49	7.94	-23.08	-46.00	119.00	1.25
1.00	2.86	8.35	-22.05	-41.00	118.00	1.27
6.00	2.86	8.44	-22.80	-36.00	118.00	1.24
12.00	2.74	8.24	-23.25	-30.00	119.00	1.22
25.00	0.13	5.39	-23.21	-25.00	120.00	1.26
29.00	0.65	7.47	-22.32	-20.00	121.00	1.19
34.00	1.29	7.93	-21.23	-15.00	122.00	1.20
38.00	1.76	7.82	-21.94	-10.00	126.00	1.18
43.00	2.46	7.37	-22.37	-5.00	133.00	1.21
47.00	2.57	7.28	-22.63	0.00	144.00	1.20
52.00	2.03	6.92	-22.42	5.00	159.00	1.21
56.00	2.60	7.10	-22.49	9.00	178.00	1.24
61.00	2.55	7.36	-22.43	14.00	198.00	1.32
66.00	2.76	7.34	-22.24	18.00	218.00	1.68
70.00	2.73	7.48	-22.81	23.00	236.00	1.74
75.00	2.89	7.70	-23.18	27.00	248.00	1.83
80.00	3.37	7.22	-22.76	31.00	251.00	1.75
85.00	3.24	7.40	-22.44	35.00	246.00	1.84
90.00	3.65	7.75	-22.10	40.00	232.00	1.56
96.00	3.93	8.00	-21.85	44.00	213.00	1.33
101.00	3.42	7.63	-22.13	48.00	190.00	1.28
107.00	3.29	7.83	-22.60	52.00	165.00	1.21
113.00	2.77	8.39	-21.08	56.00	144.00	1.14
120.00	2.94	7.69	-21.55	60.00	127.00	1.13
126.00	2.41	7.86	-21.59	65.00	114.00	1.25
133.00	2.61	7.48	-22.85	69.00	106.00	1.20
141.00	2.97	7.24	-22.64	74.00	99.00	1.17
148.00	2.16	7.27	-22.29	78.00	93.00	1.17
157.00	3.27	7.54	-22.34	83.00	88.00	1.16
165.00	3.28	7.67	-22.36	88.00	83.00	1.11

Vestra Gíslholtsvatn
Multi-proxy data for rhyolitic eruption H3 used for PCA (continued).

VGHV H3						
Years Before and After Tephra	%TOC	C:N	$\delta^{13}C$	Years Before and After Tephra	MS	Den
174.00	2.70	7.32	-22.65	93.00	79.00	1.07
194.00	3.55	7.53	-22.64	103.00	73.00	1.15
204.00	3.85	7.96	-22.40	109.00	73.00	1.13
				115.00	73.00	1.12
				121.00		1.10
				127.00	75.00	1.15
				133.00	77.00	1.15
				140.00	81.00	1.20
				147.00	83.00	1.20
				155.00	83.00	1.15
				163.00	84.00	1.15
				171.00	82.00	1.12
				179.00		1.16
				188.00	82.00	1.18
				197.00	80.00	1.17
				207.00	78.00	1.17

Vestra Gíslholtsvatn
Multi-proxy data for basaltic eruptions T-tephra and KN used for PCA

VGHV T-tephra							VGHV KN						
Years Before and After Tephra	%TOC	C:N	$\delta^{13}C$	Years Before and After Tephra	MS	Den	Years Before and After Tephra	%TOC	C:N	$\delta^{13}C$	Years Before and After Tephra	MS	Den
-212.00	2.55	8.40	-23.03	-210.00	80.00	1.21	-209.00	2.56	7.40	-22.65	-205.00	119.00	1.21
-196.00	2.88	8.15	-23.07	-201.00	83.00	1.21	-196.00	2.20	7.49	-22.40	-198.00	112.00	1.17
-179.00	3.20	8.33	-23.33	-192.00	83.00	1.15	-133.00	1.88	5.86	-22.42	-192.00	105.00	1.18
-163.00	3.18	8.73	-22.65	-183.00	82.00	1.17	-126.00	3.73	7.78	-23.30	-185.00	101.00	1.18
-132.00	3.43	7.94	-22.44	-174.00	80.00	1.14	-119.00	3.65	6.77	-23.60	-178.00	99.00	1.15
-120.00	3.86	8.20	-21.97	-165.00	78.00	1.13	-105.00	3.37	5.54	-22.66	-171.00	98.00	1.17
-112.00	3.79	7.68	-23.08	-156.00	77.00	1.14	-90.00	3.58	6.33	-22.86	-164.00	101.00	1.16
-104.00	3.49	7.61	-23.35	-147.00	75.00	1.14	-76.00	3.21	5.72	-23.31	-158.00	105.00	1.19
-96.00	2.93	7.63	-23.27	-138.00	74.00	1.17	-61.00	3.71	5.64	-23.10	-151.00	111.00	1.22
-88.00	3.29	7.56	-22.80	-129.00	74.00	1.16	-53.00	3.67	7.85	-22.42	-144.00	117.00	1.26
-80.00	3.49	7.79	-22.82	-120.00	72.00	1.16	-46.00	3.61	5.76	-22.78	-137.00	120.00	1.74
-72.00	3.63	7.74	-23.17	-111.00	70.00	1.13	-39.00	1.82	7.70	-22.65	-130.00	117.00	1.43
-65.00	3.97	8.07	-22.61	-103.00	68.00	1.13	-31.00	4.04	7.34	-23.39	-123.00	110.00	1.24
-57.00	2.85	7.75	-23.02	-94.00	68.00	1.12	-16.00	3.58	6.76	-22.74	-116.00	102.00	1.16
-49.00	2.51	7.42	-22.87	-85.00	68.00	1.16	15.00	0.48	4.73	-23.04	-110.00	93.00	1.13
-41.00	3.76	7.80	-22.48	-76.00	68.00	1.13	31.00	1.86	5.72	-22.48	-103.00	86.00	1.13
-33.00	3.98	7.78	-22.69	-68.00	70.00	1.10	39.00	2.22	8.07	-23.85	-96.00	82.00	1.12
-25.00	3.72	8.01	-22.74	-59.00	75.00	1.15	47.00	2.09	6.10	-22.98	-89.00	78.00	1.16
-17.00	3.52	8.01	-22.52	-50.00	81.00	1.18	55.00	2.97	7.52	-22.98	-82.00	78.00	1.13
-9.00	1.36	8.29	-20.99	-41.00	90.00	1.12	63.00		7.43	-24.32	-75.00	78.00	1.17
0.00	2.03	11.53	-15.79	-33.00	102.00	1.14	79.00	2.84	5.51	-23.51	-68.00	79.00	1.14
6.00	0.43	5.26	-22.39	-24.00	121.00	1.12	87.00	3.62	7.88	-22.82	-61.00	81.00	1.12
14.00	1.42	6.97	-22.94	-15.00	147.00	1.07	95.00	2.97	6.03	-23.52	-54.00	86.00	1.13
23.00	2.38	7.75	-22.54	-6.00	185.00	1.18	111.00	2.64	5.46	-23.41	-46.00	93.00	1.13
31.00	3.28	8.65	-22.29	2.00	232.00	1.45	128.00	3.02	7.19	-23.55	-39.00	104.00	1.10
39.00	2.83	7.30	-22.72	11.00	287.00	1.62	144.00	3.66	7.03	-23.00	-32.00	119.00	1.15
48.00	2.96	7.60	-22.91	20.00	340.00	1.91	160.00	3.79	7.84	-23.59	-25.00	137.00	1.18
56.00	3.17	7.58	-22.76	29.00	379.00	1.91	169.00	4.00	7.84	-22.90	-18.00	162.00	1.12
65.00	3.84	8.26	-23.42	38.00	395.00	1.78	177.00	4.39	8.30	-24.16	-11.00	192.00	1.20
73.00	3.04	7.18	-22.88	47.00	381.00	1.41	193.00	4.82	8.31	-23.89	-4.00	227.00	1.35
82.00	2.88	7.24	-23.03	55.00	342.00	1.25	210.00	3.95	7.14	-23.03	4.00	265.00	1.71
89.00	3.36	7.31	-22.66	64.00	290.00	1.19					11.00	301.00	1.81
99.00	3.42	7.95	-22.50	73.00	238.00	1.15					18.00	331.00	1.81
108.00	2.75	7.43	-23.09	82.00	194.00	1.15					25.00	354.00	1.86
117.00	2.74	7.34	-23.15	91.00	161.00	1.14					33.00	366.00	1.85
126.00	3.77	7.47	-22.54	100.00	137.00	1.14					40.00	369.00	1.54
135.00	3.09	7.24	-22.96	109.00	119.00	1.12					47.00	365.00	1.10

Vestra Gíslholtsvatn

Multi-proxy data for basaltic eruptions T-tephra and KN used for PCA (continued).

VGHV T-tephra						
Years Before and After Tephra	%TOC	C:N	$\delta^{13}C$	Years Before and After Tephra	MS	Den
144.00	2.88	7.42	-22.46	118.00	108.00	1.15
153.00	3.30	8.00	-22.73	128.00	100.00	1.15
162.00	1.43	7.43	-22.76	137.00	96.00	1.15
171.00	1.67	7.23	-22.97	146.00	93.00	1.17
180.00	2.98	7.62	-22.23	155.00	91.00	1.19
193.00	3.58	7.24	-22.65	164.00	90.00	1.17
212.00	3.71	7.34	-22.70	173.00	88.00	1.20
				182.00	88.00	1.15
				191.00	89.00	1.15
				201.00	89.00	1.17

VGHV KN		
Years Before and After Tephra	MS	Den
54.00	353.00	1.13
62.00	336.00	0.87
69.00	314.00	0.92
76.00	287.00	1.70
84.00	256.00	1.40
91.00	225.00	1.23
98.00	196.00	1.21
106.00	172.00	1.18
113.00	152.00	1.19
121.00	136.00	1.21
128.00	123.00	1.16
135.00	114.00	1.19
143.00	105.00	1.17
150.00	102.00	1.14
157.00	99.00	1.16
165.00	95.00	1.12
172.00	92.00	1.16
179.00	88.00	1.17
187.00	83.00	1.15
194.00	78.00	1.12
201.00	73.00	1.10

Hvítárvatn

Multi-proxy data for rhyolitic eruptions H4 and H3 used for PCA.

HVT H4							HVT H3					
Years Before and After Tephra	%TOC	C:N	$\delta^{13}C$	Years Before and After Tephra	Den	MS	Years Before and After Tephra	%TOC	C:N	$\delta^{13}C$	Years Before and After Tephra	Den	MS
-202.00	0.31	5.81	-24.61	-202.00	1.93	382.90	-214.00	0.23	5.55	-26.02	-207.00	1.99	428.70
-191.00	0.32	5.69	-23.91	-191.00	1.94	379.70	-196.00	0.29	6.18	-25.39	-199.00	1.99	427.70
-180.00	0.32	5.81	-24.10	-180.00	1.94	379.10	-177.00	0.21	5.50	-25.51	-192.00	2.00	425.90
-169.00	0.36	5.73	-23.54	-169.00	1.82	381.70	-159.00	0.37	6.45	-26.02	-185.00	1.97	424.50
-157.00	0.34	5.87	-24.02	-157.00	1.82	388.80	-141.00	0.29	5.73	-26.36	-177.00	1.94	424.80
-145.00	0.34	5.81	-24.61	-145.00	1.82	399.60	-122.00	0.26	5.82	-25.93	-170.00	2.04	424.80
-133.00	0.31	6.07	-24.53	-133.00	1.86	411.10	-103.00	0.44	6.15	-25.02	-163.00	1.97	421.80
-120.00	0.33	5.74	-24.06	-120.00	1.87	419.90	-84.00	0.28	6.39	-24.90	-155.00	2.00	416.00
-106.00	0.38	6.23	-24.49	-106.00	1.87	425.60	-64.00	0.23	5.33	-24.56	-148.00	1.92	411.10
-92.00	0.24	6.11	-25.15	-92.00	1.83	429.50	-52.00	0.49	6.76	-25.42	-141.00	1.91	409.60
-78.00	0.30	5.94	-24.48	-78.00	1.85	433.30	-43.00	0.33	5.75	-26.30	-133.00	2.00	409.80
-63.00	0.25	5.70	-24.38	-63.00	1.84	437.20	-35.00	0.39	6.49	-26.20	-126.00	1.99	409.60
-48.00	0.29	6.30	-24.28	-48.00	1.88	441.40	0.00	0.13	5.50	-25.70	-118.00	2.05	407.10
-31.00	0.28	6.29	-23.87	-31.00	1.78	449.40	4.00	0.31	7.51	-26.07	-111.00	1.97	403.20
-14.00	0.34	6.53	-24.04	-14.00	1.73	466.20	7.00	0.39	7.95	-25.94	-103.00	2.03	401.00
3.00	0.27	6.53	-25.19	1.00	2.22	301.50	11.00	0.99	9.14	-25.47	-95.00	1.91	402.60
7.00	0.46	7.52	-26.55	2.00	2.22	304.30	13.00	1.08	9.18	-26.00	-88.00	1.96	407.70
13.00	0.61	7.97	-26.51	3.00	2.14	305.90	17.00	1.40	10.48	-25.73	-80.00	1.99	414.30
21.00	0.55	8.66	-25.61	3.00	1.86	489.10	20.00	1.27	11.09	-25.28	-72.00	1.98	419.30
29.00	0.55	7.91	-26.07	5.00	2.09	306.50	24.00	1.36	10.44	-25.25	-64.00	2.06	419.70
39.00	0.42	7.97	-25.48	7.00	2.04	306.40	27.00	1.58	10.22	-25.13	-56.00	2.08	415.20
50.00	0.60	8.14	-25.51	10.00	2.04	304.50	31.00	1.36	10.32	-25.49	-48.00	1.92	410.50
62.00	0.43	7.24	-25.80	13.00	2.06	300.70	34.00	2.34	11.36	-25.37	-39.00	1.91	409.40
74.00	0.53	7.42	-25.75	17.00	2.13	295.20	38.00	1.28	9.83	-25.83	-2.00	2.03	407.80
87.00	0.55	7.23	-25.81	21.00	2.03	289.60	41.00	2.15	11.22	-25.46	0.00	2.22	399.20
100.00	0.55	7.25	-25.45	25.00	1.95	285.90	50.00	1.65	10.29	-25.56	3.00	2.23	380.40
114.00	0.43	6.95	-25.55	29.00	1.92	286.00	56.00	1.03	8.97	-25.99	5.00	2.10	354.90
128.00	0.42	6.79	-25.44	34.00	1.99	289.20	65.00	0.81	9.06	-26.31	8.00	2.00	326.30
156.00	0.48	7.26	-25.67	39.00	2.02	291.80	80.00	1.02	9.20	-26.54	11.00	1.95	299.70
170.00	0.36	6.80	-25.48	45.00	1.94	293.00	86.00	0.59	8.02	-26.50	13.00	1.75	280.70
185.00	0.56	6.37	-25.82	50.00	2.10	293.00	96.00	0.52	8.93	-26.25	16.00	1.69	270.50

Hvítárvatn

Multi-proxy data for rhyolitic eruption H3 used for PCA (continued).

HVT H4			
Years Before and After Tephra	%TOC	C:N	$\delta^{13}C$
199.00	0.55	6.72	-25.97
213.00	0.49	6.99	-25.62

HVT H4		
Years Before and After Tephra	Den	MS
56.00	2.12	291.10
62.00	1.92	286.80
68.00	1.88	281.70
74.00	1.88	277.10
80.00	1.82	275.60
87.00	1.92	276.40
93.00	1.96	278.10
100.00	1.88	280.10
107.00	1.90	281.90
114.00	1.90	282.70
121.00	1.86	281.90
128.00	1.91	279.00
135.00	1.84	277.30
142.00	1.76	282.30
149.00	1.81	294.70
156.00	1.89	311.90
163.00	1.97	324.50
170.00	2.05	328.90
178.00	1.92	325.60
185.00	1.85	320.40
192.00	1.86	318.20
199.00	1.86	320.30
206.00	1.84	326.90

HVT H3			
Years Before and After Tephra	%TOC	C:N	$\delta^{13}C$
102.00	0.18	6.95	-26.52
112.00	0.32	7.63	-26.59
118.00	0.39	7.36	-26.68
128.00	0.45	8.34	-25.78
135.00	0.48	7.77	-25.62
138.00	0.44	7.76	-25.92
145.00	0.73	8.51	-25.79
151.00	0.35	7.16	-26.07
158.00	0.29	7.36	-25.76
165.00	0.35	7.13	-26.16
171.00	0.53	8.30	-25.56
178.00	0.45	7.22	-26.43
185.00	0.56	7.45	-26.08
192.00	0.60	8.37	-25.76
199.00	0.33	7.68	-25.98
206.00	0.39	7.36	-25.60

HVT H3		
Years Before and After Tephra	Den	MS
19.00	1.71	268.30
22.00	1.77	269.40
24.00	1.79	268.60
27.00	1.87	264.40
30.00	1.75	257.40
33.00	1.75	250.50
35.00	1.69	246.00
38.00	1.69	245.00
41.00	1.75	247.00
44.00	1.68	251.70
47.00	1.72	260.20
50.00	1.79	271.80
53.00	1.79	285.70
56.00	1.83	300.20
59.00	1.93	312.30
62.00	1.86	319.80
65.00	1.84	324.30
68.00	1.89	327.40
71.00	1.82	330.60
74.00	1.88	332.50
77.00	1.94	333.10
80.00	1.90	333.70
83.00	1.87	336.70
86.00	1.91	342.50
89.00	1.86	350.40
93.00	1.91	359.50
96.00	1.90	367.50
99.00	1.86	374.50
102.00	1.95	380.60
105.00	2.01	385.90
109.00	1.89	390.00
112.00	1.93	391.80
115.00	2.03	390.60
118.00	1.96	388.30
122.00	1.92	387.60
125.00	1.95	389.80
128.00	2.09	393.00
131.00	2.06	395.50
135.00	2.09	396.90
138.00	2.05	397.60
141.00	2.08	398.00
145.00	2.12	398.80
148.00	2.09	400.20
151.00	2.10	402.60
155.00	2.11	405.70
158.00	2.13	409.80
161.00	2.11	414.40
165.00	2.14	418.90
168.00	2.14	422.30
171.00	2.14	420.80
175.00	2.14	392.60
235.00	2.26	434.20

Hvítárvatn

Multi-proxy data for basaltic eruptions T-tephra and KN used for PCA.

HVT T-tephra							HVT KN						
Years Before and After Tephra	%TOC	C:N	$\delta^{13}C$	Years Before and After Tephra	Den	MS	Years Before and After Tephra	%TOC	C:N	$\delta^{13}C$	Years Before and After Tephra	Den	MS
-218.00	0.40	6.26	-24.82	-218.00	1.67	244.90	-206.00	0.23	6.22	-26.03	-203.00	2.04	393.00
-198.00	0.45	6.22	-23.89	-198.00	1.69	253.70	-194.00	0.29	5.89	-25.96	-197.00	2.01	385.20
-178.00	0.40	6.71	-25.35	-178.00	1.72	260.20	-181.00	0.32	6.69	-25.68	-191.00	1.85	381.30

Hvítárvatn
Multi-proxy data for basaltic eruptions T-tephra and KN used for PCA (continued).

HVT T-tephra

Years Before and After Tephra	%TOC	C:N	$\delta^{13}C$
-158.00	0.29	5.62	-23.69
-138.00	0.41	5.54	-23.44
-119.00	0.48	5.93	-23.77
-114.00	0.33	6.38	-23.68
-104.00	0.42	7.24	-23.95
-94.00	0.49	6.80	-23.69
-84.00	0.52	7.26	-23.98
-74.00	0.37	7.95	-24.30
-64.00	0.30	7.31	-24.29
-54.00	0.33	6.73	-23.90
-44.00	0.50	6.90	-23.76
-34.00	0.43	6.80	-23.69
-24.00	0.30	9.08	-25.08
-14.00	0.18	7.30	-26.73
15.00	0.32	7.27	-25.19
25.00	0.36	7.61	-25.00
35.00	0.48	9.24	-25.78
45.00	0.36	7.42	-24.41
55.00	0.33	6.79	-23.95
65.00	0.42	8.94	-24.88
75.00	0.44	9.80	-24.57
86.00	0.36	7.92	-24.59
96.00	0.39	7.64	-24.11
106.00	0.38	6.94	-23.81
116.00	0.43	8.08	-24.66
126.00	0.41	6.64	-23.91
136.00	0.30	6.85	-24.45
146.00	0.24	7.52	-25.12
156.00	0.30	6.61	-25.08
166.00	0.33	8.54	-25.56
177.00	0.11	6.83	-25.05
187.00	0.26	5.95	-24.04
197.00	0.38	7.38	-24.65
207.00	0.32	5.98	-24.19

Years Before and After Tephra	Den	MS
-158.00	1.74	262.70
-138.00	1.68	262.30
-119.00	1.72	261.60
-99.00	1.67	261.40
-79.00	1.80	261.40
-59.00	1.66	263.10
-39.00	1.71	266.90
-19.00	1.96	269.10
0.00	1.85	264.70
20.00	1.69	255.90
40.00	1.67	246.30
60.00	1.69	238.20
81.00	1.69	231.10
101.00	1.63	225.90
121.00	1.71	223.60
141.00	1.67	224.00
161.00	1.90	227.40
182.00	1.59	234.20
202.00	1.66	244.10

HVT KN

Years Before and After Tephra	%TOC	C:N	$\delta^{13}C$
-169.00	0.33	6.38	-24.89
-156.00	0.29	6.11	-25.37
-143.00	0.34	6.22	-24.67
-131.00	0.37	6.88	-24.50
-118.00	0.40	6.49	-24.54
-105.00	0.49	7.79	-25.22
-71.00	0.37	7.21	-25.21
-57.00	0.26	5.95	-25.43
-37.00	0.28	6.77	-25.98
2.00	0.11	7.10	-26.73
13.00	0.18	6.40	-26.09
31.00	0.24	7.08	-25.88
50.00	0.35	6.43	-25.47
68.00	0.32	7.06	-25.69
87.00	0.30	5.80	-25.09
105.00	0.33	7.18	-25.42
124.00	0.23	6.08	-24.64
143.00	0.29	6.35	-25.95
162.00	0.21	5.71	-24.84
180.00	0.24	6.07	-25.74
199.00	0.22	5.33	-25.78
218.00	0.24	5.71	-25.58

Years Before and After Tephra	Den	MS
-185.00	1.97	383.70
-179.00	1.94	389.80
-173.00	2.05	395.80
-167.00	2.09	398.80
-161.00	2.01	401.10
-155.00	1.94	407.30
-149.00	2.08	416.90
-143.00	2.15	425.60
-137.00	2.02	431.40
-130.00	2.17	433.60
-124.00	2.16	433.00
-118.00	2.08	430.70
-112.00	2.20	426.80
-105.00	2.18	419.40
-7.00	2.16	452.80
0.00	2.17	456.20
7.00	2.13	457.40
13.00	2.11	459.60
20.00	2.20	461.60
27.00	2.27	460.60
35.00	2.23	456.30
42.00	2.25	454.00
49.00	2.22	451.10
56.00	2.35	453.60
63.00	2.30	453.20
70.00	2.18	450.70
77.00	2.18	448.50
85.00	2.08	447.40
92.00	2.18	446.60
99.00	2.14	444.90
107.00	2.06	442.90
114.00	2.08	442.20
121.00	2.09	442.40
129.00	2.10	444.60
136.00	2.04	449.80
144.00	2.04	457.50
151.00	1.99	465.80
159.00	2.09	470.50
166.00	2.15	468.00
174.00	2.06	461.60
181.00	1.99	456.00
189.00	2.03	453.80
196.00	1.97	454.40
204.00	2.05	454.90

Haukadalsvatn
Multi-proxy data for rhyolitic eruption H4 and basaltic eruption T-tephra used for PCA.

HAK H4							HAK T-tephra						
Years Before and After Tephra	%TOC	C:N	$\delta^{13}C$	Years Before and After Tephra	Den	MS	Years Before and After Tephra	%TOC	C:N	$\delta^{13}C$	Years Before and After Tephra	Den	MS
-212.00	0.83	9.65	-26.73	-203.00	1.64	787.30	-209.00	0.85	10.63	-27.25	-222.00	1.52	665.29
-195.00	1.03	9.65	-25.94	-186.00	1.68	806.62	-162.00	0.96	8.99	-27.41	-196.00	1.54	684.35
-177.00	0.72	9.32	-26.57	-167.00	1.71	813.07	-148.00	0.86	9.73	-27.02	-169.00	1.52	702.76
-158.00	1.11	9.48	-27.21	-149.00	1.71	798.08	-134.00	0.74	9.64	-27.01	-141.00	1.59	715.78
-139.00	1.06	9.69	-27.01	-130.00	1.61	771.79	-120.00	0.74	8.19	-27.31	-113.00	1.60	719.33
-95.00	0.80	8.23	-27.21	-110.00	1.41	748.14	-106.00	0.76	8.45	-27.37	-84.00	1.57	713.94
-84.50	0.97	8.63	-27.31	-90.00	1.58	730.26	-91.50	0.90	8.57	-27.29	-55.00	1.56	701.84
-74.00	1.07	8.42	-27.35	-69.00	1.45	718.04	-77.00	0.89	8.46	-27.36	-27.00	1.54	688.69

Haukadalsvatn

Multi-proxy data for rhyolitic eruption H4 and basaltic eruption T-tephra (continued).

HAK H4							HAK T-tephra						
Years Before and After Tephra	%TOC	C:N	δ^{13}C	Years Before and After Tephra	Den	MS	Years Before and After Tephra	%TOC	C:N	δ^{13}C	Years Before and After Tephra	Den	MS
-64.50	0.99	8.27	-27.28	-51.00	1.49	711.46	-62.50	0.74	8.08	-27.63	0.00	1.60	683.83
-55.50	0.89	8.70	-27.25	-33.00	1.61	708.70	-48.00	0.76	8.13	-27.39	24.00	1.59	689.22
-37.50	0.85	8.84	-26.88	-16.00	1.73	705.68	-34.00	0.82	8.37	-27.37	46.00	1.56	705.00
-28.50	0.80	9.15	-26.14	0.00	1.69	700.69	-20.00	0.89	8.54	-27.37	67.00	1.60	727.74
-20.00	0.75	9.59	-25.26	8.00	1.92	700.82	6.00	0.77	7.96	-27.85	85.00	1.62	746.94
-12.00	0.73	8.63	-27.06	15.00	1.60	710.94	18.00	0.73	8.08	-27.46	102.00	1.67	756.67
-4.00	0.27	8.01	-25.55	22.00	1.64	728.03	29.50	1.03	9.19	-27.55	117.00	1.61	760.48
-1.00	0.16	5.72	-24.14	36.00	1.70	748.00	40.50	1.09	8.42	-27.43	131.00	1.65	763.11
11.50	0.46	7.40	-27.05	49.00	1.68	768.51	51.50	1.12	8.31	-27.33	143.00	1.67	763.90
18.50	0.69	7.42	-27.44	61.00	1.68	786.12	62.00	1.01	8.48	-27.31	154.00	1.62	766.79
25.50	0.66	7.68	-27.92	72.00	1.69	797.95	71.50	0.98	8.25	-27.37	163.00	1.63	773.50
32.50	0.74	7.42	-28.07	83.00	1.65	804.39	80.50	0.99	8.41	-27.40	172.00	1.67	779.55
39.50	0.73	7.61	-27.68	93.00	1.68	805.84	89.50	1.12	9.06	-27.04	179.00	1.68	778.63
46.00	0.73	7.74	-27.53	102.00	1.71	804.52	98.00	0.89	8.81	-26.49	185.00	1.68	769.29
52.00	1.03	8.34	-27.43	110.00	1.70	804.39	106.00	0.72	8.37	-27.03	190.00	1.65	753.91
58.00	0.80	7.94	-27.37	118.00	1.69	806.62	113.50	0.82	8.28	-27.40	194.00	1.67	738.00
64.00	0.66	7.87	-27.32	125.00	1.74	806.89	120.50	0.86	8.26	-27.28	200.00	1.63	727.35
69.50	0.81	8.19	-27.45	132.00	1.68	806.23	127.50	0.79	7.85	-27.51			
75.00	0.95	8.35	-27.41	138.00	1.70	809.38	134.00	0.60	7.83	-27.15			
80.50	0.85	8.51	-27.38	144.00	1.71	815.43	140.00	0.74	8.07	-27.37			
85.50	1.21	9.85	-27.08	149.00	1.72	821.48	146.00	0.74	8.09	-27.33			
90.50	0.83	7.96	-27.61	154.00	1.71	814.91	151.50	0.81	8.39	-27.39			
95.00	0.78	7.96	-27.72	159.00	1.72	824.24	156.50	0.89	8.28	-27.43			
99.50	0.75	7.89	-27.63	163.00	1.73	818.19	161.00	1.00	8.40	-27.49			
104.00	0.74	7.80	-27.79	167.00	1.70	813.85	165.50	0.82	8.20	-27.37			
108.00	0.79	7.82	-27.57	171.00	1.69	815.30	170.00	0.77	8.27	-27.34			
112.00	0.85	8.02	-27.52	174.00	1.70	821.61	173.50	0.90	8.21	-27.35			
116.00	0.73	7.60	-27.62	177.00	1.71	828.71	177.00	0.74	8.32	-27.29			
120.00	0.68	7.58	-27.23	180.00	1.75	833.70	180.50	0.78	7.96	-27.04			
123.50	0.81	8.23	-27.64	183.00	1.72	836.86	183.50	0.68	7.97	-27.40			
127.00	0.86	8.20	-27.44	187.00	1.70	837.64	186.00	0.78	7.91	-27.53			
130.50	0.85	8.63	-27.43	190.00	1.71	835.54	188.50	0.88	8.33	-27.43			
133.50	1.07	11.26	-27.91	192.00	1.78	832.65	268.00	1.03	9.50	-27.16			
136.50	0.79	8.48	-27.51	195.00	1.73	833.04							
139.50	0.82	8.65	-27.44	198.00	1.69	839.22							
142.50	0.85	8.66	-27.56	200.00	1.73	848.16							
145.50	0.80	8.65	-27.39										
148.00	0.76	8.74	-27.81										
150.50	0.75	8.58	-27.57										
153.00	0.76	8.73	-27.40										
155.50	0.79	8.40	-27.61										
158.00	0.87	8.60	-27.65										
167.00	0.90	9.78	-27.20										
174.00	0.85	9.23	-27.34										
180.00	0.79	9.61	-27.10										
186.00	0.81	9.24	-27.46										
194.00	0.88	9.38	-27.34										
196.00	0.84	8.86	-27.59										
202.00	0.77	9.14	-27.45										

Torfadalsvatn

Multi-proxy data for rhyolitic eruption H4 and basaltic eruption Tv-5 used for PCA.

HAK H4							HAK T-tephra						
Years Before and After Tephra	%TOC	C:N	δ^{13}C	Years Before and After Tephra	Den	MS	Years Before and After Tephra	%TOC	C:N	δ^{13}C	Years Before and After Tephra	Den	MS
-211.00	7.06	7.63	-18.45	-206.00	1.21	49.82	-216.00	7.09	8.10	-18.98	-201.00	1.17	44.52
-196.50	4.68	7.43	-18.69	-199.00	1.21	49.32	-191.00	6.89	7.96	-19.30	-195.00	1.16	44.72
-182.50	6.48	7.46	-18.82	-192.00	1.22	49.08	-167.00	7.23	8.11	-19.41	-189.00	1.17	44.81
-168.50	7.02	7.48	-18.81	-185.00	1.22	49.02	-142.00	7.28	8.29	-19.52	-183.00	1.16	44.87

Torfadalsvatn

Multi-proxy data for rhyolitic eruption H4 and basaltic eruption Tv-5 used for PCA (continued).

HAK H4						
Years Before and After Tephra	%TOC	C:N	$\delta^{13}C$	Years Before and After Tephra	Den	MS
-139.50	7.09	7.58	-19.11	-178.00	1.24	49.32
-125.50	6.92	7.37	-18.96	-171.00	1.25	49.89
-115.00	6.74	7.39	-19.13	-164.00	1.25	50.82
-108.00	7.27	7.52	-18.87	-157.00	1.23	52.12
-100.00	7.88	8.12	-19.91	-149.00	1.23	53.98
-93.00	7.11	7.51	-18.97	-142.00	1.23	56.21
-86.00	7.23	7.52	-19.09	-135.00	1.22	58.70
-79.00	7.44	7.79	-19.66	-128.00	1.14	61.31
-72.00	6.59	7.43	-19.09	-121.00	1.17	63.78
-65.00	7.45	7.87	-19.58	-114.00	1.20	40.65
-58.00	6.57	7.46	-18.98	-107.00	1.18	38.66
-50.00	7.51	7.56	-18.85	-100.00	1.21	37.04
-43.00	8.99	8.02	-18.62	-92.00	1.22	35.80
-36.00	7.99	7.64	-18.77	-85.00	1.22	34.87
-29.00	7.56	7.56	-19.12	-78.00	1.21	34.25
-22.00	8.20	7.84	-19.77	-71.00	1.21	34.12
-15.00	8.02	8.17	-20.50	-64.00	1.19	34.00
-8.00	6.87	7.40	-19.53	-57.00	1.20	34.19
0.00	3.86	8.84	-21.48	-50.00	1.19	34.57
28.00	4.95	9.58	-22.17	-42.00	1.21	35.18
35.00	4.80	8.04	-19.06	-35.00	1.21	36.05
42.00	7.42	8.07	-18.66	-28.00	1.19	37.35
50.00	9.03	9.72	-19.91	-21.00	1.19	38.90
57.00	4.46	8.16	-19.73	-14.00	1.20	40.77
64.00	7.45	8.00	-19.03	-7.00	1.21	42.75
71.00	7.29	7.91	-19.02	0.00	1.23	44.86
78.00	7.45	7.95	-19.12	8.00	1.28	46.73
85.00	7.57	8.02	-19.06	15.00	1.32	48.22
92.00	7.34	7.98	-18.78	22.00	1.39	49.01
100.00	6.08	9.01	-21.12	29.00	1.50	49.08
107.00	7.06	8.82	-19.68	36.00	1.47	48.33
114.00	7.49	7.84	-18.72	43.00	1.29	46.91
121.00	7.52	7.68	-19.19	50.00	1.21	45.11
128.00	7.10	7.60	-19.20	58.00	1.16	43.24
135.00	8.61	8.45	-19.98	65.00	1.18	41.26
142.00	10.41	10.01	-20.00	72.00	1.20	39.46
150.00	7.94	7.84	-18.80	79.00	1.21	37.85
157.00	7.94	7.78	-18.83	86.00	1.17	36.37
164.00	7.27	8.06	-19.84	93.00	1.17	35.05
171.00	7.68	7.91	-19.36	100.00	1.18	33.88
178.00	7.48	7.98	-19.12	108.00	1.17	32.89
185.00	7.46	7.72	-19.21	115.00	1.17	31.89
192.00	7.56	7.80	-18.88	122.00	1.18	30.90
200.00	7.32	7.57	-19.01	129.00	1.16	29.97
207.00	7.61	7.87	-18.86	136.00	1.17	29.10
				143.00	1.18	28.30
				150.00	1.17	27.68
				158.00	1.17	27.18
				165.00	1.15	26.81
				172.00	1.15	26.55
				179.00	1.17	26.43
				186.00	1.17	26.24
				193.00	1.16	26.25
				200.00	1.16	26.19

HAK T-tephra						
Years Before and After Tephra	%TOC	C:N	$\delta^{13}C$	Years Before and After Tephra	Den	MS
-117.00	7.87	8.45	-19.02	-176.00	1.18	44.87
-93.00	6.92	8.08	-20.33	-170.00	1.19	44.87
-87.00	6.56	8.08	-20.43	-164.00	1.20	44.82
-81.00	6.85	8.47	-20.84	-157.00	1.19	44.81
-74.00	6.89	8.12	-20.09	-151.00	1.20	44.76
-68.00	6.79	7.99	-20.12	-144.00	1.18	44.72
-62.00	6.69	8.05	-20.24	-138.00	1.17	44.81
-56.00	6.86	8.07	-20.14	-132.00	1.18	44.87
-50.00	7.17	8.15	-20.10	-125.00	1.17	45.02
-43.00	6.81	8.12	-19.98	-119.00	1.18	45.21
-37.00	6.57	8.19	-19.99	-113.00	1.19	45.46
-31.00	6.85	8.27	-19.80	-106.00	1.18	45.81
-25.00	6.81	8.54	-19.76	-100.00	1.17	46.15
-19.00	9.94	10.01	-21.07	-94.00	1.16	46.49
-13.00	7.54	8.34	-19.46	-87.00	1.17	46.89
-6.00	7.96	9.22	-21.10	-81.00	1.17	47.29
0.00	5.97	7.99	-19.86	-75.00	1.18	47.83
6.00	6.69	7.94	-19.48	-69.00	1.18	48.42
18.00	5.71	9.00	-18.81	-62.00	1.19	49.12
24.00	4.10	7.98	-20.04	-56.00	1.19	50.00
30.00	5.44	8.18	-19.50	-50.00	1.17	50.99
36.00	6.41	8.94	-18.93	-44.00	1.18	52.22
42.00	6.31	8.79	-19.10	-37.00	1.17	53.65
48.00	7.09	9.53	-17.62	-31.00	1.18	55.43
55.00	8.99	10.30	-16.47	-25.00	1.17	57.56
61.00	6.35	8.45	-19.22	-19.00	1.18	60.02
67.00	6.12	8.45	-19.35	-13.00	1.19	62.69
73.00	6.30	8.51	-19.46	-6.00	1.19	65.26
79.00	6.76	8.76	-18.79	0.00	1.21	67.24
85.00	7.18	8.79	-18.77	6.00	1.30	68.07
91.00	7.25	8.73	-18.51	12.00	1.57	67.58
97.00	7.85	9.03	-18.20	18.00	1.57	65.71
103.00	10.46	10.12	-16.84	24.00	1.29	62.99
109.00	7.69	8.97	-18.82	31.00	1.20	59.78
132.00	6.65	8.02	-19.27	37.00	1.20	56.52
156.00	7.02	8.18	-18.96	43.00	1.22	53.51
180.00	7.99	8.83	-17.84	49.00	1.20	50.94
204.00	7.26	8.00	-18.81	55.00	1.20	48.77
				61.00	1.22	47.03
				67.00	1.21	45.66
				73.00	1.19	44.62
				79.00	1.20	43.87
				85.00	1.21	43.43
				92.00	1.21	43.23
				98.00	1.23	43.23
				104.00	1.23	43.48
				110.00	1.22	43.83
				116.00	1.11	44.22
				122.00	1.17	44.67
				128.00	1.26	45.06
				134.00	1.27	45.36
				140.00	1.26	45.51
				146.00	1.25	45.51
				152.00	1.25	45.41
				158.00	1.24	45.21
				164.00	1.23	45.02
				170.00	1.21	44.82
				176.00	1.21	44.76
				182.00	1.20	44.76
				188.00	1.22	44.87
				194.00	1.21	44.96
				200.00	1.20	45.06

Additional tephra layers within time series for basaltic tephra horizons of interest

Tephra layers in T-tephra time series as geochemically identified by T. Thordarson, and G. Jóhannsdóttir and visually identified/confirmed by C. Christensen.

Lake	Formation	Year before or after T-tephra/Tv-5	Thickness (cm)	Composition	Analysis method	Source
Vestra Gíslholtsvatn		-54	0.15	Mixed	Geochemical	Katla? Askja?
		-9	0.20	Basaltic, SILK?	Geochemical	Katla
	T-tephra	0	1.60	Basaltic	Geochemical	Hekla
		171	0.25	Basaltic	Geochemical	Katla
Hvítárvatn		-89	0.10	Basaltic	Visual	?
		-23	0.30	Basaltic	Geochemical	?
	T-tephra	0	0.50	Basaltic	Geochemical	Hekla
		131	0.15	Basaltic	Visual	?
		159	0.15	Basaltic	Visual	?
Haukadalsvatn	T-tephra	0	0.40	Basaltic	Geochemical	Hekla
Torfadalsvatn	Tv-5	0	0.70	Basaltic	Visual	Katla

Tephra layers in KN time series as geochemically identified by T. Thordarson, A. Jagan, and G. Jóhannsdóttir and visually identified/confirmed by C. Christensen.

Lake	Formation	Year before or after KN	Thickness (cm)	Composition	Analysis method	Source
Vestra Gíslholtsvatn		-189	0.20	Basaltic	Geochemical	Katla
		-140	0.70	Basaltic	Geochemical	Katla
		-20	0.20	Basaltic, SILK-like?	Geochemical	Katla
	HS	-7	0.45	Mixed	Geochemical	Hekla
	KN	0	5.00	Basaltic	Geochemical	Katla
Hvítárvatn		-195	0.20	Basaltic	Visual	?
		-181	0.50	Basaltic	Visual	?
	KN	0	5.00	Basaltic	Geochemical	Katla
		105	0.50	Basaltic	Visual	?

Additional tephra layers within time series for rhyolitic tephra horizons of interest

Tephra layers in basaltic tephra H4 time series as geochemically identified by T. Thordarson, A. Jagan, and G. Jóhannsdóttir and visually identified/confirmed by C. Christensen.

Lake	Formation	Years before or after H4	Thickness (cm)	Composition	Analysis method	Source
Vestra Gíslholtsvatn		-191	0.70	Basaltic	Geochemical	Hekla?
	F-layer	-179	1.10	Basaltic	Geochemical	Hekla
		-164	0.30	Basaltic	Geochemical	Hekla?
		-121	0.10	Basaltic	Geochemical	Katla
		-26	0.20	Basaltic, SILK-like?	Geochemical	Hekla, Katla
	H4?	0	0.65	Andesitic, Rhyolitic	Geochemical	Hekla
		69	0.55	Basaltic, Icelanditic	Geochemical	Hekla
Hvítárvatn	H4	0	7.50	Rhyolitic, Mixed	Geochemical	Hekla
		10	0.80	Basaltic	Visual	?
		49	0.50	Basaltic	Visual	?
		86	0.30	Basaltic	Visual	?
		90	0.10	Mixed	Geochemical	Hekla
Haukadalsvatn		-48	0.30	Dacitic	Geochemical	Katla
	H4?	0	0.90	Mixed	Geochemical	Hekla
Torfadalsvatn	H4	0	1.20	Rhyolitic	Visual	Hekla

Additional tephra layers within time series for rhyolitic tephra horizons of interest (continued).

Tephra layers in basaltic tephra H3 time series as geochemically identified by T. Thordarson and A. Jagan and visually identified by C. Christensen.

Lake	Formation	Years before or after H3	Thickness (cm)	Composition	Analysis method	Source
Vestra Gíslholtsvatn		-130	0.70	Basaltic	Geochemical	Katla
		-105	0.20	Basaltic, Icelanditic	Geochemical	Hekla
	H3	0	0.40	Rhyolitic	Geochemical	Hekla
	KE?	14	1.70	Basaltic	Geochemical	Katla
		23	0.80	Basaltic	Geochemical	Katla
	H-B	181	0.20	Mixed	Geochemical	Hekla
Hvítárvatn		-21	0.20	Basaltic	Visual	?
	H3	0	8.00	Rhyolitic, Mixed	Geochemical	Hekla
		17	0.10	Basaltic	Visual	?
		20	0.20	Basaltic	Visual	?
	H-C	86	0.50	Mixed	Geochemical	Hekla
		112	0.30	Basaltic	Visual	?
	H-B	160	0.30	Mixed	Geochemical	Hekla

APPENDIX 3: PROXY TIME SERIES AND BIPLOTS FOR SURROUNDING TEPHRA HORIZONS OF INTEREST

A3.1 Time Series

Time series data before and after significant tephra deposition events was smoothed by application of a Stineman function to account for natural variability in proxy values. A description of sampling practices can be found under subsection *6.5.1 Sediment Cores and Samples*.

A3.1.1400 year Rhyolitic Tephra Time Series

A3.1.1.1 Physical Proxies

MS is largely controlled by the type of erosional products and organic matter (OM) content found in lake sediments, thus lakes in different catchments with different sediment sources and/or terrestrial and aquatic vegetation will have vastly different background levels of MS. The four lakes in this study vary dramatically in background MS (see Table 5.3) however changes observed after the rhyolitic tephra horizons H4 and H3 are fairly consistent between lakes except in HVT. VGHV, HAK, and TORF all exhibit an increase in MS immediately after the tephra horizons while MS in HVT decreases (Fig. A3.1 a, b). The increases are likely because of an increase in the proportion of minerogenic material relative to the background state (e.g. Rosenbaum et al., 2012). VGHV displays the largest increases in MS after H4 and H3 with multiple peaks in the time series correlated to groups of additional tephra layers (Fig. A3.1e, f) but values return to pre-tephra levels within ~75 years of the final tephra in the time

Figure A3.1 Rhyolitic tephra time series for physical proxies in all lakes a. and b. MS around H4 and H3 respectively; c. and d. Density around H4 and H3 respectively; e. and f. Tephra layers and their thicknesses in the H4 and H3 time series respectively

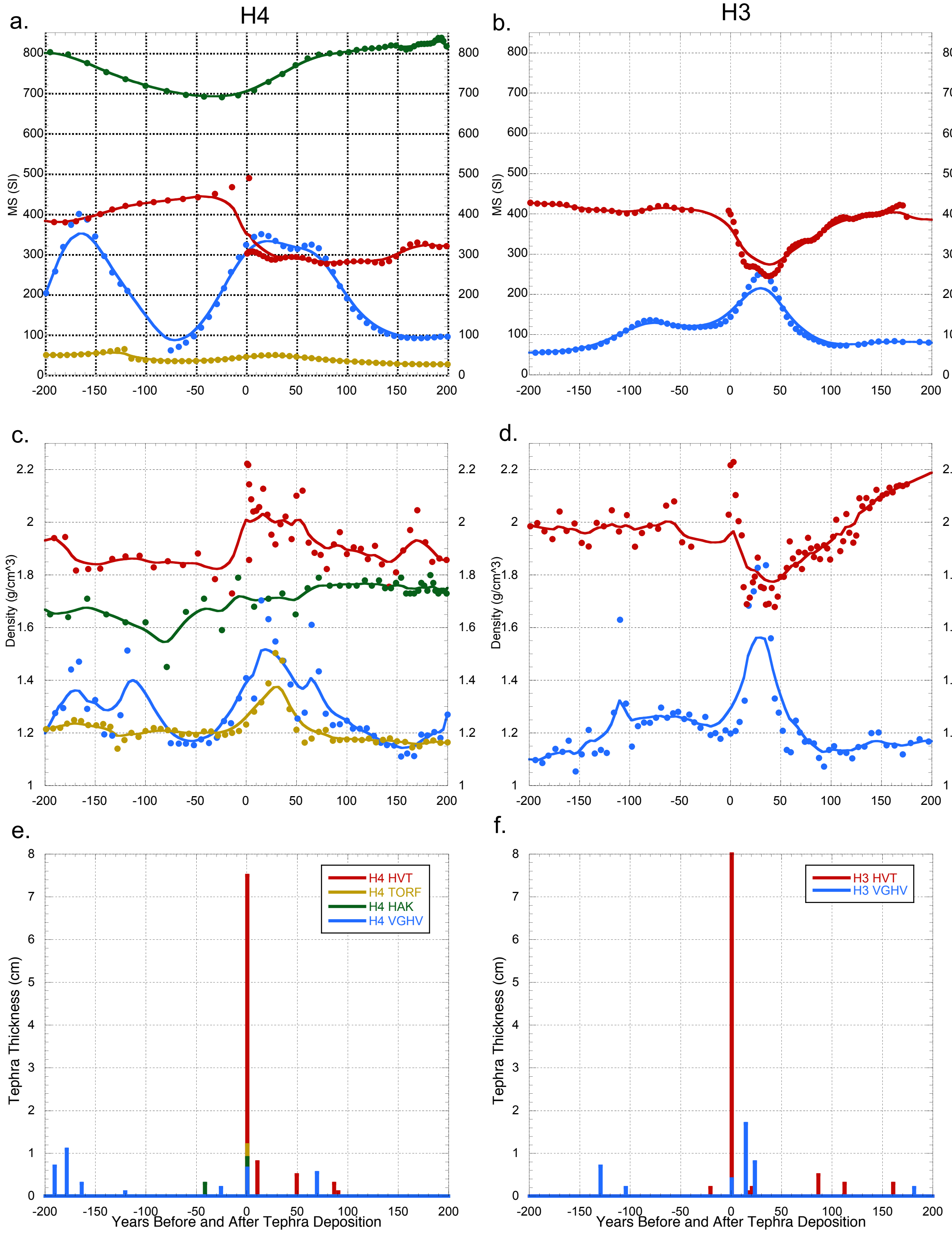

series. In HAK MS gradually decreases early in the time series with the lowest values occurring prior to H4. After H4, MS increases for ~100 years and elevated values persist for the remainder of the time series. As in VGHV, TORF peaks in MS following the tephra, and returns to low values within ~75 years. The elevated values in the first 100 years of the TORF time series are from a core break skewing the data and should be ignored. HVT is the anomalous lake in this data set as it abruptly decreases at the tephra horizons with continuous low values after H4 and a temporary low for ~50 years after H3 before gradually increasing for the rest of the time series. This decrease is due to the low MS of rhyolitic tephra and an increase in the proportion of organic material relative to the background state.

Bulk sediment density, like MS varies greatly between lakes as it depends upon the same variables, the minerogenic and OM content of sediment. Density abruptly increases in all lakes except HAK where the increase is more gradual following H4 tephra horizon. These elevations are temporary in VGHV and TORF but persistent in HVT and HAK (Fig A3.1c, d). Peaks in VGHV and TORF are related to the high density of the tephra layers relative to the background state while the long-term increases in HVT and HAK are more likely from an increase in the minerogenic flux from landscape destabilization. VGHV displays a similar trend in the H3 time series. After the H3 tephra horizon HVT has an abrupt increase followed by an abrupt decrease in density that lasts for ~50 years. This is followed by a continuous increase for the rest of the time series. The changes observed in HVT during the H3 time series can be attributed to deposition of the tephra layer and a large in wash of organic material followed by a persistent increase in minerogenic material. Additional tephra layers in VGHV and HVT also create short-lived positive tephra anomalies that extend for several decades, as tephra is typically denser than average lake sediment (Beierle and Bond, 2002).

Both HVT and VGHV have multiple tephra layers within the H4 and H3 time series while HAK has two tephra horizons and TORF one in the H4 time series. VGHV has the greatest number of tephra layers within both time series however the tephra horizons of interest, H3 and H4, are substantially thicker in HVT than in any other lake (see Fig. A3.1e, f). The other tephra layers in HVT are fairly thin relative to H4 and H3 and influence the physical proxies to a small degree. Meanwhile, VGHV has several tephra layers of greater or equal thickness to H4 and H3 producing additional variability in the data.

A3.1.1.2 Organic Matter Proxies

Background values of %TOC vary greatly between lakes with the average %TOC in TORF nearly an order of magnitude greater than in HAK, and the average %TOC in VGHV nearly an order of magnitude higher than in HVT (see Table 5.3). Following deposition of the H4 tephra %TOC increases in HVT and decreases in VGHV, HAK, and TORF. Unlike VGHV; HAK and TORF recover to pre-eruption levels within ~50 years while VGHV takes ~100 years to reach stable values (Fig. A3.2a). Decreased %TOC began before deposition of H4 in both VGHV and HAK with initiations corresponding to earlier tephra horizons. The influence of tephra on this preemptive decrease is supported by low %TOC in VGHV early in the time series coinciding with three tephra layers, two of which are of comparable to thickness to H4. VGHV shows a similar response to tephra perturbation in the H3 time series (Fig. A3.2b). As the H3 tephra horizon is nominal in VGHV there is no response however two thick basaltic

Figure A3.2 Rhyolitic tephra time series for biological proxies in all lakes a. and b. %TOC around H4 and H3 respectively; c. and d. C:N around H4 and H3 respectively; e. and f. d13C around H4 and H3 respectively; g. and h. Tephra layers and their thicknesses in the H4 and H3 time series respectively

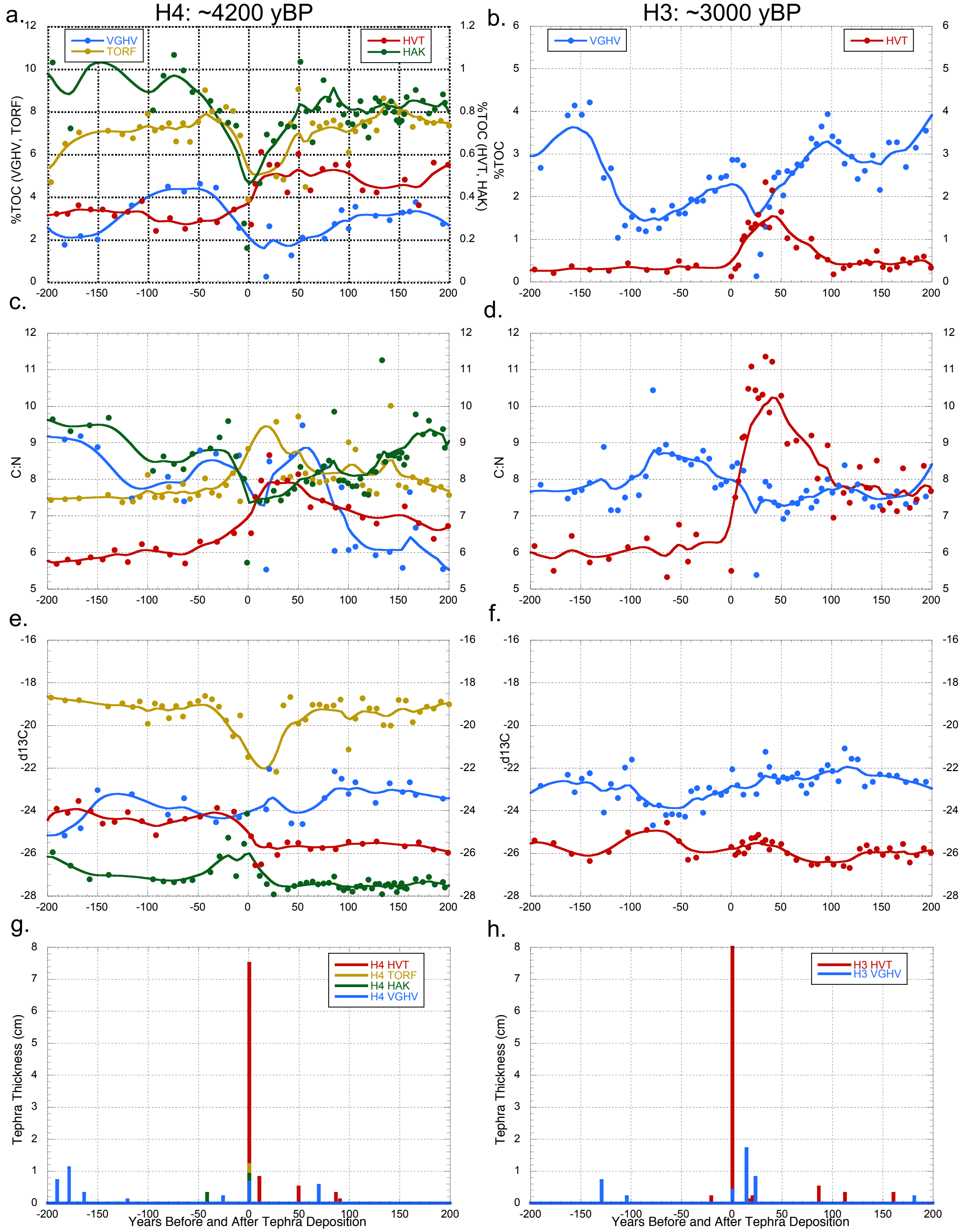

tephra horizons within three decades of H3 are associated with a substantial decrease in %TOC with another abrupt low in time series occurring after two other tephra layers.

Compared to the other lakes HVT has an opposite signal for %TOC following rhyolitic tephra perturbations. Immediately after the H4 tephra horizon %TOC increases by ~67% staying elevated for the remainder of the time series (Fig. A3.2a). The H3 tephra horizon is followed by the largest relative change observed in any lake with %TOC abruptly increasing by >600% and elevated values falling off gradually to achieve slightly elevated pre-eruption levels within 100 years of H3 (Fig. A3.2b). It is noted that the structure of %TOC correlates with MS and density in HVT and HAK, and anti-correlates in VGHV and TORF. This trend indicates the influence of minerogenic material on the signal of %TOC with correlated relationships suggesting high %TOC is associated with a high minerogenic flux. As HVT is an ultraoligotrophic lake the signal of %TOC observed after rhyolitic tephra layers can be attributed to an increase in terrestrial carbon entering the lake from the catchment (Larsen et al., 2011; 2012).

The ratio of carbon and nitrogen (C:N) indicates the proportion of terrestrial versus aquatic organic material preserved in the lake sediment (Meyers, 1997). VGHV and HAK both have one point negative deviations in C:N (from ~9 to ~5.5) after the H4 tephra horizon. As with %TOC, C:N in VGHV returns to pre-H4 values within several decades while HAK quickly reaches C:N=7.5 but does not return to pre-eruption values for 150 years (Fig. A3.2c). ~75 years after H4, C:N abruptly decreases again in VGHV and persists at C:N = 6 for the rest of the time series. This decline has the same timing as a basaltic tephra layer of similar thickness to H4. During the H3 time series, lower values of C:N also correspond to basaltic tephra layers in VGHV (Fig. A3.2d) with the thick tephra horizons after H3 producing a one point negative deviation in C:N (from ~8 to ~5.5). As in the H4 time series for VGHV C:N returns to pre-tephra values within decades. The decrease in C:N is likely an artifact of an increase in incoming minerogenic material from the landscape temporarily diluting a larger terrestrial component as the catchment is well vegetated (Hallsdóttir and Caseldine, 2005). HVT and TORF increase in C:N after H4 (Fig. A3.2c). C:N briefly increases in TORF from 7.5 to 9.5 before returning to pre-eruption values within several decades while the C:N increase in HVT (6 to 8.5) is followed by a gradual decrease but never returns to pre-eruption levels. C:N has a similar signal in HVT during the H3 time series increasing abruptly from 6.5 to 11.5 after the H3 tephra horizon (Fig A3.2d). These elevated values remain for 50 years before gradually falling off reaching a new equilibrium of C:N = 8 ~100 years after H3. Increased C:N in TORF is possibly related to increased water turbidity and reduced aquatic primary productivity following the H4 tephra horizon (Grobbelaar, 1985) while the increases in HVT is likely from more terrestrial carbon entering the catchment after rhyolitic tephra horizons (Larsen et al., 2011; 2012).

Stable carbon isotopes ($\delta^{13}C$) are controlled by a range of factors so interpretations are dependent upon the ecosystems processes of individual lakes (Meyers and Teranes 2001). As with MS, density and %TOC all four lakes vary greatly in average $\delta^{13}C$ (Table 5.3). Tephra deposition appears to have no immediate impact on stable carbon isotopes in VGHV, however $\delta^{13}C$ increases by ~2‰ early in the H4 time series at the same timing as a decrease in C:N. Another increase in $\delta^{13}C$ of ~1‰ occurs ~75 years after H4 coinciding with an abrupt decrease in C:N. Increasing $\delta^{13}C$ with decreasing C:N is an indicator of either reduced terrestrial OM input into a lake and/or increased aquatic primary productivity. TORF, HAK, and HVT all show more negative $\delta^{13}C$ after the H4 tephra horizon (Fig. A3.2e). A ~3‰ decrease in TORF persists for ~25 years before increasing back to pre-H4 values, while ~2‰ declines in HAK and HVT continue for the remainder of the time series. The decrease of $\delta^{13}C$ in TORF can be attributed to a temporary reduction in aquatic mosses and/or increased terrestrial carbon in the lake. The decrease in HAK and HVT however is most likely related to climate and/or an increased terrestrial component in the sediment. Interestingly, $\delta^{13}C$ in HAK briefly increases by ~1‰ following the earlier tephra layer in the time series and only after the H4 tephra horizon does $\delta^{13}C$ decrease. $\delta^{13}C$ does not change in HVT or VGHV following the H3 tephra horizon. However, it is noted that values in VGHV are ~1‰ higher on average post-H3. Low values of $\delta^{13}C$ and high values of C:N occur pre-H3 following a rhyolitic tephra layer of similar thickness to H3. This signal is consistent with landscape instability in all lakes. $\delta^{13}C$ in HVT remains at the post-H4 value of ~-25.5‰ the same value of terrestrial soil in the catchment after deposition of the H3 tephra (Fig. 5.3; Fig. A3.2f).

A3.1.2 400 year Basaltic Tephra Time Series

A3.1.2.1 Physical Proxies

Changes in MS and density associated with tephra layers during the KN and T-tephra time series are similar to responses in rhyolitic tephra time series for VGHV, TORF, and HAK. In HVT there is no significant variability in the physical proxies following basaltic tephra horizons (Fig. A3.3a, b, c, d). The different response at HVT in MS and density can likely be attributed to no change in erosion following deposition of the basaltic tephra horizons. VGHV and TORF show an increase in MS and density after basaltic tephra horizons returning to pre-eruption values within ~50 years for the KN and T-tephra time series. Average bulk sediment density is lower during the T-tephra time series than in any other time window observed for this study. This is because the T-tephra eruption occurred near the end of the HTM when all lakes indicate more productive ecosystems in their catchments (Hallsdóttir and Caseldine, 2005; Axford et al., 2007; Larsen et al., 2012; Geirsdóttir et al., in review). During the T-tephra time series at each tephra horizon in HVT density has one-point positive deviations above a background state of ~1.7 g/cm^3. In HVT steady increase in density lasting several decades follows the KN tephra horizon after which density gradually decreases for the remainder of the time series. The decrease in density can likely be attributed to an increase in the OM content and/or reduction of the minerogenic component of the sediment. The T-tephra horizon is not especially thick in any of the lakes relative to the other tephra layers of interest in this study. Several additional thin tephra horizons are dispersed in VGHV and HVT during this time window but the T-tephra is the only tephra layer found in HAK and TORF for the allocated time period. KN is the thickest tephra in VGHV and one of the thicker basaltic layers post-Saksunarvatn in HVT. Additional layers of tephra are dispersed before and after the KN horizon in HVT and VGHV with one moderately thick tephra layer in VGHV coinciding with a positive deviation in MS and density early in the time series (Fig. A3.3e, f).

Figure A3.3 Basaltic tephra time series for physical proxies a. and b. MS around the T-tephra and KN respectively; c. and d. Density around the T-tephra and KN respectively; e. and f. Tephra layers and their thicknesses in the T-tephra and KN time series respectively

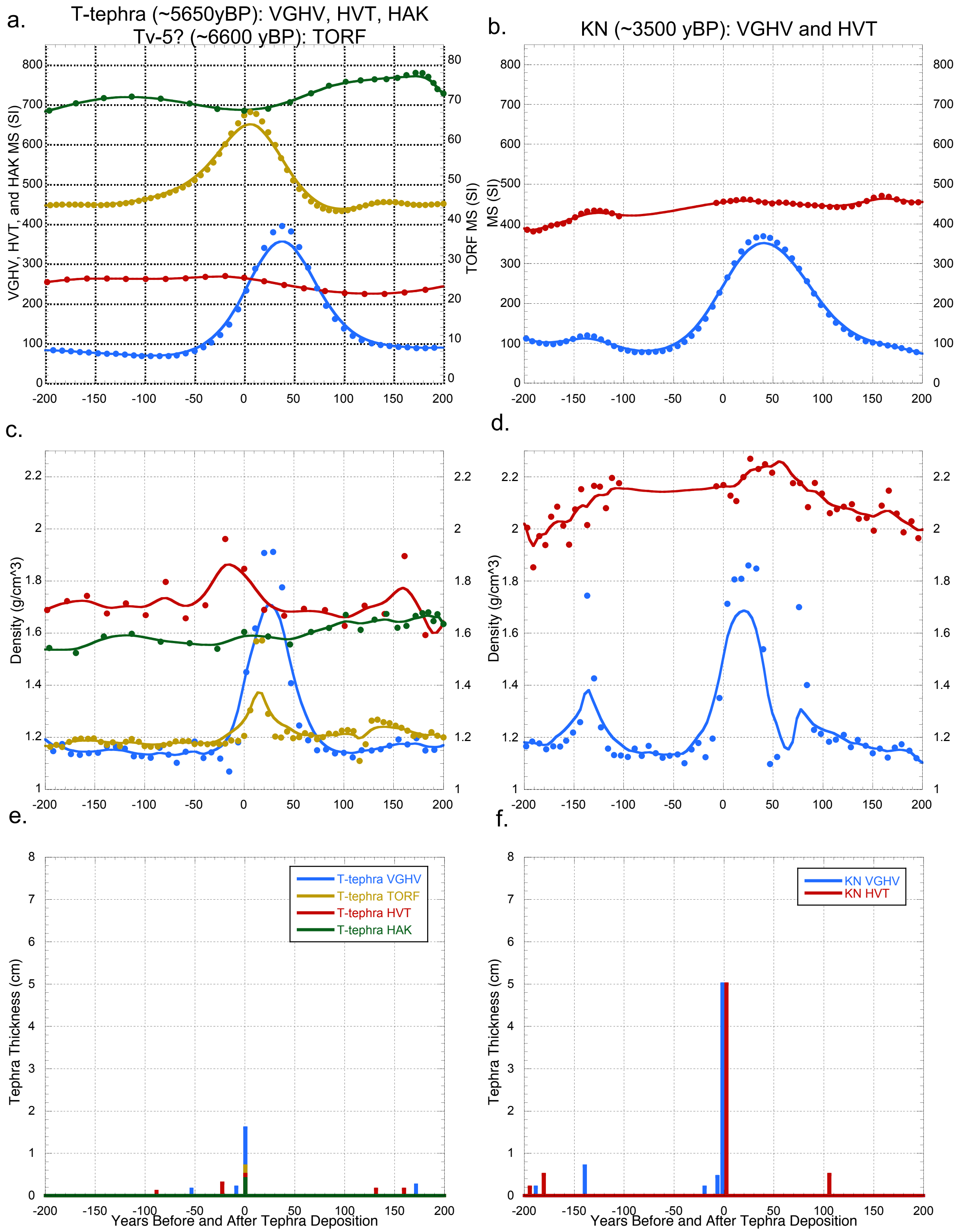

A3.1.2.2 Organic Matter Proxies

OM proxies indicate no persistent changes following deposition of the T-tephra. %TOC expresses a short-lived decrease in VGHV, HVT, and TORF after the T-tephra horizon however this decline initiates before the tephra in all three lakes suggesting earlier tephra horizons, sampling errors, tephra migration, or some other factor may be influencing the signal at this transition. Despite the decrease, all lakes return to pre-tephra values within ~50 years (Fig. A3.4a). After returning to pre-tephra values a subtle increasing trend persists for at least 50 years in TORF while no such change occur in VGHV or HVT. The brief decrease in %TOC is likely from a short-lived landscape disturbance caused by deposition of the tephra (Ayris and Delmelle, 2012). HAK has no immediate change post-T-tephra. However, ~25 years after the tephra horizon %TOC to a new high for ~75 years. This temporary increase in %TOC is increases likely related to increased productivity in HVT after the T-tephra as it is prior to the 5.5 ka transition into Neoglacial cooling (Geirsdóttir et al., in review). %TOC before and after the KN tephra horizon is more variable in VGHV and HVT (Fig. A3.4b). Both lakes show a decrease in %TOC following the KN tephra lasting ~50 years with low values of %TOC also associated with tephra layers earlier in the time series. After returning to pre-KN values HVT gradually decreases while VGHV gradually increases for the rest of the time series. The signal of %TOC suggests increased primary productivity and/or decreased erosion with the juxtaposition between the signal of %TOC in both lakes from different catchment processes during this period of Neoglacial cooling (Geirsdóttir et al., in review). It is noted that the structure of MS, density and %TOC are roughly anticorrelated in all lakes during the T-tephra time series while they are anticorrelated in

Figure A3.4 Basaltic tephra time series for biological proxies in all lakes a. and b. %TOC around the T-tephra and KN respectively; c. and d. C:N around the T-tephra and KN respectively; e. and f. d13C around T-tephra and KN respectively; g. and h. Tephra layers and their thicknesses in the T-tephra and KN time series respectively

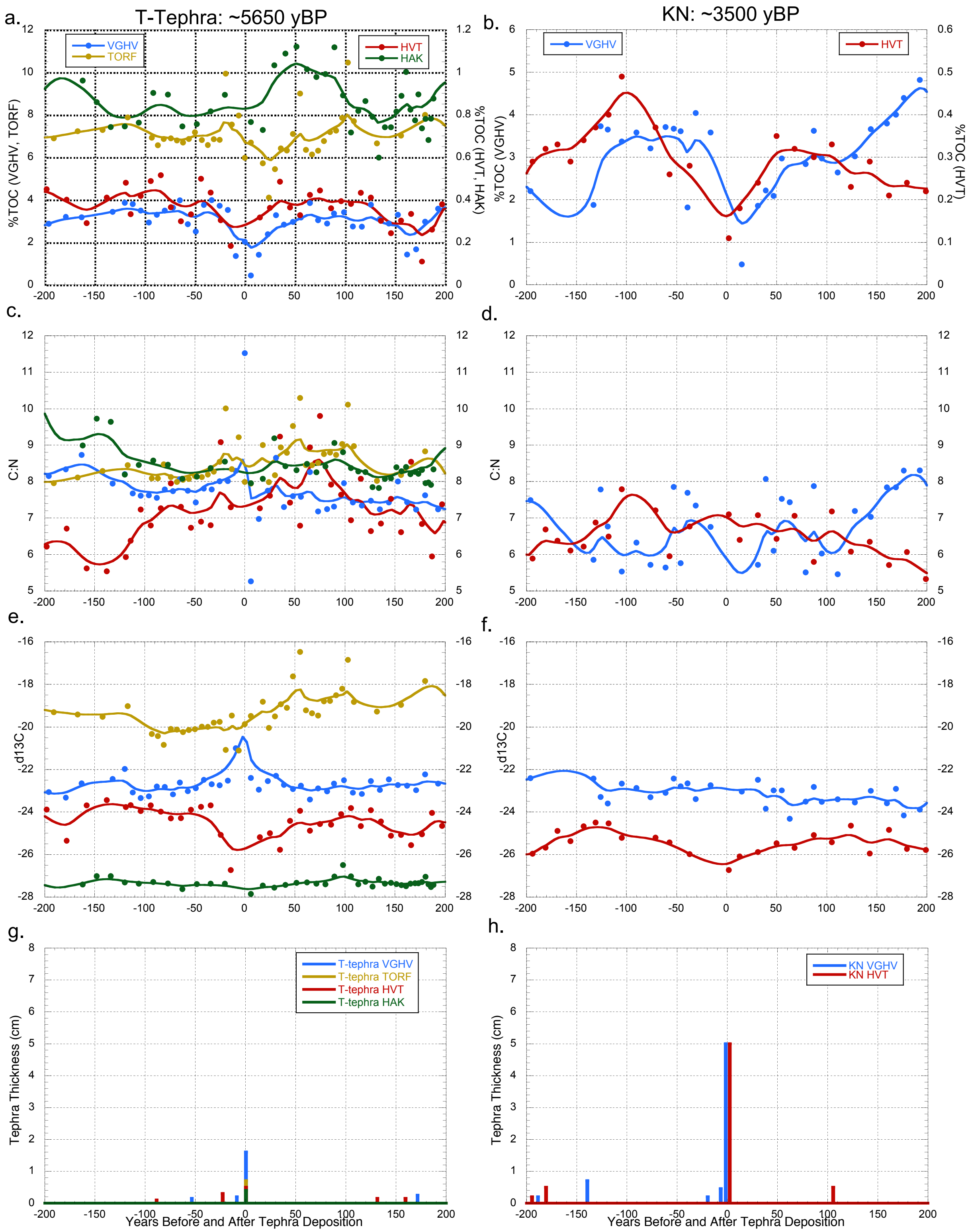

VGHV and correlated in HVT for the KN time series. This trend is telling of the influence of minerogenic material on the signal of %TOC with correlations indicating high %TOC associated with a high minerogenic flux.

C:N is fairly consistent for both basaltic time series (Fig. A3.4c, d). A gradual negative trend occurs in VGHV and HAK throughout the T-tephra time series in which C:N in VGHV has a one point positive deviation followed by a significant negative deviation and rapid recovery to pre-T-tephra values before continuing its decline. The same signal occurs in VGHV immediately after the KN tephra horizon. However, a rapid increase in C:N begins ~100 years after the tephra horizon and persists through the end of the time series. Deposition of the T-tephra if followed by no immediate response in C:N in HAK and TORF. In TORF, a gradual positive trend and increased variability occurs for at least 100 years after the tephra horizon while HAK indicates no change through time. For ~75 years after the T-tephra, C:N in HVT also gradually increases with heightened variability before slowly declining over the remainder of the time series. Following the KN tephra horizon in HVT C:N has a gradually decreasing trend that continues to the end of the time series. Trends in C:N suggest stable or increased aquatic productivity in all lakes following the thick basaltic tephra layer.

Stable carbon isotopes do not vary significantly after the basaltic tephra horizons. In the T-tephra time series $\delta^{13}C$ is correlated with %TOC in HVT and TORF, anticorrelated in VGHV, while no change occurs in HAK (Fig. A3.4e). After the T-tephra horizon a one point positive deviation takes place in VGHV before returning to pre-eruption values. In TORF a gradual positive trend begins after deposition of the tephra stabilizing after ~100 years. A multipoint negative deviation begins before deposition of the T-tephra in HVT with $\delta^{13}C$ returning to values ~0.5‰ lower than before the T-tephra within 50 years. There are no immediate changes in $\delta^{13}C$ after KN in VGHV but, a gradual negative trend persists throughout the time series with $\delta^{13}C$ decreasing by ~2‰ over 400 years (Fig. A3.4f). A brief negative deviation in $\delta^{13}C$ also occurs after the KN tephra horizon in HVT but, $\delta^{13}C$ returns to pre-KN values within 50 years. It is noted the average $\delta^{13}C$ in HVT during the KN time series is similar to post-H4 values of ~-25.5‰. Stable carbon isotope signals suggest no change or increased aquatic productivity after brief destabilization of the system following the tephra horizons.

A3.2 Bi-plots

The large number of proxies required use of bi-plots to identify significant co-variation and consistent relationships between variables for the different tephra deposition events and lakes. To observe trends more clearly proxies from the rhyolitic tephra series and the basaltic tephra series were plotted on separate graphs for both physical and OM proxies and each lake was plotted individually for OM proxies. Physical proxy bi-plots covered the entire 400 year time series while biological proxies bi-plots were divided into 200 year pre- and post-deposition of the tephra horizons of interest. For each time period best-fit lines and linear correlation coefficients were calculated. Co-variations are considered strong if ($R > 0.40$).

A3.2.1Bi-plots for Rhyolitic Tephra Series

A3.2.1.1 MS vs. Density

For the H4 time series MS and density have strong positive correlation in VGHV ($R = 0.74$), HAK ($R = 0.61$), and TORF ($R = 0.48$) and strong negative correlation in HVT ($R = -0.41$) (Fig. A3.5a). However, in the H3 time series MS and density are strongly correlated in both VGHV (R = 0.82) and HVT (R = 0.80) (Fig. A3.5b). Negative correlation for HVT proxies in the H4 time series occurs because the rhyolitic tephra had significantly lower MS than the background values skewing the data.

Figure A3.5 MS vs. Density for Rhyolitic tephra time series data in all lakes a. H4 time series data; b. H3 time series data

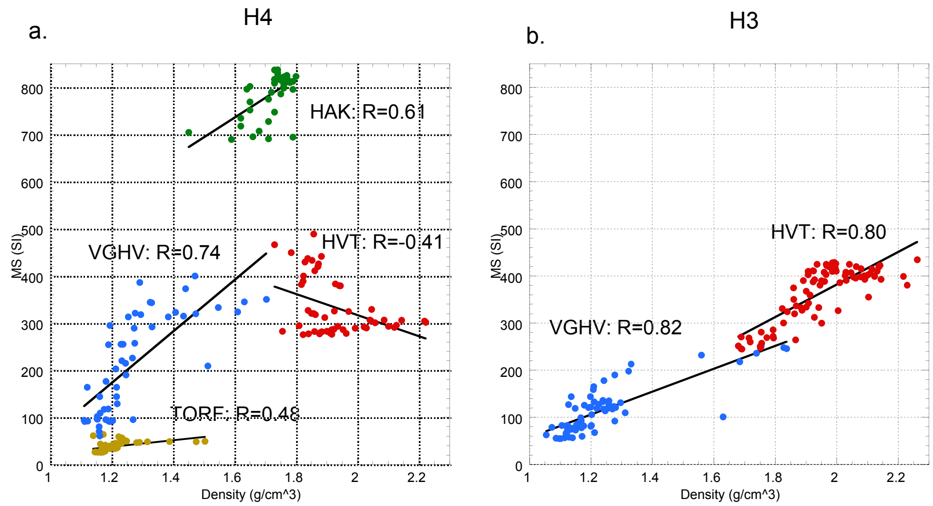

A3.2.1.2 C:N vs. %TOC

The relationship between C:N and %TOC (Fig. A3.6a, b; A3.7a, b) depends upon the ecosystem processes taking place in and around each lake. Strong co-variation suggests that both %TOC and C:N vary for the same reasons, be it changes in erosion or primary productivity in the catchment. Positive co-variations in ultraoligotrophic lakes (HVT and HAK) are likely from changes in erosive processes while positive co-variations in productive lakes (VGHV and TORF) indicate variability in primary productivity with high C:N suggesting low algal productivity. %TOC and C:N are well correlated before H4 in HAK (R = 0.70) and TORF (R = 0.69) but have moderate and weak anticorrelation in VGHV (R = -0.38) and HVT (R = -0.03) respectively for the same time period. Post-H4, both proxies in HAK show significant correlation ($R = 0.68$) and a similar range of %TOC and C:N. In TORF, C:N and %TOC are more variable immediately after H4 producing no significant correlation ($R=0.06$) between the two proxies. However, most of the data is tightly clustered at slightly elevated pre-eruption values (see Fig. A3.6a, b). VGHV has weak negative correlation ($R = -0.16$) between the two proxies before and after H4 with a negative shift in C:N post-H4. Weak anticorrelation ($R = -0.30$) is also present in VGHV pre-H3 with proxy values similar in range to pre-H4 values. After H3 %TOC and C:N have strong co-variation ($R = 0.49$) with a similar range of values observed pre-H3. C:N and %TOC are moderately well correlated ($R = 0.40$) in HVT after H4 with a positive shift in both proxies. Pre-H3 values are similar to pre-H4 values with stronger positive co-variation ($R = 0.81$). The already high correlation in HVT is improved post-H3 ($R = 0.93$) covering a large range of values (Fig. A3.7a, b).

A3.2.1.3 $\delta^{13}C$ vs. %TOC

The relationship between $\delta^{13}C$ and %TOC is dependent upon ecosystem and erosional processes in each lake as background values vary greatly for both proxies. We observed no coherent trends in $\delta^{13}C$ vs. %TOC between lakes for any of the time periods of interest (See Fig. A3.6c, d; Fig. 3.7c, d). After H4, TORF temporarily experiences lower values of %TOC accompanied with more negative $\delta^{13}C$ and co-variation changes sign from negative to positive. $\delta^{13}C$ permanently shifts to lower values post-H4 in HAK and HVT and is associated with no significant co-variation ($R = 0.07$) and strong negative co-variation ($R = -0.43$) respectively. In HVT pre-H3 proxy values are similar to post-H4 albeit with greater variability and no significant correlation

Figure A3.6 Bi-plots comparing relationships between biological proxies before and after deposition of the rhyolitic tephra horizons of interest for HAK and TORF a. and b. C:N vs. %TOC in HAK and TORF respectively; c. and d. d13C vs. %TOC in HAK and TORF respectively; e. and f. C:N vs. d13C in HAK and TORF respectively

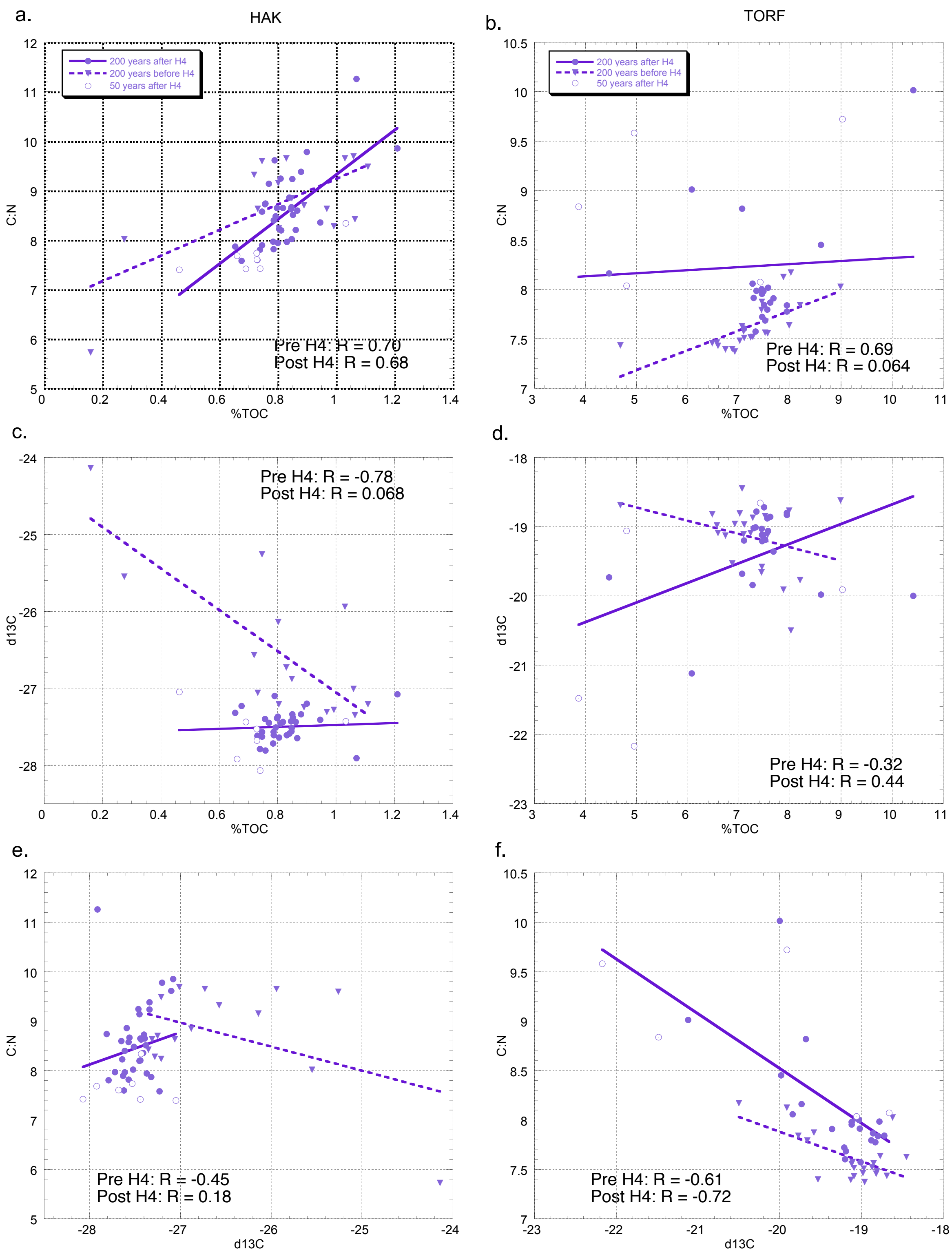

Figure A3.7 Bi-plots comparing relationships between biological proxies before and after deposition of the rhyolitic tephra horizons of interest for VGHV and HVT a. and b. C:N vs. %TOC in VGHV and HVT respectively; c. and d. d13C vs. %TOC in VGHV and HVT respectively; e. and f. C:N vs. d13C in VGHV and HVT respectively

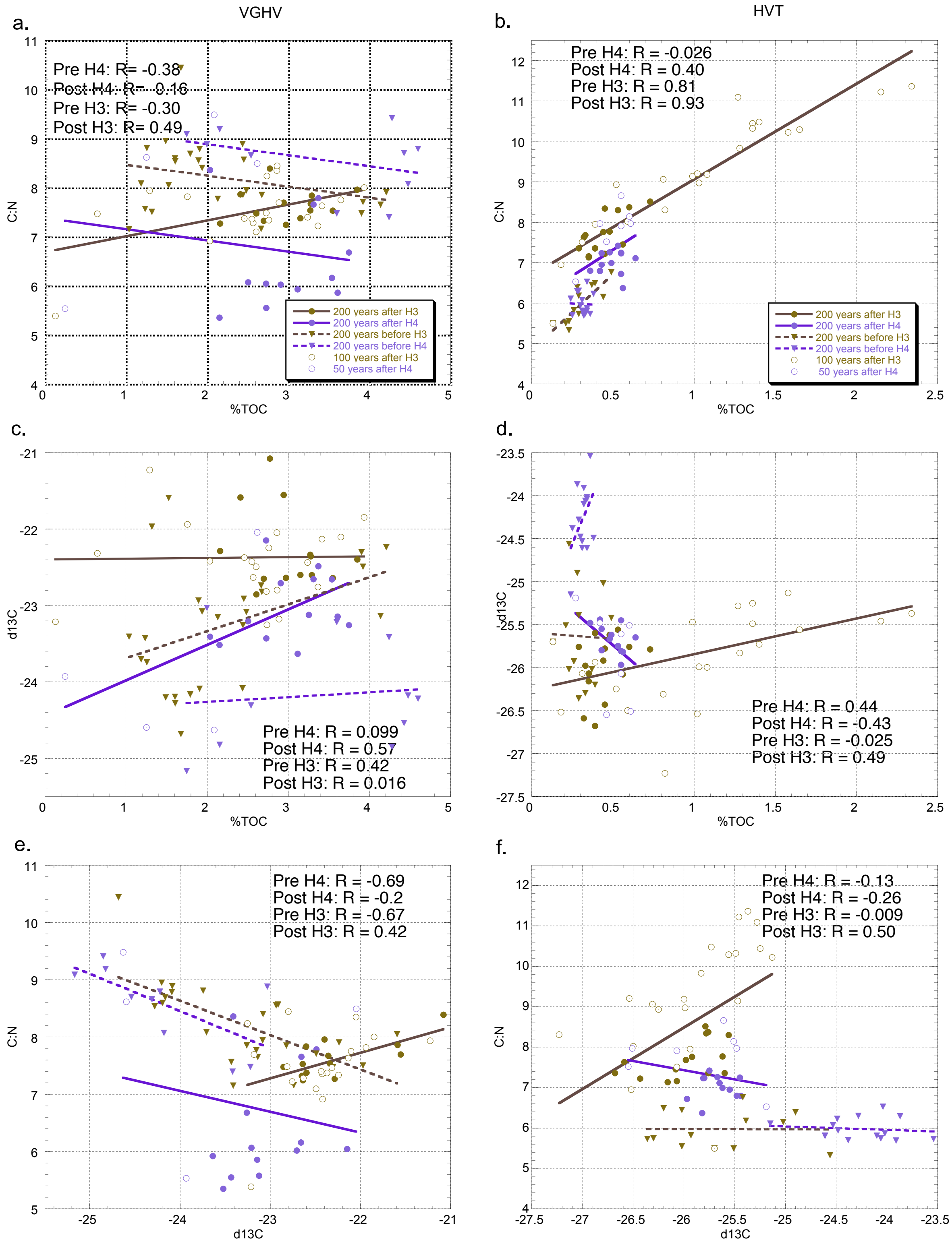

(R = -0.3). Strong positive co-variation (R = 0.49) is evident in HVT post-H3 but there is no significant shift in $\delta^{13}C$. No relationship between the proxies occurs in VGHV before H4 but after the eruption strong co-variation (R = 0.57) emerges. Values and trends of $\delta^{13}C$ vs. %TOC are similar before H3 in VGHV (R = 0.42) but following the H3 tephra horizon co-variation dissolves (R = 0.02) with values of $\delta^{13}C$ again greater on average while %TOC covers a similar range. The large shifts or change in sign of the relationship between $\delta^{13}C$ and %TOC in all lakes before and after the H4 tephra horizon supports ecosystem transitions observed in the Holocene paleoenvironmental records of VGHV, HAK and HVT (Hallsdóttir and Caseldine 2005; Larsen et al., 2012; Geirsdóttir et al., in review; Chapter 4). A shift is also observed after the H3 tephra horizon in HVT suggesting another period of significant environmental change.

A3.2.1.4 C:N vs. $\delta^{13}C$

The relationship between C:N and $\delta^{13}C$ signifies variability in OM source. Bi-plots of C:N vs. $\delta^{13}C$ have moderate to strong anticorrlation between the two proxies before H4 in all lakes except HVT, where the negative correlation is weak (see Fig. A3.6e, f, A3.7e, f). Following H4 the negative co-variation persists in all lakes except HAK where a small range of C:N and $\delta^{13}C$ masks any correlation. After the H4 tephra, HAK, TORF and HVT show a negative shift in $\delta^{13}C$ associated with higher values of C:N while VGHV displays the opposite. Pre-H3 HVT and VGHV indicate weak (R = -0.01) and significant (R = -0.67) anticorrelation respectively. After H3 both lakes have strong positive co-variation between the two proxies. The change in sign of co-variation between the post-H3 and post-H4 indicate OM sources preserved in the sediment was different.

A3.2.2Bi-plots for Basaltic Tephra Series

A3.2.2.1 MS vs. Density

MS and density have moderate to strong co-variation in all lakes for both the T-tephra and KN time series (See Fig. A3.8a, b). This trend was also observed in the rhyolitic tephra time series indicating that the minerogenic component of sediment primarily drives variations in MS and density.

A3.2.2.2 C:N vs. %TOC

All lakes show positive correlation between C:N and %TOC in the 200 years following thick basaltic tephra layers (See Fig. A3.9a, b, A3.10a, b). HAK and TORF indicate weak (R = 0.23) and strong (R = 0.90) positive correlation respectively before the T-tephra and strong positive co-variation after (R = 0.67 and R = 0.72 respectively). Prior to the T-tephra and KN tephra horizons correlation is more variable with proxies in VGHV supporting weak anticorrelations (R = -0.21 and R = -0.12 respectively). HVT displays weak negative correlation between proxies before the T-tephra (R=-0.25) and significant positive correlation post-T-tephra (R=0.59) and pre-KN (R=0.78). Post-KN co-variation is weak (R=0.10) in HVT suggesting reduced landscape erosion. Positive co-variations after the basaltic tephra layers indicate both proxies vary for consistent reasons however values of C:N and %TOC also cover smaller ranges than observed in the rhyolitic tephra time series for all lakes except TORF, in which the two are comparable.

Figure A3.8 MS vs. Density for Basaltic tephra time series data in all lakes a. T-tephra time series data; b. KN time series data

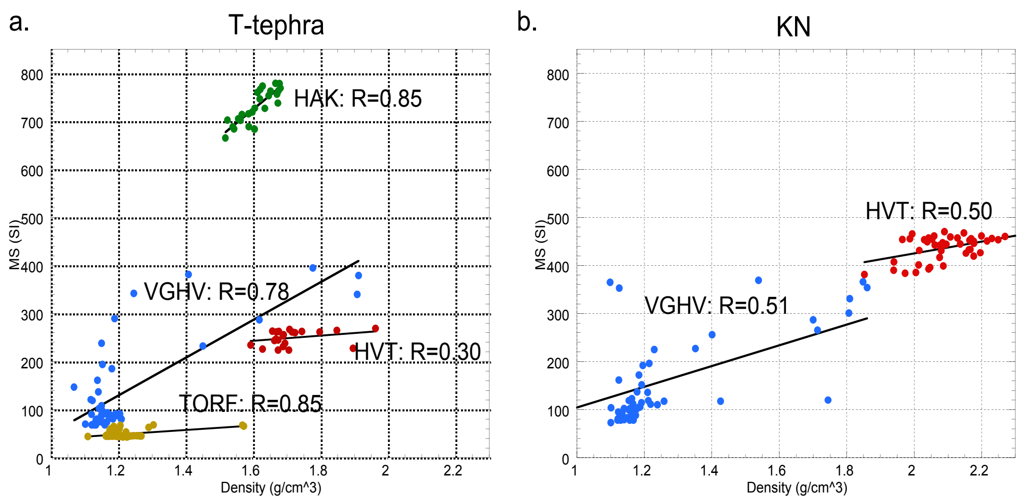

A3.2.2.3 δ^{13}C vs. %TOC

As in rhyolitic tephra bi-plots there is no consistent relationship between lakes for δ^{13}C and %TOC (See Fig. A3.9c, d, A3.10c, d). VGHV and HAK show no significant change before and after the tephra layers of interest. Proxies in VGHV have moderate to strong negative co-variation between proxies and a similar range of values before and after the KN and T-tephra horizons. HAK has no correlation and no change in proxies before and after the T-tephra. HVT has strong positive co-variation for all time periods of interest except after the T-tephra. TORF has moderate anticorrelation before the T-tephra but this is skewed by one data point. After the T-tephra, TORF has a strong positive correlation (R = 0.86) between the proxies. The lack of changes in sign and decreased correlation after most basaltic layers supports little change to ecosystem processes and a reduction in the extent %TOC controls values of δ^{13}C. As with the other two OM proxies, δ^{13}C covers a smaller range of values in all lakes except TORF, where more positive values are present.

A3.2.2.4 C:N vs. δ^{13}C

All lakes except HVT have moderate to strong positive co-variation between C:N and $\delta^{13}C$ following deposition of the T-tephra (See Fig. A3.9e, f, A3.10e, f). This relationship suggests increased primary productivity of aquatic algae and macrophytes. Both HAK and VGHV have positive correlation before and after the T-tephra. TORF has anticorrelation before and positive correlation after the T-tephra while HVT has strong negative co-variation before and after the T-tephra supporting little terrestrial input. Both VGHV and HVT show weak positive correlations between proxies before the KN horizon and moderately strong anticorrelation following the tephra indicating a different system state at the time of eruption. In all lakes except TORF the data is fairly well clustered around a small range of $\delta^{13}C$ and C:N values.

A3.3 Summary of Proxy Time Series and Bi-Plots

Generalized trends and response time of proxies to tephra perturbations can seen in Table A1.1. Short-lived positive density anomalies occur coupled with peaks in MS in lakes with low %TOC (VGHV and TORF) at rhyolitic and basaltic tephra horizons. MS and density in HVT and HAK vary in their response to tephra perturbations as they have significantly higher background states due to relatively high minerogenic sediment fluxes in each lake. Despite this, HAK and HVT show more persistent changes in MS and density following rhyolitic tephra layers but little change after basaltic tephra layers. However, HVT does show a gradual decrease in MS following the KN tephra suggesting a lower minerogenic flux. In all time series except one (HVT at H4) MS and density have a moderate to strong positive correlation suggesting a relationship driven by the minerogenic component in the sediment. Additional tephra horizons are most prominent in VGHV and HVT and dominated by layers of basaltic composition.

Figure A3.9 Bi-plots comparing relationships between biological proxies before and after deposition of the basaltic tephra horizons of interest for HAK and TORF a. and b. C:N vs. %TOC in HAK and TORF respectively; c. and d. d13C vs. %TOC in HAK and TORF respectively; e. and f. C:N vs. d13C in HAK and TORF respectively

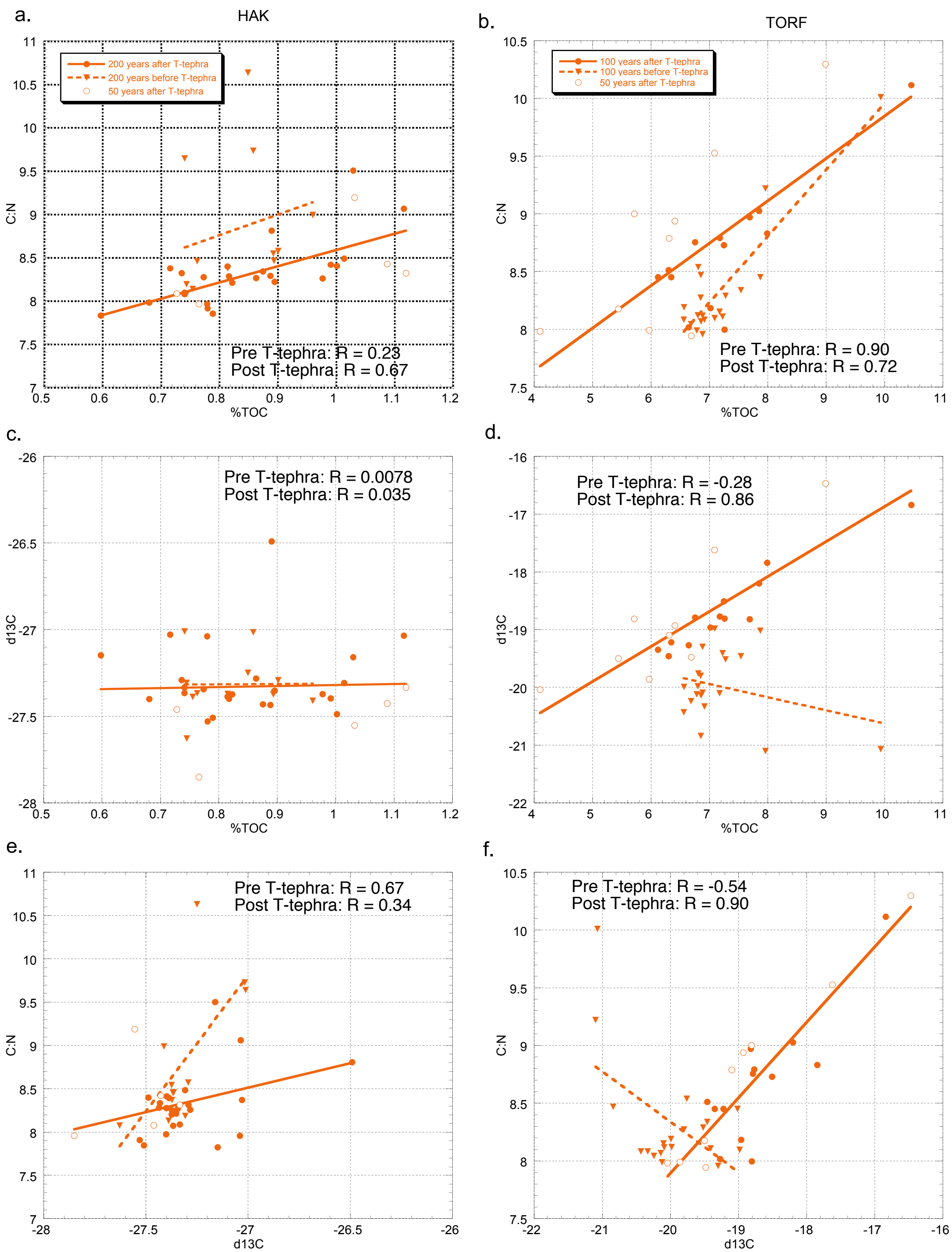

Figure A3.10 Bi-plots comparing relationships between biological proxies before and after deposition of the basaltic tephra horizons of interest for VGHV and HVT a. and b. C:N vs. %TOC in VGHV and HVT respectively; c. and d. d13C vs. %TOC in VGHV and HVT respectively; e. and f. C:N vs. d13C in VGHV and HVT respectively

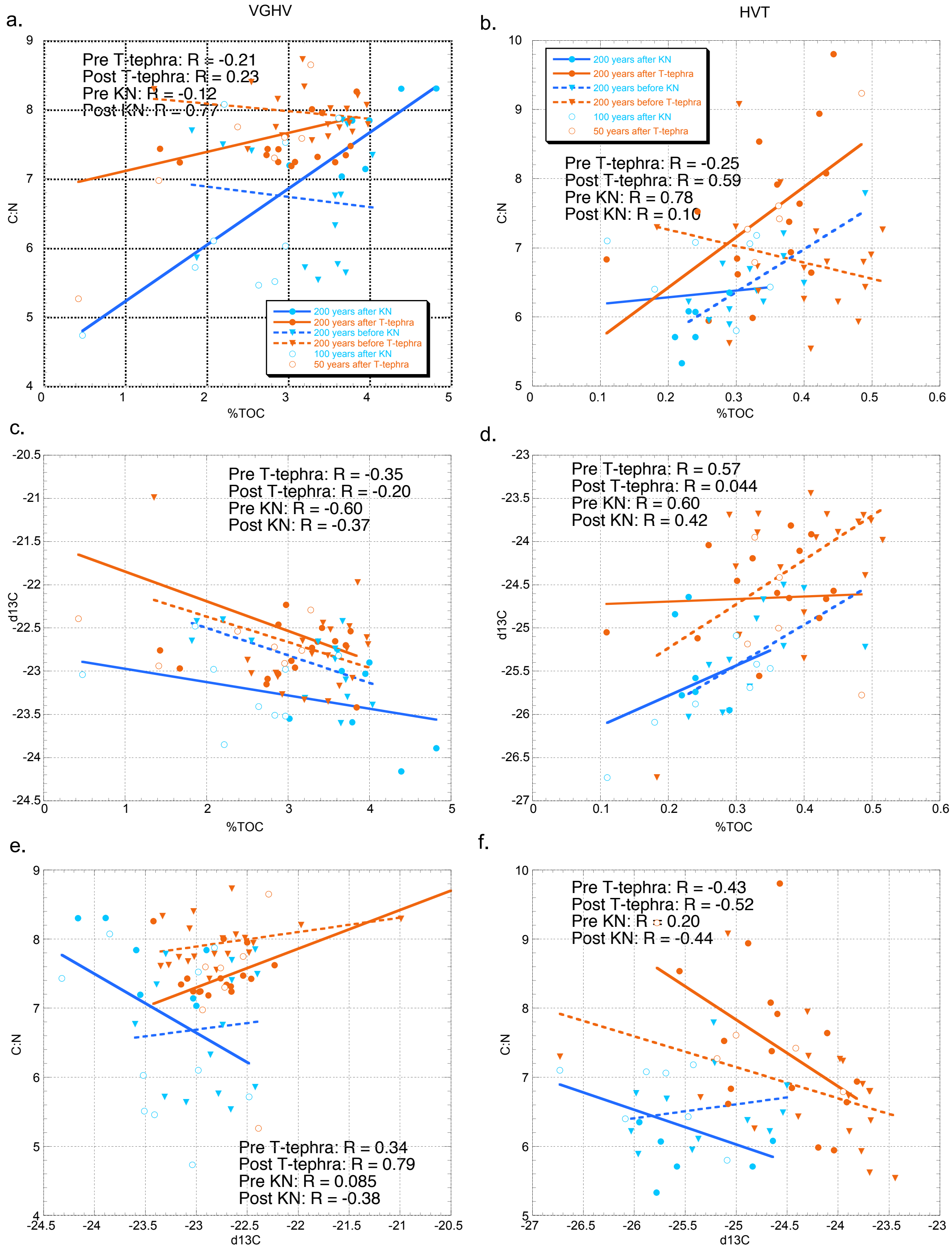

Table A3.1 General trend of proxies in lakes in response to the tephra layers of interest. +: positive response, -: negative response, 0: no response, S: short response <100 years, L: long response ≥ 100 years

Lake	Rhyolitic Tephra	MS	Den	%TOC	C:N	$\delta^{13}C$	Basaltic Tephra	MS	Den	%TOC	C:N	$\delta^{13}C$
VGHV	H4	+ S	+ S	- S	- S	+ L*	T-tephra	+ S	+ S	- S	- S	+ S
HVT		- L	+ L	+ L	+ L	- L		0	0	- S	+/- L	- S
HAK		+ L	+ L	- L	- L	- L		?	?	+ S	0	0
TORF		+ S	+ S	- S	- S	- S		+ S	+ S	-/+ L	+ L	+ L
VGHV	H3	+ S	+ S	- S	- S	+ L*	KN	+ S	+ S	-/+ L	-/+ L	- L
HVT		-/+ L	-/+ L	+ L	+ L	0		0	- L	- L	- L	- S

*trends likely skewed due to the presence of thick basaltic tephra layers in the time series in addition to the rhyolitic tephra horizons of interest.

All lakes except HVT have negative anomalies in %TOC for ≤100 years following rhyolitic eruptions indicating short-lived landscape disturbance after tephra deposition. Subsequent the rhyolitic tephra layers HVT experiences a long-lived increase in %TOC consistent with high landscape instability in the catchment (Larsen et al., 2011; 2012). Abrupt changes in C:N occur after rhyolitic tephra horizons: negative changes in VGHV and HAK and positive changes in TORF and HVT consistent with an increased minerogenic flux, decreased in-lake primary productivity, and/or increased terrestrial erosion. The longevity of these changes varies between lakes lasting the longest in HVT. After H4 HAK and HVT experience a persistent decrease in $\delta^{13}C$ while TORF has a temporary decrease and VGHV a long-lasting increase, with changes corresponding to an increased terrestrial and aquatic components respectively (Meyers and Lallier-Vergès, 1999). The H3 tephra horizon produces little change in $\delta^{13}C$ in HVT and VGHV.

Following basaltic tephra layers negative anomalies in %TOC occur in all lakes except HAK. However, unlike signals after the rhyolitic tephra layers of interest these changes are shorter lived and not associated with abrupt changes in C:N except in VGHV. A one point positive anomaly is followed by a short lived negative anomaly in VGHV while HAK has no change in C:N after the T-tephra. Meanwhile a gradual increases in C:N occur in HVT and TORF post-T-tephra. In HVT C:N begins to decrease ~75 years after the tephra layers of interest. $\delta^{13}C$ does not change significantly following basaltic tephra horizons. HVT and VGHV experience short-lived decreases and increase respectively but quickly recover to the pre-eruption background state of $\delta^{13}C$ while TORF gradually increases to more positive values. The changes observed in all lakes following the thick basaltic tephra layers support some degree of landscape stabilization and/or increased aquatic productivity after a brief disturbance.

Bi-plots indicate some consistent trends between lakes and between eruption types such as negative co-variation between $\delta^{13}C$ and C:N after H4 in all lakes and positive co-variation after H3 in VGHV and HVT. Additionally all lakes except for VGHV show positive correlation between %TOC and C:N subsequent the rhyolitic tephra layers of interest. VGHV only has such a correlation after the H3 tephra horizon. $\delta^{13}C$ vs. %TOC shows no consistent relationship between lakes and eruption types but, do indicate shifts in $\delta^{13}C$ (i.e. the OM source) through time. Following basaltic tephra horizons C:N and %TOC have moderate to strong positive co-variation in the lakes. All lakes except HVT are negatively correlated between $\delta^{13}C$ and C:N after the T-tephra. After KN, $\delta^{13}C$ and C:N are positively correlated in HVT and VGHV. A significant transition in the state of the system appears to occur after H4 and H3 in all lakes where little change takes place in most lakes following the T-tephra and KN.